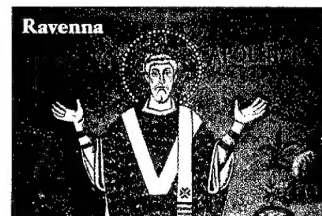


# PROGRAM and ABSTRACTS

## DRIP IX

### 9<sup>th</sup> International Conference on Defects - Recognition, Imaging and Physics in Semiconductors

**RIMINI, Italy**  
**September 24-28, 2001**



**Sotto l'Alto Patronato  
del Presidente della Repubblica**

**Under the High Patronage of the  
President of the Italian Republic**

sponsored by  
CNR - MASPEC  
CNR - MADESS II

**OFFICE OF NAVAL RESEARCH INTERNATIONAL FIELD OFFICE  
PROVINCIA DI RAVENNA, UFFICIO TURISMO**

20020405 054

AQ F02-07-1182

**The 9<sup>th</sup> International Conference on  
Defects - Recognition, Imaging and Physics in  
Semiconductors  
DRIP IX**

**was held under the**

**HIGH PATRONAGE of  
the PRESIDENT of the ITALIAN REPUBLIC**

**and sponsored by**

**CNR - MASPEC**

**CNR - MADESS II**

**OFFICE OF NAVAL RESEARCH INTERNATIONAL FIELD OFFICE  
PROVINCIA DI RAVENNA, UFFICIO TURISMO**

**REPORT DOCUMENTATION PAGE**

Form Approved OMB No. 0704-0188

Public reporting burden for this collection of information is estimated to average 1 hour per response, including the time for reviewing instructions, searching existing data sources, gathering and maintaining the data needed, and completing and reviewing the collection of information. Send comments regarding this burden estimate or any other aspect of this collection of information, including suggestions for reducing this burden to Washington Headquarters Services, Directorate for Information Operations and Reports, 1215 Jefferson Davis Highway, Suite 1204, Arlington, VA 22202-4302, and to the Office of Management and Budget, Paperwork Reduction Project (0704-0188), Washington, DC 20503.

1. AGENCY USE ONLY (Leave blank)		2. REPORT DATE September 2001		3. REPORT TYPE AND DATES COVERED September 26-28, 2001 Final	
4. TITLE AND SUBTITLE International Conference on Defects – Recognition, Imaging and Physics in Semiconductors (9 <sup>th</sup> ) (DRIP IX) Held in Rimini, Italy on September 24-28, 2001. Program and Abstracts..				5. FUNDING NUMBERS	
6. AUTHOR(S)					
7. PERFORMING ORGANIZATION NAME(S) AND ADDRESS(ES) National Research Council of Italy Il Consiglio Nazionale delle Ricerche (CNR) Aldo Large square Moor, 7 00185 Rome, Italy				8. PERFORMING ORGANIZATION REPORT NUMBER	
9. SPONSORING/MONITORING AGENCY NAME(S) AND ADDRESS(ES)  Office of Naval Research, European Office PSC 802 Box 39 FPO AE 09499-0039				10. SPONSORING/MONITORING AGENCY REPORT NUMBER	
11. SUPPLEMENTARY NOTES This work relates to Department of the Navy Grant issued by the Office of Naval Research International Field Office. The United States has a royalty free license throughout the world in all copyrightable material contained herein.					
12a. DISTRIBUTION/AVAILABILITY STATEMENT  Approved for Public Release; Distribution Unlimited. U.S. Government Rights License. All other rights reserved by the copyright holder.				12b. DISTRIBUTION CODE  A	
12. ABSTRACT (Maximum 200 words) Conference topics included: Photoluminescence, Other optical methods, Nanoscanning techniques, Defects in silicon, contactless techniques, Electron beam methods, Electrical methods, Defects in wide-gap semiconductors, cathodoluminescence, X-ray techniques, Miscellaneous techniques and Defects in devices.					
13. SUBJECT TERMS DRIP IX, ONRIFO, EOARD, Foreign reports				15. NUMBER OF PAGES	
				16. PRICE CODE	
17. SECURITY CLASSIFICATION OF REPORT  UNCLASSIFIED	18. SECURITY CLASSIFICATION OF THIS PAGE  UNCLASSIFIED	19. SECURITY CLASSIFICATION OF ABSTRACT  UNCLASSIFIED	20. LIMITATION OF ABSTRACT  UL		

NSN 7540-01-280-5500

Standard Form 298 (Rev. 2-89)  
Prescribed by ANSI Std. Z39-18  
298-102

## DRIP IX COMMITTEES

### DRIP IX PROGRAM

MONDAY 24 September	
	16:00 – 20:00 Registration & Reception 20:00 – 21:30 Welcome Dinner
TUESDAY 25 September	
08:45 – 09:00 Opening Address 09:00 – 10:25 <b>SESSION 1</b> 10:25 – 10:55 Coffee Break 10:55 – 12:35 <b>SESSION 2</b> 12:35 – 14:10 Lunch	14:10 – 15:50 <b>SESSION 3</b> 15:50 – 16:20 Coffee Break 16:20 – 16:50 <b>SESSION 3</b> 16:50 – 18:30 <b>SESSION 4</b> 18:45 – 20:00 <b>POSTER SESSION 1</b> 20:00 – 21:30 Dinner
WEDNESDAY 26 September	
08:30 – 10:10 <b>SESSION 5</b> 10:10 – 10:40 Coffee Break 10:40 – 12:20 <b>SESSION 6</b> 12:20 – 14:00 Lunch	14:00 – 15:15 <b>POSTER SESSION 2</b> 15:15 – 16:40 <b>SESSION 7</b> 16:40 – 17:10 Coffee Break 17:10 – 18:35 <b>SESSION 8</b> 18:35 – 20:00 <b>SESSION 9</b> 20:00 – 21:30 Dinner
THURSDAY 27 September	
08:30 – 10:10 <b>SESSION 10</b> 10:10 – 10:40 Coffee Break 10:40 – 12:20 <b>SESSION 11</b> 12:20 – 13:40 Lunch	13:40 – 19:30 <b>EXCURSION to URBINO</b> 20:00 – 23:00 <b>GALA DINNER</b>
FRIDAY 28 September	
09:00 – 10:25 <b>SESSION 12</b> 10:25 – 10:50 Coffee Break 10:50 – 12:30 <b>SESSION 13</b> 12:30 – 13:50 Lunch	13:50 – 15:30 <b>SESSION 14</b> 15:30 – 15:45 Closing ceremony



## **DRIP IX COMMITTEES**

### **Conference Chairman**

Cesare Frigeri                      CNR-MASPEC

### **International Steering Committee**

Martina Baeumler	Germany
Paul D. Brown	United Kingdom
Mike Brozel	United Kingdom
Iain Calder	Canada
Anna Cavallini	Italy
Joerg D. Donecker	Germany
Jean Pierre Fillard	France
Cesare Frigeri	Italy
Juan Jimenez	Spain
Alan Mickelson	Usa
Paul Montgomery	France
Tomoya Ogawa	Japan
Ingrid Rechenberg	Germany
Michio Tajima	Japan
Zhanguo Wang	China
Jan L. Weyher	Poland, The Netherlands

### **Scientific Program Committee**

R. Blunt	United Kingdom
W. K. Chim	Singapore
C. Claeys	Belgium
A. Gasparotto	Italy
M. Itsumi	Japan
B. Jenichen	Germany
M. Kamp	Germany
A. N. Larsen	Denmark
S. Martinuzzi	France
Y. Otoki	Japan
D. Pavlidis	USA
S. Pearton	USA
J. Piqueras	Spain
M. Yamada	Japan

### **Local Organising Committee**

A. Cavallini	University of Bologna
R. Fornari	CNR-MASPEC
E. Gombia	CNR-MASPEC
R. Magno	CNR-MASPEC
R. Mosca	CNR-MASPEC
G. Salviati	CNR-MASPEC

<http://www.maspec.bo.cnr.it/ut/d11200/NEWS/drip9/drip9.html>

# PROGRAM

## MONDAY 24 SEPTEMBER, 2001

16:00-20:00      **REGISTRATION**

20:00              **WELCOME    DINNER**

## TUESDAY 25 SEPTEMBER, 2001

8:45-9:00        **OPENING    ADDRESS**  
C. Frigeri, Chairman DRIP IX

### **SESSION 1. PHOTOLUMINESCENCE    1** *Chair : Tajima Michio*

- 9:00    **S1-1**    **Daniel T. CASSIDY**  
**Invited**    Spatially-resolved and polarization resolved-photoluminescence for  
study of dislocations and strain in III-V materials
- 9:40    **S1-2**    **M. Baeumler, M. Maier, W. Jantz, Th. Bunger, J. Stenzenberger**  
2K PL topography of silicon doped VGF GaAs wafers
- 9:55    **S1-3**    **Masahiro Yoshimoto**  
Sub-micron scale photoluminescence images of wide bandgap  
semiconductors by cryogenic scanning optical microscope
- 10:10   **S1-4**    **L. Masarotto, J. M. Bluet, M. Berenguer, P. Girard and G. Guillot**  
UV scanning photoluminescence spectroscopy applied to silicon  
carbide characterization

10:25-10:55      **COFFEE    BREAK**

### **SESSION 2. PHOTOLUMINESCENCE    2** *Chair : Montgomery Paul*

- 10:55   **S2-1**    **Michio TAJIMA** and Shigeo Ibuka  
**Invited**    Condensate luminescence under ultraviolet excitation: Application to  
the study of ultrathin SOI layers

- 11:35 S2-2 **Hiroshi Tsuji, Ryangsu Kim, Toshifumi Shyano, Tetsuya Hirose, Yoshinari Kamakura, and Kenji Taniguchi**  
Photoluminescence study of {311} defect-precursors in self-implanted silicon
- 11:50 S2-3 **J. W. Tømm, A. Maaßdorf, and Y. I. Mazur, S. Gramlich, E. Richter, K. Brunner, M. Weyers, G. Tränkle, D. Nickel, V. Malyarchuk, T. Günther, Ch. Lienau, A. Bärwolff, T. Elsaesser**  
The impact of defects to minority-carrier kinetics in heavily doped GaAs:C analyzed by transient photoluminescence spectroscopy
- 12:05 S2-4 **H. D. Geiler, H. Karge, M. Wagner, A. Ehlert, E. Daub**  
Detection and Analysis of Crystal Defects in Silicon by Scanning Infrared Depolarization and Photoluminescence Heterodyne Techniques
- 12:20 S2-5 **N. D. Zharov, P. Werner, G. Gerth, U. Gösele, G. Cirlin, V. A. Egorov, B. V. Volovik, N. N. Ledentsov, V. M. Ustinov**  
Structure and optical properties of periodic submonolayer insertions of Ge in Si grown by MBE

12:35-14:10 **LUNCH TIME**

### **SESSION 3. OTHER OPTICAL METHODS**

**Chair : Wang Zhanguo**

- 14:10 S3-1 **Jean-Pierre LANDESMANN**  
**Invited** Micro-PL for the visualisation of defects, stress and temperature profiles in high-power III-V's devices
- 14:50 S3-2 **Xiaoling Ye, Yonghai Chen, Bo Xu, Z. G. Wang**  
Detection of Indium segregation effects in InGaAs/GaAs quantum wells using reflectance-difference spectrometry
- 15:05 S3-3 **M. R. Islam, Prabhat Verma, M. Yamada, S. Kodama, Y. Hanaue, and K. Kinoshita**  
The influence of residual strain on Raman scattering in  $\text{In}_x\text{Ga}_{1-x}\text{As}$  single crystals
- 15:20 S3-4 **M. Ardila, O. Martínez, M. Avella, J. Jiménez, E. Gil-Lafon, B. Gérard**  
Study of defects in conformal GaAs/Si layers by optical techniques and photoetching
- 15:35 S3-5 **P. J. Wellmann, R. Weingärtner, M. Bickermann, T. L. Straubinger, and A. Winnacker**  
Optical quantitative determination of doping levels and their distribution in SiC

15:50-16:20 **COFFEE BREAK**

- 16:20 S3-6 P. C. Montgomery, A. Benatmane, J. P. Ponpon, and E. Fogarassy  
Large area, high resolution measurement of surface roughness of semiconductors using interference microscopy
- 16:35 S3-7 Kazuo Moriya  
Inspection of Si wafer by Laser Scattering Topography

#### SESSION 4. NANOSCANNING TECHNIQUES

*Chair : Baeumler Martina*

- 16:50 S4-1 Christoph LIENAU, Francesca Intonti, Tobias Günther,  
**Invited** Valentina Emiliani, and Thomas Elsaesser  
Temporally- and spectrally resolved near-field optics of semiconductor nanostructures
- 17:30 S4-2 P. Tománek, M. Benelová, P. Dobis, L. Grmela  
Near field photoluminescence and photoreflectance measurements of semiconductor structures
- 17:45 S4-3 I. Goldfarb and G. A. D. Briggs  
Analysis of complex heterogeneous surfaces by scanning tunneling microscopy/spectroscopy and surface electron diffraction
- 18:00 S4-4 Masamichi Yoshimura, Mitsumasa Odawara, and Kazuyuki Ueda  
Atomic defects generated by hydrogen on Si (110) surface as revealed by scanning tunneling microscopy
- 18:15 S4-5 S. Selci, M. Righini, G. Latini  
STM topography and barrier imaging of InAs/GaAs dots

18:45-20:00 **POSTER SESSION 1**  
**POSTERS P1-01 to P1-54**

20:00 **DINNER**

**WEDNESDAY 26 SEPTEMBER, 2001**

#### SESSION 5. DEFECTS IN SILICON 1

*Chair : Cavallini Anna*

- 8:30 S5-1 G. BORIONETTI  
**Invited** A review of in line/off line defect characterization techniques applied to control and improve electronic grade silicon wafer manufacturing processes

- 9:10 S5-2 **T. Matsumoto, Y. Yamanaka and N. Inoue**  
Infrared absorption measurement of nitrogen in CZ-Si crystal
- 9:25 S5-3 **Kazuhiko Kashima, Hiroyuki Fujimori, Yumiko Hirano and Hiroshi Shirai**  
Behaviors of oxygen precipitation in D-like defect zone and ring-OSF zone in nitrogen-doped CZ silicon single crystals
- 9:40 S5-4 **R. Krause-Rehberg, F. Börner, F. Redmann, J. Gebauer, R. Kögler, W. Skorupa, P. Sperr, W. Triftshäuser**  
The microscopic nature of gettering defects at  $R_p/2$  in high-energy self-implanted silicon
- 9:55 S5-5 **T. Hirose, T. Shano, R. Kim, H. Tsuji, Y. Kamakura, and K. Taniguchi**  
Atomic configuration study of implanted F in Si based on experimental evidences and ab-initio calculations

10:10-10:40 **COFFEE BREAK**

## **SESSION 6. CONTACTLESS TECHNIQUES**

***Chair : Yamada Masayoshi***

- 10:40 S6-1 **Dieter K. SCHRODER**  
**Invited** Contactless Surface Charge Semiconductor Characterization
- 11:20 S6-2 **Piotr Edelman, Jacek Lagowski, Alexandre Savtchouk, Marshall Wilson, Andrey Aleynikov and Joaquin Navarro**  
Full wafer non-contact mapping of electrical properties of ultra-thin advanced dielectrics on Si
- 11:35 S6-3 **O. Palais, E. Yakimov and S. Martinuzzi**  
Minority carrier lifetime scan maps applied to iron concentration mapping in silicon wafers
- 11:50 S6-4 **V. Raineri and F. Giannazzo**  
Scanning Capacitance Microscopy on semiconductor materials
- 12:05 S6-5 **G. Citarella, S. von Aichberger and M. Kunst**  
Microwave photoconductivity techniques for the characterization of semiconductors

12:20-14:00 **LUNCH TIME**

## **14:00-15:15 POSTER SESSION 2**

**POSTERS P2-01 to P2-56**

## **SESSION 7. DEFECTS IN SILICON 2**

**Chair : Martinuzzi Santo**

- 15:15 S7-1 **E. SIMOEN and C. Claeys**  
**Invited** Random Telegraph Signals: a local probe for single point defect studies in solid-state devices
- 15:55 S7-2 **Tao Chu, Masayoshi Yamada, Joerg Donecker, Volker Alex, and Helge Riemann**  
Optical anisotropy and strain-induced birefringence of dislocation-free silicon single crystals
- 16:10 S7-3 **F. Nishihori, K. Kashima and M. Watanabe**  
Effect of germanium and boron co-doping during CZ-Si crystal growth
- 16:25 S7-4 **Kazutaka Terashima and Suzuka Nishimura**  
Annealing effect and impurity doping effects on the defect generation in interstitial-rich Si crystals observed by infrared microscope

16:40-17:10 **COFFEE BREAK**

## **SESSION 8. ELECTRON BEAM METHODS**

**Chair : Weyher Jan W.**

- 17:10 S8-1 **P. E. BATSON**  
**Invited** Direct Atomic Resolution Measurement of Electronic Structure Using EELS
- 17:50 S8-2 **H. S. Leipner, H. Lei, N. Engler**  
Agglomeration of point defects at dislocations in compound semiconductors
- 18:05 S8-3 **Alexander Satka, Daniel Donoval**  
Frequency-domain EBIC method for mapping of noise and instability regions in semiconductor devices
- 18:20 S8-4 **T. Sekiguchi, S. Ito and A. Kanai**  
Cathodoluminescence and EBIC study of twist and tilt boundaries in bonded silicon wafers

## **SESSION 9. ELECTRICAL METHODS**

**Chair : Blunt Roy**

- 18:35 S9-1 **K. IRMSCHER**  
**Invited** Electrical properties of SiC: characterisation of bulk crystals and epilayers
- 19:15 S9-2 **T. Wosinski, T. Figielski, A. Makosa, W. Dobrowolski, O. Pelya and B. Pécz**  
Quantum effects associated with misfit dislocations in GaAs-based heterostructures

- 19:30 S9-3 **B. Gründig, M. Jurisch, and J. R. Niklas**  
Defect specific topography of GaAs wafers by microwave- detected  
Photo Induced Current Transient Spectroscopy
- 19:45 S9-4 **M. Fukuzawa, M. Yoshida, M. Yamada, Y. Hanaue and K. Kinoshita**  
Non destructive measurement of resistivity in bulk  $\text{In}_x\text{Ga}_{1-x}\text{As}$  crystals
- 20:00 **DINNER**

## THURSDAY 27 SEPTEMBER, 2001

### SESSION 10. DEFECTS IN WIDE-GAP SEMICONDUCTORS

*Chair : Piqueras Javier*

- 8:30 S10-1 **D. CHERNS**  
**Invited** TEM characterisation of defects, strains and local electric fields in  
 $\text{AlGaIn}/\text{InGaIn}/\text{GaIn}$  structures
- 9:10 S10-2 **J. L. Weyher, H. W. Zandbergen, F. D. Tichelaar, L. Macht, P. Hageman**  
Complementary study of defects in GaN by photo-etching and TEM
- 9:25 S10-3 **M. Ahoujja, J. L. McFall, Y. K. Yeo, R. L. Hengehold, J. E. Van Nostrand**  
Electrical and optical investigation of MBE grown Si-doped  $\text{Al}_x\text{Ga}_{1-x}\text{N}$  as a function of Al mole fraction up to 0.5
- 9:40 S10-4 **N. Kamata, J. M. Zanardi Ocampo, W. Okamoto, K. Hoshino, T. Someya, Y. Arakawa and K. Yamada**  
Below-gap recombination dynamics in GaN revealed by time-resolved and two-wavelength excited photoluminescence
- 9:55 S10-5 **A. Castaldini, A. Cavallini, L. Polenta, N. Armani and G. Salviati**  
Electrical and optical properties of defects in proton-irradiated GaN epilayers

10:10-10:40 **COFFEE BREAK**

### SESSION 11. CATHODOLUMINESCENCE

*Chair : Sekiguchi Takashi*

- 10:40 S11-1 **U. JAHN**  
**Invited** Cathodoluminescence of  $(\text{Al,Ga})\text{As}$  and  $(\text{Al,Ga,In})\text{N}$  heterostructures grown by molecular beam epitaxy

- 11:20 S11-2 **S. M. Hubbard, D. Pavlidis, V. Valiaev, M. A. Stevens-Kalceff, I. M. Tiginyanu**  
Electrical Characterization and Cathodoluminescence Microanalysis of AlN/GaN Heterostructures
- 11:35 S11-3 **Toshivuki Isshiki, Hiroshi Saijo, Shigehiro Nishino, Makoto Shiojiri**  
Cathodoluminescence microscope observation of hollow caves induced in 6H-type SiC wafer
- 11:50 S11-4 **J. Schreiber, L. Höring, U. Hilpert**  
Dyn SEM CL of glide dislocations in GaAs and CdTe
- 12:05 S11-5 **A. Urbieta, Ch. Hardalov, P. Fernández, J. Piqueras and T. Sekiguchi**  
Cathodoluminescence and scanning tunneling spectroscopy of ZnO single crystals
- 12:20-13:40 **LUNCH TIME**
- 13:40 **EXCURSION TO URBINO**
- 20:00 **GALA DINNER**

## FRIDAY 28 SEPTEMBER, 2001

### SESSION 12. X-RAY TECHNIQUES

*Chair : Jiménez Juan*

- 9:00 S12-1 **N. HERRES, L. Kirste, H. Obloh, K. Köhler, J. Wagner, D. G. Ebling, P. Koidl**  
Invited  
X-ray diffractometry on (Al,Ga,In)-nitride layers
- 9:40 S12-2 **Bernd Jenichen, Vladimir M. Kaganer, Frank Schippan, Wolfgang Braun, Lutz Däweritz, and Klaus H. Ploog**  
Strain mediated phase coexistence in MBE-grown MnAs films on GaAs
- 9:55 S12-3 **I. Yonenaga, T. Taishi, X. Huang, K. Hoshikawa**  
X-ray topographic observation of dislocation generation at the seed/crystal interface of CZ-Si highly doped with impurities
- 10:10 S12-4 **C. Ferrari, G. Rossetto, E. A. Fitzgerald**  
Misfit dislocation and threading dislocation distributions in InGaAs and GeSi/Si partially relaxed heterostructures
- 10:25-10:50 **COFFEE BREAK**



### SESSION 13. MISCELLANEOUS TECHNIQUES

*Chair : Jenichen Bernd*

- 10:50 S13-1 Maya KISKINOVA  
**Invited** Scanning photoelectron microscopy and its application in characterisation of semiconductor interfaces
- 11:30 S13-2 Wei-Yuan Ting, Adrian H. Kitai, and Peter Mascher  
Crystallization Phenomena in  $\beta$ -Ga<sub>2</sub>O<sub>3</sub> Investigated by Positron Annihilation Spectroscopy
- 11:45 S13-3 N. Konofaos, C. T. Angelis, E. K. Evangelou, N. A. Hastas, Y. Panayiotatos, C. A. Dimitriadis, S. Logothetidis  
The effects of interface and bulk defects on the electrical performance of amorphous carbon/silicon heterojunctions
- 12:00 S13-4 R. Cantelli, F. Cordero, O. Palumbo, F. Trequattrini, B. Molinas and G. M. Guadalupi  
Anelastic Spectroscopy as a Probe for the Structure and Dynamics of Defects in Semiconductors
- 12:15 S13-5 A. Gasparotto, T. Cesca, N. El Habra, B. Fraboni, F. Boscherini, F. Priolo, E.C. Moreira, G. Ciatto, G. Scamarcio  
Implant and characterization of highly concentrated Fe deep centers in InP

12:30-13:50 **LUNCH TIME**

### SESSION 14. DEFECTS IN DEVICES

*Chair : Yonenaga Ichiro*

- 13:50 S14-1 Tsuguru SHIRAKAWA  
**Invited** Effect of defects on the degradation of ZnSe-based white LEDs
- 14:30 S14-2 A. Gerhardt, J. W. Tamm, A. Bärwolff, J. Donecker  
Measurement of mounting-induced and grown-in strain in high-power laser diodes using Fourier-transform photo-current spectroscopy
- 14:45 S14-3 J. P. Bergman and E. Janzén  
Optical mapping of defects in SiC
- 15:00 S14-4 J. P. Rakotoniaina, O. Breitenstein, M. Langenkamp  
Localization of Weak Heat Sources in Electronic Devices Using Highly Sensitive Lock-in Thermography
- 15:15 S14-5 M. Bettiati, C. Starck, M. Pommies, N. Broqua, G. Gelly, M. Avella, J. Jiménez, I. Asaad, B. Orsal, J. M. Peransin  
Gradual degradation in 980 nm InGaAs/AlGaAs pump lasers

15:30-15:45 **CLOSING CERIMONY**



# FT-IR Spectroscopy

## The Complete Spectrometer Line

### VECTOR 22/33

Compact, robust and affordable FT-IR spectrometer for "routine" analytical applications without compromising performance and reliability. The intuitive OPUS™ software package provides an easy approach to FT-IR. The VECTOR 33 offers quick range extension to the near IR.

### VECTOR 22/N

A series of FT-NIR spectrometers for rapid and reliable QA/QC work and process monitoring. A wide range of fiber optic probes and sampling accessories are available.

### MATRIX

An industry hardened FT-NIR system for process monitoring and control. All components are adapted to 19" rack geometry. Several standard formats for communication with process control systems are offered.

### RFS 100/S, FRA 106/S

Stand-alone RFS 100/S FT-Raman spectrometer for fluorescence-free Raman measurements in the NIR spectral range. The **FRA 106/S** FT-Raman module is an externally adapted option for BRUKER FT-IR spectrometers.

### EQUINOX 55

Versatile FT-IR spectrometer for demanding analytical application with rapid and step scan option, automated sample changers, hyphenated techniques such as TGA/GC/LC-IR and IR-microscope with the new focal plane array (FPA) HYPERION detector for IR-imaging.

### IFS 66/S, IFS 66v/S

For challenging measurement problems in R&D. Ultra fast rapid and step scan for kinetic and signal modulated time resolved experiments. The IFS 66v/S offers high sensitivity and moisture free spectra ranging from the very far IR up to the UV by use of vacuum optics.

### IFS 120HR

Highest resolution (better than  $0.001 \text{ cm}^{-1}$ ) research spectrometer for measurement on single crystals at low temperature and on gas phase samples. The IFS 120M is designed for mobile studies of constituents in the upper atmosphere.

---

#### In Europe:

Bruker Optik GmbH  
Rudolf-Plank-Str. 23, D-76275 Ettlingen  
Tel.: ++49 7243 504 600, Fax: -698  
Email: [optik@bruker.de](mailto:optik@bruker.de)  
[www.bruker.de/optik](http://www.bruker.de/optik)

---

#### In North America:

Bruker Optics Inc  
19 Fortune Drive, Manning Park, Billerica  
MA 01821 - 3991 USA  
Tel.: ++1 978 439 - 9899, Fax: - 663 - 9177  
Email: [optics@bruker.com](mailto:optics@bruker.com)  
[www.brukeroptics.com](http://www.brukeroptics.com)

## POSTER SESSION 1

**Tuesday 25 September, 2001**

**18:45 - 20:00**

### *P1 - A : DEFECTS IN WIDE GAP SEMICONDUCTORS*

- P1-01**    **M. Bosi, R. Fornari, N. Armani**  
Effects of thermal annealing on GaN epilayers deposited on (0001) sapphire
- P1-02**    **C. Grazzi, H. P. Strunk**  
Structure and optical properties of epitaxial gallium nitride layers
- P1-03**    **E. Zielinska-Rohozinska, M. Regulska, V. S. Haroutyunian, K. Pakula**  
High resolution X-ray diffraction defect structure characterization in Si doped and undoped GaN films
- P1-04**    **R. Paszkiewicz, B. Paszkiewicz, J. Kozlowski, M. Tlaczala**  
Correlation between crystallographic structure and electrical characteristic of (Al,Ga)N epitaxial layers grown by MOVPE method
- P1-05**    **A. Cremades and J. Piqueras**  
Study of carrier recombination at structural defects in InGaN films
- P1-06**    **J. Skriniarová, A. van der Hart, H. P. Bochem, P. Kordos**  
Photoenhanced wet chemical etching of n+-doped GaN
- P1-07**    **Junyong Kang, Yaowen Shen, Zhanguo Wang**  
Effects of residual C and O impurities on luminescence in undoped GaN epilayers
- P1-08**    **L. Ottaviani, M. Lazar, M. L. Locatelli, V. Heera, W. Skorupa, M. Voelskow, J. P. Chante**  
Annealing studies of Al-implanted 6H-SiC in an induction furnace

### *P1 - B : DEFECTS IN SILICON*

- P1-09**    **O. González-Varona, B. Garrido, A. Pérez-Rodríguez, J. R. Morante, C. Bonafos, M. Carrada, L. F. Sanz, M. A. González, J. Jiménez**  
Analysis of the white emission from ion beam synthesised layers by in depth resolved scanning photoluminescence microscopy
- P1-10**    **Y. Tokuda, T. Murase, T. Namizaki, T. Hasegawa and H. Shiraki**  
Hydrogen introduction into p+ silicon by boiling in water and its application to deep-level transient spectroscopy measurements
- P1-11**    **Yoshimori Ishizuka, Takayuki Uchihashi, Haruhiko Yoshida, and Seigo Kishino**  
Electrical characterization of SOI wafers at sub-micron scale by scanning capacitance microscopy

- P1-12**     **Shiho Sasaki, Tomio Izumi and Tohru Hara**  
Delamination of Si by high dose H-ion implantation through thin SiO<sub>2</sub> film (ESR characterization)
- P1-13**     **Minya Ma, Cesare Frigeri, Toshiharu Irisawa and Tomoya Ogawa**  
Analysis of extended defects in CZ silicon annealed in either oxygen or nitrogen by optical and electron beams methods
- P1-14**     **Kovacsics Csaba**  
Reflection mode scanning infrared microscope (SIRM) and its applications to defect detection in silicon
- P1-15**     **I. Ohkubo, T. Mikayama, H. Harada and N. Inoue**  
Analysis on localized vibration of nitrogen in silicon
- P1-16**     **Y. Kamiura, K. Fukuda, Y. Iwagami, Y. Yamashita and T. Ishiyama**  
Comparative Study of the Electronic States and Atomic Configurations of Two H-Related (H-C and Pt-H<sub>2</sub>) Complexes in Silicon
- P1-17**     **N. A. Sobolev, E. M. Emel'yanov, E. I. Shek, V. I. Vdovin, T. G. Yugova, S. Pizzini**  
Structural defects and dislocation-related photoluminescence in Erbium-implanted silicon
- P1-18**     **S. Saramad, A. Moussavi-Zarandi**  
Study of the effect of clustered defects on macroscopic behaviour of hadron irradiated silicon detectors
- P1-19**     **A. Fedotov, A. Mazanik, K. Enisherlova**  
The electrical characterization of interface in the unitive directly-bonded silicon wafers
- P1-20**     **N. Yu. Arutyunov and V. Yu. Trashchakov**  
Positron as a microprobe of oxygen-related "as-grown" defects in Si and 1D-ACAR spectroscopy
- P1-21**     **V. A. Stuchinsky, G. N. Kamaev, K. Yu. Khoroshilov, V. V. Bolotov, Yu. A. Sten'kin**  
Further development of electrical characterization method for unipolar semiconductor/semiconductor junctions and its application to studying the effect of gamma-irradiation on directly bonded p-Si/p-Si structures
- P1-22**     **B. Zebentout, Z. Benamara, H. Sehil, H. Dib, T. Mohammed-Brahim**  
Study of grain boundary effect on photovoltaic parameters in polycrystalline silicon homojunction pin solar cells

#### *P1 - C : DEFECTS IN COMPOUND SEMICONDUCTORS*

- P1-23**     **G. Kowalski, I. Frymark, A. Krotkus, K. Bertulis, M. Kaminska**  
On the properties of the Be-doped low temperature MBE GaAs layers
- P1-24**     **R. Mosca, P. Bussei, S. Franchi, P. Frigeri, E. Gombia, A. Carnera, M. Peroni**  
Modelling of Be diffusion in GaAs layers grown by MBE

- P1-25** A. Tukiainen, J. Dekker, T. Leinonen, and M. Pessa  
Characterization of deep levels in rapid thermal annealing treated AlGaInP
- P1-26** E. Gombia, R. Mosca, S. Amighetti, C. Ghezzi, P. Frigeri, S. Franchi  
Electrical characterization of self-assembled InAs/GaAs quantum dots by capacitance techniques
- P1-27** A. T. Gorelenok, V. F. Andrievskii, A. V. Kamanin, S. I. Kohanovskii, M. M. Mezdrogina and N. M. Shmidt  
Peculiarities of defect and impurity behavior in gallium arsenide after surface gettering
- P1-28** W. Siegel, A. Sidelnicov and G. Kühnel  
Electrical studies in the micro-environment of dislocations in undoped high-resistivity GaAs
- P1-29** Th. Steinegger, B. Gründig, M. Baeumler, M. Jurisch, W. Jantz, and J. R. Niklas  
Photoluminescence Topography, PICTS and Microwave Conductivity Investigation of EL6 in GaAs
- P1-30** P. Kaminski and R. Kozlowski  
High-resolution photoinduced transient spectroscopy as a new tool for quality assessment of semi-insulating GaAs
- P1-31** M. Herms, G. Goerigk, G. Irmer, E. Bedel, and A. Claverie  
Precipitation in low temperature grown GaAs
- P1-32** K. Sivaji, C. S. Sundar, G. Amarendra, S. Sankar, P. Jayavel and V. Ravichandran  
2D-ACAR studies of high energy swift heavy ion implanted GaAs
- P1-33** K. D. Chtcherbatchev, A. D. Sequeira, N. Franco, N. Barradas, M. Myronov, O. A. Mironov, E. H. C. Parker  
Application of High-Resolution X-ray Diffraction techniques to study strain status in  $\text{Si}_{1-x}\text{Ge}_x/\text{Si}_{1-y}\text{Ge}_y/\text{Si}$  (001) heterostructures
- P1-34** Chtcherbatchev K.D.  
Reconstruction of depth strain profile in ion-doped structures from High-Resolution X-ray Diffraction data using fitting procedure based on genetic algorithm
- P1-35** R. Singh, S. K. Arora, J. P. Singh, Renu Tyagi, S. K. Agarwal and D. Kanjilal  
Effect of 200 MeV  $^{107}\text{Ag}^{14+}$  ion irradiation on the electrical characteristics of Ni/n-GaAs epitaxial Schottky diode
- P1-36** K. Zdansky and O. Procházková  
P-type InP grown by LPE from melts with rare earth admixtures
- P1-37** O. Procházková, K. Zdansky, J. Zavadil  
Preparation of InP-based semiconductor materials with low density of defects: Effect of Nd, Tb and Yb addition
- P1-38** V. Corregidor, V. Babentsov, E. Dieguez, T. Feltgen, M. Fiederle, K. Benz  
Study of high resistivity CdTe based material by PL and IR absorption

- P1-39**     **J. L. Plaza, P. Hidalgo, B. Méndez, J. Piqueras and E. Diéguez**  
Study of the defect structure, compositional and electrical properties of  $\text{Er}_2\text{O}_3$ -doped n-type GaSb:Te crystals grown by the vertical Bridgman technique
- P1-40**     **V. Rakovics, S. Püspöki, J. Balázs, I. Réti, and C. Frigeri**  
Spectral characteristics of InP/InGaAsP Infrared Emitting Diodes grown by LPE
- P1-41**     **V. Rakovics, A. L. Tóth, B. Pödör, C. Frigeri, J. Balázs, and Z. E. Horváth**  
LPE growth and characterization of  $\text{In}_x\text{Ga}_{1-x}\text{As}_y\text{Sb}_{1-y}$  quaternary alloys
- P1-42**     **E. P. Skipetrov, N. A. Chernova, L. A. Skipetrova and E. I. Slyn'ko**  
Electric and magnetic characterization of impurity-induced states in diluted magnetic semiconductor  $\text{Pb}_{1-y}\text{Yb}_y\text{Te}$
- P1-43**     **E. P. Skipetrov, E. A. Zvereva, O. S. Volkova, E. I. Slyn'ko, A. M. Mousalitin**  
On Fermi level pinning in lead telluride based alloys doped with mixed valence impurities
- P1-44**     **B. Pavlyk, B. Tsybulyak**  
Evolution of metastable centers on the CdS surface stimulated by temperature decrease

#### ***PI - D : METHODS AND TECHNIQUES***

- P1-45**     **Hiroshi Saijo, Toshiyuki Isshiki, Giuseppe Pezzotti, Shigehiro Nishino and Makoto Shiojiri**  
Detection of hidden electronic states in semiconductors by multi-band cathodoluminescence electron microscopy
- P1-46**     **M. Nazarov**  
Cathodoluminescence defectoscopy of II-VI compounds
- P1-47**     **V. M. Popov, A. S. Klimenko, A. P. Pokanevich**  
Investigation of electrically active defects in Si-based semiconductor structures
- P1-48**     **H. Väinölä, J. Storgårds, M. Yli-Koski and J. Sinkkonen**  
Effect of light induced change in built-in potential on carrier lifetime in epitaxial wafers
- P1-49**     **V. V. Sirotkin and E. B. Yakimov**  
Computer simulation of excess carrier distribution for the phase shift microwave detected photoconductivity technique
- P1-50**     **E. I. Rau and J. Wernisch**  
Correlation between BSE energy and X-ray spectra of multilayered microelectronics structures

#### ***PI - E : MISCELLANY***

- P1-51**     **C. Scholz, K. Boucke, R. Poprawe**  
Investigation of indium solder interfaces for high-power diode lasers

- P1-52**    **J. Arbiol, F. Peiró, A. Cornet, J. R. Morante, J. A. Pérez-Omil and, J. J. Calvino**  
Computer Image HRTEM Simulation of Catalytic Nanoclusters on Semiconductor Gas Sensor Materials Supports
- P1-53**    **O. I. Shpotyuk and J. Filipecki**  
Radiation-induced point defects in vitreous chalcogenide semiconductors studied by positron annihilation method
- P1-54**    **H. Tabet-Derraz, N. Benramdane, D. Nacer, A. Bouzidi, M. Medles**  
Investigations on  $Zn_xCd_{1-x}O$  Thin Films Obtained by Spray Pyrolysis

## POSTER SESSION 2

**Wednesday 26 September, 2001**

**14:00 - 15:15**

### *P2 - A : DEFECTS IN WIDE GAP SEMICONDUCTORS*

- P2-01**    **A. Castaldini, A. Cavallini, L. Polenta and C. Diaz-Guerra**  
Characterization of thin films of n- and p-type GaN
- P2-02**    **Junyong Kang, Shin Tsunekawa, Shun Itoh**  
Precipitates in AlGaIn epilayers grown by metallorganic vapor phase epitaxy
- P2-03**    **G. Nowak, R. Czerwinski, M. Leszczynski, I. Grzegory**  
Removal of defects formed due to micro-masking on Ga-polar surface of GaN single crystals after reactive ion etching
- P2-04**    **R. Srnanek, A. Vincze, J. Kovac, I. Gregora, V. Gottschalch**  
A Raman study of GaAsN, GaInAsN layers on beveled samples
- P2-05**    **M. Senthil Kumar, D. Kanjilal and J. Kumar**  
Effect of high energy nitrogen irradiation in GaN
- P2-06**    **E. Zielinska-Rohozinska, M. Regulska, K. Pakula, J. M. Baranowski, A. Kasinska**  
High resolution x-ray diffraction investigations of thin  $Al_xGa_{1-x}N$  films

- P2-07**     **A. M. Strel'chuk, N. S. Savkina, A. N. Kuznetsov, A. A. Lebedev, A. S. Tregubova**  
 Characterization of p-n structures grown by sublimation heteroepitaxy of 3C-SiC on 6H-SiC
- P2-08**     **N. Savkina, A. Tregubova, M. Scheglov, G. Mosina, L. Sorokin, V. Solov'ev, A. Volkova, A. Lebedev**  
 Characterization of 3C-SiC epilayers grown on 6H-SiC substrates by vacuum sublimation

***P2 - B : DEFECTS IN SILICON***

- P2-09**     **T. Okumura, A. En, K. Eguchi and M. Suhara**  
 Contactless Characterization of Surface and Interface Band-bending in Silicon-On-Insulator (SOI) Structures
- P2-10**     **A. Castaldini, D. Cavalcoli, A. Cavallini, M. Rossi**  
 Scanning Kelvin probe and surface photovoltage analyses of polycrystalline silicon
- P2-11**     **Nobuya Takabatake, Takeshi Kobayashi, Yoshiyuki Show, and Tomio Izumi**  
 Photoacoustic (PA) evaluation of defects and thermal conductivity in the surface layer of ion implanted semiconductor
- P2-12**     **G. Citarella, O. Abdallah and M. Kunst**  
 The optoelectronic characterization of the silicon/silicon nitride interface
- P2-13**     **L. V. Antonova**  
 Extraction of parameters of deep centers and interface traps in SOI structures by using DLTS measurements
- P2-14**     **M. V. Zamoryanskaya, V. I. Sokolov, I. M. Kotina**  
 Cathodoluminescence of thin films of silicon oxide on silicon
- P2-15**     **B. M. Efros, A. Misiuk, N. V. Shishkova, A. M. Prudnikov**  
 Application of gasketed diamond anvil cell for optical and spectroscopical study of semiconductors under pressure
- P2-16**     **B. Efros, N. Shishkova, A. Misiuk and A. Prudnikov**  
 DAC optical absorption studies of the Si-O (SiO<sub>2-x</sub>) semiconductor system
- P2-17**     **Jinggang Lu, Deren Yang, Luixin Fan, Xiangyang Ma, Liben Li, Duanlin Que**  
 The impacts of nitrogen on power diodes characteristics
- P2-18**     **Sobolev N. A.**  
 Characterization of structural, electrical and optical properties of rare-earth doped Si-based light emitting diodes
- P2-19**     **V. Bondarenko, V. Yakovtseva, L. Dolgyi, M. Balucani, G. Lamedica and A. Ferrari**  
 X-ray diffractometry of Si epilayers grown on porous silicon



- P2-20**     **C. Bocchi, F. Germini, E. Kh. Mukhamedzhanov, L. Nasi, V. Privitera and C. Spinella**  
Damage profiles determination in ultra-shallow implantated Si by triple crystal x-ray diffraction
- P2-21**     **T. Baumbach, L. Helfen, P. Pernot, M. Herms, C. Landesberger, and G. Schwinn**  
Characterization of ultrathin wafers by X-ray topography and micrometer-resolved area diffraction
- P2-22**     **K. Sivaji, C. S. Sundar, R. Rajaraman, Padma Gopalan, S. Sankar and V. Ravichandran**  
2D-ACAR studies of microstructure characteristics of porous silicon

#### ***P2 - C : METHODS AND TECHNIQUES***

- P2-23**     **V. A. Stuchinsky**  
DLTS-analysis of kinetics of charge-carrier capture by dense planar array of deep traps
- P2-24**     **Rau E. I.**  
Comparison of the scanning electron microscopy methods of semiconductors: SEBIV, SEAM, SCEBIC
- P2-25**     **E.I. Rau, E.B. Yakimov**  
Determination of diffusion length and surface recombination velocity by the surface electron beam induced voltage method
- P2-26**     **V. Sirotkin, S. Zaitsev, E. Yakimov**  
Multi-electrode LBIC method for characterization of 1D "hidden" defects
- P2-27**     **J. Ph. Piel, A. Dubois, L. Vabre, P. Boher, L. Escadafals, R. Tirmarche, A. C. Boccara, J. L. Stehlé**  
Optical profilometry applied to the characterization of surfaces in the microelectronic field
- P2-28**     **F. Corni, R. Tonini, G. Pavia, G. Queirolo, R. Zonca**  
In-situ time-resolved reflectivity: a technique useful for solid-state transformations
- P2-29**     **Ma. Bouloudenine, D.E. Mekki and R.J. Tarento**  
Effect of minority charge carrier lifetime general form on EBIC – Case of Au-nSi Schottky diode

#### ***P2 - D : DEFECTS IN COMPOUND SEMICONDUCTORS***

- P2-30**     **K. Wieteska, W. Wierzchowski, W. Graeff, M. Lefeld-Sosnowska, M. Regulska**  
Studies of growth bands in Si:Ge crystals
- P2-31**     **A. A. Podolyan and O. A. Korotchenkov**  
Acoustic-wave effects on space charge defect states in SiGe heterostructures

- P2-32**     **O. A. Korotchenkov and D. S. Kim**  
 Ultrasonic manipulation of bound exciton luminescence in GaAs quantum wells
- P2-33**     **M. Righini, F. Fernández-Alonso, A. D'Andrea, D. Schiumarini, S. Selci and N. Tomassini**  
 Spontaneous quantum dot formation at  $\text{In}_x\text{Ga}_{1-x}\text{As}/\text{In}_y\text{Ga}_{1-y}\text{GaAs}$  interfaces
- P2-34**     **G. A. Lyubas, V. V. Bolotov**  
 Polarization resolved-photoluminescence for study of GaAs/AlAs interfaces in corrugated and flat ultra-short-period superlattices
- P2-35**     **V. V. Bolotov, V. A. Sachkov**  
 The investigation of quantum islands structures on (001) GaAs surface at submonolayer MBE growth from calculation of phonon spectrum
- P2-36**     **O. Martínez, M. Avella, A. M. Ardila, J. Jiménez, B. Gérard and M. Philippens**  
 Properties of AlGaAs layers grown on Si by the Conformal method
- P2-37**     **M. D. Efremov, V. A. Volodin, V. A. Sachkov, V. V. Preobrazhenski, B. R. Semyagin**  
 Raman investigation of interface atomic reconstructions in GaAs/AlAs superlattices grown on (100) substrates
- P2-38**     **M. D. Efremov, V. A. Volodin, V. A. Sachkov, V. V. Preobrazhenski, B. R. Semyagin, N. N. Ledentsov, V. M. Ustinov, I. P. Soshnikov, D. Litnikov, D. Gerthsen**  
 Influence of disorder on Raman spectra of GaAs quantum wires grown with partial filling of corrugated (311)A AlAs surfaces
- P2-39**     **Vincenzo Grillo, Laura Lazzarini, Thilo Remmele**  
 On the morphology and composition of InAs/GaAs quantum dots
- P2-40**     **C. Pelosi, G. Attolini, S. Scardova, F. Germini, O. Martinez, L. F. Sanz, M. A. Gonzales, J. Jimenez**  
 Optical and structural characterization of LP MOVPE grown lattice matched GaInP/GaAs heterostructures
- P2-41**     **V. Eremenko, L. Gonzalez, Y. Gonzalez, V. Vdovin, L. Vazquez, G. Aragon, M. Herrera and F. Briones**  
 AFM and TEM study of the lateral composition modulation in the etched and photoetched  $\text{In}_x\text{Ga}_{1-x}\text{P}$  epitaxial layers
- P2-42**     **P. Jayavel, K. Santhakumar and J. Kumar**  
 Investigations of swift heavy ion implantation on semi-insulating GaAs
- P2-43**     **S. K. Guba, S. I. Krukovsky, A. B. Smirnov, A. I. Vlasenko**  
 Improvement of the parameters of devices on the base of GaAs epilayers by isovalence doping by liquid phase epitaxy
- P2-44**     **M. Kaniewska and K. Klima**  
 Investigations on surface defects of GaAs grown by Molecular Beam Epitaxy
- P2-45**     **Bobrovnikova I. A., Lavrentieva L. G., Ivonin I. V., Subach S. V., Vilisova M. D., Preobragenski V. V., Putjato M. A., Semjagin B. R.**  
 Doping and impurity defect formation in epitaxial GaAs

- P2-46**     **V. A. Gnatyuk**  
Transformation of defect structure and electrophysical properties of III-V semiconductors by pulsed laser irradiation
- P2-47**     **D. Korytar, P. Bohacek, C. Ferrari, B. Surma, F. Dubecky, J. Huran, B. Zatkó, V. Smatko, R. Fornari and S. Strzelecka**  
Correlation of crystal defects and galvanomagnetic parameters of semi-insulating InP with performance of radiation detectors fabricated from characterized materials
- P2-48**     **Youwen Zhao, Niefeng Sun, Hongwei Dong, Jinghua Jiao, Jianqun Zhao, Zhengping Zhao, Tongnian Sun and Lanying Lin**  
Characterization of defects and whole wafer uniformity of annealed undoped semi-insulating InP wafers
- P2-49**     **K. Jarasiunas, N. Lovergine**  
Characterization of bulk crystals and structures by light-induced transient grating technique
- P2-50**     **N. Armani, C. Ferrari, G. Salviati, F. Bissoli, M. Zha, L. Zanotti**  
Crystal defects and optical transitions in high purity, high resistivity CdTe for device applications
- P2-51**     **V. Corregidor, E. Saucedo, L. Fornaro, E. Diéguez**  
Defects in CdTe films doped with Zn and Ge
- P2-52**     **A. Baidullaeva, O. I. Vlasenko, P. O. Mozol'**  
Behaviour of defects in ZnSe crystals at laser shock wave passage
- P2-53**     **D. Sugak, A. Matkovskii, A. Durygin, A. Suchocki, P. Potera**  
Transient and stable absorption of radiation induced defects in oxide crystals
- P2-54**     **S. V. Belyaev, G. I. Zhovnir, S. A. Sypko**  
Surface states of  $\text{Cd}_{1-x}\text{Zn}_x\text{Te}$  crystals
- P2-55**     **M. M. Pociask, E. M. Sheregii**  
Heterojunction and periodical structures in MCT solid solution: the results of laser annealing
- P2-56**     **Pavel Y. Pak, Valeriy V. Shashkin**  
Using spatially resolved techniques for investigating defects through HgCdTe IR FPA technological process



**September 25, 9:00 - 10:25**

**Session 1**

**Photoluminescence 1**





**Spatially-resolved and polarisation-resolved photoluminescence  
for study of  
dislocations and strain in III-V materials**

**Daniel T. Cassidy**

**McMaster University  
Department of Engineering Physics  
Hamilton, Ontario, Canada  
L8S 4L7  
cassidy@mcmaster.ca  
voice: (905) 525-9140 ext 24565  
FAX: (905) 527-8409**

Unstrained III-V material has a cubic structure and, owing to symmetry, the probabilities of light being emitted with polarisation along or perpendicular to a selected direction are equal. Mechanical strain, in general, reduces the symmetry of III-V material and the probabilities of light being emitted with polarisation along or perpendicular to a selected direction are not necessarily equal. Thus the strain in III-V material can be deduced from measurement of the degree of polarisation (DOP) of luminescence. We take the DOP to be  $(L_{xx} - L_{yy})/(L_{xx} + L_{yy})$  for light that is propagating in the  $z$  direction, where  $z$  is a normal to the surface of the material under study, and  $L_{xx}$  and  $L_{yy}$  are the powers of the luminescence that are polarised in the  $x$  and  $y$  directions. We find the DOP to be equal to, under the assumption of isotropic material,  $-K_e(\epsilon_{xx} - \epsilon_{yy})$  where  $K_e$  is a positive constant of calibration, and  $\epsilon_{xx}$  and  $\epsilon_{yy}$  are the components of strain along the  $x$  and  $y$  directions.

Measurement of the DOP is fast (there is no need to resolve spectrally the light) and the DOP is a sensitive function of strain. Thus maps of the DOP of luminescence can be made in reasonable time with a spatial resolution of the order of  $1\ \mu\text{m}$  and a noise level equivalent to a strain of approximately  $10^{-5}$ .

Dislocations create characteristic strain fields. The type, direction, and Burgers vector of dislocations near the surfaces of luminescent III-V material can be determined by matching measured patterns of DOP with predicted patterns that are based on the characteristic strain fields of dislocations. In addition, strain and strain patterns for defects, quantum wells, interfaces, and steps of fabrication in luminescent III-V devices and materials can be imaged and investigated by analysis of the DOP of luminescence.

## 2K PL Topography of Silicon doped VGF GaAs wafers

**M. Baeumler, M. Maier, W. Jantz**

Fraunhofer Institut Angewandte Festkörperphysik, Tullastr. 72, 79108 Freiburg, Germany  
Tel. +49 761 5159 511 Fax. +49 761 5159 423 e-mail: martina.baeumler@iaf.fhg.de

**Th. Bünger, J. Stenzenberger**

Freiberger Compound Materials GmbH, Am Junger Löwe Schacht 5, 09599 Freiberg, Germany

The vertical gradient freeze (VGF) growth technique is utilized to produce semiconducting Si doped GaAs substrates. Very low dislocation density (typically  $< 500 \text{ cm}^{-2}$ ) is obtained, resulting in improved performance and reliability of laser and high brightness light emitting diodes. A homogeneous distribution of the dopant and carrier concentrations is also desired and is achieved by appropriate control of VGF process parameters.

Laterally resolved photoluminescence topography (PLT) is an established analytic technique to assess the macroscopic lateral homogeneity of substrates and to study localized variation patterns. The predicative capability of PLT is significantly enhanced if the distribution of specific radiative centers can be imaged selectively, requiring that PLT is done at low temperature with high spectral resolution.

Four PL bands are observed in GaAs:Si and assigned as follows: <sup>1</sup>

Label	wavelength (nm)	transitions from conduction band and shallow donors to
A	832	shallow acceptors and valence band
B	922	$B_{As}^{-/-}$
C	1100	$Si_{Ga}-V_{Ga}$
D	1250	unidentified deep center

We report full wafer and magnified small area PLT investigations, recorded at these four wavelengths, of six VGF GaAs:Si wafers. The wavelength-specific images exhibit various correlations and anti-correlations. Analysis of these dependencies, supported by SIMS analysis, allows to distinguish between macroscopic and local fluctuations due to

- stoichiometric variations replicating the dislocation pattern
- stoichiometric variations due to growth inhomogeneities
- variations of the silicon and boron concentration.

The intensity variations will be discussed with respect to competitive radiative and non-radiative recombination processes. For example, if the Si concentration across the wafer is constant, as determined by SIMS, the intensity of transition A replicates the dislocation pattern, while the intensities of C and D show inverse contrast.

The anticorrelation of topograms recorded for shallow (A,B) and deep (C,D) centers is not observed if the Si content varies. We show that the relative intensity and high energy tail of line A can be related to variations of the Si concentration.

<sup>1</sup>M.Tajima, Inst. Phys. Conf. Ser. 149, 259 (1996)





## Sub-micron Scale Photoluminescence Images of Wide Bandgap Semiconductors by Cryogenic Scanning Optical Microscope

Masahiro Yoshimoto

Kyoto Institute of Technology, Department of Electronics and Information Science,  
Matsugasaki, Sakyo, Kyoto 606-8585, Japan.  
email: yoshimot@dj.kit.ac.jp, fax: +81-75-724-7400, phone: +81-75-724-7484

Microscopic photoluminescence (micro-PL) measurements using a conventional optical system have been widely used in order to analyze local electronic structures of semiconductors and their devices. The spatial resolution ( $\Delta$ ) of a micro-PL equipment is determined by wavelength ( $\lambda$ ) of the light and the numerical aperture (NA) of the objective in the form of  $\Delta = 0.52 \lambda / \text{NA}$ . Using an available objective with the maximum NA of 0.95, the resolution becomes approximately one-half the wavelength of the observed light. The large value of NA improves the optical throughput of PL signal.

To surpass the diffraction limit, scanning near-field optical microscope (SNOM) has been extensively studied. While a high optical throughput was achieved in a SNOM equipment showing a resolution of approximately 100 nm, the optical throughput exponentially decreases with improving spatial resolution of SNOM. Although the spatial resolution is limited to one-half the wavelength of the observed light in the PL microscope using a conventional optical system, it has an advantage in terms of the high optical throughput with simple configuration and procedure.

Micro-PL measurements with the sub-micron resolution at room temperature have been already realized using a high-resolution objective with a large NA. In micro-PL measurements at a low temperature using a conventional objective, the sample is mounted inside a cryostat, and an objective or a focusing device is positioned outside the cryostat. The large working distance between the objective and the sample limits NA to a small value, resulting in a low spatial resolution in micro-PL measurements at a low temperature.

In this report, a new PL microscope has been developed to obtain a spatial resolution equal to one-half the wavelength of the observed light at a low temperature. The objective and sample were put in the identical vacuum chamber to ensure thermal insulation between them. The spatial resolution at 15 K was confirmed to be 300 nm at a wavelength of 488 nm, which is almost equal to the diffraction limit.

The PL microscope clearly discriminated PL emissions ascribed to free excitons (3.494 eV) and excitons bound to donors (3.487 eV) from laterally overgrown GaN with a spatial resolution of 300 nm at 15 K. Cross-sectional micro-PL images depicted an inhomogeneous incorporation of donors in the GaN film.

At a line-shaped surface defect in a 4H-SiC homoepitaxial layer, a PL image ascribed to excitons bound to neutral nitrogen atoms showed a dark line coincident with the defect, indicating that a nonradiative recombination dominates the excitonic emission at the surface defect. The microscopic PL imaging with the sub-micron resolution is promising for characterization of spatial distributions of impurities and defects in widegap semiconductors such as SiC and GaN.



## UV Scanning Photoluminescence Spectroscopy applied to Silicon Carbide Characterization

**L. Masarotto, J.M. Bluet, M. Berenguer, P. Girard and G. Guillot**

*Laboratoire de Physique de la Matière - CNRS (UMR5511)  
INSA de Lyon - Domaine Scientifique de la Doua - Bâtiment Blaise Pascal  
7, avenue Jean Capelle, 69621 Villeurbanne Cedex - FRANCE  
e-mail: [bluet@insa-lyon.fr](mailto:bluet@insa-lyon.fr) Tel: 33 (0)4 72 43 87 32 Fax: 33 (0)4 72 43 85 31*

In spite of tremendous progress in SiC bulk growth and epitaxy the rise of high performance and high reliability devices is still limited by the material quality. In the case of SiC wafers, while the micropipes density has been strongly reduced down to  $10 \text{ cm}^{-2}$ , the dislocation density is still of typically  $10^4 \text{ cm}^{-2}$ . These defects, reproduced in the epitaxial layers, are deleterious for high power devices. Additionally, in semi-insulating substrates, deep levels acting as carrier traps affect the devices performance [1]. For epitaxial layers, the main problem is doping inhomogeneities exceeding 20% on a two inches wafer. The presence of polytypes inclusions in substrates as well as in epitaxial layers is also a recurrent problem in SiC wafers. In order to analyse these defects, to understand their origin and their impact on devices performance, non destructive and few time consuming characterization tools are strongly needed.

For such a tight quality control of the wafers, we have developed a scanning photoluminescence (SPL) apparatus, initially conceived for III-V compounds analysis. Indeed, the first results reported [2, 3] indicate that SPL is a very promising tool for SiC material characterization. The PL mapping is obtained by scanning the sample, fixed to an x-y stage with  $1 \mu\text{m}$  minimal step, under a doubled  $\text{Ar}^+$  laser beam (244 nm) focused by an achromatic microscope objective (x52). For this excitation the spot diameter is about  $2 \mu\text{m}$  and the penetration depth is below  $1 \mu\text{m}$  for 4H-SiC. The PL signal can be either directly detected, giving integrated PL intensity, either dispersed using a monochromator, giving spectrally resolved PL (1 nm resolution).

The optical signature of different defects will be presented. For example, the gettering effect of non radiative traps around dislocations results in a denuded zone in the vicinity of the defect. This phenomenon is characterized by an exhaust of the photoluminescence intensity near the dislocation. From this observation, the density on epitaxial layers can be obtained without using chemical etching. The presence of micropipes can also be detected by photoluminescence mapping without using KOH etching. We will show that non emergent micropipes (not visible with optical microscope focussed on the surface) can be revealed. Some examples of polytypes mixtures on epitaxial layers (cubic inclusions) and bulk samples (4H and 6H distinct zone) will also be presented.

[1] N. Sghaier, A. Souifi, J.M. Bluet, O. Noblanc, C. Brylinsky and G. Guillot, *MRS Fall Meeting (Boston 2000)*, to be published.

[2] M. Tajima, Y. Kumagaya, T. Nakata, M. Inoue and A. Nakamura, *Jpn. J. Appl. Phys.*, Vol 36 (1997), L1185-L1187.

[3] L. Masarotto, J-M Bluet, M. Berenguer, P. Girard and G. Guillot, *Mat. Science For.* 333-356, (2001), p 393-396.

**September 25, 10:55 - 12:35**

**Session 2**

**Photoluminescence 2**





## Condensate Luminescence under Ultraviolet Excitation: Application to the Study of Ultrathin SOI Layers

Michio Tajima and Shigeo Ibuka

Institute of Space and Astronautical Science, 3-1-1 Yoshinodai, Sagami-hara 229-8510, Japan

E-mail: [tajima@pub.isas.ac.jp](mailto:tajima@pub.isas.ac.jp), Phone: +81-42-759-8325, Fax: +81-42-759-8463

The condensate luminescence, photoluminescence (PL) from the condensed phase of electrons and holes in semiconductors, was one of the most exciting topics in 1970's. The condensed phase below the critical temperature is known as an electron-hole droplet (EHD). The nucleation and annihilation mechanism of the EHD was investigated in detail based on its analogy with vapor-liquid phase transitions. In spite of the great progress in understanding the EHD properties, useful applications were not found and the research field became outdated. We have revived the condensate luminescence in characterizing silicon-on-insulator (SOI) wafers. Ultrathin SOI wafers are most promising substrates for low-power, high-speed, and highly integrated devices as well as for radiation and high-temperature tolerant devices. Characterization of the SOI wafers is indispensable for improving their quality, and the physical analysis of a superficial Si layer as thin as 0.1  $\mu\text{m}$  is quite challenging. In this paper we demonstrate that the PL under ultraviolet (UV) excitation induces the condensate luminescence in SOI wafers, and show its effectiveness for the characterization.

In bulk Si wafers we need a very high excitation intensity to induce the condensate luminescence. In contrast, the condensed phase is easily realized in SOI wafers under UV excitation. The UV excitation increases the density of electrons and holes in the superficial Si layer, since the UV light is predominantly absorbed in that layer and the excited carriers cannot diffuse into the substrate because of the presence of a buried oxide (BOX) layer which acts as a diffusion barrier. As a result, a high density of electrons and holes are transferred to the condensed phase, emitting the characteristic condensate luminescence. Since the luminescence is sensitive to the crystalline and interfacial defects, its analysis allows us to perform an accurate characterization of these wafers.

We excited samples with a continuous-wave  $\text{Ar}^+$  laser operated at 350 nm for spectroscopy and a pulsed  $\text{N}_2$  laser operated at 337 nm for decay time measurement. Samples were immersed in liquid He in a glass cryostat. The EHD luminescence was always observed in commercial SOI wafers if the superficial Si layer was thermally oxidized. The decay time of the EHD luminescence varied depending on the wafer vendors, reflecting the quality of the materials. We combined this luminescence with the PL under visible and near infrared light excitation on both the front and back sides of the wafers, which allowed us to characterize the quality of not only the superficial Si layer, but also the surface/interface and substrate of the SOI wafers. The technique was applied to analysis of the annealing process in wafers synthesized by separation by implantation oxygen (SIMOX wafers). We found that the  $\{311\}$  interstitial defects were generated below the BOX layer by  $\text{O}^+$  implantation and transferred to dislocations during annealing. PL intensity mapping was done of wafers fabricated by bonding and  $\text{H}^+$  splitting technique (Unibond<sup>®</sup> wafers) at room temperature. We showed that the defects in the wafers originate in the oxygen precipitation which occurs during the two-step annealing of the process. The present technique is thus demonstrated to be quite useful in making an accurate and nondestructive characterization of SOI wafers.

This work was partly supported by JSPS Research for Future Programs under the project: "Ultimate Characterization Technique of SOI Wafers for Nano-Scale LSI Devices."

## Photoluminescence study of {311} defect-precursors in self-implanted silicon

**Hiroshi Tsuji, Ryangsu Kim, Toshifumi Shyano, Tetsuya Hirose, Yoshinari Kamakura, and Kenji Taniguchi**

*Department of Electronics and Information Systems, Osaka University,  
2-1 Yamada-oka, Suita, Osaka 565-0871, Japan  
TEL and FAX : +81-6-6879-7792  
E-mail : tsuji@eie.eng.osaka-u.ac.jp*

An accurate physical model of the formation and dissolution of {311} defects is essential to simulate transient enhanced diffusion (TED) of implanted dopants in IC fabrication processes. Since very little is known about the nucleation of {311} defects, we have studied the transition from the smaller precursor interstitial clusters to {311} defects during thermal annealing with photoluminescence (PL) measurements.

Czochralski Si wafers with a boron concentration of  $3 \times 10^{17} \text{ cm}^{-3}$  were implanted with 50 keV Si ion with fluence of  $5 \times 10^{13} \text{ cm}^{-2}$ . After implantation the samples were annealed at 620 or 670°C in nitrogen ambient for times in the range of 1 min to 810 min. PL measurements were performed at 10 K using the 476.5 nm line of an argon laser.

A broad PL peak at 0.94 eV due to implantation damage is observed after annealing at 670°C for 1 min as shown in Fig. 1. As annealing time increases, the peak energy shifts continuously toward lower energy down to 0.900 eV after 270 min annealing which is associated with {311} defects [1]. The broad PL peak is also observed in low temperature annealing at 620°C, with similar peak energy shifts in Fig. 2. Note that no {311} defects were observed with high resolution TEM in all the samples except the one annealed at 670°C for 270 min annealing. These results strongly suggest that the broad PL peak at 0.94 eV is associated with precursors of {311} defects. A first principle calculation study is now under way to investigate the existence of the precursors.

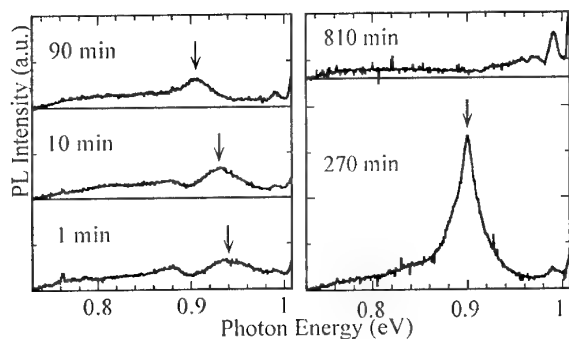


Fig. 1. PL spectra from samples annealed at 670°C

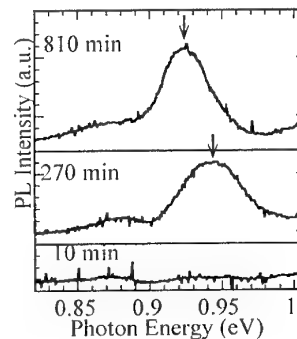


Fig. 2. PL spectra from samples annealed at 620°C

[1] S.Coffa, S.Libertino, and C.Spinella, Appl. Phys.Lett. **76**, 321 (2000).



## The impact of defects to minority-carrier kinetics in heavily doped GaAs:C analyzed by transient photoluminescence spectroscopy

**J. W. Tomm<sup>a)</sup>, A. Maaßdorf<sup>b)</sup>, and Y. I. Mazur<sup>a)</sup>, S. Gramlich<sup>b)</sup>, E. Richter<sup>b)</sup>,  
K. Brunner<sup>b)</sup>, M. Weyers<sup>b)</sup>, G. Tränkle<sup>b)</sup>, D. Nickel<sup>a)</sup>, V. Malyarchuk<sup>a)</sup>,  
T. Günther<sup>a)</sup>, Ch. Lienau<sup>a)</sup>, A. Bärwolff<sup>a)</sup>, T. Elsaesser<sup>a)</sup>**

<sup>a)</sup> Max-Born-Institut, Max-Born-Str. 2 A, 12489 Berlin, Germany  
Tel. +49-30-63921453, Fax. +49-30-63921459, tomm@mbi-berlin.de,  
<http://www.mbi-berlin.de/>

<sup>b)</sup> Ferdinand-Braun-Institut, Albert-Einstein-Str. 11, 12489 Berlin, Germany

We report room-temperature photoluminescence (PL) decay time measurements in heavily doped GaAs:C-layers which are designed as base layer for heterojunction bipolar transistors (HBT). HBT current gains are proportional to the non-equilibrium carrier lifetime ( $\tau$ ) within the base.

This study is done with the main objective to derive reliable room-temperature  $\tau$  data from transient PL. Time resolved PL appears either as mono- or bi-exponential transients.

A number of extrinsic effects that influence the PL transients are carefully analyzed:

- For a number of GaAs:C samples but also for GaAs-bulk very fast (50-200 ps) transients appeared. These transients, that vanish for high excitation densities, are interpreted as fast carrier trapping. Experiments with intentionally treated surfaces indicate, that this trapping effect is related to surface states.
- Analysis of steady state and transient PL spectra indicate the absence of pronounced hot electron and stimulated emission effects at room-temperature.
- Furthermore, we show that a doublet structure in the room-temperature PL spectrum is caused by a geometry effect.

We are able to give experimental conditions that allow to minimize the impact of extrinsic effects. For the excitation density a compromise between the necessity to saturate traps and avoiding stimulated emission is found. At room-temperature an excitation density of  $10^{17}$ - $10^{18}$  cm<sup>-3</sup> per pulse meets this demand. Detection should be limited to a spectral window well above the gap of GaAs, i.e. beyond 1.5 eV.

Our methodical investigations allow us to perform reliable PL decay time measurements providing  $\tau$ -data for MOCVD optimization.

$\tau$ -data from one sample group are well explained by intrinsic Auger and radiative recombination. This is an excellent confirmation of the success of our work to minimize the impact of extrinsic effects on our  $\tau$ -data.

Thus we show how PL decay time measurements can be used as a robust tool for the estimation of expected HBT current gains on wafer scale immediately after epitaxial growth.





**September 25, 14:10 - 15:50**  
**16:20 - 16:50**

## **Session 3**

### **Other Optical Methods**





## **Micro-PL for the visualisation of defects, stress and temperature profiles in high-power III-V's devices**

**Jean-Pierre Landesman**

Laboratoire des Plasmas et des Couches Minces

Institut des Matériaux – Jean Rouxel

2, rue de la Houssinière – BP 32229

44322 Nantes Cedex 3

☎ 02 40 37 39 55 – [Jean-Pierre.Landesman@cnrs-imn.fr](mailto:Jean-Pierre.Landesman@cnrs-imn.fr)

(work done at Thales - Laboratoire Central de Recherches  
Domaine de Corbeville, 91404 Orsay Cedex)

Several different applications of the micro-photoluminescence ( $\mu$ -PL) mapping technique to the evaluation of (high power) semiconductor devices are demonstrated, mainly in the framework of reliability investigations for these devices.

The measurements involve a spectroscopic optical micro-probe equipment, in which the devices (which can be under operation for some of the applications demonstrated in this talk) are scanned by a focused laser beam. The required information is derived from the back-scattered photoluminescence signal, which is collected and analysed using a semi-automated procedure in each point of analysis. The spot size at the device surface is in the range of 1  $\mu$ m, which is also in most cases the final spatial resolution.

In this presentation, the applications mentioned will be:

- Local temperature mapping either in individual devices or in circuits like MMICs (Monolithic Micro-Wave Integrated Circuits) based on PHEMTs (Pseudo-morphic High Electron Mobility Transistors) or HBTs (Hetero-junction Bipolar Transistors) on GaAs substrates.
- Mapping of the local mechanical stress, in relation with the packaging, in high-power GaAs/GaAlAs laser diode arrays designed for emission at 808 nm.

Both types of mapping are done by analysis of the  $\mu$ -PL peak shifts associated with either heating or mechanical stress in the semiconductor materials. As will be shown, this very simple approach is well adapted to automatic measurements, which in turn allows measurements on a large number of samples, or for a number of different operating conditions for temperature measurements. In the case of temperature measurements, details of the heat dissipation in the transistors will be shown, which could not be obtained from any of the available commercial techniques (like temperature variations along the gates of the PHEMTs, or differences in heat dissipation in the emitters of multi-emitter HBTs, which can be related to the topology of these transistors). In the case of mechanical stress, the potential of the  $\mu$ -PL technique will be illustrated first for a quantitative, local evaluation of the amount of stress induced in the device by the packaging procedure (with special emphasis on the type of solder used), and then for a more microscopic investigation of the defects responsible for the lifetime limitation in high-power laser diode arrays.

## Detection of Indium segregation effects in InGaAs/GaAs quantum wells using reflectance-difference spectrometry

Xiaoling Ye, Y. H. Chen, Bo Xu, Z. G. Wang

Laboratory of Semiconductor Materials Science, Institute of Semiconductors, Chinese Academy of Sciences, P.O. Box 912, Beijing 100083, P. R. China

Segregation effects at semiconductor heterojunctions lead an ultimate limitation to the achievement of perfectly abrupt interfaces for high-control growth technique such as molecular-beam epitaxy (MBE) or metalorganic chemical-vapor deposition (MOCVD). Several methods, including *in situ* reflection high-energy electron diffraction (RHEED)<sup>1</sup> and *ex situ* x-ray diffraction measurements<sup>2</sup>, etc., have been employed to investigate the effects. As an interface-sensitive and non-destructive technique, reflectance-difference spectroscopy (RDS) has not been reported in *ex situ* detection of the segregation effects. In this paper, we will study the relations between the interfacial asymmetry induced by the segregation and the lineshapes of the RDS.

Two samples used in the study were grown on Semi-insulating GaAs (001) substrate in a MBE chamber with the same substrate temperature (~520°C) and the growth rate (~1ML/s). Sample 1 is a  $\text{In}_{0.2}\text{Ga}_{0.8}\text{As}$  (70 Å) / GaAs single quantum well, and Sample 2 is a 10 periods of  $\text{In}_{0.15}\text{Ga}_{0.85}\text{As}$  (70 Å) / GaAs (130 Å) superlattice. Their RDS spectra show dissimilar characters: in Sample 1, the signs of the anisotropy of 1H1E (1HH→1CB) transition and 1L1E transition are opposite, and the anisotropy of the forbidden 2H1E transition also has the opposite sign to that of 1H1E; while for Sample 2, though 1H1E and 1L1E transitions still have opposite signs, 2H1E transition turns to have the same sign as 1H1E. Because the anisotropy of 2H1E transition is very sensitive to the interfacial asymmetry<sup>3</sup>, it demonstrates that the two quantum wells should have different interfacial shape. The best agreement between observed and calculated RDS lineshape is obtained if Sample 1 has a symmetric-shape well; but for Sample 2, the agreement can be achieved only if it has an asymmetric well: the interface widths are ~2 and 5 ~ 6 monolayers for  $\text{In}_{0.15}\text{Ga}_{0.85}\text{As}$ -on-GaAs and GaAs-on- $\text{In}_{0.15}\text{Ga}_{0.85}\text{As}$  respectively. It confirms that In segregation depends not only on the substrate temperature and the growth rate, but also on other growth conditions.

1 J.-M. Gérard, J. Crystal Growth **127**, 980 (1993)

2 P. Auvray, M. Baudet, C. Deparis and J. Massies, J. Crystal Growth **127**, 821(1993)

3 Y. H. Chen, Z. Yang, Z. G. Wang, Xu Bo et al., Phys. Rev. **B60**,1783(1999)



## The influence of residual strain on Raman scattering in $\text{In}_x\text{Ga}_{1-x}\text{As}$ single crystals

M.R. Islam<sup>a</sup>, Prabhat Verma<sup>a</sup>, M. Yamada<sup>a</sup>, S. Kodama<sup>b</sup>, Y. Hanaue<sup>c</sup>, and K. Kinoshita<sup>c</sup>

<sup>a</sup>Department of Electronics and Information Science, Kyoto Institute of Technology, Kyoto 606-8585, Japan.

<sup>b</sup>Fujitsu Laboratories Ltd. 10-1 Morinosato-wakamiya, Atsugi 243-0197, Japan.

<sup>c</sup>National Space Development Agency of Japan, Tsukuba 305-8505, Japan.

Email: [islam@djedu.kit.ac.jp](mailto:islam@djedu.kit.ac.jp) Fax.: 81-075-724-7400 Phone: 81-075-724-7422

$\text{In}_x\text{Ga}_{1-x}\text{As}$  bulk crystal is an attractive lattice matched substrate material for fabricating InGaAs-based optoelectronic devices. However, there is a problem that the samples are often cracked due to the residual strain during growth process, which is developed in the crystals because of inhomogeneous compositional distribution in the crystal. Therefore, spatial homogeneity in composition is the basic requirement to eliminate residual strain. But it is a big challenge for the crystal growers to grow compositionally homogeneous  $\text{In}_x\text{Ga}_{1-x}\text{As}$  single crystal, because convective flow in the melt leads to the compositional fluctuation in the resultant material. Hence, it is very important to characterize these samples, particularly, the composition using a non-destructive accurate method, such as Raman scattering. Composition-dependent shift of optical phonon in Raman spectra provides convenient estimation of the composition with high accuracy.

The effect of residual strain in Raman measurement of epilayers is reported in the past by several authors[1]. In these investigations, it is found that the observed shift in optical phonons contains composition-dependent shift as well as strain-induced shift. Hence, using Raman scattering, the exact composition can be obtained after separating out the shift induced by residual strain. The release of residual strain in cracked samples is reported [2] using photoelastic measurement in GaP wafers. In this investigation, it is noticed that the residual strain is relaxed proportionally with the size of the cracked part.

In this paper, we report the influence of residual strain on Raman spectra of  $\text{In}_x\text{Ga}_{1-x}\text{As}$  single crystal. The sample used in our measurement was a wafer sliced from a crystal grown by multi-component zone melting method [3]. This wafer was found to contain cracks due to the residual strain. The sample was cracked into three pieces along two lines. Some microscopic pieces were also found at the joining point of the cracked lines. Room temperature Raman spectra were measured from both the sides of the cracked line and also from the microscopic pieces. The Raman spectrum measured from a microscopic piece was compared to the spectrum measured from a nearby point on the big piece. It was found in the previous study [2] that the residual strain decreases with the size of the broken piece. In the case of microscopic pieces, the residual strain becomes negligible. It is observed that the spectrum obtained from the microscopic piece is shifted by about  $5\text{ cm}^{-1}$  (LO-like phonon) compared to the spectrum obtained from the big piece. The intensity of the spectrum obtained from the microscopic piece is about two times larger compared to the intensity of the spectrum obtained from the big piece. The linewidth of the spectrum obtained from the big piece is broadened compared to the linewidth of the spectrum obtained from microscopic piece. Since the spectra were measured from the two close points of the sample, therefore, it can be considered that the two points have same composition. Hence, the  $5\text{ cm}^{-1}$  frequency shift in the optical phonon is induced by strain alone. The changes in the linewidths and intensities also indicate the relaxation of residual strain in microscopic pieces. On the other hand, if we compare the spectra obtained from two close points on the big pieces across the cracked line the difference of frequency shift is about  $1\text{ cm}^{-1}$  (LO-like phonon). Therefore, big broken pieces are not free from residual strain. From this study we can estimate the strain-induced shift in Raman spectrum, which is very useful to estimate the compositional profile of an  $\text{In}_x\text{Ga}_{1-x}\text{As}$  single crystal where the observed shifts in phonon contain strain-induced as well as composition-induced shifts.

[1] J. Groenen, G. Landa, R. Carles, P. S. Pizani, and M. Gendry, J. Appl. Phys. **82** (1997) 803.

[2] M. Yamada, J. Appl. Phys. **74**(10), 1993.

[3] S. Kodama, Y. Furumura, K. Kinoshita, H. Kato, and S. Yoda, NASDA Tech. Memorandum, (1999) 57.

## Study of defects in conformal GaAs/Si layers by optical techniques and Photoetching

A.M. Ardila<sup>1,2</sup>, O. Martínez<sup>1</sup>, M. Avella<sup>1</sup>, J. Jiménez<sup>1</sup>, E. Gil-Lafon<sup>3</sup>, B. Gérard<sup>4</sup>

<sup>1</sup>Departamento de Física de la Materia Condensada, Facultad de Ciencias, Universidad de Valladolid, Valladolid, 47011, Spain

<sup>2</sup>Departamento de Física, Facultad de Ciencias, Universidad Nacional de Colombia, Ciudad Universitaria, Santa Fe de Bogotá, Colombia

<sup>3</sup>LASMEA UMR CNRS 6602, Université Blaise Pascal, Les Cézeaux, 63177 Aubière Cedex, France

<sup>4</sup>THALES, Corporate Research Laboratory, 91404 Orsay Cedex, France

We present herein the results obtained from the characterization of crystal defects in GaAs layers grown on silicon substrates by the conformal growth method. This technique consists of a lateral growth confined by the substrate and an overhanging dielectric cap layer. These layers grow with a reduced density of crystal defects, e.g. dislocations, which are effectively filtered by the substrate and the overhanging layer. The samples were analysed by microRaman Spectroscopy, Cathodoluminescence, Phase Stepping Microscopy and were etched by the DSL (Diluted Stirl Solution applied with light) method. Several structures were revealed; in particular a quasi-periodic array of hillocks and valleys that are spatially correlated with fluctuations of the luminescence intensity. The etching rate was controlled by the distribution of deep levels, which were found to be accumulated in the regions under tensile stress; the etching rate reproduces the stress distribution generated by the interaction between the conformal layer and the thin SiO<sub>2</sub> passivating layer formed on the silicon surface during the underetching stage prior to the GaAs lateral deposition. Dislocations were not revealed by DSL, which is in agreement with the drastic reduction of the dislocation density. Other crystal defects were identified, in particular some grooves parallel to the seeds were observed. These grooves were analysed and the stress distribution was obtained. Some dark lines crossing the conformal layer from seed to end were also revealed. The main properties of these defects and their possible origin are studied.



## Optical quantitative determination of doping levels and their distribution in SiC

**P.J. Wellmann, R. Weingärtner, M. Bickermann, T.L. Straubinger,  
and A. Winnacker**

Materials Department 6, University of Erlangen, Martensstr. 7, 91058 Erlangen,  
GERMANY.

Phone: +49-9131-85-27635, Fax: +49-9131-85-28495,

Email: peter.wellmann@ww.uni-erlangen.de

Wide bandgap semiconductor materials like silicon carbide (SiC) have gained much interest for high-power, high-frequency and high-temperature device applications. The knowledge of the doping level and doping level distribution of n- and p-type doped 4H- and 6H-SiC substrate wafers is of particular interest due to their impact on the electrical properties of SiC based power devices and GaN based optoelectronic devices.

SiC exhibits unique mid-bandgap optical absorption bands which show a strong, linear dependence on the charge carrier concentration. In addition a large impact of the charge carrier concentration on band gap related absorption transitions is observed due to doping induced band gap shrinkage effects.

Based on these electronic features we have developed a quantitative characterization tool for SiC wafers using optical absorption measurements which is as accurate as electrical Hall measurements (15%...20%) and serves all the advantages of optical methods like being non-contact, non-destructive and quick.

Using spectrally resolved absorption measurements we were able to distinguish the doping type (n- or p-type) and to determine the doping level ( $n, p = 5 \cdot 10^{16} \text{ cm}^{-3} \dots 1 \cdot 10^{19} \text{ cm}^{-3}$ ). Performing absorption mappings at specific optical transitions enabled us to reveal the spatial doping level homogeneity. Numerical calculations as well as electrical Hall measurements were performed in order to quantify the experimental absorption data. Calibration plots for all technological important SiC polytypes (n-/p-type 6H-SiC, n-/p-type 4H-SiC and n-type 15R-SiC) were evaluated.

The presentation will also include a discussion of the physical nature of the optical absorption transitions in order to further support the confidence in the reliability of the new characterization method. In a final part the potential of the measurement tool will be demonstrated by showing several examples of SiC wafer doping level mappings.

## Large area, high resolution measurement of surface roughness of semiconductors using interference microscopy

**P.C. Montgomery<sup>(1)</sup>, A. Benatmane<sup>(1)</sup>, J.P. Ponpon<sup>(1)</sup>, and E. Fogarassy<sup>(1)</sup>**

<sup>(1)</sup> Laboratoire de Physique et Application des Semi-conducteurs, C.N.R.S.,  
23 rue du Loess, BP 20 CR, 67037 STRASBOURG Cédex 2 – FRANCE.

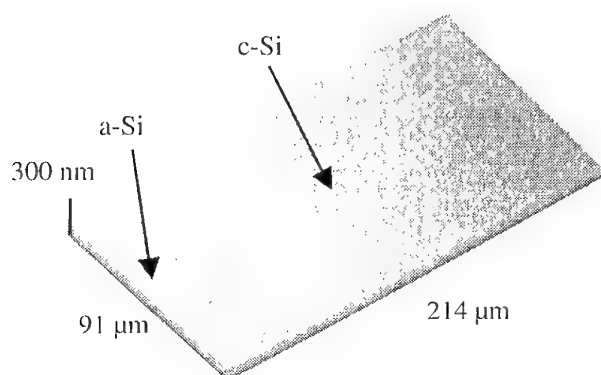
E-mail: monty@phase.c-strasbourg.fr

Tel: (33) 03.88.10.62.31.

Fax: (33) 03.88.10.62.30.

Nanometre to multi-micron surface roughness of semiconductors can be measured rapidly and non-destructively using interference microscopy. This technique is the only one available for measuring the surface roughness of certain materials that are particularly fragile such as  $\text{HgI}_2$  and  $\text{PbI}_2$  since they do not support the vacuum conditions of electron microscopy nor even the light stylus force used in AFM.

Being a far-field optical technique, the lateral resolution is limited by diffraction, but the use of blue/UV light enables resolutions of  $<0.3 \mu\text{m}$  to be achieved. One of the problems in measuring larger areas with a lower power objective is that the resolution decreases due to the smaller numerical aperture. One way round this is to scan the sample using the same high power objective and to use "image stitching" to create a large area high resolution measurement. Several other improvements have been introduced over the past decade in interference microscopy that improves the efficiency in the use of computer memory, the measurement speed, and the precision. We discuss these improvements as applied to the analysis of surface polish of  $\text{HgI}_2$  and the grain shape of  $\text{PbI}_2$  for nuclear detectors, and the optimisation of c-Si grain size after laser annealing of a-Si layers for flat panel displays.



Large area measurement using "image stitching" in Phase Stepping Microscopy to analyse the distribution in grain size of c-Si at the edge of a laser annealed a-Si flat panel display sample

### References :

1. Montgomery P.C. and Montaner D., *Deep submicron 3D surface metrology for 300 mm wafer characterization using UV coherence microscopy*, Microelectronic Engineering, **45**, pp. 291-297, 1999.
2. Ponpon J.P., Montgomery P.C., Sieskind M. and Amann M., *Photoetching effects in mercuric iodide*, Applied Surface Science, **165**, pp. 233-240, 2000.



## Inspection of Si wafer by Laser Scattering Topography

Kazuo MORIYA  
MITSUI KINZOKU

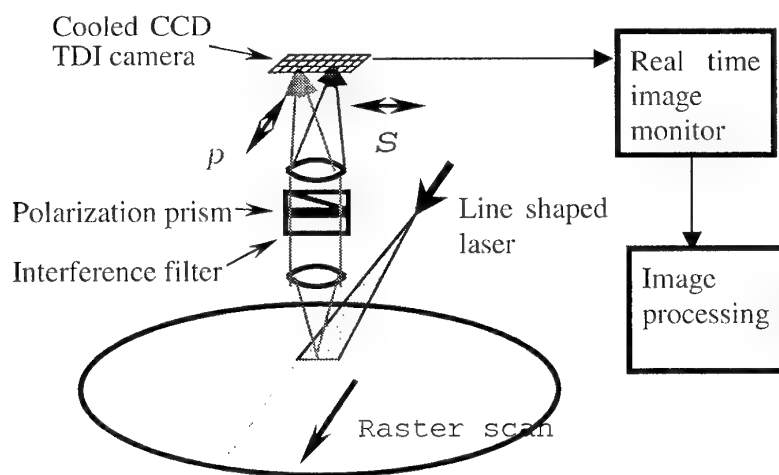
[k\\_moriya@mitsui-kinzoku.co.jp](mailto:k_moriya@mitsui-kinzoku.co.jp) TEL:048-773-7964, FAX:048-776-4743

Laser scattering inspection system was newly developed for reveal the surface haze, scratch, particles, Photo-luminescence and inside defects.

Principle of this instrument is oblique incident laser beam lineally shaped about 1mm in length, and the scattered light is received by CCD camera as shown in Figure. Image formation is performed by raster scanning of wafer. The discrimination methods for such scattering centers are developed as follows.

- 1) Haze is defined as background scattering, and orientation dependence measurement is effective to know the surface micro texture i.e. micro steps due to the heat treatment or off-angle.
- 2) Scratch lines are recognized as line shaped scattering centers on the real time scattering image .
- 3) Particles and inside defects are discriminated as 99% probability by polarization ratio measurement of scattered light.
- 4) PL and scattered light are separated by interference filters. PL intensity map is related to the lifetime map.
- 5) Orientation dependence of scattered light is effective to know the defect shape.
- 6) Wavelength dependence of scattering from inside defects are useful to discuss the depth profile of defect density.
- 7) Direct observation of defects can be observe by TEM using laser marking function of this instrument.

Problem to be solve is improvement of detection limits. Detection limit of void defect is estimated about 50nm in diameter, and this value is strongly affected by surface roughness. Ideal and theoretical detection limit of polished wafer is calculated about 30nm in diameter.





**September 25, 16:50 - 18:30**

**Session 4**

**Nanoscanning Techniques**





## Temporally- and spectrally resolved near-field optics of semiconductor nanostructures

**Christoph Lienau, Francesca Intonti, Tobias Günther, Valentina Emiliani, and Thomas Elsaesser**

Max-Born-Institut für Nichtlineare Optik und Kurzzeitspektroskopie,  
Max-Born-Str. 2A, D-12489 Berlin, Germany  
Tel. ++49-30-6392-1476, Fax. ++49-30-6392-1489, lienau@mbi-berlin.de

We discuss ultrahigh spatial, spectral and temporal resolution near-field spectra of single quantum wires and thin quantum wells recorded by low-temperature near-field scanning optical spectroscopy. In such disordered quantum systems, localized exciton states play a key role for the optical and transport properties. The disorder-induced broken translational symmetry of the nanostructure leads to slightly different exciton eigen and thus optical transition energies. This gives rise to inhomogeneously broadened far-field optical spectra. On the other hand, in highly spatially and spectrally resolved experiments the smooth inhomogeneously broadened line of macroscopic PL spectra breaks up into many narrow spikes from single localized excitons whose individual spectral widths are often determined by experimental resolution or by the natural line width.

In experiments on single quantum wires, we demonstrate that the localization length of the different excitonic eigenstates in such disorder systems may vary over a wide range between typically 10 nm up several microns. The optical signatures of these excitonic states in high spectral resolution near-field images will be shown to be clearly different, a behavior that is well accounted for by theoretical calculations of exciton states in a disorder potential.

Experiments on single thin quantum wells demonstrate that the statistical properties of the different localized exciton states bear precise information about the nature of the underlying disorder potential, specifically its correlation length. We subject a set of several hundred near-field spectra displaying sharp emission lines to an analysis of the two-energy autocorrelation function [1]. An accurate comparison with a quantum theory of the exciton center-of-mass motion in a two-dimensional spatially-correlated disordered potential reveals clear signatures of quantum-mechanical energy level repulsion, giving the spatial and energetic correlations of excitons in disordered quantum systems.

In the last part of this talk we present first femtosecond time-resolved reflectance spectra of single localized excitons. We demonstrate a novel technique that is capable of mapping the time-dependent density matrix of single exciton eigenstates in thin quantum wells or, e.g., self-assembled InAs quantum dots. The potential of the technique and first applications that resolve the incoherent carrier trapping and relaxation dynamics in disorder quantum wells are discussed.

[1] F. Intonti et al., Phys. Rev. Lett. **87**, 076801 (2001).



## Near field photoluminescence and photoreflectance measurements of semiconductor structures

**P. Tománek, M. Benelová, P. Dobis, L. Grmela**

Brno University of Technology

Faculty of Electrical Engineering and Computer Science, Physics Department

Technická 8, 616 00 Brno, Czech Republic

e-mail: tomanek@dphys.fee.vutbr.cz, Fax: + 420-5-4114 3133, Tel: + 420-5-4114 3278

Photoluminescence (PL) and photoreflectance (PR) spectroscopic techniques have demonstrated to be helpful experimental method to investigate the properties of bulk semiconductors, microstructures, surfaces and interfaces. In PR spectroscopy, the periodical modulation of the intrinsic field by photogenerated electron-hole pairs produces sharp, derivative-like features in the region of interband (or intersubband) transitions.

We present near-field local photoluminescence and photoreflectance spectroscopic study of semiconductor quantum structures using a technique of reflection scanning near-field optical microscopy (SNOM) in combination with Nitrogen laser and dye laser in one arm and He-Ne lasers in the other. Because of derivative-like nature of the PR spectra, a large number of sharp spectral features can be observed, even in the room temperature, which allows that this technique can be used as an effective and powerful spectroscopic and imaging tool. The optical properties of GaAs/AlGaAs quantum well were measured at 300 K by means of photoluminescence and photoreflectance spectroscopy using SNOM with shear force control of the distance. The pump light from dye and alignment light from He-Ne lasers are focused into a single mode fiber and the light reflected by the sample is collected by the same fiber and then detected by a photodiode.

The experiments in the photoluminescence and the photoreflectance have been performed as a function of the excitation intensity, tip-surface distance, and sample position. By using the sharp feature of photoreflectance signal, more sensitive and spatially resolved variation of energy fluctuations could be obtained. From the results, it is obvious that this method has several advantages over conventional optical techniques, working in the optical far-field region, including higher signal-to-noise ration, and better spatial resolution.



## **Analysis of complex heterogeneous surfaces by scanning tunneling microscopy/spectroscopy and surface electron diffraction**

**I. Goldfarb and G.A.D. Briggs**

Department of Solid Mechanics, Materials and Systems

The Fleischman Faculty of Engineering

Tel Aviv University, Ramat Aviv 69978, Israel

e-mail: [ilang@eng.tau.ac.il](mailto:ilang@eng.tau.ac.il), phone: +972-3-6407079, fax: +972-3-6407617

URL: <http://www.eng.tau.ac.il/~ilang>

Department of Materials, Oxford University, Parks Road, Oxford OX1 3PH, UK

In future devices, the size of active regions and separations may be in the order of few atomic rows, which facilitates the need not only for new physical concepts of operation and advanced production techniques, but for more powerful characterization methods, as well. There are many methods to probe surface structure and chemistry. Low- (LEED) and reflection high- (RHEED) energy electron diffraction are amongst the most widely used techniques for surface structure identification, and Auger electron (AES) and X-ray photoelectron (XPS) spectroscopies are popular methods for obtaining chemical information. While these, and other methods, are useful and important, the information they provide is averaged over rather large areas. In other words, they are not site-selective, and lack the required nanometer spatial resolution. Scanning tunneling microscopy (STM), on the other hand, is a very powerful method for surface visualization with sub-nanometer resolution, and scanning tunneling spectroscopy (STS) contains information directly linked to the surface density of states of features as small as a single atom. However such resolution comes at the expense of large fields of view. Also, when, due to various reasons, atomic resolution is not possible, the crystallographic information from STM is limited. Hence the above-mentioned methods are complementary, and should be used in conjunction with each other.

One of the other powerful STM features is the so-called "bias-dependant imaging", especially for analyzing defects, which has also been used to distinguish between topographic and electronic contrast. In this work we present analysis of various multicomponent surfaces, such as Si-Ge, Co-Ge, and Co-Si, by combined STM, STS, RHEED and LEED. The work also emphasizes the need for a wider theoretical support in interpreting both tunneling and diffraction phenomena.



## Atomic Defects Generated by Hydrogen on Si(110) Surface as Revealed by Scanning Tunneling Microscopy

Masamichi Yoshimura, Mitsumasa Odawara, and Kazuyuki Ueda

Toyota Technological Institute, Hisakata, Tempaku, Nagoya 468-8511, Japan  
e-mail: yoshi@toyota-ti.ac.jp

The Si(110) substrate is of great importance for future quantum devices because of its lower dimensional nature as compared with (100) or (111) plane. The clean surface shows “16x2” reconstruction, in which upper and lower terraces with 2.5nm in width are alternatively arranged into one direction [1]. The terrace consists of periodical arrays of pentagonal units of Si atoms (“pentagon” hereafter) and the tetramer-interstitial model was recently proposed [2]. It is noted in the model that the one atom of the pentagon is not adatom but a substrate atom which is lifted up by the interstitial. Since each atom of the pentagon has one dangling bond, the pentagon units are expected to play an important role in chemical reactions.

In this study we investigate hydrogen adsorption processes on the clean Si(110) “16x2” surface by ultrahigh vacuum-scanning tunneling microscopy (UHV-STM). Atomic hydrogen was irradiated stepwisely onto the surface at room temperature, as monitored by time-of-flight type electron stimulated desorption spectroscopy (TOF-ESD). The STM observations were performed at room temperature using chemically sharpened tungsten probe. Upon exposure of atomic hydrogen, atom-like bright spots were observed randomly on the surface and their number increased with the H-exposure. These spots are classified into three types from the appearance and the location. It is found that all the three types are positioned close to the lift-up substrate atom described above. This indicated high reactivity of the lift-up site through its structural specificity, and we tentatively assign the bright spot to the defect produced by hydrogen at this site. Beside the bright spots, we found that the reaction occurred in another path through the island formation along the terrace. The detailed reaction mechanism is presented.

- [1] E. J. van Loenen, D. Dijkkamp, and A. J. Hoeven, *J. Microsc.* 152 (1988) 487.
- [2] T. An, M. Yoshimura, I. Ono, and K. Ueda, *Phys. Rev. B* 61 (2000) 3006.



**STM topography and barrier imaging of InAs/GaAs dots****S. Selci, M. Righini, G. Latini**

Istituto di Struttura della Materia-CNR, Via del Fosso del Cavaliere 100 - 00133 Rome,  
 ITALY – E-mail: [selci@ism.rm.cnr.it](mailto:selci@ism.rm.cnr.it); Fax: +390649934153; Tel: +390649934167

We have performed Scanning Tunneling Microscopy (STM) imaging in air of self assembled InAs dots on GaAs surfaces (by MASPEC-CNR, Parma Italy).

Both constant current map as well gap-modulated images are obtained. The results reveal a clear difference of the dots profile between the topography, that shows dome shaped dots, and the barrier mode that shows sharp pyramids, while the two are acquired just on the same place and at the same time. Possible contrast mechanisms involved in both types of images are discussed. In particular, it is well known that tunnelling barrier modulation techniques is able to produce the local work function

$$\phi \approx 0.95 \left( \frac{d \ln I}{dW} \right)^2$$

However, at short distances or in presence of contamination intermediates, like for a air-operated STM, a Morse function for the local forces can be used to get into account possible tunnelling gap elastic modification of the sample and/or the tip. Therefore, the observed  $z$  is related to the true tunnelling gap  $W$ <sup>1</sup>:

$$dz/dW \cong 1 - \gamma \left( e^{-k(W-W_0)} - 2e^{-2k(W-W_0)} \right)$$

being  $\gamma$  proportional to the chemical bonding between tip and sample. Therefore  $dI/dW$  can produce compliance profiles<sup>2</sup> with the sensitivity to chemical local properties. These results can be inserted in the current debate on the actual shape of InAs dots, and claim for a more realistic interpretation of scanning probes results.

Also laser modulation of the sample surface has been used to enhance the difference between dots and wetting layer through different conductivity properties, as clearly shown by composite images obtained mixing standard topographic and laser modulated data.

<sup>1</sup> C.J.Chen, loc. cit., pag. 207

<sup>2</sup> H. Rohrer, Scanning Tunneling Microscopy - Methods and Variations, in Tunneling Microscopy and Related Methods, Kluwer Academic Publishers 1990, pg. 20



**September 26, 8:30 - 10:10**

**Session 5**

**Defects in silicon 1**





**A review of in line/off line defect characterization techniques applied to control and improve electronic grade silicon wafer manufacturing processes**

**G. Borionetti**

MEMC Electronic Materials SpA, Viale Gherzi, 31 28100 Novara Italy  
e-mail: gborionetti@memc.it  
tel: +39 0321 334387  
fax +39 0321 691000

Electronic grade silicon wafer manufacturing industry, as well as IC manufacturing industry to which is primary supplier, has continuously to face extremely challenging parametric roadmaps combined with shorter and shorter time to market cycles of new products development, efficient volume production and contained manufacturing costs. Within this scenario, an intelligent use and development of characterization techniques able to combine the necessity of very advanced material properties investigation with real time process /product control is one of the key winning factors.

First section of the paper will be a review of silicon wafer present and future quality requirements included the associated metrological needs, in the three main areas of surface and in bulk metal purity, surface and in bulk extended defects and silicon wafer flatness. Basic principles of the main characterization tools used in electronic industry to test silicon wafer properties in these fields will be included.

Then, the paper will examine recent examples of new products introduction to the market where a combination of in line and off line characterization techniques is necessary at least in the first manufacturing phase. Discussion will include considerations regarding the impact that advanced characterization techniques may have on manufacturing cost and cycle time.



## Infrared absorption measurement of nitrogen in CZ-Si crystal

T. Matsumoto, Y. Yamanaka and N. Inoue

JEITA Nitrogen Task Team, RIAST, Osaka Prefecture University

E-mail: yamanaka@riast.osakafu-u.ac.jp, Fax: +81-722-54-9935, Tel: +81-722-54-9831

In recent years, small crystalline defects have influenced the performance of the semiconductor devices. It is reported that nitrogen doping reduces these defects. Therefore, it is important to characterize nitrogen. Nitrogen concentration [N] in FZ-Si has been measured by infrared absorption. But, it is difficult to measure [N] in CZ-Si. Here, we report nitrogen measurement in CZ-Si and propose the detailed method.

The samples used were cut from the CZ-Si crystals of 5 inches diameter and their surface was mirror polished. The sample thickness was 10 mm. The [N] ranges from  $2 \times 10^{14}$  to  $4 \times 10^{15} \text{ cm}^{-3}$  which was estimated from the distribution coefficient. We used both MCT and TGS detectors. The measurement was done at room temperature and the resolution was  $2 \text{ cm}^{-1}$ . The absorbance noise level was below 0.0002 which was equivalent to the absorption peak with  $1.0 \times 10^{14} \text{ cm}^{-3}$ .

The absorption peaks of  $963 \text{ cm}^{-1}$  and  $764 \text{ cm}^{-1}$  were observed in samples with [N] more than  $2 \times 10^{14} \text{ cm}^{-3}$  and high resistivity (non dope). We used the peaks at  $963$ ,  $995$  and  $1018 \text{ cm}^{-1}$ , which correspond to N [1], NO [2] and  $\text{NO}_2$  [3] respectively. The full widths at half maxima were  $6.1$ ,  $5.7$  and  $3.8 \text{ cm}^{-1}$  respectively. We established the baselines inside the small satellite peaks in the foot of the main peaks.

The relative ratio of the three peaks changed from sample to sample. So we think that the total [N] is obtained by the sum of three peaks. The conversion coefficient between the absorption coefficient and the nitrogen concentration was obtained to be  $2.1 \times 10^{17} \text{ cm}^2$  which is nearly equal to the reported value of  $1.82 \times 10^{17}$  for FZ-Si [4]. Thus, the nitrogen concentration was successfully determined by the established measurement method. This work is partially supported by JSPS for the future program.

[1] R. Jones et al., Phys. Rev. Lett. **72** (1994) 1882.

[2] R. Jones et al., Semicond. Sci. Technol. **9** (1994) 2145.

[3] P Wagner et al., Appl. Phys. A **46** (1988) 73.

[4] Y. Itoh et al., Appl. Phys. Lett. **47** (1985) 488.



## Behaviors of Oxygen Precipitation in D-like defect Zone and Ring-OSF Zone in Nitrogen-doped CZ Silicon Single Crystals

Kazuhiko KASHIMA, Hiroyuki FUJIMORI,  
Yumiko HIRANO and Hiroshi SHIRAI

TOSHIBA CERAMICS Co.,Ltd.  
30,Soya, Hadano-shi, Kanagawa 257-8566, Japan  
E-mail: [kkashima@tocera.co.jp](mailto:kkashima@tocera.co.jp)  
Phone: +81-463-84-6625  
Facsimile: +81-463-81-8416

Recently, since LSI's pattern design becomes fine, strong gettering ability is required. Therefore it will become important to understand behavior of IG (Internal gettering) due to oxygen precipitation in the bulk. In CZ silicon crystal, nitrogen doping effect can extend Ring-OSF zone and reduce void size and enhance effectively oxygen precipitation<sup>1)</sup>. CZ silicon crystal without nitrogen can precipitate oxygen in the D-like defect (i.e. void / COP) zone, but cannot in the Ring-OSF zone. CZ silicon crystal with nitrogen can precipitate oxygen in the both zones<sup>2)</sup>.

Using IR-tomography, TEM with EDX and FTIR, we invest grown-in oxygen precipitates in nitrogen-doped CZ silicon crystal and show difference between the both nitrogen doping effects on oxygen precipitation in the D-like defect zone and in the Ring-OSF zone. Grown-in oxide precipitates in Ring-OSF zone are {111} octahedral shape and 14-sided polyhedral shape bounded eight {111} and six {100} with the small whisker-like defects less than 5 nm long. These defect size is about 20 nm. It is important to detect nitrogen in these defects. The number density is about  $10^9$  to  $10^{10}/\text{cm}^3$ . On the other hand, nitrogen is not detected in the as-grown defects of D-like defect zone. The shapes are octahedral and 14-sided polyhedral without whisker-like defects. The size is 20 to 30nm. The other defects are platelet void/oxide 100nm long.

After hydrogen annealing at 1200C for 1 hour, these grown-in defects change to octahedral shapes with whisker-like defects. In the case of the Ring-OSF zone, nitrogen is detected from surface covered the octahedral oxide precipitate and the whisker-like defects. On the other hand, in the case of D-like defect zone, nitrogen isn't detected.

Nitrogen doping effect on oxide precipitate in D-like defect zone would increase excess vacancies and enhance oxygen precipitation due to the many vacancies. Nitrogen doping effect in Ring-OSF zone would enhance immediately oxygen precipitation. Maybe nitrogen would become nuclei of oxygen precipitates.

Moreover, difference between the both effects will be shown clearly due to the proportion among  $996\text{cm}^{-1}(\text{N}_2)$ ,  $996\text{cm}^{-1}(\text{NO})$  and  $1018\text{cm}^{-1}(\text{NO}_2)$  absorptions<sup>3)</sup> using FTIR method. But we cannot still get the results using FTIR.

1) M.Iida, W.Kusakai, M.Tamatsuka et al.: Defect in Silicon, ECS PV99-1(1999), p499.

2) K.Nakai, Y.Inoue, H.Yokota, A.Ikari, J.Takahashi and W.Ohashi: Proc. of the 3<sup>rd</sup> International Sympo. on Adv. Scie. and Tech. of Silicon Materials(2000), p88.

3) N.Inoue and K.Tanahashi: JAPS Spring Mtg. Proc. (in Japanese), p473, 28p-S-7.



**The microscopic nature of gettering defects at  $R_p/2$   
in high-energy self-implanted silicon**

**R. Krause-Rehberg<sup>1</sup>, F. Börner<sup>1</sup>, F. Redmann<sup>1</sup>, J. Gebauer<sup>1</sup>, R. Kögler<sup>2</sup>,  
W. Skorupa<sup>2</sup>, P. Sperr<sup>3</sup>, W. Triftshäuser<sup>3</sup>**

<sup>1</sup>*Fachbereich Physik, Universität Halle, D-06099 Halle, Germany*

<sup>2</sup>*FZ Rossendorf, Postfach 510119, D-01314 Dresden, Germany*

<sup>3</sup>*Univ. der Bundeswehr, Inst. f. Nukl. Festkörperphysik, D-85577 Neubiberg, Germany*

contact: krause@physik.uni-halle.de; Phone +49-345-5525567; Fax +49-345-5527160

Gettering effects of diffusing Cu have been studied in high-energy self-implanted silicon (3.5 MeV). After implantation and subsequent RTA annealing (30 sec at 900°C), Cu diffusion was performed. Two getter zones at  $R_p$  and  $R_p/2$  were found by SIMS measurements in accordance to earlier literature results. The defects at  $R_p/2$  were studied using the positron beam technique with an improved depth resolution. Vacancy defects were found to exist in this zone. Positron lifetime spectroscopy shows that small vacancy clusters ( $n > 5$ ) are detected. Moreover, the S-W analysis of Doppler-broadening spectroscopy reveals that these vacancy clusters must contain Cu atoms. This is confirmed by the Doppler coincidence spectroscopy. The analysis of the spectra in the high-momentum region proves that the annihilation of positrons trapped in the vacancy clusters occurs partly by Cu core electrons. A quantitative estimation of Cu atoms detected in these clusters gives evidence that the vacancy clusters are the dominating gettering centers at  $R_p/2$ .



## Atomic configuration study of implanted F in Si based on experimental evidences and *ab-initio* calculations

**T. Hirose, T. Shano, R. Kim, H. Tsuji, Y. Kamakura, and K. Taniguchi**

Department of Electronics and Information Systems, Osaka University.  
hirose@cie.eng.osaka-u.ac.jp, Tel: +81-6-6879-7792, Fax: +81-6-6879-7792

Recently, we observed that implanted F atoms significantly suppress the activation and transient enhanced diffusion of boron in pre-amorphous Si layer. In order to elucidate physical mechanisms behind the experimental findings, we investigated the kinetics of F in Si through the experiments and *ab-initio* calculations.

Key features of the experimental results performed were as follows;

- (A) F atoms implanted into crystalline Si at 5 keV,  $1 \times 10^{15} \text{ cm}^{-2}$  diffuse out of the Si, after annealing at 820 °C for 1 min while those implanted into re-crystallized pre-amorphous layer remain in the bulk Si as shown in Fig.1.
- (B) B and F co-implantation into re-crystallized pre-amorphous layer suppresses boron activation in the tail region. The amount of deactivated boron was found to be proportional to that of F remaining in Si.

The experimental results (A) suggest that V type defects formed in the re-crystallized layer<sup>[1]</sup> capture implanted F atoms in the layer. From the experimental results (B), it is plausible that F-V and F-B interaction involve the suppression of B activation and diffusion as well.

In order to study the microscopic mechanisms behind the experimental results, we investigated F-V and F-B interaction by using *ab-initio* calculation based on a generalized gradient approximation. We used the efficient plane-wave ultrasoft pseudopotential code, and optimized Si lattice constants of 5.40 angstrom as well as a kinetic-energy cutoff of 150 eV, 64-atom supercells, and  $2 \times 2 \times 2$  Monkhorst-Pack **k**-point sampling.

The calculated results revealed that F interacts strongly with V and B. For the case of F-V calculations, F moving around V is captured with a Si dangling bond. There exist two types of stable F configuration around V without appreciable energy difference; planar (Fig 2) and three-dimensional structures. F-B calculation also demonstrated that F atom intrudes into a Si-B bond and pushes the substitutional B away from its position, resulting in one stable configuration.

[1] Jun Xu et al., Appl. Phys. Lett. 74, 997

(1997)

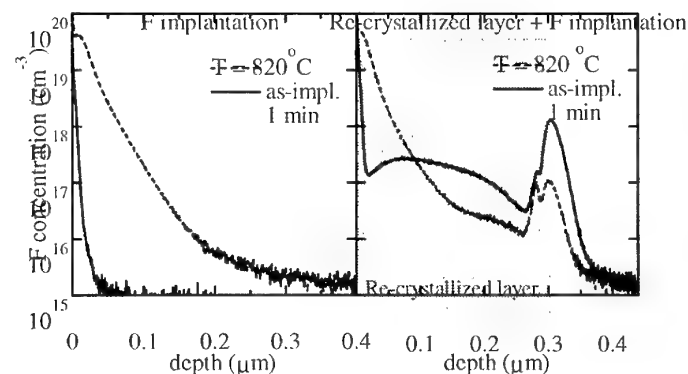


Fig 1. Experimental results

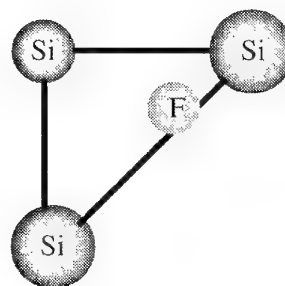


Fig 2. One of the stable F-V configurations



**September 26, 10:40 - 12:20**

**Session 6**

**Contactless Techniques**





## **Contactless Surface Charge Semiconductor Characterization**

**Dieter K. Schroder**

Department of Electrical Engineering, Center for Solid State Electronics Research,  
Arizona State University Tempe, AZ 85287-5706  
Tel.: (480) 965-6621, Fax: (480) 965-8118, e-mail: [schroder@asu.edu](mailto:schroder@asu.edu)

Surface voltage and surface photovoltage have become important semiconductor characterization tools, largely because of their contactless nature and the availability of commercial equipment. The use of these contactless measurement techniques has broadened from initial application of minority carrier diffusion length measurements to a wide variety of semiconductor characterization, including surface voltage, surface barrier height, flatband voltage, oxide thickness, oxide charge density, interface trap density, mobile charge density, oxide integrity, generation lifetime, recombination lifetime, and doping density. It is likely that this range of application will broaden further. As with all characterization techniques, there are limitations but they are compensated by the contactless nature of the measurement.

## Full wafer non-contact mapping of electrical properties of ultra-thin advanced dielectrics on Si

**Piotr Edelman, Jacek Lagowski, Alexandre Savtchouk, Marshall Wilson, Andrey Aleynikov and Joaquin Navarro**

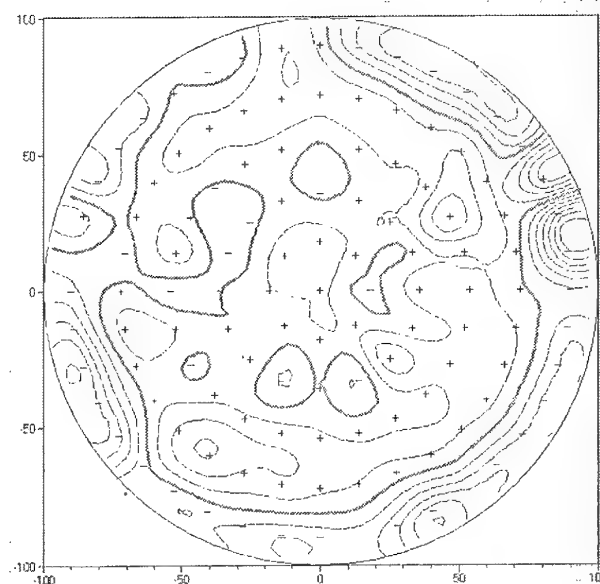
Semiconductor Diagnostics Inc. 3650 Spectrum Blvd. #130, Tampa, FL 33612 USA  
phone: 813.977.2244, fax: 813.977.2450, e-mail: [sditampa@sditampa.com](mailto:sditampa@sditampa.com)

The shrinking size of semiconductor devices had created the need to increase the capacitance per unit area of CMOS gates. This led to manufacturing of extremely thin  $\text{SiO}_2$  layers (5 to 20 Å), approaching their limits in terms of leakage and reliability, and to a search of advanced dielectrics with higher dielectric constants. The ability to characterize the fundamental properties of these materials, like electrical capacitance and thickness, is becoming essential to development of new technologies.

An answer to these needs is coming from a new dielectric metrology that involves controlled deposition of thermalized ions with a corona discharge and non-contact measurement of the dielectric response with a Kelvin or Monroe type probe. At DRIP 1997 we presented fundamentals of this metrology and typical applications for  $\text{SiO}_2$  with thickness exceeding 40 Å. Extension to ultra-thin dielectrics has been realized only recently. It required overcoming the effects of direct tunneling leakage current that neutralizes corona ions. This paper discusses a corresponding Self-Adjusting-Steady-State (SASS) method that enables very precise measurement of oxide with thickness below 20 Å with sensitivity of 0.01 Å. SASS whole wafer maps of oxide capacitance or electrical oxide thickness are presented together with non-contact I-V characteristics and maps of the oxide leakage current measured in a direct tunneling regime. SASS  $T_{\text{ox}}$  and SASS I-V are two of the most important parameters in characterization of advanced gate dielectrics for semiconductor IC's.

SASS  $T_{\text{ox}}$  map for 200mm wafer. Thicker contour line denotes the average thickness, + and - signs mark areas above and below the average

min: 13.5Å; max: 15.6Å;  
avg: 14.7Å; stddev: 0.31Å;  
increment: 0.17 Å; 12 levels



## MINORITY CARRIER LIFETIME SCAN MAPS APPLIED TO IRON CONCENTRATION MAPPING IN SILICON WAFERS

**O. PALAIS<sup>1</sup>, E. YAKIMOV<sup>2</sup> AND S. MARTINUZZI<sup>1</sup>**

<sup>1</sup>UMR TECSSEN, University of Marseilles

Faculté des Sciences et Techniques de Marseille St Jérôme, Case 231

13397 Marseille Cedex 20, France

e-mail: olivier.palais@tecsen.u-3mrs.fr

<sup>2</sup>Institute of Microelectronics Technology – Russian Academy of Science

Chernogolovska 142432, RUSSIA

In processed silicon wafers, impurity concentrations in the  $10^{10}\text{cm}^{-3}$  range (and below) can be deduced from minority carrier lifetime  $\tau$  measurements when the impurity atoms are the main source of recombination centers. Moreover, in some cases, as in the case of iron, it is possible to ascribe the recombination centers to a specific impurity and to evaluate its concentration.

$\tau$  can be determined by the contact-less phase-shift  $\mu\text{W-PS}$  technique i.e. by the measurements of phase shift between a near infrared modulated optical excitation and the reflected power of microwaves. Such a technique works at a practically constant injection level and is suited to obtain scan maps of  $\tau$  with a lateral resolution of  $50\mu\text{m}$ , when the samples are moved by an X-Y stage powered by step motors.

In the present paper intentionally and in inadvertently iron contaminated Cz, FZ and multicrystalline p-type silicon wafers were studied by the phase-shift  $\mu\text{W-PS}$  technique. Contaminations resulted of in-diffusion of iron at  $900^\circ\text{C}$  for 1 hour from an electron gun evaporated iron layer or of samples annealed at  $1050^\circ\text{C}$  in an open tube furnace. Under phase-shift measurements wafer surfaces were passivated by an aqueous solution of iodine polyvidone.  $[\text{Fe}_i]$  was evaluated by the measurement of  $\tau$  before and after sample annealing at  $210^\circ\text{C}$  for 10min, which dissociates the iron boron pairs in p-type silicon.

The influence of the injection level was taken into account. Deep Level Transient Spectroscopy (DLTS) was used to determine  $[\text{Fe}_i]$  in boron doped FZ wafers (in the range  $5.10^{13}$  to  $3.10^{16}\text{cm}^{-3}$ ), to evaluate the dopant concentration for which our technique works at a low injection level and to precize the value of K in the formula which gives  $[\text{Fe}_i]$ :

$$[\text{Fe}_i] = K (1/\tau_{\text{Fei}} - 1/\tau_{\text{FeB}}) (\text{cm}^{-3})$$

The dependence of K on dopant concentration was measured and simulated. It is shown that the phase-shift technique allows to evaluate recombination center densities in the range  $10^9$  to  $10^{10}\text{cm}^{-3}$ . Iron concentration scan map (in fact interstitial iron associated with boron) in wafers with high enough dopant concentration was obtained by our technique with a lateral resolution of  $50\mu\text{m}$  and a sensitivity of a few  $10^{10}\text{cm}^{-3}$ .

In Cz wafers, the conventional ring pattern structure was revealed by the  $\mu\text{W-PS}$  technique in the lifetime scan map. In multicrystalline silicon it was found that the formation of iron-boron pairs does not occur at grain boundaries, probably because iron atoms precipitate preferentially at such defects and cannot form FeB pairs.



## Scanning Capacitance Microscopy on Semiconductor Materials

**V. Raineri**

*CNR-IMETEM Stradale Primosole, 50 - I 95121 Catania, Italy*

**F. Giannazzo**

*Dipartimento di fisica ed astronomia dell'Università, Corso Italia 57, 95129 Catania, Italy*

Scanning capacitance microscopy (SCM) provides images of the two dimensional (2D) free carrier distribution in a semiconductor with a spatial resolution of 20 nm and a dynamic range from  $10^{14}$  to  $10^{20}$  cm<sup>-3</sup> representing a quite powerful tool for characterisation of state-of-the art Si devices. According to the scaling trend in the silicon device roadmap, an improvement of this lateral resolution is necessary in order to characterise future ultra large scale integration (ULSI) devices. The technique can be applied to many semiconductor materials, and in particular we applied it to characterise implanted layers in SiC and base and emitter regions in SiGe HBTs. We demonstrate that it is also possible to obtain a higher resolution magnifying the sample region under investigation by angle bevelling. This approach obviously imposes to consider the carrier spilling in samples with junctions. An extensive study has been performed on many samples obtained by P or B implantation into both p and n-type (100) wafers, and the results indicate that the amount of spilling effect is in agreement with the models developed to date. The method was successfully applied directly to silicon devices (LDMOS, MDMOS, HBT) and it demonstrates that accuracy well below tip dimensions can be reached. Furthermore, for the first time we are experimentally determining the resolution on delta layers formed by MBE. We applied the techniques to ultra shallow structures, shallow junctions obtained by laser annealing of Si samples implanted with 20 keV BF<sub>2</sub> and on ultra-shallow junctions obtained by B implantation at energy below 1 keV and subsequent rapid thermal annealing. Moreover, Implants have been performed into patterned wafers with different feature sizes ranging from 0.8 to 5 µm. It is demonstrated that the B transient enhanced diffusion is strongly reduced with decreasing feature size below about 2 µm. This effect is related to the integral number of interstitials produced during ion implantation. The implication for the formation of ultra-shallow junctions in device structures is also discussed.

### **Presenting and contacting author:**

Filippo Giannazzo  
CNR-IMETEM  
Stradale Primosole, 50  
I-95121 Catania  
Italy

Tel.: 39 095 591912  
Fax: 39 095 7139154  
Email: raineri@imetem.ct.cnr.it





## **Microwave Photoconductivity Techniques for the characterization of semiconductors**

**G. Citarella, S. von Aichberger and M. Kunst**

Hahn-Meitner-Institut, Dept. Solare Energetik (SE5), Glienicker Strasse 100, 14109  
Berlin, Germany; e-mail: citarella@hmi.de, phone: 0049 (0)30 80622189,  
fax: 0049 (0)30 80622434

Photoconductivity is an excellent tool for the characterization of semiconductors or semiconductor devices for (opto)electronic applications. Photoconductivity can be measured in a contactless and non-invasive way in the microwave frequency range. For these reasons measurements of photoconductivity in the microwave frequency range are highly interesting.

In this work first the different ways to obtain the photoconductivity in the microwave frequency range will be discussed shortly. The standard method where photoconductivity is determined from the change of the microwave power reflection upon illumination will be treated more in detail.

Then the different ways of excitation:

- By pulse illumination
- By (harmonically) modulated illumination
- By stationary illumination

will be compared and the respective merits and appropriate applications discussed. Also the performance of spatially resolved measurements will be considered. The concepts developed will be illustrated at the end of experiments on Si wafers.

It will be shown that modulated illumination is appropriate for the determination of the minority carrier lifetime as a function of the injection level but details as storage of excess charge carriers in the space charge region cannot easily be distinguished and can even lead to an erroneous interpretation of the experimental data. These details can be observed after pulsed illumination, but a determination of lifetime as a function of the injection may be intricate. Scanning measurements appear to be most efficient with pulsed illumination where the spatial resolution is optimal and the measurements can be faster performed.



**September 26, 15:15 - 16:40**

**Session 7**

**Defects in silicon 2**





## Random Telegraph Signals: a local probe for single point defect studies in solid-state devices

**E. Simoen and C. Claeys<sup>1</sup>**

IMEC, Kapeldreef 75, B-3001 Leuven

[simoen@imec.be](mailto:simoen@imec.be); fax: (32) 16 281 844; phone: (32) 16 281 381

<sup>1</sup>also at E.E. Dept., KU Leuven, Kasteelplein 10, B-3001 Leuven, Belgium

Whenever the charge transport through a solid-state device is governed by a single defect, this will give rise to a discrete switching of the current through it. Different names exist, like burst or popcorn noise, although the most often used term is Random Telegraph Signal (RTS). Especially for small-area scaled devices, RTSs become increasingly important, so that there exists more than just academic interest in the subject nowadays.

The paper is organised as follows. In a first part, the main features of RTS will be defined and described. These comprise the amplitude and the up and down time constants. In many cases, the up time corresponds to the time it takes to capture a carrier, while carrier release (emission) governs the down period. Besides studying RTS in the time domain, one can also take the Fourier transform, resulting in a spectrum in the frequency domain. The spectral type corresponding to an RTS is a Lorentzian spectrum, characterised by a constant power spectral density at low frequency ( $f$ ) and a roll-off with  $f^2$  for higher frequencies. The corner frequency  $f_0$  corresponds to the 3dB point of the spectrum and is also related to the reciprocal characteristic time constant of the underlying trap.

In the second part, the RTS behaviour in submicron area MOSFETs will be described and methods for extracting the trap parameters will be highlighted. Besides the amplitude and the time constants, it is also possible to extract the position of the trap. In most cases, an RTS in a MOSFET originates from a defect in the oxide close to the Si-SiO<sub>2</sub> interface. By analysing the gate, drain and substrate bias dependence of the time constants and/or the amplitude, it is possible to extract both the lateral, i.e., along the channel and the depth position, i.e., the distance from the interface. However, as will be demonstrated, some types of RTSs occur in the bird's beak region of the LOCOS device isolation. Temperature dependent measurements enable to extract the activation energy for the carrier capture and emission. In addition, depending on the character of the underlying trap (attractive, neutral, repulsive) a different impact of the vertical electric field on the trap dynamics will be observed. Evidence will be given that for repulsive traps, Coulomb blockade effects can occur during carrier capture.

In a third part, it will be demonstrated that an RTS can also be used as a local probe for detecting other defects/charges at the interface. This will be illustrated for the case of a hot-carrier damaged MOSFET. Particularly in weak inversion, when few carriers populate the channel, RTS will be very sensitive to the local environment.

Finally, some examples will be given where RTSs occur in real-life applications. It has for example been observed that in proton-irradiated Charge-Coupled-Devices used in space, RTSs occur after some time. They are thought to originate from radiation defects/clusters, created in the silicon substrate. More recently, similar effects have been observed in CMOS imagers. From this, it is expected that the study of RTSs will become even more important when entering the nano-electronics and single-electronics era.



## Optical Anisotropy and Strain-induced Birefringence of Dislocation-free Silicon Single Crystals

**Tao CHU, Masayoshi YAMADA,  
Joerg DONECKER\*, Volker ALEX\*, and Helge RIEMANN\***

Dept. of Electronics and Information Science, Kyoto Institute of Technology,  
Matsugasaki, Sakyo-ku, Kyoto 606-8585, Japan

\* Institute of Crystal Growth, Max-Born-Strasse 2, Berlin, Germany

E-mail: [tchu@djedu.kit.ac.jp](mailto:tchu@djedu.kit.ac.jp), Tel:+81-75-724-7422, Fax:+81-75-724-7400

Cubic crystals such as silicon should be optically isotropic according to classical crystal optics that neglects spatial dispersion and takes into account only dipole-type transitions. However, Lorentz indicated the possibility of optical anisotropy in cubic crystals if one considers the polarization in a given point to be dependent not only on the value of the local field at that point but also its value in the close neighborhood, i.e., polarization being not only frequency but also wave vector dependent, and then predicted that the birefringence due to the optical anisotropy is a maximum for the cubic crystal for the light propagation along  $\langle 110 \rangle$  directions. Pastrnak and Vedam<sup>1)</sup> experimentally observed a small amount of birefringence due to this  $\langle 110 \rangle$  optical anisotropy and claimed that no birefringence was observed for  $\langle 100 \rangle$  and  $\langle 111 \rangle$  directions of propagation. In order to measure the birefringence induced in Si by residual strain as well as process-induced strain, our research group has recently developed a high-sensitive scanning infrared polariscope (SIRP)<sup>2)</sup>. By improving the SIRP, we followed the work done by Pastrnak and Vedam using dislocation-free Si single crystals. The improved SIRP was so sensitive to detect a small amount of strain induced by the gravity as well as by an extremely small external stress, although those effects were avoided in the actual experiment by using a special sample holder. We observed for the first time the optical anisotropy for  $\langle 100 \rangle$  direction of propagation, which was very small while observing the same optical anisotropy for  $\langle 110 \rangle$  direction of propagation. The  $\langle 100 \rangle$  optical anisotropy was not constant over the (100) cross-section of crystal measured but it was distributed inhomogeneously. The distribution could be separated into two components, i.e., one was symmetric to crystal orientation and the other was irregular. At the present stage, we presume that the origin of symmetric one is due to point defects and that of irregular one is due to surface chipping. More details will be discussed in the conference.

1) J. Pastrnak and K. Vedam, Phys. Rev. **B3**, 2567 (1971).

2) M. Fukuzawa and M. Yamada, J. Crystal Growth, in press (2001).



## Effect of Germanium and Boron co-doping during CZ-Si crystal growth

**F. Nishihori, K. Kashima and M. Watanabe**

Toshiba Ceramics Co., Ltd. 30, Soya, Hadano, Kanagawa, Japan.

E-mail : [nishihori@tocera.co.jp](mailto:nishihori@tocera.co.jp)

fax : +81-463-81-8416

phone : +81-463-84-6646

It was recently reported that a dislocation-free Si crystal could be grown by CZ method from un-doped melt without Dash-necking process using a heavily B and Ge co-doped seed with their concentration ratio of about 1/4 to 1/6<sup>(1)</sup>. In some similar experiments we also confirm that kind of seed is so useful that any types of dislocations caused by a thermal shock or a lattice misfit are not generated. But in spite of using the seeds, many dislocations caused by a lattice misfit at the interface between the seeds and the grown crystals are generated run by run. So, In order to determine the most suitable B/Ge concentration ratio to compensate the silicon lattice strain, we have measured the lattice constant parameters of silicon crystals with different B/Ge concentration ratio and un-doped silicon crystal. The B and Ge concentration of the crystals ranged  $(2.6 \text{ to } 2.7) \times 10^{19} \text{ atoms/cm}^3$  and  $(0 \text{ to } 2.5) \times 10^{20} \text{ atoms/cm}^3$  respectively. The B/Ge concentration ratio ranged 0 to 9.6. The oxygen concentration of all samples ranged  $(1.28 \text{ to } 1.38) \times 10^{18} \text{ atoms/cm}^3$  (old ASTM). We find out that the lattice constant parameter for un-doped silicon is 0.3571167(11) nm and the closest value to that is 0.3571106(26) nm for B/Ge co-doped silicon with B/Ge ratio 1/6.6. This value almost corresponds to the predicted value 1/6.15, when the lattice contraction/expansion coefficients of B and Ge are assumed to be  $5.46 \times 10^{-24} \text{ cm}^3/\text{atoms}$  and  $-8.87 \times 10^{-25} \text{ cm}^3/\text{atoms}$  respectively. These values are calculated based on the Vegard's law<sup>(2)</sup> using the tetrahedral covalent radii  $r(\text{B})=0.0853\text{nm}$  for B,  $r(\text{Ge})=0.1225\text{nm}$  for Ge and  $r(\text{Si})=0.1173\text{nm}$  for Si. Therefore we must research the generation mechanism of the misfit dislocation related to the growth condition and the diffusion of the impurities at the growth interface, but we cannot still get the result as for this issue.

- 1) X.Huang et al, JAPS Spring Mtg. Proc.(2001), p. 331, 31a-W-1, (in Japanese)
- 2) L.Vegard, Z. Phys. 5 (1921) p. 17
- 3) J.A.Van Vechten and J.C.Phillips, Physical Review B 2 (1970) p. 2160

## **Annealing Effect and Impurity Doping Effects on the Defect Generation in Interstitial-rich Si Crystals Observed by Infrared Microscope**

**Kazutaka Terashima<sup>1</sup> and Suzuka Nishimura<sup>2</sup>**

<sup>1</sup> Department of Materials Science and Technology,  
Shonan Institute of Technology  
1-1-25 Tsujido-Nishikaigan, Fujisawa, Kanagawa, 251-8511, Japan  
e-mail ; terasima@mate.shonan-it.ac.jp  
TEL +81-466-30-0226  
FAX+81-466-30-0226

<sup>2</sup> Keio University Faculty of Science and Technology  
3-14-1 Hiyoshi Kouhokuku, Yokohama, Kanagawa 223-8522, Japan  
e-mail; nishimura@stnt.elec.keio.ac.jp

We have reported the surface tension and viscosity of silicon melts decrease with adding boron into the melts(1). The temperature distribution was measured by inserting thermocouples into the growing crystals. These melt property variations change the temperature distribution at the growing interface. It has been found that the temperature gradient at the growing interface increases with boron addition, while the temperature gradient in the bulk melt decreases. This result indicates that the interstitial has a tendency to be dominant in the boron doped crystals.

We studied the extended defects in quenched crystals, prismatic punching out dislocations have been found in a crystals. These dislocations disappeared depending on the holding time just after pulling from the melt. This phenomenon is closely related with diffusion of point defects during the holding at high temperature.

We have next studied the extended defects in boron doped crystals. It should be noted that the prismatic dislocations have been markedly decreased in a boron doped crystals being interstitial rich even in quenched crystals without holding time. The crystal becomes remarkably uniform. This means the mechanical strength at high temperature much increases or the behavior of interstitial and/or oxygen atoms widely varied by doping boron. These defects were observed by infrared transparency microscope.

This paper describes the temperature distribution in a growing crystal with and without boron doping. And the generation of the extended defects in quenched crystals and annealing effects will be discussed in terms of quenching conditions. The effect of annealing with in-situ observation will also presented.

### References

- 1) H. Nakanishi, K. Nakazato and K. Terashima, Jpn. J. of Appl. Phys. 39 (2000) 6487.



**September 26, 17:10 - 18:35**

## **Session 8**

### **Electron Beam Methods**





## Direct Atomic Resolution Measurement of Electronic Structure Using EELS

P. E. Batson

IBM Thomas J. Watson Research Center  
Yorktown Heights, New York 10598

It has become increasingly clear in recent years that integrated circuits will soon rely on switching devices that are only a few atoms in size. These devices will probably rely on physical behavior that is unique to this very small size. A good example of this might be the single electron transistor, which depends on Coulomb blocking of the conductance channel by the presence of a single additional electronic charge. It becomes necessary, therefore, that analytical equipment become sensitive to the electronic behavior of atomic-sized regions of materials.

The Scanning Transmission Electron Microscope (STEM), operating in the 100-200KeV range, has obtained electron probe sizes of 0.15-0.3nm routinely. Electron Energy Loss Spectroscopy, using equipment that is compatible with the small probe, has obtained 0.2-2eV resolution spectra. This combination has allowed experiments using 1.0-20.0nm sized objects: large defects, thin layers, and small particles.

Some studies have been done to show the power of this combination: for instance atomic bonding at the Si-SiO<sub>2</sub> interface, bonding in grain boundaries in the strontium titanate materials, and electronic structure at different atomic positions in a misfit dislocation at the GeSi-Si interface.

Future work will require that these studies become much more reproducible and accurate. Probe sizes must become smaller than 0.05-0.10nm in order to become sensitive to isolated regions near single atoms. This is becoming possible by use of computer controlled multipole lens combinations to reduce and optimize electron optical aberrations in the probe forming system. Electron energy loss resolution must be reduced to the 20-100meV level so that these experiments will can reveal electronic structure which is relevant to operation of the switching device. This operation requires invention of electron source monochromatization and improved spectrometers. The new instruments will be operated through use of extensive digital control, increasing the precision and reproducibility of the results.

Results obtained at this level will not only reveal expected behavior at greater precision, but should also reveal new, unexpected behavior. Therefore, the new equipment will require that we improve theoretical methods for understanding the results. For instance, it is commonly expected that X-ray Absorption and EELS experiments should produce similar results at some level of accuracy. On the other hand, it is also well known that EELS results can be more complex in detail, for instance depending on electron channeling conditions. In addition, electron scattering experiments clearly have an additional complication: an extra nearby charge introduced by the probe electron. New theoretical techniques need to be invented to predict the outcome of these conditions.

As these developments come together during the next few years, we can expect STEM and EELS will become essential to the successful development of sub-nm sized electron switching devices. This is truly an exciting time for instrumental and technique development.

## **Agglomeration of point defects at dislocations in compound semiconductors**

**H. S. Leipner, H. Lei, N. Engler**

Fachbereich Physik, Martin-Luther-Universität, D-06099 Halle  
leipner@physik.uni-halle.de, phone +49-345-55 25 453, fax +49-345-55 27 212

Line and point defects are influencing each other with respect to structure and properties. We have investigated in well-defined diffusion experiments the formation of extended point defect clouds around dislocations introduced by plastic deformation of GaAs and InP. Transmission and analytical electron microscopy, scanning cathodoluminescence microscopy, and micro-Raman investigations have been used to characterize various point defect complexes and microdefects agglomerated near the dislocations. The defect atmosphere around dislocations can only be described as a Cottrell cloud of dissolved impurities, when no precipitation of impurities occurs on the dislocation. In the other case, the point defect cloud can extend up to several micrometers, depending on the thermal treatment and cooling conditions. The experiments have been carried out with impurities diffusing on the Ga sublattice (copper) and with impurities on the As sublattice (sulfur). The simulation of the diffusion-drift behavior of sulfur and copper at dislocations provides in accordance with the experiment a non-equilibrium atmosphere. The numerical solution of the drift-diffusion equations taking into account the substitutional-interstitial diffusion mechanism yields not only the accumulation of impurities at dislocations but also of the interstitials taking part in the kick-out reaction of the diffusion. From the model experiments with copper and sulfur conclusions are drawn on the formation of an extended defect zone around dislocations in as-grown GaAs doped with Te, Si, and other impurities.



## Frequency-Domain EBIC Method for Mapping of Noise and Instability Regions in Semiconductor Devices

Alexander Satka and Daniel Donoval

*FEI STU, Department of Microelectronics, Ilkovicova 3, SK - 812 19 Bratislava,  
Slovakia*

*e-mail: [satka@elf.stuba.sk](mailto:satka@elf.stuba.sk), fax: 421-7-65423480, phone: 421-7-60291656*

Various defects, inhomogeneities, related noise and instabilities or oscillations and other non-standard phenomena play more and more important role in advanced semiconductor and optoelectronic devices. There exist various methods of their characterisation and analysis, but many of them suffer in providing the values averaged over the real-space because of a port nature of the device and unavailability to observe instant changes in given space at instant time.

We report on a frequency-domain EBIC method for investigation and analysis of noise enhancement and/or instabilities stimulated by generation-recombination effects under electron beam excitation of semiconductor devices. The main goal of the proposed method is direct mapping and visualisation of regions in which noise or instabilities are generated at different working conditions so that an increase in noise or instabilities can be directly attributed to real space.

Presented method is similar to static or quasi-static EBIC method. The excess carriers are generated by time-stable electron beam as in steady state EBIC method, which prevents any initialisation of oscillations or noise enhancement by time-varying or pulsing electron beam. Generated carriers are then collected by space charge region. In difference to the conventional EBIC method frequency spectra of induced current are calculated and subsequently saved for each position of a digitised rectangular raster. Resulting frequency-resolved real-space EBIC maps contain characteristics and quantitative values of noise or instabilities.

As an example frequency domain EBIC spectra were taken for different samples. The InGaAsP/InP avalanche photodiodes were investigated both by quasi-static and frequency domain EBIC method. Regions of noise enhancement corresponding to microavalanche defects have been clearly detected and visualised. Instability domains in Au / SI GaAs Schottky diode detector structures were mapped upon our best knowledge for the first time.

In conclusion, novel modification of EBIC method has been proposed and realised. It is the promising and effective non-destructive method for analysis of generation-recombination stimulated noise and instabilities present in semiconductor and optoelectronic devices. The method is supplementary but not complementary method to Time Resolved EBIC. In connection with the other SEM analytical methods it offers a new possibility to exactly investigate the phenomena in this area.



## CATHODOLUMINESCENCE AND EBIC STUDY OF TWIST AND TILT BOUNDARIES IN BONDED SILICON WAFERS

**T. Sekiguchi<sup>1</sup>, S. Ito<sup>2</sup> and A. Kanai<sup>3</sup>**

<sup>1</sup> Nanomaterials Laboratory, National Institute for Materials Science, Tsukuba 305-0047, Japan

<sup>2</sup> Institute for Materials Research, Tohoku University, Sendai 980-8577, Japan

<sup>3</sup> Naoetsu Electronics Co. Ltd., Kubiki-mura 942-0193, Japan

Presenting author: e-mail: sekiguchi.takashi@nims.go.jp

Phone: +81-298-59-2750, Fax: +81-298-59-2701

Direct bonding is a promising technique to fabricate artificial structures such as abrupt p-n junctions, 3-dimensional device structures etc.

Even in the bonding of flat surface wafers, the misorientation of two wafers inevitably introduces dislocation networks at the interface. We have regarded such bonding interfaces as the ideal grain boundaries and studied their electrical properties by means of electron-beam-induced-current (EBIC) technique. [1]

In this article, we have fabricated not only twist but also tilt boundaries of certain misorientation angles. Transmission electron microscopy showed that the dislocation networks were formed at the interfaces according to the twist and/or tilt angles if the bonding procedure was properly taken place.

The luminescence property of grain boundary was studied by cathodoluminescence (CL). At present, only one broad peak was observed in the CL spectra. The energy position of this peak was varied between 0.80 and 0.85 eV among the specimens. Such luminescence may be related to D1 or D2 lines of dislocation related defects rather than D3 and D4. No systematic relation with the misorientation angle was found yet.

The electrical activities of grain boundaries were observed by EBIC method. The EBIC contrast at room temperature was increased with the twist or tilt angle.

The control of electrical activities by decorating dislocation network with metallic impurities or hydrogen is now carrying out.

[1] K. Ikeda et al., J. Crystal Growth 210 (2000) 90.

**September 26, 18:35 - 20:00**

## **Session 9**

### **Electrical Methods**







## Electrical properties of SiC: characterisation of bulk crystals and epilayers

K. Irmscher

Institut für Kristallzüchtung, Max-Born-Strasse 2, D-12489 Berlin, Germany  
Tel: +49-(0)30-6392-3090, Fax: +49-(0)30-6392-3003, E-mail: irmscher@ikz-berlin.de

The recent progress in SiC semiconductor device technology for electronic and optoelectronic applications is based on the ability to grow high quality SiC substrates and epitaxial layers. Physical vapor transport (PVT) using a seed is at present the only growth method of technological importance for the bulk crystals. It takes place at high temperatures (about 2200 °C). Therefore, special care must be taken to avoid high concentrations of unintentional impurities and intrinsic point defects in the grown crystals to obtain the desired electrical parameters. The growth of homoepitaxial layers on PVT substrates by chemical vapor deposition (CVD) at temperatures of 1500..1600 °C improves the crystalline perfection and minimizes the incorporation of residual background impurities. This is a prerequisite for a reproducible adjustment of low concentrations of shallow-level dopants. For instance, high-voltage devices require active layers in the doping range down to  $10^{14} \text{ cm}^{-3}$ . The utmost importance of electrical characterization of the grown bulk crystals and epilayers is obvious. Whenever possible the electrical measurements should be combined with defect identifying methods like electron paramagnetic resonance (EPR) or luminescence.

After a short review of the published data on electrically active defects and impurities in SiC (with emphasis on the polytypes 4H and 6H) it is reported about the electrical characterization techniques which are applied to the crystals grown in our institute. Capacitance-voltage ( $C$ - $V$ ) measurements and deep-level transient spectroscopy (DLTS) are dealt with in more detail. For the necessary routine measurements of the shallow-level doping the  $C$ - $V$  method using Schottky contacts as probes has the following advantages over temperature dependent Hall effect measurements: (1) Even for ionization energies of the dopants greater than 50 meV the net doping concentration can be obtained at room temperature. (2) Epilayers on highly conductive substrates of the same conductivity type can be measured. (3) Depending on the contact area a moderate lateral resolution is attained making  $C$ - $V$  mappings a valuable tool. (4) It is possible to determine depth profiles. (5) The  $C$ - $V$  method is in a way non-destructive (at least the wafers can be recycled). Measurement examples are presented which demonstrate these advantages.

Because of the well known effect of deep-level defects (impurities) on minority carrier lifetime or on compensation they are also of special interest in SiC. Here it is reported on the incorporation of some metal impurities during the PVT growth of 6H-SiC bulk crystals. These investigations combine DLTS and EPR.



## Quantum effects associated with misfit dislocations in GaAs-based heterostructures

**T. Wosinski<sup>a</sup>, T. Figielski<sup>a</sup>, A. Makosa<sup>a</sup>, W. Dobrowolski<sup>a</sup>, O. Pelya<sup>a</sup> and B. Pécz<sup>b</sup>**

<sup>a</sup>*Institute of Physics, Polish Academy of Sciences, 02-668 Warsaw, Poland  
e-mail: wosin@ifpan.edu.pl, fax: +48 22 843 0926*

<sup>b</sup>*Research Institute for Technical Physics and Materials Science, Hungarian Academy  
of Sciences, Budapest 1525, Hungary*

In this paper we discuss a phenomenon of quantum interference of charge carriers flowing around misfit dislocations in heterostructures of III-V compound semiconductors. Misfit dislocations are formed at the interface in these heterostructures during their epitaxial growth to accommodate lattice mismatch between the substrate and the epilayer. Localized states of the dislocation core usually accept majority carriers from the corresponding energy band, thus causing that the dislocation line becomes electrically charged and is screened by a cylindrical region (so-called Read cylinder) of the space charge of opposite sign, formed by ionized donors or acceptors.

We investigated two types of heterostructures,  $p^+-n$  GaAs/GaAsSb junctions, grown by liquid phase epitaxy, and  $n^+-p$  GaAs/InGaAs junctions, grown by molecular beam epitaxy, containing up to 3% of Sb or In in the ternary compound. Owing to a small lattice mismatch between different components of the heterostructures regular arrays of  $60^\circ$  misfit dislocations were generated at their interfaces. They have been revealed by means of transmission electron microscopy applied in both cross-sectional and planar configurations.

We have found that the misfit dislocations give rise to low-temperature magnetoconductance oscillations in both types of heterostructures. Under high magnetic field, transverse with respect to the current through the heterostructure, the oscillations are periodic in magnetic field. Their period, of the order of 1 T, varies with the angle between the magnetic field direction and the dislocation axes. A peculiar feature of the oscillations is that the positions of individual conductance maxima and minima shift on the magnetic field scale with varying bias voltage applied to the heterostructure.

We interpret the revealed oscillations in terms of quantum interference of charge carriers flowing across an array of parallel dislocations. Under strong magnetic field, applied parallel to the dislocation axes, localized orbits encircling Read cylinders around dislocations are formed cyclically whenever the magnetic flux enclosed inside the cylinder is changed by one flux unit  $h/e$ . Capture of free charge carriers on these quasi-stationary orbits give rise to oscillations of the structure conductance. We discuss a possible use of the discovered phenomenon as a tool for the investigation of misfit-dislocation features inaccessible by other methods.



## Defect Specific Topography of GaAs Wafers by Microwave- detected Photo Induced Current Transient Spectroscopy

B. Gründig\*, M. Jurisch\*\*, and J.R. Niklas\*

\* Technical University Bergakademie Freiberg, Germany,  
email: [niklas@physik.tu-freiberg.de](mailto:niklas@physik.tu-freiberg.de)

fax: (+49)-(0)3731-39-4314, phone (+49)-(0)3731-39-2860

\*\* Freiburger Compound Materials GmbH, Freiberg, Germany

Topographic experiments turned out to be very powerful tools for the technological improvement and for a better basic understanding of the properties of inhomogeneous materials such as GaAs. As it is well known, these experiments in general deliver valuable pieces of information for the optimisation of different parameters in material production. On the other hand, also a deeper understanding of the correlation between defect spatial distribution and mesoscopic inhomogeneities of e.g. the electrical conductivity arises from different topographic experiments. So far mainly photoluminescence, infrared absorption, light scattering and dc-conductivity experiments were developed for topographic purposes and successfully applied.

However, despite these possibilities there was so far a clear lack of methods capable of providing direct identification of defect species along with their spatial distribution. The situation was even worse for the investigation of lower resistance GaAs material or for epitaxial layers. For the identification of defects, the well known Deep Level Transient Spectroscopy (DLTS) turned out to be the most appropriate tool to characterise defects by their energetic level position and their crosssection for the interaction with charge carriers. In many respects similar results can be obtained by measuring photoconductivity transients and evaluating them like the capacitance transients in DLTS experiments. These so-called Photo Induced Current Transient Spectroscopy (PICTS) experiments are feasible also for high resistance material, however, an exact information about the absolute concentration of defects is lost.

Recently, considerable progress was possible when detecting photoconductivity and even small transients of photoconductivity without the use of contacts by very high sensitivity microwave absorption. In GaAs it turned out that photoconductivity within a volume of a few  $(\mu\text{m})^3$  as induced by a small laser spot of bandgap light suffices for these experiments. This opens instantaneously the possibility of high resolution photoconductivity topography as a new tool of non-destructive material homogeneity inspection. The contrast in these topograms is determined by the total lifetime of excess carriers which is of direct relevance for many devices. Moreover, these experiments could now also be carried out under the constraints of a variable low temperature of the sample enabling the first non-destructive highly spatially resolved PICTS experiments for a directly defect specific topography.

Using various GaAs samples of different preparations, the possibilities of this new tool are demonstrated along with the first results for technologically relevant extrinsic and intrinsic defects. Similar results are also possible for other semiconductor materials.

**Nondestructive measurement of resistivity in bulk  $\text{In}_x\text{Ga}_{1-x}\text{As}$  crystals****M. Fukuzawa<sup>a</sup>, M. Yoshida<sup>a</sup>, M. Yamada<sup>a</sup>, Y. Hanaue<sup>b</sup> and K. Kinoshita<sup>b</sup>**<sup>a</sup>Kyoto Institute of Technology, Kyoto 606-8585, Japan<sup>b</sup>National Space Development Agency of Japan, Tsukuba 305-8505, Japan

E-mail: fukuzawa@dj.kit.ac.jp, FAX: +81-75-724-7400, Phone: +81-75-724-7439

$\text{In}_x\text{Ga}_{1-x}\text{As}$  crystals, which can realize much less lattice mismatch with  $\text{In}_x\text{Ga}_{1-x}\text{As}$ -based epitaxial layer than InP crystals used currently, are promising materials as substrates for fabricating laser diodes for the optical communication system. However, it is difficult to grow homogeneous  $\text{In}_x\text{Ga}_{1-x}\text{As}$  crystals on the ground, because of strong segregation and convective flow in the melt. Under microgravity environments in space, NASDA has planned to grow homogeneous  $\text{In}_x\text{Ga}_{1-x}\text{As}$  crystals [1]. If such a crystal is successfully grown in space, it becomes a quite unique and precious sample. Therefore, it is strongly required to evaluate nondestructively the characteristics such as resistivity which is generally evaluated destructively. For nondestructive measurement of resistivity in compound semiconductor, we have developed a non-destructive resistivity measurement (NDRM) technique [2,3], which is based on a Fourier analysis of charge response in a metal-insulator-semiconductor-metal (MISM) structure, not on the direct measurement of time-dependent charge response [4]. The MISM structure consists of a probing electrode, an air gap, a slice of semiconductor sample and a plate electrode on which the sample is placed. We applied a symmetrical bipolar square wave to the MISM structure and analyzed its charge response by Fourier transform. These techniques enable us to avoid unwanted effects such as constant charge-up in sample which increases measurement time in mapping of resistivity and to compensate transfer function of whole electronic circuits which cover from the probing electrode to the output of charge-amplifier. In this paper, we present two-dimensional maps of resistivity measured in bulk  $\text{In}_x\text{Ga}_{1-x}\text{As}$  crystals. Samples used here were sliced along and across the growth axis of cylindrical ingot grown by normal freezing with vertical Bridgman method. Indium composition was, in advance, also estimated nondestructively by using micro-Raman analysis [5]. Two-dimensional NDRM maps measured in several samples reveal inhomogeneous distribution of resistivity which may reflect crystal defects and/or inhomogeneity of impurities. The magnitude of resistivity is also varied with the increase of indium composition. From the experimental results, we can conclude that the nondestructive technique used here is useful for evaluating crystal quality of bulk  $\text{In}_x\text{Ga}_{1-x}\text{As}$ .

- [1] NASDA-TMR-990006E, National Space Development Agency of Japan (1999).
- [2] M. Fukuzawa and M. Yamada, in preparation.
- [3] M. Yamada, M. Fukuzawa, M. Akita, M. Herms, M. Uchida, and O. Oda, Proc. of the 10<sup>th</sup> Conference on Semiconducting and Insulating Materials (SIMC-X), pp.45-48, (1999).
- [4] R. Stibal, J. Windscheif and W. Jantz, Semicond. Sci. Technol. 6, pp.995-1001, (1991).
- [5] M. R. Islam, P. Verma, M. Yamada, M. Tatsumi and K. Kinoshita, Proc. of 12<sup>th</sup> Indium Phosphide and Related Materials (IPRM'01), in press (2001).

**September 27, 8:30 - 10:10**

**Session 10**

**Defects in  
Wide-gap Semiconductors**





**TEM characterisation of defects, strains and local electric fields in  
AlGaIn/InGaIn/GaN structures**

**D. Cherns**

H.H. Wills Physics Laboratory, University of Bristol, Tyndall Avenue, Bristol BS8  
1TL, UK

Tel: +44 117 9288702, Fax: +44 117 9255624, e-mail: [D.Cherns@bris.ac.uk](mailto:D.Cherns@bris.ac.uk)

GaN heterostructures have been used for a range of light-emitting diodes and laser diodes working towards the blue end of the visible spectrum, and are being intensively studied for high speed, high power electronic devices. It is clear, however, that the performance of these devices is dependent on the presence of threading defects, which can be present at densities up to  $10^{10} \text{ cm}^{-2}$ , and of local electric fields, which can exceed  $1 \text{ MV cm}^{-1}$ , in the vicinity of the active layers.

In our work, we have developed a range of electron microscope techniques to characterize the defects, their optoelectronic properties and the local electric fields in InGaIn/GaN and AlGaIn/GaN structures grown in the wurtzite structure on (0001)sapphire. Transmission electron microscopy (TEM) and convergent beam electron diffraction (CBED) have been used to clarify the nature of threading dislocations, nanopipes and inversion domains. Large angle CBED (LACBED) has been used to examine the local strains, thereby clarifying, for example, how dislocations propagate in epitaxial laterally overgrown (ELO) GaN. Electron holography (EH), carried out in a field emission TEM, has been used to profile the piezoelectric fields generated across strained InGaIn quantum wells, and, very recently, to show directly that threading edge dislocations in n-GaN are highly charged.

The paper will explain the techniques employed, and how the results have yielded an improved understanding of the role of microstructure on the performance of GaN devices.

## Complementary study of defects in GaN by photo-etching and TEM

J.L. Weyher<sup>1,2)</sup>, H.W. Zandbergen<sup>3)</sup>, F.D. Tichelaar<sup>3)</sup>, L. Macht<sup>1)</sup>, P. Hageman<sup>1)</sup>

<sup>1)</sup> Exp. Solid State Physics III, RIM, University of Nijmegen,  
Toernooiveld 1, 6525 ED Nijmegen, The Netherlands

Tel. +31 (0)24 365 3436, Fax +31 (0)24 365 2620, email jlw@sci.kun.nl

<sup>2)</sup> High Pressure Research Center, Polish Academy of Sciences, ul. Sokolowska 29/37,  
01-142 Warsaw, Poland

<sup>3)</sup> National Centre for HREM, Laboratory of Materials Science, Delft University of  
Technology, Rotterdamseweg 137, 2628 AL Delft, The Netherlands

Hetero-epitaxial GaN layers are characterized by a very high density of defects, which in the material grown on sapphire is in the range  $10^8$ - $10^{10}$  cm<sup>-2</sup>. In addition to this very high density of defects, different types of them are present depending on the growth conditions and polarity of the layer. In [0001] (i.e. Ga-polar) material dislocations constitute the predominating type of defects, while in [000-1] (i.e. N-polar) material also inversion domains (IDs) occur with a density approaching that of dislocations [1,2].

In this communication the results of photo-etching in aqueous KOH solutions under Xe lamp illumination (PEC method after Youtsey et al. [3]) of Ga- and N-polar hetero-epitaxial GaN layers grown on sapphire by MOCVD technique are presented. In Ga-polar layers PEC etching reveals threading dislocations in the form of typical straight nanometer-scale filamentary features. It has been confirmed by cross-sectional TEM on etched specimens that there is a one-to-one correspondence between the whiskers and threading dislocations. In N-polar layers more complicated etch features appeared after PEC etching. Detailed cross-sectional TEM study of this material revealed that apart from dislocations also inversion domains give rise to the formation of etch features. When the diameter of IDs remains in the tens of nanometer range, the defects are entirely resistant to the etching medium. However IDs with diameters approaching micrometer size are preferentially etched in their centers, resulting in the formation of pronounced crater-like etch features. This points at the recombinative property of inversion domain boundaries (IDBs). (PEC etching mechanism of GaN is similar to the mechanism of photo-etching of other III-Vs, e.g. GaAs, and depends upon supply of holes [4,5], therefore a local decrease of the etch rate at the defect site indicates a decrease of carriers (holes) which are necessary for dissolution of GaN). To the best of our knowledge this is a first experimental evidence of electrical activity of IDBs in GaN. In order to explain the behavior of IDs during PEC etching the models of IDBs and a possible influence of decoration by native defects will be discussed.

1. J-L. Rouviere et al., Inst. Phys. Conf. Ser. No 157 (1997) 173
2. P.D. Brown, J. Crystal Growth 210 (2000) 143
3. C. Youtsey et al., Appl. Phys. Lett. 73 (1998) 797
4. I.M. Huygens et al. J. Electrochem. Soc. 147 (2000) 1797.
5. G. Nowak et al. J. Crystal Growth 222 (2001) 735.





## Electrical and optical investigation of MBE grown Si-doped $\text{Al}_x\text{Ga}_{1-x}\text{N}$ as a function of Al mole fraction up to 0.5

M. Ahoujja<sup>a</sup>, J. L. McFall<sup>b</sup>, Y. K. Yeo<sup>a\*</sup>, R. L. Hengehold<sup>a</sup>, and J. E. Van Nostrand<sup>b</sup>

<sup>a</sup> Air Force Institute of Technology, Wright-Patterson Air Force Base, OH, USA

<sup>b</sup> Air Force Research Laboratory, Wright-Patterson Air Force Base, OH, USA

\* Yung.Yeo@afit.edu; Tel: (937) 255-3636 ext.4532; Fax: (937) 255-2921

$\text{Al}_x\text{Ga}_{1-x}\text{N}$  is of interest in the fabrication of high-temperature and high-frequency electronic devices as well as blue to UV light emitting and detecting devices. Despite the considerable effort concentrated on GaN, there have been relatively few studies on the growth, characterization, and device fabrication of  $\text{Al}_x\text{Ga}_{1-x}\text{N}$  alloys, especially for  $x > 0.3$ . In order to better understand the effects of impurities and native defects on the properties of  $\text{Al}_x\text{Ga}_{1-x}\text{N}$  films, we investigated the electrical and optical properties of  $\text{Al}_x\text{Ga}_{1-x}\text{N}$  as a function of Al mole fraction  $x$  up to 0.5, using temperature dependent Hall effect (TDH) and cathodoluminescence (CL) measurements.

$\text{Al}_x\text{Ga}_{1-x}\text{N}$  was grown by gas source molecular beam epitaxy (MBE) at 800 °C on  $\text{Al}_2\text{O}_3(0001)$  substrates with a 200 Å AlN buffer layer, followed by 1 μm of  $\text{Al}_x\text{Ga}_{1-x}\text{N}$ . The nominal Si doping level was  $1 \cdot 10^{18} \text{ cm}^{-3}$ . The CL spectra for the GaN show a donor bound exciton ( $\text{D}^0, \text{X}$ ) peak, a donor-acceptor pair (DAP) peak, and a yellow peak, which is believed to be due to a transition between a shallow donor and a deep level acceptor defect complex. On the other hand, the CL spectra for the  $\text{Al}_x\text{Ga}_{1-x}\text{N}$  show strong ( $\text{D}^0, \text{X}$ ) peaks and (DAP) peaks, but do not show the defect-related yellow peak. Although the value of the Al mole fraction was confirmed by x-ray diffraction, the band gap energies of  $\text{Al}_x\text{Ga}_{1-x}\text{N}$  estimated from the ( $\text{D}^0, \text{X}$ ) peak positions agreed with the predicted bandgap energies only for the  $x \leq 0.3$ , and did not correlate well with those for the  $x = 0.4$  and 0.5. This discrepancy is attributed to a large number of doped impurities and a large increase in the extended defects observed to occur for  $x > 0.3$ .

The TDH measurements for  $x \leq 0.3$  show that carrier concentration remains constant up to 30K, then decreases with temperature, reaching a minimum at 200K, and finally increases exponentially with temperature up to 650K. The constant carrier concentration below 30K is evidence of a parallel conduction path, which is believed to be due to dislocation defects near the interfacial region between the AlGaN and the sapphire substrate. For  $\text{Al}_x\text{Ga}_{1-x}\text{N}$  with  $x \geq 0.4$ , there are no measurable carriers and mobilities below 300 K, but carriers increase exponentially with temperature from 300 to 650K. These observations are consistent with TEM measurements that showed a dislocation density to be  $\sim 10^9 \text{ cm}^{-2}$  near the AlGaN/GaN interface. A two conducting-layer model was used to separate the carriers in the  $\text{Al}_x\text{Ga}_{1-x}\text{N}$  layer alone from the degenerate interfacial defect conducting layer. The carrier concentrations of  $\text{Al}_x\text{Ga}_{1-x}\text{N}$  samples were found to be significantly higher than the nominal doping value of  $1 \times 10^{18} \text{ Si/cm}^3$ .

In summary, both the electrical and optical measurements indicate that the properties of AlGaN layers are significantly affected by the native defects and the interfacial defect layers. The measurements also indicate that good quality  $\text{Al}_x\text{Ga}_{1-x}\text{N}$  films can be grown for  $x$  up to 0.3 by the gas source MBE method, but lesser quality films are obtained for  $x > 0.3$ , thus indicating a need for further improvement of the MBE growth technique.

## Below-Gap Recombination Dynamics in GaN Revealed by Time-Resolved and Two-Wavelength Excited Photoluminescence

**N. Kamata, J. M. Zanardi Ocampo, W. Okamoto, K. Hoshino\*,  
T. Someya\*, Y. Arakawa\* and K. Yamada**

Dept. of Functional Materials Science, Saitama University, Urawa, Saitama 338-8570,  
Japan e-mail:kamata@fms.saitama-u.ac.jp, Fax/Phone:+81-48-858-3529

\*Res. Center for Adv. Science and Techn., Univ. of Tokyo, Meguro-ku, Tokyo 153-  
8904, Japan

In order to optimize GaN-based light emitting devices, it is crucial to understand the origin of below-gap states and their nonradiative recombination (NRR) dynamics. We have selected a pair of below-gap states which gives rise to yellow luminescence (YL) in GaN and succeeded in determining their NRR parameters quantitatively by measuring a time-resolved and two-wavelength excited photoluminescence (PL).

Our typical sample, a 2.1  $\mu\text{m}$ -thick unintentionally doped GaN with a 25 nm-thick low-temperature buffer layer grown by MOCVD on a sapphire substrate, showed YL (2.26 eV) with an intensity  $I_A$  at 77 K under a conventional above-gap excitation (AGE) of 4.12 eV[1]. By superposing a below-gap excitation (BGE) light of 1.165 eV, the intensity decreased down to a new value  $I_{A+B}$ . This is interpreted in our two-states model, in which an optical excitation from a lower-energy state (state1) to higher one (state2) takes place and the increase of electronic population at state2 results in an enhancement of total NRR rate[2].

After interrupting BGE under constant AGE, the YL intensity recovered from  $I_{A+B}$  to its steady-state value  $I_A$  gradually with a time constant  $\tau$  which reflects directly the de-trapping process from the state2. With increasing BGE density to 5.2 mW/mm<sup>2</sup>, the ratio  $I_{A+B}/I_A$  decreased down to 0.20, while  $\tau$  increased up to 28 s at an AGE density of 2.21 nW/mm<sup>2</sup>. These data were utilized to determine the concentration and hole capture rate of the state2 as  $N_2=2.5 \times 10^{16} \text{ cm}^{-3}$  and  $C_{p2}=2.7 \times 10^{-9} \text{ cm}^3/\text{s}$ , respectively. The use of  $\tau$  released us from a fitting procedure on excitation-density dependence and improved the accuracy essentially.

Since the NRR parameters of the state1 were obtained by conventional PL as  $N_{t1}=5.2 \times 10^{14} \text{ cm}^{-3}$ ,  $C_{p1}=3.8 \times 10^{-6} \text{ cm}^3/\text{s}$  and  $C_{n1}=9.6 \times 10^{-11} \text{ cm}^3/\text{s}$ , quantitative understanding on the NRR process among below-gap states became possible based on this method. The BGE-energy dependence of  $\tau$  and  $I_{A+B}/I_A$  showed close correlation with YL spectrum, indicating the energy dependent recombination dynamics among below-gap states.

[1] J. M. Zanardi Ocampo et al., Proc. Int. Workshop on Nitride Semicond., IPAP Conf. Ser., 1, pp. 544-547, 2000; N. Kamata et al., Proc. Int. Conf. on Phys. Semicond., E21, 2000.

[2] N. Kamata et al., Recent Research Developments in Quantum Electronics, 1, pp. 123-135, Transworld Res. Network, 1999.

## Electrical and optical properties of defects in proton-irradiated GaN epilayers

A.Castaldini\*, A.Cavallini\*, L.Polenta\*, N.Armani<sup>#</sup> and G.Salviati<sup>#</sup>

\* INFN and Dipartimento di Fisica, Università di Bologna, Italy

<sup>#</sup> Istituto CNR-MASPEC, Parco Area delle Scienze, Parma, Italy

Electrical and optical activity of defects in GaN layers grown by hydride vapor phase epitaxy (HVPE) on a sapphire substrate has been investigated before and after irradiation. The influence of native and of irradiation-induced defects, both point-like and extended, on the electrical and optical characteristics has not yet fully understood, although it has been assessed that the dislocations from the epilayer-sapphire substrate interface to the GaN bulk severely affect the transport properties.

This contribution deals with defect induced by proton irradiation in GaN epilayers. To investigate the defect nature the epilayers, the thickness of which ranged between 30 and 40  $\mu\text{m}$ , have been irradiated with 24 GeV protons at a fluence of  $7.5 \times 10^{13} \text{ cm}^{-2}$ .

Electron Beam Induced Current (EBIC) and CathodoLuminescence (CL) analyses have been performed before and after irradiation. The CL spectra have been collected at electron energies varying from 0.5 to 40 KeV and from cryogenic to room temperature. EBIC and CL results have been acquired both in planar and normal collector geometry and compared to get deeper information on the role that deep levels associated to defects play in the recombination mechanism.

This investigation has evidenced the presence of a radiation induced clustering mechanism of electrically activated dislocations.

Spectral photocurrent (PC) analyses have been also carried out. They have clearly shown four well separated emission bands underneath the broad yellow band typical of GaN layers, whose wavelengths correspond to blue, green, yellow and red emission.

In the irradiated samples CL and PC results obtained in normal collector geometry have evidenced the increase of the yellow band intensity by approaching the buffer/substrate interface and a decrease of the near band edge emission. Also DLTS performed in planar and cross-sectional configurations have shown an in-depth distribution of deep levels than can be related to the yellow luminescence.



**September 27, 10:40 - 12:20**

**Session 11**

**Cathodoluminescence**



## **Cathodoluminescence of (Al,Ga)As and (Al,Ga,In)N heterostructures grown by molecular beam epitaxy**

**U. Jahn**

Paul-Drude-Institut für Festkörperphysik, Hausvogteiplatz 5-7, 10117 Berlin, Germany  
[ujahn@pdi-berlin.de](mailto:ujahn@pdi-berlin.de), phone: (030)20377523, fax: (030)20377515

Lateral inhomogeneous distributions of non-radiative recombination centers and lateral parameter variations affecting the band edge energy of semiconductors are easily imaged by luminescence methods in connection with scanning techniques. Advantages of cathodoluminescence spectroscopy (CL) in a scanning electron microscope are the adjustable excitation depth and unlimited possibilities in terms of the excitation for wide band gap semiconductors. Monochromatic CL images of semiconductor quantum wells (QW) show usually a random bright/dark pattern reflecting lateral parameter fluctuations. For correlation lengths of the fluctuations on a nm-scale, the period of the respective CL intensity variation is determined by the lateral resolution. The modulation depth of the CL intensity, however, contains information about the length scale of the fluctuation. Examples of growth related parameter variations of GaAs/(Al,Ga)As QW structures fabricated by molecular beam epitaxy on patterned and unpatterned GaAs substrates are discussed. The CL contrast in quantum well wire structures (QWR) is a measure for the transfer efficiency of injected carries between the connecting QW regions and the QWRs. Its temperature dependence reveals carrier loss mechanisms such as thermally activated non-radiative recombination channels or re-emission out of the QWRs and QWs.

Electronic properties of (Al,Ga,In)N heterostructures grown on sapphire or SiC substrates are essentially governed by strain induced piezoelectric fields, which in turn contribute to an enhancement of lateral fluctuations of both the CL peak energy and the CL intensity. The influence of inhomogeneous electric fields and localization effects due to composition fluctuations has been investigated in (In,Ga)N/GaN multiple QWs with different well widths containing a fully screened single QW. The presence of electric fields has been checked by variations of the CL excitation density (field screening) and by time resolved photoluminescence investigations. Depending on the growth conditions, the temperature dependence of the CL peak energy is dominated by localization and tail state filling or by electric field effects. Threading dislocations appear to serve as accumulation centers for In decomposition.

Plastic deformation properties of 1  $\mu\text{m}$  thick GaN layers grown on sapphire have been investigated by nano-indentation in connection with CL and transmission electron microscopy (TEM). In the CL images, the indentation is surrounded by dark line defects arranged in a hexagonal symmetry indicating a high crystalline quality of the layers. The region of these extended defects is characterized by a blue-shift of the near-band-gap CL indicating the presence of tensile strain, which is clearly correlated with the appearance of the dark lines. For large loads, the formation of dark line defects is accompanied by the occurrence of micro-cracks in the layer.

## Electrical Characterization and Cathodoluminescence Microanalysis of AlN/GaN Heterostructures

**S. M. Hubbard<sup>1</sup>, D. Pavlidis<sup>1</sup>, V. Valiaev<sup>1</sup>, M. A. Stevens-Kalceff<sup>2</sup>, I. M. Tiginyanu<sup>3</sup>**

- 1) EECS Department, The University of Michigan, 1301 Beal Ave., Ann Arbor, MI 48109-2122, USA, Tel: (734) 763-6132, Fax: (734) 763-9324, E-mail: [hubbards@umich.edu](mailto:hubbards@umich.edu)
- 2) Department of Applied Physics, University of Technology, Sydney, NSW 2007, Australia
- 3) Lab of Low-Dimensional Semiconductor Structures, TU Moldova, Chisinau 2004, Moldova

MODFET's based on the III-Nitride group of materials have recently shown great promise for high-frequency/high-power applications. For the most part, these devices are based on low Al composition AlGaN/GaN type heterostructures. However, because AlN has proved to be a good insulating material with high dielectric constant, we consider here the possibility of using an AlN/GaN system to create metal-insulator-semiconductor field effect transistors (MISFETs). Low-pressure OMVPE is used to grow AlN/GaN MIS-type heterostructures with AlN thickness between 30 Å and 300 Å. X-Ray Diffraction, X-Ray Reflectivity and Atomic Force Microscopy were used to probe GaN and AlN material quality, thickness and surface morphology, respectively. The electronic properties of the 2DEG were investigated using temperature dependent Van der Pauw Hall-effect measurements. Surfaces of the thicker AlN layers exhibit defects 100-200 nm in size propagating out from dislocations in the underlying GaN channel layer. These defects are seen to decrease in size and density for very thin AlN layers, indicating the presence of an initial AlN wetting layer. As the AlN thickness was increased, 2DEG sheet carrier concentration increased and Hall mobility decreased. The decrease in electron mobility with increasing AlN thickness is related to a higher percent of the sheet carrier concentration being located very near the interface for thicker AlN. The optimal AlN thickness was found to be approximately 50 Å. The measured room temperature and 20K mobilities for this sample were 980 cm<sup>2</sup>/Vs ( $n_s=8.14 \times 10^{12}$  cm<sup>-2</sup>) and 3230 cm<sup>2</sup>/Vs ( $n_s=7.76 \times 10^{12}$  cm<sup>-2</sup>), respectively. The Cathodoluminescence (CL) experiments were carried out in a Scanning Electron Microscope (SEM) equipped with CL imaging and spectral analysis system. CL and SEM images taken from different areas of the same sample prove the uniformity of emission characteristics and morphology along the surface. CL spectra consist of two GaN-related bands with the maxima at 3.4 eV and 1.9-2.3 eV. Under surface excitation (electron beam energy 3 keV) the intensity of the red-yellow CL relative to the intensity of the UV emission was found to increase with the increase of the AlN film thickness. The increase in red-yellow CL intensity correlates well with the decrease in electron mobility, indicating a relationship between recombination and scattering processes in GaN at the interface. Study of morphology, electrical characterization and CL microanalysis show the possibility to use OMVPE for growth of device quality AlN/GaN MIS-type heterostructures. This work was supported by ONR under Grants N00014-92-J-1552 and N00014-00-1-0879 as well as by NRC under COBASE Program.



## Cathodoluminescence Microscope Observation of Hollow Caves Induced in 6H-type SiC Wafer

**Toshiyuki ISSHIKI<sup>a</sup>, Hiroshi SAIJO<sup>a</sup>, Shigehiro NISHINO<sup>a</sup> and  
Makoto SHIOJIRI<sup>a, b</sup>**

<sup>a</sup>Department of Electronics and Information Science, Kyoto Institute of  
Technology, Matsugasaki, Sakyo-ku, Kyoto 606-8585, Japan

<sup>b</sup>Department of Anatomy, Kanazawa Medical University, Uchinada,  
Ishikawa 920-0293, Japan

E-mail: [issniki@dj.kit.ac.jp](mailto:issniki@dj.kit.ac.jp) Phone & Fax: +81-75-724-7448

Silicon carbide (SiC) is expected as a material for devices usable at high temperature and for high power electric circuits. However, development of the SiC devices is prevented by the defects such as stacking faults and micropipe. This paper deals the cathodoluminescence (CL) microscopy on defects in 6H-type SiC wafer.

An SiC wafer was epitaxially grown using the modified Lely method [1], where purified SiC powder was deposited on 6H-type (0001) SiC substrate in a graphite crucible heated at 2100 °C, in an atmosphere of  $2 \times 10^{-4}$  Pa Ar gas. The wafer grew with 6H structure having *c* axis perpendicular to the substrate and the wafer thickness was 1.5 mm after 3-hour growth. The (0001) grown surface of the wafer was mechanically polished with diamond paste. CL images were obtained with a microscope based on Topcon DS-130 secondary electron microscope (SEM) operated by RGB full-color mode [2] using two dichroic mirrors for color separation at 500 and 600 nm. The polished surface of the wafer and its cross-section exposed by cleavage were observed.

Luminescence patterns having hexagonal outline of several ten  $\mu\text{m}$  in size and yellowish green color were observed in a CL image of the polished surface, while no corresponding pattern appears in an SEM image of the same area. The difference between the images suggests that a structure giving the luminescence stays not near the polished surface but deep inside. A wavelength of the luminescence is about 580 nm and the luminescence around the hexagonal pattern is stronger than one from the inside. Cross-sectional SEM observation revealed that a hollow cave surrounded by flat surfaces exists in the cleaved wafer. Size of the cave is several ten  $\mu\text{m}$  in width and several  $\mu\text{m}$  in height. Strong CL emission at the area within  $1\mu\text{m}$  from the surface of the cave and weak one at belt like area from an edge of substrate side to the cave with almost the same width as the cave was detected at wavelength of 580nm. The result of cross-sectional observation agrees with one obtained by observation of the polished surface about the wavelength and size of radiation area. Therefore, there are the caves having hexagonal shape inside the SiC wafer. The strong CL emission suggests that radiation centers of the luminescence are localized at the region within  $1\mu\text{m}$  from the surface of the cave. It can be considered that the lattice distortion and/or impurities on the surface provide a lot of recombination sites and affect badly the electronic property. More results of observations for other defects will be discussed in the conference.

[1] Yu.M. Tairov and V.F. Tsvetkov, *J. Crystal Growth*, **52**, 146 (1981).

[2] H. Koike, T. Nakano, T. Fujimoto and K. Ogawa, "Proc. EUREM88", **3** 591 (1988). T. Nakano, T. Fujimoto, H. Koike and K. Ogawa, *Acta Histochem. Cytochem.* **23**, 753-767 (1990).

## Dyn SEM CL of glide dislocations in GaAs and CdTe

**J. Schreiber, L. Höring, U. Hilpert**

Fachbereich Physik, Friedemann-Bach-Platz 6, Martin-Luther Universität, D-06108  
Halle, Germany

Dynamic mode of high-resolution CL microscopy as provided by SEM technique, referred to as Dyn SEM CL, is employed in detailed studies of the relationship between dynamic properties and intrinsic recombination activity of glide dislocations in GaAs and CdTe as typical semiconductor materials with zincblende structure. Systematic examinations have been performed at crystallographically defined defect configurations generated in the stress fields of microindents and scratches on the low-indexed (001), (110) and (111) sample surfaces. The occurring edge-type dislocation segments with polar A(g) and B(g) core structure as well as the screw dislocation segments were characterised by radiative or non-radiative CL contrast behaviour. The Dyn SEM CL findings reflect their recombination activity during glide movement.

Distinct tangential glide processes in various  $\{111\}\langle 1-10 \rangle$  glide geometries, in particular, nucleation and propagation of extended surface-parallel dislocation half-loops consisting of a polar A(g) or B(g) edge-type dislocation accompanied by corresponding screw-type line segments, have been observed by means of the REDG effect and under conditions of in-situ micro-deformation at low temperature.

In GaAs, Dyn SEM CL experiments revealed differences in the dynamics of the Ga(g), As(g), and screw dislocation segments belonging to same half-loop structure, and gave evidence for the formation of  $30^\circ$  and  $90^\circ$  perfect dislocations as parts of the glide dislocation configuration. By the in-situ microdeformation studies in CdTe, an unexpected high dislocation mobility at low temperature ( $T=72\text{K}$ ) could be established. The microscopically resolved dislocation dynamics was further used to look for effects on the dislocation contrast behaviour due to defect reactions, e.g. annihilation of dislocation segments, dislocation bunching or variations of the geometrical defect position. A new mechanism of defect-related CL contrast formation found to be specific for high-speed dislocations (appearing in GaAs!) is discussed.

The results of the Dyn SEM CL observations confirm intrinsic recombination activity in all cases of the particular dislocation types investigated in both materials. However, dislocation recombination activity evaluated by values of measured line recombination velocity is found to be stronger in GaAs than in CdTe. In addition to their distinct recombination activities, the REDG response of dislocations in GaAs and CdTe turns out to be clearly different. For CdTe showing only weak REDG effect, a stress and thermal activation controlled kink dynamics may be concluded, whereas, in GaAs possessing a high Peierls potential, kink formation and migration are obviously affected by the local carrier recombination. There is no indication of kink sites as recombination centres to derive from the contrast behaviour during glide movement of the dislocations.

Most of the experimental results are prepared as movies for MS-powerpoint presentation supported by oral explanation.



## CATHODOLUMINESCENCE AND SCANNING TUNNELING SPECTROSCOPY OF ZnO SINGLE CRYSTALS

A.Urbieta<sup>1</sup>, Ch. Hardalov<sup>1\*</sup>, P. Fernández<sup>1</sup>, J.Piqueras<sup>1</sup> and T.Sekiguchi<sup>2</sup>

<sup>1</sup>Departamento de Física de Materiales, Facultad de Físicas, Universidad Complutense,  
28040 Madrid, Spain

<sup>2</sup> National Institute for Materials Science, 1-2-1 Sengen, Tsukuba 305-0047, Japan  
Presenting author: e-mail: arana@eucmax.sim.ucm.es.  
phone: 34-913944550, fax: 34-913944547

Bulk ZnO single crystals grown by the hydrothermal and alkali flux methods have been investigated by means of scanning tunnelling spectroscopy and time resolved cathodoluminescence. Measurements were performed in the different crystalline faces. The results from these measurements show that both, surface electrical properties and luminescent characteristics depend on the face studied.

Polar O-terminated surfaces show an intrinsic conduction behaviour with a surface band gap ranging from 0.4 to 0.8 eV. Zn-terminated surfaces show mainly n-type conduction. The non polar faces present either intrinsic or p-type behaviour. Cathodoluminescence spectra show that the relative intensity of the different components of the deep level band also depends on the atomic structure of the face under study. This complex behaviour is clearly revealed from the time resolved spectra. The differences observed are attributed to the nature of the defects present in each case and, in particular, to different impurity incorporation processes that could be mainly controlled by the atomic configuration and polarity of the planes.

\* Permanent address: Technical University, Department of Applied Physics, blvd.  
Kliment Ochridski No 8, Sofia, Bulgaria



**September 28, 9:00 - 10:25**

**Session 12**

**X-ray Techniques**





### X-ray diffractometry on (Al,Ga,In)-nitride layers

**N. Herres<sup>1</sup>, L. Kirste<sup>1,2</sup>, H. Obloh<sup>1</sup>, K. Köhler<sup>1</sup>, J. Wagner<sup>1</sup>, D.G. Ebling<sup>2</sup>, P. Koidl<sup>1</sup>**

<sup>1</sup>Fraunhofer-Institut für Angewandte Festkörperphysik (IAF)

Tullastrasse 72, D-79108 Freiburg, Germany

Email: [nikolaus.herres@gmx.de](mailto:nikolaus.herres@gmx.de)

FAX: +49 (761) 5159-400

Phone: +49 (761) 5159-578

<sup>2</sup>Freiburger Materialforschungszentrum

Stefan-Meier-Straße 21, D-79104 Freiburg, Germany

(Al,Ga,In)-Nitrides are important materials for photonic and electronic applications. The physical properties of the epitaxial layers depend on structural features like phase purity, texture, mosaicity, strains and chemical composition. These topics can be addressed by various X-ray diffraction techniques, which have been refined over the years to keep pace with the requirements.

After a brief overview on how X-ray diffraction can be applied to address problems common to the growth of III-V nitrides, we will concentrate on two aspects:

- ◆ *The X-ray determination of the composition of  $Al_xGa_{1-x}N$  and  $Ga_{1-x}In_xN$  layers.*  
We will present a safe and quick technique to accurately determine strained metrics from peak positions of the film alone without recurrence to eventually unreliable or unavailable lattice parameters of the substrate. The procedure works, no matter if a layer is pseudomorphically strained, partially relaxed, or completely relaxed, as long as the strain can be described as a uniaxial distortion parallel to the growth direction. A mathematical / graphical evaluation procedure will be shown which yields the layers chemical composition, once its strained metric has been determined.
- ◆ *The evaluation of a layer's defect structure from Reciprocal Space Maps.*  
Crystal defects usually lead to changes in the width and shape of X-ray diffraction peaks. The amount and orientation of the „peak broadening“ depends on the nature of the crystal defect and will in general be different for different reflections. Very often the broadening of a „rocking curve“ is used to quantify e.g. dislocation densities. However, such rocking curves represent *convoluted*, *projected* and *experimentally distorted* images of the actual situation in Reciprocal Space and should be looked upon with suspicion unless the nature of the crystal defect present is well known. We will detail several crystal defects typical for III-Vs and show their impact on the situation in Reciprocal Space. Based on these considerations, multiple-crystal X-ray measurements of an MBE grown  $Al_{0.5}Ga_{0.5}N$  film showing „natural“ ordering will be explained.

## X-ray topographic observation Strain mediated phase coexistence in MBE-grown MnAs films on GaAs

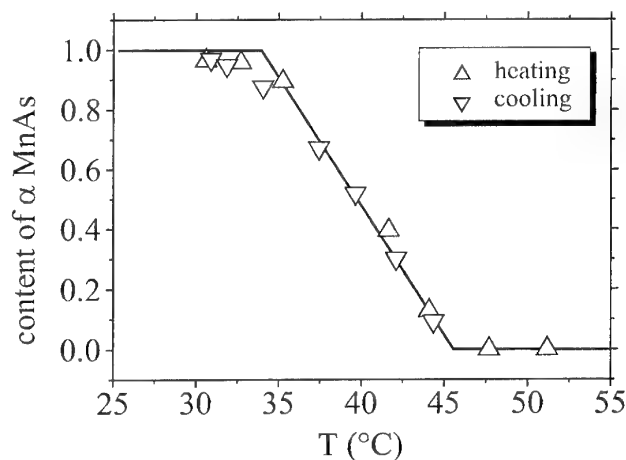
**Bernd Jenichen, Vladimir M. Kaganer, Frank Schippan,  
Wolfgang Braun, Lutz Däweritz, and Klaus H. Ploog**

Paul-Drude-Institut für Festkörperelektronik Hausvogteiplatz 5-7, 10117 Berlin (D)

Recently considerable effort has been made in connecting semiconductor and ferromagnetic materials to obtain hybrid magnetic-semiconductor devices e.g. in order to achieve spin injection. GaAs as a substrate allows the coupling of a magnetic material to semiconductor electronics and photonics. Thin ferromagnetic metal layers of MnAs have been grown epitaxially on GaAs and characterised by different methods [1,2]. For growth on As-stable GaAs (001) a unique orientation of the epitaxial MnAs layers is achieved with (-1100) MnAs parallel to the (001) GaAs surface and [0001] MnAs along the [1-10] GaAs direction. Transmission electron microscopy studies [2] show that every sixth GaAs {220} plane fits to every fourth MnAs {0002} plane resulting in a remaining effective mismatch of 5%. This mismatch, as well as the misfit of 7% in the perpendicular direction are released at the growth temperature by regular arrays of misfit dislocations. Difference in the thermal expansion coefficients results in strain at room temperature. We have determined the temperature dependence of strain by measuring the curvature of the samples.

The bulk MnAs crystals experience, near 40°C, a first order phase transition from the low temperature hexagonal ferromagnetic  $\alpha$ -phase to the high temperature orthorhombic paramagnetic  $\beta$ -phase. At this transition the unit cell shrinks in the hexagonal plane, while the height of the prism does not change. For thin epitaxial layers we have found that this phase transition does not occur at a certain temperature like in the bulk material. Rather, both phases coexist in a temperature range of about 10°C [3]. The fraction of the  $\alpha$ -phase shown in the figure is calculated from the integrated intensities of the observed hexagonal (-1100) and orthorhombic (020) reflections.

This phase coexistence is explained by a constraint of the lateral expansion of epitaxial layers which gives rise to strain in the layer. The phase coexistence is treated as a growth of elastically strained domains inside the layer.



[1] M. Tanaka et al. J.Appl.Phys.,  
76(1994)6278

[2] F. Schippan et al. J. Vac.  
Sci. Technol 17(1999)1716

[3] V.M. Kaganer et al.  
Phys. Rev. Lett. 85(2000)341





## **X-ray topographic observation of dislocation generation at the seed/crystal interface of CZ-Si highly doped with impurities**

**I. Yonenaga, T. Taishi,\* X. Huang\* and K. Hoshikawa\***

Institute for Materials Research, Tohoku University, Sendai 980-8577, Japan

\* Faculty of Education, Shinshu University, Nagano 380-8544, Japan

(E-mail: yonenaga@imr.edu, fax: +81 22 215 2041, phone: +81 22 215 2042)

The Dash necking with a 3-5 mm neck is generally recognized as a standard method to avoid dislocation introduction during crystal growth in the industry for more than 40 years. Recently, dislocation-free silicon crystals without the Dash necking has been successfully grown by the Czochralski (CZ) method using high doping of B impurity [1,2]. The success is important for development of large size Si crystals, being heavier than 500kg and is related closely to the suppression of the dynamic activities of dislocations by B impurity during the crystal growth [3]. In such a highly impurity doped Si crystals, it is found that an isolate dislocation is strongly immobilized by the impurities, which is interpreted in terms of dislocation locking due to impurity segregation. In the X-ray topographic experiments by which the elimination of dislocations from the grown crystals were confirmed, some interesting features on dislocation generation at the seed/crystal interface have been recognized on the dislocation generation during the seeding process affected by the concentration of B impurity and the concentration difference of the seed/crystal. Generally in the low B concentration case dislocations slipped by the thermal shock at dipping crystals were observed, while in the high B concentration case dislocations were generated parallel to the growth axis, caused by the misfit between seed and crystal. The results are very important to clarify the dislocation generation not only in the seeding process of bulk crystal growth but also in the hetero epitaxial growth, which are even now unclear. This paper reports the results of the X-ray topographic investigation undertaken with such a purpose in a consideration of dislocation activities in highly impurity doped Si crystals.

1. X. Huang, T. Taishi, I. Yonenaga and K. Hoshikawa, J. Cryst. Growth 216, 283 (2000).
2. X. Huang, T. Taishi, I. Yonenaga and K. Hoshikawa, Jpn. J. Appl. Phys. 39, L1115 (2000).
3. I. Yonenaga, T. Taishi, X. Huang and K. Hoshikawa J. Appl. Phys. (2001) in press.

## Misfit Dislocation and Threading Dislocation Distributions in InGaAs and GeSi/Si Partially Relaxed Heterostructures

<sup>a</sup>C. Ferrari, <sup>b</sup>G. Rossetto, <sup>c</sup>E. A. Fitzgerald

<sup>a</sup>C.N.R. Maspec Institute, Parco Area delle Scienze 37/A, 43010 Fontanini, Parma Italy. Email: [ferrari@maspec.bo.cnr.it](mailto:ferrari@maspec.bo.cnr.it), tel. 0039 0521 269222, fax 269206

<sup>b</sup>C.N.R. Ictima, Corso Stati Uniti 4, 35127 Padova, Italy

<sup>c</sup>Massachusetts Institute of Technology, Massachusetts Av., Cambridge, MA02139 USA

Single and compositionally graded InGaAs/GaAs and SiGe/Ge partially relaxed heterostructures of equivalent lattice mismatch and thickness have been characterized by high resolution X-ray diffraction and by X-ray double crystal topography in order to evaluate the degree of strain release and the distribution of misfit dislocations.

X-ray topography evidences a rapid decrease of the average length of misfit dislocation segments with the increase of the density of misfit dislocations both in InGaAs and GeSi/Si structures. For an equivalent amount of strain release, in SiGe/Si heterostructures shorter misfit dislocation lengths have been evidenced with respect to InGaAs/GaAs heterostructures.

The decrease of the misfit dislocation length is due to the blocking mechanism proposed by Samavedam and Fitzgerald [1]. The reduction of misfit dislocation length in GeSi/Si heterostructures with respect to InGaAs/GaAs ones can be probably attributed to the lower glide mobility of dislocations in Si based materials, as confirmed by a topograph of a metastable GeSi/Si heterostructure beyond the critical thickness.

If the threading dislocation density is evaluated from the lattice mismatch and the average length of the misfit dislocations on the basis of a simple formula, GeSi/Si heterostructures exhibit a much rapid increase of threading dislocation density as a function of strain release in comparison to equivalent InGaAs/GaAs ones.

Compositionally graded InGaAs/GaAs heterostructures show much longer misfit dislocation segments with respect to equivalent single heterostructures, thus confirming the effectiveness of composition grading to reduce the dislocation interaction ([2]-[3]).

[1] S. Samavedam and E. A. Fitzgerald, J. Appl. Phys., 81 (1997), 3108-3116

[2] Tersoff, J. 1992, Appl. Phys. Lett., 62, 693

[3] C. Ferrari, S. Gennari, and A. V. Drigo, Current Topics in Crystal Growth Research, Vol. 3 (1997) p. 143

**September 28, 10:50 - 12:30**

**Session 13**

**Miscellaneous Techniques**





## Scanning photoelectron microscopy and its application in characterisation of semiconductor interfaces

Maya Kiskinova

Sincrotrone Trieste, Area di Ricerca, 34012 Trieste, Italy

The ultrabright third generation soft x-ray sources have enabled us to overcome the poor spatial resolution of electron spectroscopy for chemical analysis (ESCA), considered as one of the major limitations of this most widely used method for investigating the composition, chemical state and electronic structure of solid surfaces and interfaces [1]. The access of photoelectron spectromicroscopy to microscopic properties of semiconductor materials and interfaces will be illustrated by some recent results for metal/Si and metal/GaN interfaces and micro-structured Si device with p-doped and n-doped regions, obtained by means of the scanning photoelectron microscope (SPEM) at the ELETTRA light source [2-6]. The discussed case metal/semiconductor studies will illustrate the potential of SPEM in (i) distinguishing the different phases and mass transport phenomena at morphologically complex metal/Si interfaces [2-4], (ii) development of chemical heterogeneity related to the defective structure of the GaN epilayers and its effect on the local band bending [5]; (iii) identification of edge and contamination effects on the surface electronic states of devices with p-n junctions [6].

[1] see e.g. J. Electr. Spectr. Rel. Phenom. 84 (1997), Ed. H. Ade, special issue on Spectromicroscopy.

[2] M. Kiskinova, Surf. Int. Anal. 30 (2000) 464.

[3] L. Gregoratti et al, Phys. Rev. B57 (1998) L2134; *ibid.* B 59 (1999) 2018.

[4] L. Gregoratti et al, Surf. Sci. 439 (1999) 120.

[5] A. Barinov et al, Phys. Rev. B63 (2001) and in preparation.

[6] R. J. Phaneuf et al, J. Appl. Phys. 88 (2000) 863

## Crystallization Phenomena in $\beta$ -Ga<sub>2</sub>O<sub>3</sub> Investigated by Positron Annihilation Spectroscopy

Wei-Yuan Ting, Adrian H. Kitai, and Peter Mascher

Centre for Electrophotonic Materials and Devices,  
Department of Engineering Physics  
McMaster University, Hamilton, Ontario, Canada L8S 4L7

In this paper, we present recent results of our ongoing studies of the defect characteristics in wide band gap oxides, which are used extensively for applications as luminescent phosphors, especially when doped with rare earth atoms.  $\beta$ -Ga<sub>2</sub>O<sub>3</sub> is one of the newly discovered oxide phosphors with highly anisotropic crystal structures that feature interconnected tetrahedra or octahedra chains forming a large "tunnel" through the crystal. This tunnel is believed to play a role in transporting the "hot" electrons that are necessary for electroluminescent emission. Knowledge of the defect characteristics, which can influence device efficiency either through the scattering of the hot electrons or quenching of radiative emission, is very important. Furthermore, defects in EL phosphors can provide local crystal fields that promote a non-radiative transition in the luminescent centres.

In this work, samples of single- and polycrystalline  $\beta$ -Ga<sub>2</sub>O<sub>3</sub>, undoped and doped with Tb<sup>3+</sup> or Dy<sup>3+</sup> were investigated by positron lifetime and Doppler broadening spectroscopy as well as by x-ray diffraction analysis. The positron annihilation data show that there are more large open-volume defects (large voids or pores) in the samples sintered at 800°C than in the samples sintered at higher temperatures (1200°C and 1500°C). Also, intergranular precipitation of second-phase particles (crystallites) of RE<sub>3</sub>Ga<sub>5</sub>O<sub>12</sub> is seen for the doped samples sintered at 1200°C and 1500°C, and is confirmed by the X-ray diffraction data. It is suggested that these second-phase particles are inclined to precipitate either along grain boundaries or at surfaces of pores. For the samples sintered at 800°C, most rare earth ions are in the oxide forms and the second phase of RE<sub>3</sub>Ga<sub>5</sub>O<sub>12</sub> is not nucleated. This indicates that a sintering temperature of 800°C may not be high enough to trigger the growth of the second phase of RE<sub>3</sub>Ga<sub>5</sub>O<sub>12</sub>.

For all of the sintered samples, crystallization processes are observed. Furthermore, the segregation of insoluble rare earth atoms at grain boundaries, which has been suggested earlier, is not confirmed and most insoluble rare earth atoms are likely to be in the second-phase particles of RE<sub>3</sub>Ga<sub>5</sub>O<sub>12</sub> when the sintering temperature is high enough to allow the nucleation of this phase.

The x-ray diffraction data suggest that a second phase of RE<sub>3</sub>Ga<sub>5</sub>O<sub>12</sub> (where RE stands for Rare Earth atom / ion) is present in the doped samples sintered at 1200°C and 1500°C.

## **The effects of interface and bulk defects on the electrical performance of amorphous carbon/silicon heterojunctions.**

**N.Konofaos, C.T.Angelis, E.K.Evangelou, N.A.Hastas, Y.Panayiotatos,  
C.A.Dimitriadis and S.Logotheidis**

Department of Physics, University of Ioannina, P.O.Box 1186,  
45110 Ioannina, Greece  
tel: +30-651-98498, fax: +30-651-45631, email: nkonofa@otenet.gr  
Department of Physics, University of Thessaloniki,  
54006 Thessaloniki, Greece

Amorphous diamond-like (DLC) carbon-Silicon heterojunctions with a high rectification ratio were developed by rf magnetron sputtering from a carbon target on Si(100) n-type substrates at room temperature <sup>(1)</sup>. Subsequent metalization by deposition of sputtered TiN on top of the carbon films resulted in the creation of effective heterojunction devices, as shown by electrical characterisation <sup>(2,3)</sup>. An investigation of the behaviour of the Current-Voltage (I-V) and Capacitance-Voltage (C-V) curves revealed asymmetric p-n junction characteristics.

The classical current-voltage (I-V) measurements at various temperatures are a useful tool for deriving the conduction mechanisms that dominate in the heterojunctions of amorphous carbon on silicon (a-C/Si). The conduction mechanism is directly related with the number of defects of the heterojunction in the bulk of the material or at the interface between the Si and the amorphous carbon.

Low frequency noise measurements in room temperature is a very precise technique for determining the concentration of states or traps that create the fluctuation of the current through the device <sup>(4)</sup>. It can also determine where they are lying in the heterojunction and so can clarify the role of them as far as the electrical properties of the material are concerned.

Low temperature admittance spectroscopy was also used to measure the density of interface traps and the results were found to agree with those of the noise measurements. In particular, the density of states was found to be of the order of  $10^{12}$  eV<sup>-1</sup>cm<sup>-2</sup> and their time constant of the order of  $10^{-4}$  sec. All of the above were suitable used in order to model the defects contribution on the conduction mechanisms and the device behaviour.

1. P.Patsalas and S.Logotheidis, J. Appl. Phys., 88, p.6346, 2000.
2. N.Konofaos, C.T.Angelis, E.K.Evangelou, S.Logotheidis and C.A.Dimitriadis, Appl. Phys. Lett. 78(12), 1649, 2001.
3. N.A.Hastas, C.A.Dimitriadis, P.Patsalas, Y.Panayiotatos, D.H.Tassis and S.Logotheidis, J. Appl. Phys. 89(5), 2832, 2001.
4. N.A.Hastas, C.A.Dimitriadis, S.Logotheidis, C.T.Angelis, N.Konofaos and E.K.Evangelou, Sem. Sci. & Tech. (in press).

## Anelastic Spectroscopy as a Probe for the Structure and Dynamics of Defects in Semiconductors

**R. Cantelli<sup>a</sup>, F. Cordero<sup>b</sup>, O. Palumbo<sup>a</sup>, F. Trequattrini<sup>a</sup>, B. Molinas<sup>c</sup> and G.M. Guadalupi<sup>c</sup>**

<sup>a</sup> Dipartimento di Fisica, Università di Roma "La Sapienza", P.le A. Moro 2, I- 00185 Roma, Italy, and INFN, e-mail: [cantelli@roma1.infn.it](mailto:cantelli@roma1.infn.it), tel./fax 06-49914388.

<sup>b</sup> Istituto di Acustica "O.M. Corbino", CNR, Area della Ricerca di Roma-Tor Vergata, I-00133 Roma, Italy, and INFN. <sup>c</sup> Venezia Tecnologie SpA (ENI Group), Via delle Industrie 39, I-30175 P. Marghera (VE), Italy

The anelastic spectroscopy is a powerful method for studying the dynamics and geometry of defects and excitations carrying a local distortion. The complex elastic modulus, whose imaginary part is the elastic energy absorption, is measured by electrostatically exciting the vibration modes of the sample. The vibrational stress affects the energy levels of the defects, which approach the dynamically perturbed thermal equilibrium giving rise to dissipation of energy. The analysis of anelastic spectra provides the values of the defect jumping (or transition) rates and of the associated energy barriers. Furthermore, the application of the stress along different crystallographic directions gives indications on the symmetry of the relaxing defects. In this manner, important information on some hydrogenated complexes in semiconductors has been obtained. Hydrogen easily contaminates the crystals during their growth and can form stable complexes with the dopants and various defects, often neutralizing their electrical activity. The formation and reorientational dynamics of the dopant-H(D) complexes has been studied in Si:B, Si:P and GaAs:Zn. In the case of Si the anelastic measurements agree with other types of experiments and allow deviations from the classical Arrhenius law to be observed. Instead, in GaAs:Zn an extraordinarily fast relaxation rate has been measured. A possible explanation is that H is displaced from the usual bond-center position around Zn; H might tunnel within the rings of off-centre sites around a same bond and reorient to a different bond at a very fast rate, since the separation between off-centre sites in adjacent bonds is smaller than that between bond-center sites.

Recent anelastic measurements on InP lead to the formulation of a model explaining the conversion to the semiinsulating state (SI), which is necessary for applications in optical fibre communication systems, but whose achievement is still on empirical basis. The anelastic measurements on Fe-doped and Fe-free InP samples cut along different crystallographic directions and subjected to different thermal treatments reveal a new relaxation process, which is present only in the SI state, and has been identified with the hopping of H atoms trapped at In vacancies. The hydrogenated In vacancies, whose presence is deduced by other experiments, would form during the sample preparation with the liquid encapsulated Czochralski method. H atoms would dissolve from the capping liquid containing H<sub>2</sub>O and form relatively stable H-P bonds, and hence H saturated In vacancies.





## Implant and characterization of highly concentrated Fe deep centers in InP.

**A. Gasparotto<sup>1</sup>, T. Cesca<sup>1</sup>, N. El Habra<sup>1</sup>, B. Fraboni<sup>2</sup>, F. Boscherini<sup>2</sup>, F. Priolo<sup>3</sup>,  
E.C. Moreira<sup>3</sup>, G. Ciatto<sup>4</sup>, G. Scamarcio<sup>5</sup>.**

1) INFN and University of Padova, Italy - gasparotto@padova.infn.it, phone +39 0498277001, fax +39 0498277003.

2) INFN and University of Bologna, Italy.

3) INFN and University of Catania, Italy.

4) CNR, GILDA CRG, ESRF Grenoble, France.

5) INFN and University of Bari, Italy.

Fe is an important substitutional impurity in InP. It acts as a deep acceptor, with a well known near-midgap level associated to the  $\text{Fe}^{2+}$  charge state, which is mainly used for compensation of unintentional n doping in order to produce semi-insulating bulk or epitaxial InP. Moreover,  $\text{Fe}^{2+}$  centers have also interesting optical properties in the mid-infrared portion of the electromagnetic spectrum.

Fe solubility in InP is rather low, causing precipitation and limiting to  $< 1 \times 10^{17} \text{ cm}^{-3}$  the equilibrium concentration of  $\text{Fe}^{2+}$  active centers. We used ion implantation as a non-equilibrium technique in order to increase the  $\text{Fe}^{2+}$  concentration well above the solubility limit. The substrates were kept at  $T \geq 200^\circ \text{C}$  during implantation: this dramatically reduces the implant-induced damage thanks to dynamic annealing effects. A post-implantation annealing (in phosphine flux) is necessary to activate the  $\text{Fe}^{2+}$  centers. A wide range of different experimental conditions (varying implanted doses and energies, substrate doping, annealing temperatures) was explored.

A great variety of techniques is necessary to characterize the various aspects of both the implantation induced and the Fe-related defects: structural, electrical, electronical and optical. Lattice damage was detected by RBS-channeling, whereas the local environment of Fe atoms was studied by PIXE-channeling and EXAFS measurements. In order to assess the electrical activity of the Fe-related centers current-voltage (I-V) measurements on mesa diodes were done, while the deep level structure was examined by photo induced current transient spectroscopy (PICTS). Mid-infrared photoluminescence (PL) measurements were also performed.

Our results show that a strong increase of the  $\text{Fe}^{2+}$  concentration is reached with respect to the equilibrium values: I-V curves demonstrate compensation of n-doping levels up to  $10^{19} \text{ cm}^{-3}$ , confirmed by both PICTS and PL results. Nevertheless, the situation appears to be rather complex, with a limited fraction (of the order of 10%) of the implanted Fe being activated and a strong dependence on the substrate doping level of the  $\text{Fe}^{2+}$  concentration. PIXE and EXAFS measurements seems to indicate that most of the Fe atoms reside on non-substitutional sites after annealing, most likely in Fe-P agglomerates. These structures do not show any detrimental effects on the  $\text{Fe}^{2+}$ -related electrical and optical properties.



**September 28, 13:50 - 15:30**

**Session 14**

**Defects in Devices**





## Effect of defects on the degradation of ZnSe-based White LEDs

Tsuguru SHIRAKAWA

Production Group of E&E Component, Sumitomo Electric Industries Ltd.  
E-mail: [sirakawa@asd.sei.co.jp](mailto:sirakawa@asd.sei.co.jp), Fax. +81-6-6466-5592, Tel. +8-6-6466-5733

A phosphor-free white LED based on II-VI compound materials is demonstrated. Our device utilizes a phenomenon unique to ZnSe homo-epitaxy, where a portion of the main greenish-blue emission from the active layer of a pn junction diode is absorbed by the substrate, which in turn gives off an intense broad-band yellow emission centered around 585nm by photoluminescence. These two emission bands combine to give a spectrum which appears white to naked eye. The optical output power and forward voltage of a typical ZnSe-based white LED lamp at a drive current of 20mA are 4.3mW and 2.7 V, respectively. The luminous efficiency estimated from these results is 20lm/W. Device lifetimes (half-life) at  $I_F=5\text{mA}$  have exceeded  $2.5 \times 10^3$  hours at 60 °C (estimated lifetime at 25 °C:  $2 \times 10^4$  hours). These properties make our white LEDs an attractive candidate for application as backlights for LCDs in personal handy phones.

The effect of defects on the lifetime properties of ZnSe white LEDs is complex due to the multi-layered structure of the device. Defects taking part in the device degradation are dislocations, point defects, impurities in the substrate and epitaxial layers as well as structural defects originating at the epilayer interfaces. Among them, perhaps the most important ones are dislocations in the substrate as well as those originating at the epilayer/substrate interface. The latter depends on the surface preparation method of the substrate, and its density needs to be suppressed to less than  $1 \times 10^4 \text{cm}^{-2}$  in order to obtain practical lifetimes. Another important type of defect that needs to be considered are point defects originating in the  $\text{p-Zn}_x\text{Mg}_{1-x}\text{S}_y\text{Se}_{1-y}$  cladding layer. Nitrogen-related complexes caused by p-type doping in the cladding layer have been reported to be responsible for degradation of ZnSe-based laser diodes. Though we have not yet found any direct evidence for this type of defect to take part in the degradation of our white LEDs, its possibility cannot be neglected.

Aging experiments have shown that the degradation of our white LEDs consists of several modes which are directly related to the defects mentioned above. The mechanism responsible for such behaviour will be discussed at the conference.

## Measurement of mounting-induced and grown-in strain in high-power laser diodes using Fourier-transform photo-current spectroscopy

A.Gerhardt<sup>1</sup>, J.W.Tomm<sup>1</sup>, A.Bärwolff<sup>1</sup>, J.Donecker<sup>2</sup>

<sup>1</sup> Max-Born-Institut für nichtlineare Optik und Kurzzeitspektroskopie,  
Max-Born-Str. 2a, 12489 Berlin, Germany, <http://www.mbi-berlin.de>  
Tel.: +49-30-63921444, Fax: +49-03-63921459, [gerhardt@mbi-berlin.de](mailto:gerhardt@mbi-berlin.de)

<sup>2</sup> Institut für Kristallzüchtung, Max-Born-Str. 2, 12489 Berlin, Germany

We introduce Fourier-Transform (FT) Photo-Current (PC) spectroscopy as a nondestructive method to investigate strain in high-power laser diodes. The method provides a direct quantitative insight into the strain distribution of laser diodes.

High reliability and efficiency are necessary for many applications and any commercial application of high power laser diode arrays. Despite a high efficiency high-power operation of so-called cm-laser bars leads to a substantial heating at the epitaxial layer during operation. For an efficient heat removal the epitaxial layer is directly soldered onto a heat sink. Different thermal expansion coefficients cause thermally induced strain. This additional strain in the epitaxial layer changes laser parameters and limits the lifetime of the devices. Our method offers a way to detect and quantify this strain contribution.

We measure the PC spectra of the laser structures using a commercial Fourier-Transform Infrared (FTIR) spectrometer. The laser array works like a typical photo detector. No additional preparation of the sample is necessary for the PC-measurement. All PC-measurements are carried out at room temperature.

Analyzing the PC-spectra we find the absorption of the quantum-well to be the main contribution. We identify the interband transitions within the quantum-well, namely the 1hh-1c- and the 1lh-1e-transitions as well as the edge of the bulk-like  $\text{Ga}_{0.7}\text{Al}_{0.3}\text{As}$  waveguide. The spectral positions of these transitions are connected with the band structures and react very sensitive to strain. A change of the strain leads to a shift of the accompanied characteristic photon energies.

We examine  $\text{In}_{0.09}\text{Al}_{0.1}\text{Ga}_{0.81}\text{As}/\text{Ga}_{1-x}\text{Al}_x\text{As}$  double quantum wells (QW) structures at GaAs substrate which are mounted at different types of heat sinks. The PC-spectra's of these differently strained devices show a characteristic shift of the related optical transitions. After calibration the spectral position of the transitions serves as a measure of strain.

Scans along 'cm-bars' allow us to determine lateral strain distributions. We find typical distributions for compressive respectively tensile strained arrays depending on the heat spreader materials. We gain independent information from the QW and the wave guide. So we are able to distinguish between mounting- grown-in induced and strain.

## Optical mapping of defects in SiC

J.P. Bergman<sup>1,2</sup>, and E. Janzén<sup>1</sup>

<sup>1</sup>, Department of Physics and Measurement Technology,  
Linköping University,  
S-58183 Linköping, Sweden  
and

<sup>2</sup>, ABB Corporate Research  
S-72178 Västerås, Sweden  
Email: ped@ifm.liu.se  
Tel: +46 13 282382  
Fax: +46 13 142337

SiC is a material of increasing interest for high power and high frequency applications. The material quality of both substrate and epitaxial layers is currently a limiting factor. There is a large need for material characterization and understanding, in connection with the growth development, and since SiC is a relatively expensive material, different non destructive optical methods are very useful.

In this work we will describe different techniques for high resolution luminescence and time resolved luminescence mapping of 4H SiC epitaxial layers. These have been used to measure carrier lifetime both during high and low excitation conditions, and to determine the presence and distribution of defects in the epitaxial layers. These techniques which to a large extent are utilized as large area routine characterizations have been complemented with more detailed measurements such as spectral photoluminescence measurements, cathodeluminescence, synchrotron topography, XRD topography and electrical measurements on devices processed on the material.

From these measurements we have been able to determine that the values and variations of the carrier lifetime in the epitaxial layer are strongly related to the substrate quality. Structural defects present in the substrate are replicated into the epitaxial layers, and we have specially shown that screw dislocations and low angle grain boundaries are connected with regions of local reduction of the carrier lifetime.

Finally, we will describe how the above mentioned techniques have been used to characterize and to identify a critical, generated defect in high power SiC bipolar devices. We have shown that these phenomena are related to the generation of stacking faults in the SiC basal plane. This can be seen as a local reduction of the carrier lifetime, in triangular or rectangular shape, which explains the increased forward voltage drop in the diodes. The stacking faults and their bounding partial dislocations are seen and identified using synchrotron topography. The entire stacking faults are also optically active as can be seen as dark triangles and rectangles in low temperature cathodeluminescence and as bright emitting features at higher temperatures.



## Localization of Weak Heat Sources in Electronic Devices Using Highly Sensitive Lock-in Thermography

**J. P. Rakotoniaina, O. Breitenstein, M. Langenkamp**

Max-Planck-Institut für Mikrostrukturphysik, Weinberg 2, D-06120 Halle, Germany

Phone : +49-345-5582-760, Fax +49-345-5511-223, E-mail: pati@mpi-halle.de

Leakage currents in electronics devices are sources of heat. These heat sources can be localized using an IR camera. Thus IR thermography has become a useful method to detect defects in electronic devices. However, if the heat source is weak, hence if the temperature signal is below the detection limit of a conventional IR camera (around 20 mK for a good thermocamera), the defects cannot be detected. Therefore the use of a higher sensitive detection system to localize weak heat sources is necessary. One possibility is the use of lock-in thermography. Using lock-in techniques the detection limit of IR thermography can be drastically improved below 100  $\mu$ K owing to the signal averaging. Furthermore the poor spatial lateral resolution for silicon devices in stationary thermography due to the high lateral heat conductivity can be improved. In lock-in thermography the spatial resolution is related to the thermal diffusion length, which decreases with the square of the lock-in frequency and has the value of about 1 mm at  $f_{\text{lock-in}} = 30$  Hz for silicon. For microscopic surface-near heat sources, however, the spatial resolution may be well below the thermal diffusion length. Using a microscope objective the lateral resolution of lock-in thermography can be as good as 5  $\mu$ m.

In this paper we describe the principle of lock-in thermography. Then applications to the investigation of shunts in solar cells and the detection of weak leakage current in integrated circuits (ICs) are introduced to demonstrate the potential of the lock-in thermography technique. For solar cell investigations lock-in thermography enables the non-destructive localization and the quantitative analysis of internal shunts. Shunts are defects in the p-n junction, which locally enhance the forward current. Therefore they reduce the open circuit voltage and the fill factor of the cells. In ICs local heat sources may be caused by electrostatic pulse induced leakage currents of MOS gates, by shorts between metallization lines, or by other heat dissipations related to the normal operation of the IC or to internal faults. Both for the investigation of solar cells and ICs, the combination of lock-in thermography with microscopic analytical techniques (e.g. TEM with focused ion beam preparation, EBIC) can be used to understand the physical reasons for the defects.

Lock-in thermography doesn't need any surface preparation, it is not sensitive to temperature drifts, and it shows a unique thermal sensitivity. Therefore lock-in thermography is an advantageous alternative to liquid crystal and fluorescence microthermal investigations (FMI), which are presently widely used in thermal electronic device testing.





## Gradual degradation in 980nm InGaAs/AlGaAs pump lasers

**M.Bettiati, C.Starck, M.Pommies, N.Broqua, G.Gelly (\*)**

**M.Avella, J.Jiménez (+)**

**I.Asaad, B.Orsal, J.M.Peransin (α)**

(\*) OPTO+, Groupement d'Interêt Economique, Route de Nozay - 91460 Marcoussis  
France CA: [mauro.bettiati@optoplus.fr](mailto:mauro.bettiati@optoplus.fr), t:+33 1 6963 1138, f: + 33 1 6963 1813

(+) Fisica de la Materia Condensada, ETSII, 47011 Valladolid - Spain

(α) CEM2, Université de Montpellier 2 - P.O.Box 84 - 34095 Montpellier - France

**Abstract :** High temperature (140°C) and high current density (17 kA/cm<sup>2</sup>) aging tests have been applied to InGaAs/AlGaAs 980nm single-mode pump lasers. The use of low reflectivity ( $\cong 1\%$ ) coatings on both facets leads to a symmetrical cavity configuration with relatively low power per facet emission ( $\approx 50\text{-}60\text{mW}$ /per facet). In this way, a quasi-uniform strongly accelerated stress is applied to the laser cavity and the normally very low gradual degradation rates become observable after a few hundreds hours of operation as a strong threshold current shift, while the external efficiency of the laser is almost unaffected. The degradation of the laser structure has been studied by low level I(V) curves analysis, Low Temperature (80°K) Spectrally Resolved Cathodoluminescence (LT-SRCL) and Electrical/Optical Noise (EON) techniques ; the degradation seems to be longitudinally uniform and localized in the vicinity of the QW. Some laser thus degraded has been subsequently aged in more standard conditions, after applying an high reflection coating on the back facet; preliminary results of these tests are discussed.



**September 25, 18:45 - 20:00**

**POSTER Session 1**





## Effects of thermal annealing on GaN epilayers deposited on (0001) sapphire

M. Bosi, R. Fornari, N. Armani

Istituto MASPEC-CNR, Area delle Scienze 37/A, 43010 Fontanini, Parma (Italy)  
[fornari@maspec.bo.cnr.it](mailto:fornari@maspec.bo.cnr.it) fax 39 0521 269206 phone 39 0521 269201

GaN is a wide gap semiconductor suitable for blue/green optoelectronics. Furthermore, its stability and high thermal conductivity make it a promising material for high power/high temperature electronics. High quality layers with low defect concentration are necessary for long lifetime devices. However, the GaN layers grown on foreign substrates often exhibit a high density of extended and point defects in addition to a high concentration of free carriers.

In this work the effects of thermal annealing on the electrical and optical characteristics of GaN layers grown by Hydride-VPE at 650 °C on (0001) sapphire in a vertical reactor with two main lines for the Ammonia and the HCl/H<sub>2</sub> mixture. The 7x7 mm<sup>2</sup> GaN samples submitted to thermal treatments were cleaved from 2" substrates and were about 1.2 µm thick. They were kept under flowing nitrogen at temperatures of 800 – 900 °C for periods ranging between 3 and 20 hours and subsequently cooled at different cooling rates.

The electrical properties were observed to change dramatically corresponding to annealing at 900 °C and cooling to room temperature at a rate of 100 °C/h. Indeed the free carrier concentration was reduced of more than two orders of magnitude while the Hall mobility did not show consistent changes. Similar anneals carried out on GaN grown at 1000-1050 °C did not result in such large variations of carrier concentration, although a free carrier reduction of 30-60 % was still observable.

The characterisation by SEM showed that the surface morphology had benefited from the thermal annealing with an apparent reduction of the roughness.

The cathodoluminescence measurements carried out before and after annealing showed that the CL spectra changed remarkably: an additional large band centred at about 390 nm appeared close to the near-band edge signal; the near-band edge itself was seen to be strongly dependent upon the penetration depth of the excitation beam as the signal taken at the substrate/film interface was very low while at the surface it resulted enhanced. The yellow band was not significantly affected by the thermal processing though it appeared slightly shifted towards lower energies.

This fact suggests that the residual carriers in samples grown at low temperature are mostly related to point defects rather than impurities. Therefore, their concentration may drastically be changed by post-growth thermal treatments. On the other side, samples grown at about 1000 °C have already experienced the high-temperature conditions, during and immediately after the deposition step and are thus relatively insensitive to post-growth annealing.



## Structure and optical properties of epitaxial gallium nitride layers

**C. Grazzi, H.P. Strunk**

*Erlangen-Nürnberg University, Department of Materials Science and Engineering,  
Institute of Microcharacterisation, Cauerstr 6, D-91058 Erlangen, Germany*

Cristina Grazzi, e-mail: grazzi@ww.uni-erlangen.de;

Tel: 0049 9131 8528612(13) ; Fax: 0049 9131 8528602

In this work nominally undoped gallium nitride layers grown by molecular beam epitaxy (MBE) onto sapphire substrates were studied by means of different Transmission Electron Microscopy (TEM), Photoluminescence spectroscopy (PL) and Electron Beam Induced Current (EBIC) techniques. Energy Dispersive X-ray spectroscopy (EDX) measurements show no significant amount of dopants and contaminants elements.

The TEM analyses of the microstructure show a high density of extended defects. Threading dislocations with a, a+c and c-type Burgers vector are present with a density of  $\sim 4 \times 10^9 \text{ cm}^{-2}$ . Planar defects such as stacking faults are also present.

PL spectra were measured at 300, 77 and 12 K in the wavelength range from ultraviolet to infrared. These spectra are characterised by near-edge band transitions in the ultraviolet range and a broad, but sharply structured PL band in the visible region with the most intensive peak at around 540 nm. The PL spectra in the ultraviolet region change drastically with lowering the temperature. Two phonon peaks appear at 12 K in addition, while the strong emission and the structure PL band is practically independent of the temperature.

The unexpected emission in visible region can be evaluated to yield recombination lifetime and free carrier concentration. These values agree reasonably well with those evaluated from temperature dependent Hall measurements and EBIC analyses. This agreement of characteristic volumetric properties indicates that the emission in visible region can be ascribed to the defect structure.



## High resolution x-ray diffraction defect structure characterization in Si doped and undoped GaN films

E. Zielińska – Rohozińska, M. Regulska, V.S. Haroutyunian\*, K. Pakuła

Institute of Experimental Physics, University of Warsaw, Hoża 69, 00-681, Warsaw, PL

Email: [mreg@fuw.edu.pl](mailto:mreg@fuw.edu.pl), fax: (48-22) 622 61 54

\* On leave from Department of Solid State Physics, Yerevan State University,  
A. Manukian 1, 375049 Yerevan, Armenia.

Si doped ( $N_{Si}=3 \times 10^{18} \text{ cm}^{-3}$  - free carriers concentration were determined by Hall measurements) and undoped GaN layers grown by MOCVD on the  $c$  plane of sapphire using the same growth conditions have been investigated. The heterostructure is composed of GaN sublayer and GaN overlayer (Si doped or undoped). Both are of about  $3 \mu\text{m}$  thick. Prior to the deposition of GaN layers a low temperature GaN buffer layer of thickness of 25 nm was grown. Triple axis diffractometry (x-ray diffraction profiles and reciprocal space maps) and atomic force microscopy were applied to study stress relaxation and the dislocation structure. The symmetrical and asymmetrical diffraction profiles for all basic crystallographic directions (azimuths) of scattering vector  $\mathbf{q}_x$  were measured. It was found that coexistence of biaxial and hydrostatic strains of the same order appears for moderate Si doping of GaN layer. Both undoped and Si doped GaN layers are under compression but with higher stress in the undoped sample while the hydrostatic strain component remains unchanged. For GaN epilayers the hydrostatic strain, biaxial out-plane and in-plane strains (of order of  $\langle \epsilon_{\parallel} \rangle = 2.1 \times 10^{-4}$ ,  $\langle \epsilon_{bc} \rangle = 3.6 \times 10^{-4}$  and  $\langle \epsilon_{ba} \rangle = 2.0 \times 10^{-4}$ ,  $\langle \epsilon_{ba} \rangle = -6.8 \times 10^{-4}$ ,  $\langle \epsilon_{ba} \rangle = -3.2 \times 10^{-4}$  for undoped and Si doped, respectively) are extracted from the measured ones. The measured broadening of the radial  $\phi$  scans performed on asymmetric reflections were used to determine twist angle  $\alpha_{\phi}$  of hexagonal GaN columnar grains and threading edge type dislocation densities. The lateral correlation length  $L$  and tilt angles  $\alpha_{\Omega}$  of columnar crystallites, and screw dislocation density  $N_{[001]}$  was determined from Williamson-Hall plot applied to  $\omega$  scans. It was found that introduction of Si reduced the lateral correlation lengths and increased magnitudes of the tilt angles. For both samples sixfold symmetry is observed for random distribution of edge type dislocations  $N_E$ . When  $N'_E$  is dislocation density piled up in small angle grain boundaries and  $N_{[001]}$  denotes screw dislocation density we can observe: Si doping of GaN with the concentration of  $3 \times 10^{18} \text{ cm}^{-2}$  decreases the density of edge type threading dislocation  $\langle N_E \rangle$  from  $6.53 \times 10^{11} \text{ cm}^{-2}$  to  $4.8 \times 10^{11} \text{ cm}^{-2}$ , piled up in small angle boundaries  $\langle N'_E \rangle$  from  $2.64 \times 10^{10} \text{ cm}^{-2}$  to  $2.28 \times 10^{10} \text{ cm}^{-2}$  while the averaged screw dislocation density  $\langle N_{[001]} \rangle$  increases from  $9.18 \times 10^7 \text{ cm}^{-2}$  up to value of  $1.52 \times 10^8 \text{ cm}^{-2}$ . Quasi-homogeneous radius of curvature  $R$  (convex) is observed for undoped GaN layer. Unlikely, inhomogeneous bending, even local reversing sign of  $R$  (convex  $\rightarrow$  concave) is observed in sample with Si doped GaN overlayer.

Si doping of GaN with the moderate concentration of  $3 \times 10^{18} \text{ cm}^{-2}$  changes the structural quality of epitaxial layers.



## **Correlation between crystallographic structure and electrical characteristic of (Al,Ga)N epitaxial layers grown by MOVPE method**

**R.Paszkwicz, B. Paszkiewicz, J.Kozłowski, M.Tlaczala**

Institute of Microsystems Technology, Wrocław University of Technology,  
Janiszewskiego 11/17 50-372 Wrocław, Poland, phone/fax: 48(71)3283504,  
e-mail: rpsz@wt.ite.pwr.wroc.pl

Gallium nitride and its related alloy AlGa<sub>0.2</sub>N are important materials for short wavelength optical devices and high power, high frequency devices due to their wide band gap and good thermal, chemical and mechanical stability.

The lack of bulk substrates for nitrides growth caused that epitaxial layers deposited on heteroepitaxial substrates have the mosaic structure with the great amount of dislocations. The typical epitaxial layer consists of grains with the lateral diameters equal to few hundred of nanometers. The mosaic structure determines diffusion length and lifetime of minority carrier and influences the charge transport in epitaxial layer. Because all nitrides heteroepitaxial layers always have mosaic structure it is essential to determine which of them are suitable for devices preparation. The attempt was made to correlate the crystallographic structure and electrical characteristic of GaN and AlGa<sub>0.2</sub>N layers grown by MOVPE method on c-plane sapphire substrates.

Structural characterisation was performed by means of X-ray diffractometry. In order to obtain the necessary information the high resolution as well as parallel beam optics were applied. The following epitaxial layer parameters were determined: distribution of the GaN and AlGa<sub>0.2</sub>N lateral and vertical lengths, strains, twist and tilt mosaicities. The grain sizes were calculated on the basis of peak profile analysis and solution of the Fredholm equations. Twist and tilt mosaicities were measured directly from the specially chosen rocking curves. In order to obtain such reflections the new geometry of scans was proposed, where the edge (not surface) of the sample was illuminated. Additionally, the data obtained for the typically measured rocking curves and reciprocal lattice points were presented and discussed.

The electrical properties of epitaxial structures were determined by C-V measurements. If such measurements are performed in the wide range of frequencies by impedance spectroscopy methods enabling the equivalent circuits evaluation not only the carrier concentration but also many others epitaxial layer parameters can be obtained. It is possible to observe the deep level relaxation phenomena and determine the layer resistivity, carriers mobility and shunt resistance. The paper presents the study of correlation between the material structure and the equivalent circuits parameters of the Schottky contact to epitaxial layer. The correlation enables the comparison of two non-destructive methods results, their physical interpretation and verification of epitaxial structures usefulness for devices application especially with Schottky gate.





## Study of carrier recombination at structural defects in InGaN films

A.Cremades and J. Piqueras

Dpto. Física de Materiales, Facultad de Ciencias Físicas, Universidad Complutense  
de Madrid, 28040 Madrid, Spain

E-mail: [cremades@eucmax.sim.ucm.es](mailto:cremades@eucmax.sim.ucm.es)

Phone: 34-913944521. Fax: 34-913944547

The study of the carrier recombination properties of InGaN films is of interest due to their use as active layers of blue lasers and LEDs.

A series of 100 nm thick InGaN films with Indium content up to 14% has been grown by MOVPE on SiC substrates. An AlN and GaN layer of total thickness 1  $\mu\text{m}$  was used as a buffer layer. Cathodoluminescence (CL) and remote electron beam induced current (REBIC) in the scanning electron microscope have been applied to investigate with spatial resolution the recombination of carriers at the structural defects present in the films. These defects are mainly pinholes (pits in the shape of open inverted pyramids) formed at the surface. The density of pinholes increases with the In content in the layers, which can be explained by elastic relaxation at pinholes.

Cathodoluminescence images show the spatial distribution of the emission sites. For pinholes with diameter in the  $\mu\text{m}$  range we observe enhanced luminescence around the pinhole and a reduced luminescence at the apex. Pinholes are observed as dark spots surrounded by a bright halo in REBIC images. The halo spreads over an area bigger than the pinhole, with a diameter of about 3-4  $\mu\text{m}$ . Also a cell-like dislocation structure have been observed in some samples in the CL and REBIC images.

CL spectra were carried out at low temperature and at different accelerating voltages. A complex emission in the blue range and a broad structured band centered about 670 nm are the common features in the CL spectra of the samples. Local spectra on different zones have been recorded in order to investigate the origin of the observed bands. The influence of the inhomogeneous Indium incorporation on the luminescence of the films is discussed.

## Photoenhanced wet chemical etching of $n^+$ -doped GaN

**J. Skriniarová<sup>1</sup>, A. van der Hart<sup>2</sup>, H.P. Boehm<sup>2</sup>, P. Kordos<sup>2</sup>**

<sup>1</sup>Department of Microelectronics, Slovak University of Technology, Ilkovicova 3,  
SK- 812 19 Bratislava, Slovakia

Tel.: +421 7 60291 271, Fax.: +421 7 654 65423 480, E-mail: skriniar@elf.stuba.sk

<sup>2</sup>Institute of Thin Film and Ion Technology, Research Centre Jülich, D-52425 Jülich,  
Germany

Gallium nitride based structures for high frequency and optoelectronic applications require patterning of the semiconductor material on micrometer and submicrometer scales. For gate recessing of MESFET and HEMT structures, shallow etching of a region with a typical width of 0.5 – 3  $\mu\text{m}$  is necessary for the purposes of source-drain separation. Also for laser structures a smooth etched surface is required for processing the corrugated distributed Bragg reflector. The typical size of patterned features is about 300 – 500 nm. Additionally, mesa etching requires sufficiently high etch rates.

Dry etching is currently used in processing, however, it has several disadvantages, including the possibility of ion-induced damage of the surface and proton related modification of the electrical properties of the underlying layers. Wet chemical etching has been commonly used to solve these problems but only UV light assisted PEC etching was successfully applied to pattern GaN. Results of this etching technique were shown to be dependent on the electrolyte concentration and light intensity.

In our contribution, we present UV assisted PEC etching of  $n^+$ -GaN in AZ400K solution on micrometer and submicrometer scales. We have tested conditions which

lead to a rather smooth surface after etching for features with dimension of 0.5 to 10  $\mu\text{m}$ . Dependence of the etched surface quality on etchant concentration and intensity of illumination was observed. Conditions for relatively smooth final etched surfaces were applied to etch gratings in micro- and submicrometer ranges (Fig.1).

Crystallographic etching in a hot AZ400K solution is used to smooth the PEC-etched surface. Comprehensive evaluation of the resulting profiles and surface roughness by SEM is presented and discussed.

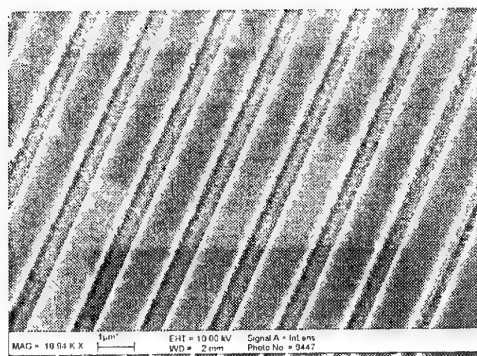


**Fig. 1:** SEM micrograph of a 500nm wide etched in AZ400K (1:250) water solution.



## Effects of residual C and O impurities on luminescence in undoped GaN epilayers

Junyong Kang<sup>1</sup>, Yaowen Shen<sup>1</sup>, Zhanguo Wang<sup>2</sup>

<sup>1</sup> Department of Physics, Xiamen University, Xiamen 361005, People's Republic of China, E-mail: jykang@xmu.edu.cn, Fax: +86-592-2189426, Tel: +86-592-2186393

<sup>2</sup> Laboratory of Semiconductor Materials Sciences, Institute of Semiconductors, Chinese Academy of Sciences, P. O. Box 912, Beijing 100083, People's Republic of China

GaN and its related semiconductor compounds are currently attracting much attention because of their advantages of wide direct band gaps, high external luminescence quantum efficiencies, high breakdown fields, and excellent chemical stability. In spite of the breakthroughs in the growth process, various residual impurities are still difficult to remove from in epilayers. It has been observed in our previous work that the residuals O and C impurities are likely to form precipitates and enhance yellow luminescence band. Recently, donor-acceptor pairs are associated to blue luminescence band. However, the relation between the luminescence bands and the residual impurities is not yet fully understood.

The samples under study were GaN epilayers grown on (0001) sapphire substrates by metalorganic vapor phase epitaxy at atmospheric pressure. A GaN buffer layer was first deposited on the (0001) surface of an Al<sub>2</sub>O<sub>3</sub> substrate at 488°C. Then, a 0.6-μm-thick GaN layer was grown at 1071 °C. None of the epilayers were intentionally doped. As-grown epilayers were transparent with specular surfaces characterized by a scanning electron microscope (SEM). The photoluminescence was excited by the 325 nm line of a He-Cd laser, dispersed by a spectrometer, and detected by a GaAs photo-multiplier connected to a lock-in amplifier.

Photoluminescence spectra of defects exhibited a series of emission peaks distributing from blue to yellow region, and a broad emission band in yellow region. The series of emission peaks and the broad emission band were resigned as the blue and yellow luminescence bands, respectively. The intensity of the blue band is stronger in the some epilayers with lower C concentrations while the intensity of the yellow band is stronger at precipitates of C and O impurities.

On the other hand, we calculated substitutional C and O impurities and their complexes on the first-principles with local-density-functional methods and supercell. The results show that the isolated substitutional C and O onto N are shallow acceptor and donor, respectively, which is likely to responsible for the blue luminescence band. Their complex results in deep levels that seem to be responsible for the yellow luminescence band.

## ANNEALING STUDIES OF Al-IMPLANTED 6H-SiC IN AN INDUCTION FURNACE

L. OTTAVIANI<sup>a</sup>, M. LAZAR<sup>b</sup>, M.L. LOCATELLI<sup>b</sup>, V. HEERA<sup>c</sup>, W. SKORUPA<sup>c</sup>,  
M. VOELSKOW<sup>c</sup>, J.P. CHANTE<sup>b</sup>

<sup>a</sup>UMR TECSSEN, Aix-Marseille III University, Case 231, F-13397 Marseille Cedex 20

Tel : (33) (0)4 91 28 83 46 Fax : (33) (0)4 91 28 88 52

E-mail : Laurent.Ottaviani@tecsen.u-3mrs.fr

<sup>b</sup>UMR CEGELY, INSA de Lyon, Bât.21, 20 Av. Einstein, F-69621 Villeurbanne Cedex.

<sup>c</sup>Forschungszentrum Rossendorf e.V., Postfach 510119, D-01314 Dresden, Germany

Silicon Carbide (SiC) is a wide band-gap semiconductor, which electrical properties are suitable for many applications, especially high power and high frequency devices. It is therefore needful to investigate the elaboration conditions of p<sup>+</sup>-n junctions, when such junctions are part of planar bipolar diodes .

Since the main dopant diffusion coefficients are too weak at usual temperatures, ion implantation is the only viable technique which allows to selectively dope SiC, in order to get device active layers or ohmic contacts. Due to the relatively deep energy levels of the common acceptors, which are aluminium (Ev + 200 meV) and boron (Ev + 300 meV), the hole concentrations at room temperature (RT) are very low with respect to the acceptor concentration. Getting  $p > 10^{17} \text{ cm}^{-3}$  at RT, for example, needs Al atoms concentration of at least  $10^{19} \text{ cm}^{-3}$ , which requires implantation doses very close to the SiC amorphization threshold for layer depths beneath 0.5  $\mu\text{m}$ . It is then very interesting to study the annealing of SiC amorphized by ion implantation, since it can be an usual case in device processing, even though increasing the implantation temperature can reduce material damage. Specific annealing problems can arise, such as material etching or surface roughening, and they must be well understood to optimise the resulting p<sup>+</sup>-n junction.

6H-SiC n-type layers were amorphized by five successive Al implantations at RT (from 25 to 300 keV), in order to obtain a flat p-type doping profile up to 500 nm. Two different doses were investigated ( $1.75 \times 10^{15} \text{ cm}^{-2}$  and  $3.28 \times 10^{16} \text{ cm}^{-2}$ ), probably leading to two distinct amorphous states.

The aim of the present paper is to study the following parameters : the heating rate (from 10 to 40 K/s), and the annealing set-up (sample mounting, atmosphere, furnace design). All the annealings were carried out at 1700°C during 30 minutes, in Ar atmosphere. It is found that the given parameters directly influence the Al profile detected by SIMS (surface etching, presence of pile-ups in case of solid phase epitaxy, diffusion), and the damage profile depicted by RBS/C spectroscopy. In particular, a rapid heating rate induces a RBS/C signal level similar to that of a virgin crystal (for the lowest dose), indicating a satisfactory reordering of the compound.

A correlation between the annealing conditions and the resulting observations will be tentatively discussed.

## Analysis of the white emission from ion beam synthesised layers by in depth resolved scanning photoluminescence microscopy

O. González-Varona<sup>1</sup>, B. Garrido<sup>1</sup>, A. Pérez-Rodríguez<sup>1</sup>, J.R. Morante<sup>1</sup>,  
C. Bonafos<sup>2</sup>, M. Carrada<sup>2</sup>, L.F. Sanz<sup>3</sup>, M.A. González<sup>3</sup>, J. Jiménez<sup>3</sup>

<sup>1</sup>EME, Departament d'Electrònica, Unitat Associada CNM-CSIC, Universitat de Barcelona, Martí i Franquès 1, 0028 Barcelona, Spain.

Tel: +34 93 4029069, Fax: +34 93 4021148, e-mail perez-ro@el.ub.es

<sup>2</sup>CEMES/CNRS, 29 Rue J. Marvig, 31055 Toulouse Cedex, France

<sup>3</sup>Dept. Física de la Materia Condensada, ETSII, Universidad de Valladolid, Valladolid 47011, Spain

Intense (visible to the naked eye) white emission can be achieved in SiO<sub>2</sub> films by high dose sequential implantation of Si<sup>+</sup> and C<sup>+</sup> ions. This results from the convolution of three bands in the PL spectrum: IR-red (1.45 eV), yellow (2.1 eV) and blue (2.8 eV). The microstructural characterisation of the films reveals the presence of a complex multilayer structure with different kinds of precipitates: Si nanocrystals are observed at regions above and below the C implanted peak region. In this last region, a darker amorphous contrast is observed in the cross section TEM images. Raman, XPS and electron diffraction measurements suggest the coexistence of sp<sup>2</sup> and sp<sup>3</sup> coordinated carbon, which is attributed to the presence of both C graphite and C rich SiC<sub>x</sub> amorphous particles. The three PL bands are tentatively related to the different kinds of nanoparticles. However, up to know no direct evidence on their relationship was experimentally observed.

This work reports the in-depth resolved photoluminescence (PL) analysis of these structures by scanning PL microscopy measurements on the surface of low angle bevelled samples. This allows to correlate at a microscopic level the PL bands with the different regions in the structures. The measured specimens were obtained by mechanical polishing (7° of nominal bevel angle) using the standard procedure of the Spreading Resistance technique. The PL spectra were measured by exciting the samples with an UV He-Cd laser ( $\lambda = 325$  nm) at room temperature. For scanning PL microscopy measurements, the excitation of the sample and light collection are performed with an Olympus metalographic microscope provided of a reflection objective with 0.4 numerical aperture, which allows to achieve a lateral resolution down to 1  $\mu$ m. The spectra obtained at different depths show a clear correlation of the intensity of the IR-red band with the presence of Si nanocrystals in the implanted layer, as well as the yellow band with the C implanted profile. These results provide with a direct experimental evidence which relates these two PL bands with the Si nanocrystals and C rich aggregates. The evolution of the blue band is hindered by a parasitic component and requires for further optimisation of the experimental setup. The clear correlation of the different PL bands with the different regions present in the structure demonstrates the ability of the Scanning PL technique in combination with simple bevelling processes for the in-depth analysis of complex luminescent structures.

## Hydrogen Introduction into $p^+$ Silicon by Boiling in Water and its Application to Deep-Level Transient Spectroscopy Measurements

Y. Tokuda, T. Murase, T. Namizaki, T. Hasegawa\* and H. Shiraki\*

Department of Electronics, Aichi Institute of Technology, Yakusa, Toyota 470-0392,  
Japan

E-mail: tokuda@el.aitech.ac.jp, Phone: +81-565-48-8121, Fax: +81-656-48-0020

\*Mitsubishi Materials Silicon Corporation, Nishisangao, Noda 278-0015, Japan

The silicon  $p/p^+$  structure consisting of a lightly boron-doped epitaxial layer on a heavily boron-doped substrate is a promising one for next-generation devices. Many works have been done to study electrically active defects in the  $p$  epitaxial layers by deep-level transient spectroscopy (DLTS) which is the powerful tool to detect deep-level defects of low concentrations. It is also important to estimate defects in  $p^+$  substrates for understanding of gettering behavior of detrimental impurities in  $p/p^+$  structures. However, there is some difficulty to fabricate Schottky diodes for DLTS measurements on  $p^+$  substrates due to the high carrier concentration.

In this work, for the fabrication of Schottky diodes on  $p^+$  silicon, hydrogen introduction was carried out to reduce the surface carrier concentration due to the formation of boron-hydrogen pairs. Hydrogen was introduced into  $p^+$  silicon by boiling in water without any damage. DLTS measurements were performed for hydrogenated  $p^+$  silicon which was intentionally iron-contaminated.

Samples used were single side polished, 200 mm diameter wafers cut from boron-doped (100) Czochralski-grown silicon single crystals with the resistivity of  $0.01 \Omega \text{ cm}$ . The method of hydrogen introduction into  $p^+$  samples was as follows;  $p^+$  samples were rinsed in 5% HF to remove the oxide, rinsed in de-ionized water and then boiled in de-ionized water for 0.5 h. It was found that the repetition of this process was essential to introduce a large quantity of hydrogen. Total boiling times were varied from 0.5 h to 28 h. Schottky contacts were obtained by evaporating samarium (Sm) on hydrogenated surfaces. Ohmic contacts were formed by rubbing eutectic gallium-indium on the back side of samples. Current-voltage (I-V), capacitance-voltage (C-V) and DLTS measurements were performed for fabricated diodes.

The rectifying characteristic was obtained for the Sm-boiled  $p^+$  contact. The I-V characteristics became better with longer boiling times. Correspondingly, the quantity of the decreased carrier concentration near the surface became larger. At the total boiling time of 28 h, the carrier concentration decreased from the original value of mid  $10^{18} \text{ cm}^{-3}$  to  $2 \times 10^{15} \text{ cm}^{-3}$  at the depth 170 nm. Iron-boron pairs ( $E_v + 0.1 \text{ eV}$ ) were detected by DLTS in hydrogenated  $p^+$  silicon which was iron-contaminated. It will be shown that the estimation of iron through iron-boron pairs is unaffected by hydrogen introduction. Generally, hydrogen passivation of acceptors is thought to be more predominant than that of defects. Therefore, this procedure is still useful for evaluation of defects which are partially passivated by hydrogen.

## Electrical characterization of SOI wafers at sub-micron scale by scanning capacitance microscopy

Yoshimori Ishizuka, Takayuki Uchihashi, Haruhiko Yoshida, and Seigo Kishino

Department of Electronics, Faculty of Engineering, Himeji Institute of Technology,  
2167 Shosya, Himeji 671-2201, Japan  
Email: ishi@elnics.eng.himeji-tech.ac.jp  
TEL/FAX: +81-792-67-4875

Silicon-on-insulator (SOI) devices have attracted world-wide attention in the ultra large scale integration (ULSI) industry. This is because the SOI-CMOS devices are advantageous to low-power and high speed LSIs, compared with bulk CMOS devices. It is said that these advantages will be more obvious as the scale down of device size is advanced hereafter. In the sub-micron SOI devices nanometer scale characterization of electrical properties becomes highly important for the wafer inspection. The advent of scanning capacitance microscopy (SCM) has enabled us to measure local variation of trapped charges, carrier concentration and defects of semiconductor materials on sub-micron scale through local capacitance measurement. However, there are few studies of SCM on SOI wafers, because the interpretation of local capacitance versus voltage ( $C-V$ ) curves in the case of SOI is more difficult than bulk-silicon.

In this study, we applied revised SCM to the electrical characterization of SOI wafers on sub-micron scale. We used a laboratory-built SCM equipment with a high sensitive capacitance sensor, which can directly obtain  $C-V$  curves and image a local variation of differential capacitance ( $dC/dV$ ). We firstly observed a new type of  $C-V$  curves with anomalous features using SOI wafers. We found that this  $C-V$  curve is composed of  $C-V$  characteristics on both SOI-Si layer and bulk Si. Then we obtained  $dC/dV$  image at the specific bias voltage of  $C-V$  curve on the SOI wafer. The  $dC/dV$  images have local contrast with a sub-micron scale, which depends on the bias voltage during the imaging. Furthermore, we measured  $C-V$  curves on the specific sites of the SOI wafer. As a result, it was found that the  $dC/dV$  image contrast was caused by the fluctuation of flat band voltage on an SOI wafer. Therefore, this SCM image contrast using the new  $C-V$  curve is probably due to the trapped charges in the  $\text{SiO}_2$  or the interface trapped charges of  $\text{SiO}_2/\text{SOI-Si}$ . These results indicate that the SCM is a useful tool for the characterization of local charges on SOI wafers.

## Delamination of Si by high dose H-ion implantation through thin SiO<sub>2</sub> film (ESR characterization)

Shiho SASAKI<sup>1</sup>, Tomio IZUMI<sup>1</sup> and Tohru HARA<sup>2</sup>

<sup>1</sup> Department of electronics, School of information technology and electronics,  
Tokai University, JAPAN

1117 Kitakaname, Hiratsuka, Kanagawa, 259-1292, JAPAN

Tel: +81-463-58-1211 ext.4098 Fax: +81-463-50-2031

E-mail:0aeem007@keyaki.cc.u-tokai.ac.jp

<sup>2</sup> Electrical Engineering, Hosei University, JAPAN

Silicon-on-insulator (SOI) is a promising material on the semiconductor devices with low power and high-speed operation. One of the techniques for fabricating SOI materials is the delamination method, which is high dose H<sup>+</sup> ions implantation into Si substrate through SiO<sub>2</sub> layer. It is important to reduce defects in order to apply the SOI to semiconductor devices, because high dose H<sup>+</sup> ions implantation introduces the defects in the Si substrate. In this paper, the defect structures in the H<sup>+</sup> ions implanted Si layer through the SiO<sub>2</sub> film has been studied by electron spin resonance (ESR) and thermal desorption spectroscopy (TDS) methods.

The Si surface layer was implanted with 30keV, 8x10<sup>16</sup> H<sup>+</sup>ions/cm<sup>2</sup> through thin SiO<sub>2</sub> film (50nm) at room temperature. Isochronal annealing was carried out in the temperature range of room to 1000°C in an Ar atmosphere. The defect structures in H<sup>+</sup> ions implanted layer were investigated by ESR method. The ESR measurement was carried out by using X-band microwave spectrometer at room temperature. Desorption of hydrogen atoms from the H<sup>+</sup> ions implanted layer was confirmed by TDS.

The ESR signal observed from H<sup>+</sup> implanted layer was composed of two kinds of ESR center, that is, the hydrogen associated center and the E'-center. The signal intensity of the H associated center decreased with an increase of the annealing temperature up to 300 °C. The TDS measurement exhibited that the implanted hydrogen atoms were desorbed from the implanted layer at the annealing of 400 °C. On the other hand, the ESR observation showed that the paramagnetic defects changed from the H associated center to O associated center, because of the hydrogen desorption. Moreover, the E'-center was disappeared by the annealing of 400 °C. By the annealing temperature above 500 °C, the delamination was occurred at the projected range (R<sub>p</sub>) of hydrogen.

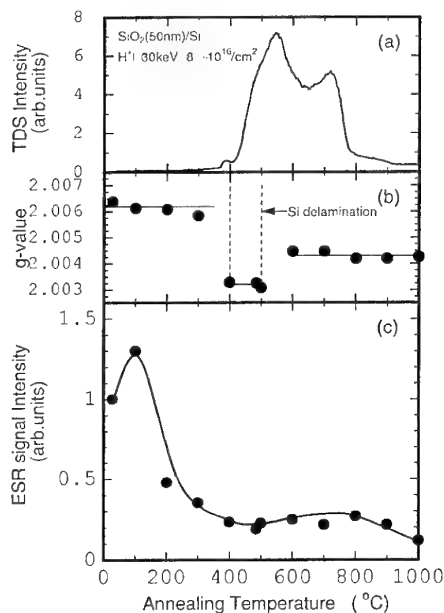


Fig.1 Changes in (a)TDS intensity (b)g-value and (c)ESR signal intensity as a function of annealing temperature.





## **Analysis of extended defects in CZ silicon annealed in either oxygen or nitrogen by optical and electron beams methods**

**C. Frigeri<sup>1</sup>, M. Ma<sup>2,3</sup>, T. Irisawa<sup>2</sup> and T. Ogawa<sup>3</sup>**

<sup>1</sup>) CNR-MASPEC Institute, Parco Area delle Scienze, 37-A, Fontanini, 43100 Parma, Italy (Fax: +39-0521-269206; e-mail: frigeri@maspec.bo.cnr.it)

<sup>2</sup>) Computer Center, <sup>3</sup>) Department of Physics, Gakushuin University, Mejiro, Tokyo, 171 Japan

Extended defects in (100) p-type CZ-Si crystals have been studied as a function of the annealing atmosphere type by using optical and electron beams based techniques such as multi-chroic infrared light scattering tomography (MC-IR-LST), transmission electron microscopy (TEM) and scanning electron microscopy in the electron beam induced current (EBIC) mode. By MC-IR-LST both scattered light and photoluminescence (PL) signal mappings could be recorded. The EBIC investigations were carried out as a function of temperature from 77 to 300 K. The samples, taken from the same ingot, were annealed in either a) oxygen atmosphere at 1150 °C for 16 hours or b) nitrogen atmosphere at 1100 °C for 16 hours. Observations were performed in the oxidation-induced stacking fault (OSF) ring area.

For both types of annealing atmospheres, LST revealed a high density of scattering centres. By TEM it was shown that the defects present in the O<sub>2</sub> annealed sample are oxygen precipitates as well as extrinsic stacking faults. Both defects can act as scattering centres. In the N<sub>2</sub> annealed sample stacking faults were not observed but only oxygen precipitates as well as tiny strain centres with loop-like diffraction contrast. These results suggest that annealing in N<sub>2</sub> atmosphere is effective to eliminate the stacking faults, whose presence is quite detrimental for device performance, while it does not prevent the formation of the oxygen precipitates which, on the contrary, can be useful for the process of impurity gettering. The elimination of the stacking faults should be due to the introduction into the Si crystal of vacancies from the nitrogen atmosphere. Very likely the Si interstitials produced because of the formation of the oxygen precipitates recombine with such extra vacancies rather than being nuclei for the extrinsic stacking faults whose formation does not thus take place. The small strain centres might be due to the precipitation of the extra vacancies which have not recombined with the Si interstitials. Such hypothesis would need further experimental evidence. The oxygen precipitates exhibit EBIC contrast at all temperatures in the sample annealed in O<sub>2</sub> but only at temperature below about 110 K for annealing in N<sub>2</sub>. Such behaviour would indicate that the oxygen precipitates are much less contaminated with deep levels after annealing in N<sub>2</sub>. This can be due to either a passivation of deep impurities due to the nitrogen ambient or a negligible introduction of contaminating impurities for annealing in N<sub>2</sub> with respect to annealing in oxygen atmosphere.



## **REFLECTION MODE SCANNING INFRARED MICROSCOPE (SIRM) AND ITS APPLICATIONS TO DEFECT DETECTION IN SILICON**

**Csaba Kovaacsics**

**SEMILAB Semiconductor physics laboratory, Inc.  
Budapest, Prielle K. u. 2. H-1117 Hungary**

An instrumentation of scanning infrared microscope is presented on photos and schemes. The performance and the limitations of this detection technique is briefly analyzed and supported with illustrative high-resolution SIRM images. Its detection capability is demonstrated through examples of various kinds of defects like oxygen precipitates, voids, dislocations, stacking faults etc. Correlation with carrier lifetime measurements ( $\mu$ PCD and SPV) and  $\Delta O_i$  data were investigated on oxygen precipitated wafers. The diameter line-scans on wafers and correlation plots show tight correlation between the data received with the above mentioned measurement techniques.

## Analysis on localized vibration of nitrogen in silicon

**I. Ohkubo, T. Mikayama, H. Harada and N. Inoue**

RIAST, Osaka Prefecture University

E-mail: harada@riast.osakafu-u.ac.jp, Fax: +81-722-54-9935, Tel: +81-722-54-9831

Nitrogen doping has attracted much attention because it reduces secondary defects [1]. It is important for clarification of this reduction mechanism and for nitrogen concentration measurement to reveal the nitrogen configurations and the origin of infrared absorption (IR) bands. In this study, the atomic-level behavior around nitrogen is revealed by using molecular orbital (MO) method and valence force method.

It is well known that the interstitial N pair (diamond-shaped  $\text{Si}_2\text{N}_2$ ) is the dominant N configuration and it causes the IR peaks of  $963\text{ cm}^{-1}$  and  $764\text{ cm}^{-1}$  [2]. We performed MO analyses by semiempirical PM3 method. The structure used was  $\text{Si}_2\text{N}_2(\text{SiH}_3)_6$  which includes the diamond-shaped  $\text{Si}_2\text{N}_2$ . It was found that the two principal asymmetric stretching modes are responsible for the observed peaks: One mode corresponds to that of  $\text{H}_2\text{O}$  type nonlinear three atom molecule, in which Si atoms adjacent to the N atoms of  $\text{Si}_2\text{N}_2$  do not move. The calculated frequency was  $752\text{ cm}^{-1}$  which is nearly equal to the observed  $764\text{ cm}^{-1}$ . The other mode corresponds to that of  $\text{BF}_3$  type planar four atom molecule, in which Si-N bonds out of the diamond-shaped  $\text{Si}_2\text{N}_2$  stretch asymmetrically. The calculated frequency was  $952\text{ cm}^{-1}$  which is nearly equal to the observed  $963\text{ cm}^{-1}$ .

As the frequencies of these modes of the  $\text{H}_2\text{O}$  and  $\text{BF}_3$  type molecules are related to the force constants of bond stretching and bond bending, the force constants were calculated. The results were  $k_1=3.3\times 10^5\text{ dyne/cm}$  and  $k_d=2.9\times 10^4\text{ dyne/cm}$ , respectively. As the valence force analysis on Si-N system was done only on amorphous Si implanted with N [3], the above result was compared to the reported values:  $k_1=2.3\times 10^5\text{ dyne/cm}$  and  $k_d=9.2\times 10^3\text{ dyne/cm}$ , respectively. Both force constants of the present case are slightly larger than those in a-Si:N, probably due to the stiffer structure of crystalline Si. This work is partially supported by the JSPS for the future program.

[1] M. Iida et al., DEFECTS IN SILICON III (The Electrochem. Soc., 1999), p. 499.

[2] R. Jones et al., Phys. Rev. Lett. **72** (1994) 1882.

[3] G. Lucovsky et al., Phys. Rev. B **28** (1983) 3234.



## Comparative Study of the Electronic States and Atomic Configurations of Two H-Related (H-C and Pt-H<sub>2</sub>) Complexes in Silicon

Y. Kamiura, K. Fukuda, Y. Iwagami, Y. Yamashita and T. Ishiyama

Faculty of Engineering, Okayama University, 3-1-1 Tsushima-naka,  
Okayama 700-8530, Japan

E-mail: kamiura@ms.elec.okayama-u.ac.jp

Fax: +81-86-251-8237, Tel.: +81-86-251-8230

The characterization and control of hydrogen in semiconductors is one of the important subjects in semiconductor technologies. Recently, we have studied the electronic states of two H-related (H-C and Pt-H<sub>2</sub>) complexes in Si by deep-level transient spectroscopy (DLTS) under uniaxial compressive stress. This paper presents the results of comparative study of these complexes, concerning their electronic states and atomic configurations.

The H-C complex has a donor level, which was detected by DLTS to lie at  $E_c-0.15$  eV. The application of  $\langle 111 \rangle$  and  $\langle 110 \rangle$  compressive stresses split the DLTS peak into two as intensity ratios of 1:3 and 1:1, respectively, which were the ratios of the low-temperature peak to the high-temperature peak [1]. No splitting was observed under the  $\langle 100 \rangle$  stress. These results indicate the  $C_{3v}$  symmetry of the H-C complex and the anti-bonding nature of its electronic state, and are consistent with the atomic model, in which the hydrogen atom occupies the bond-centered site between silicon and carbon atoms.

The atomic structure of the Pt-H<sub>2</sub> complex in Si was well established by EPR to have the  $C_{2v}$  symmetry [2], and this complex has been inferred to have a gap state at  $E_c-0.18$  eV [3]. However, no direct evidence has been obtained to connect the defect structure to the electronic state. We have observed an energy level at  $E_c-0.14$  eV related to Pt and H in Si. The application of  $\langle 100 \rangle$  and  $\langle 111 \rangle$  stresses split the DLTS peak into two with intensity ratios of 2.7 : 1 and 1.4 : 1, respectively, which were the ratios of the low-temperature peak to the high-temperature peak. Under  $\langle 110 \rangle$  stress, this peak split into three as an intensity ratio of low- to high-temperature peaks was 1.4 : 5 : 1. In addition, we observed that repeated DLTS runs at 63-150K under uniaxial stresses induced the low-temperature peak to grow with decaying high-temperature peak. This observation implies that the complex was aligned under applied stresses to the configuration corresponding to the low-temperature DLTS peak. Considering this stress-induced alignment, we have determined that the platinum-hydrogen complex observed by us has the  $C_{2v}$  symmetry and is identified as the Pt-H<sub>2</sub> complex.

We will show that the atomic configuration and thermal stability of both hydrogen-related complexes are quite different whereas their electronic states are similar.

- [1] Y. Kamiura, N. Ishiga, and Y. Yamashita, *Jpn. J. Appl. Phys.* **36**, L1419 (1997).
- [2] S. J. Uffring, M. Stavola, P. M. Williams, and G. D. Watkins, *Phys. Rev.* **B51**, 9612 (1995).
- [3] J.-U. Sachse, E. O. Sveinbjornsson, W. Jost, and J. Weber, *Phys. Rev.* **B55**, 16176 (1997).



## STRUCTURAL DEFECTS AND DISLOCATION-RELATED PHOTOLUMINESCENCE IN ERBIUM-IMPLANTED SILICON

**N.A.Sobolev<sup>1</sup>, E.M.Emel'yanov<sup>1</sup>, E.I.Shek<sup>1</sup>, V.I.Vdovin<sup>2</sup>, T.G.Yugova<sup>2</sup>, S.Pizzini<sup>3</sup>**

<sup>1</sup>Ioffe Physico-Technical Institute, 194021 St.Petersburg, Russia

E-mail: [nick@sobolev.ioffe.rssi.ru](mailto:nick@sobolev.ioffe.rssi.ru), fax: (812)2471017, phone: (812)2473885

<sup>2</sup>Institute for Chemical Problems of Microelectronics, 109017 Moscow, Russia

<sup>3</sup>INFM and Department of Materials Science, I-20126 Milano, Italy

Fabrication of light-emitting structures with a wavelength of  $\sim 1.5 \mu\text{m}$  is of great interest for optoelectronic applications. One way of producing such structures is using of luminescence determined by the presence of dislocations in the material. Formerly, the dislocation-related photoluminescence (DRL) with the wavelengths of  $\sim 1.52 \mu\text{m}$  (D1 line) and  $\sim 1.42 \mu\text{m}$  (D2 line) was detected in plastically deformed silicon and relaxed epitaxial SiGe layers. Recently, we have observed DRL in silicon implanted with erbium and annealed at  $1100^\circ\text{C}$ . This report presents the results of experiments designed to understand the nature of luminescence lines associated with erbium implantation and subsequent high temperature annealing.

Structural defects and optical features of p-type Cz-Si after implantation of erbium with 1 MeV energy and  $1 \times 10^{13}$ -  $1 \times 10^{14} \text{ cm}^{-2}$  doses followed by annealing at (620-1100)  $^\circ\text{C}$  for 0.5-3.0 hrs in chlorine-containing atmosphere or argon have been studied by transmission electron microscopy, optical microscopy in combination with selective chemical etching, and photoluminescence.

We have found that high temperature annealing in the chlorine-containing ambience gives rise to dislocation loops and pure edge dislocations with dominant dislocation-related lines in the PL spectrum. Pure edge dislocations are responsible for the appearance of the lines. The Er-related lines due to the intra-4f shell transitions in the rare earth ions dominate in the PL spectra and no structural defects are observed after annealing in argon. The remarkable difference in the defect patterns arising in erbium-implanted silicon annealed in the oxidizing or inert ambience can be explained in the following way. It is known that annealing at fairly high temperatures results in silicon supersaturation with intrinsic point defects (vacancies and self-interstitials) and the type of dominant defects varies with the annealing medium: an oxidizing ambience is favorable to the silicon supersaturation with self-interstitials, and an inert ambience promotes the supersaturation with vacancies. The interaction between the point defects generated during implantation and annealing leads to different results. In the case of annealing in an oxidizing ambience, the total silicon supersaturation with self-interstitials is high enough to form dislocation loops of the interstitial type. In contrast, during annealing in an inert ambience, the annihilation of implantation-related self-interstitials with medium annealing-related vacancies decreases the level of silicon supersaturation with self-interstitials. In the latter case, extended defects of the dislocation type do not form at all.



## STUDY THE EFFECT OF CLUSTERED DEFECTS ON MACROSCOPIC BEHAVIOR OF HADRON IRRADIATED SILICON DETECTORS

**S. Saramad, A. Moussavi-Zarandi**

Department of Physics and Nuclear Science, Amir Kabir University, Tehran, Iran  
Phone: +41 22 767 79 51, Email: Shahyar.Saramad@cern.ch

Radiation hardening of silicon detectors in extremely high fluences of irradiation in future CERN LHC experiments is an important problem. This high radiation levels will cause significant bulk damage, which controls the electrical parameters of irradiated silicon detectors. On the other hand experimental results show that with a good design and material selection the radiation induced damages can be reduced, but a complete reasonable model for describing the macroscopic parameters such as effective doping concentration ( $N_{eff}$ ) and leakage current does not exist. Detail calculations and experimental results predict that cluster defects with a non Shockley-Read-Hall statistic, by exchange charge reaction, may be responsible for this discrepancy. But for explaining the experimental  $N_{eff}$ , because of some limitations the above assumption is not satisfactory. In addition our results show that leakage current after annealing of some defects can not extracted by this method [1].

In this paper we have used the latest Deep-Level Transient Spectroscopy (DLTS) data after hadron irradiation, which identify ( $E_v+0.2$ ) eV, ( $E_c-0.45$ ) eV and ( $E_c-0.35$ ) eV levels as three states of trivacancy (V3), and also E170 (V4) and divacancy (V2) cluster defects [2] for computing the leakage current and  $N_{eff}$  by exchange charge model. Since some cross sections of these defects are not clearly known, in first step we considered equal carrier cross sections and obtained a reasonable leakage current. But for explaining  $N_{eff}$  and experimental leakage current after annealing, it was found that this assumption is not satisfactory. In second step by changing the dominant carrier cross sections for matching with experimental leakage current data, some carrier cross sections of these levels were extracted, but mismatching with experimental  $N_{eff}$  did not solved by this method. Since some experimental data of DLTS method is not reliable for cluster defects so we found that with some modification to introduction rate of these defects a reasonable model can be obtained, which can be used to study many unsolved problems in hadron irradiated silicon detectors.

1-Saramad, S. et al. (1999) Physica B 273-274,1041-1044

2-Ahmed, M. et al. (2001) Nuclear Instruments and Methods in Physics Research A 457, 588-594



## THE ELECTRICAL CHARACTERIZATION OF INTERFACE IN THE UNITYPE DIRECTLY-BONDED SILICON WAFERS

Fedotov A., Mazanik A., Enisherlova K.

Belarusian State University, F. Skaryna av. 4, 220050 Minsk, BELARUS,  
e-mail: [fedotov@phys.bsu.unibel.by](mailto:fedotov@phys.bsu.unibel.by), tel.: 375-17-2265212, fax: 375-17-2066001

Properties of electronic devices manufactured by the direct bonding of silicon wafers are strongly dependent on the state of interfaces "silicon-silicon" and "silicon-silicon oxide". Here we studied precisely the effect of the interface state (without any additional influence of p-n junction as in case of p- and n-type wafers bonding). For this reason we used unitype structures formed by the direct bonding of p-p- and n-n-type wafers (Czochralski grown, (100) and (111) oriented, 1-20  $\Omega\cdot\text{cm}$ ) without and with their pre-oxidation. Before bonding the standard cleaning, hydrophilation procedures and rinsing in deionized water were applied to the wafers. After all these procedures four groups of bonded wafers were produced: (a) silicon wafers dried and brought into face-to-face contact in the air and annealed in air at 1200 °C; (b) silicon wafers connected in the deionized water, dried and then annealed in air at 1100-1200 °C; (c) silicon wafers dried, joined in the air and then annealed in vacuum at 1200 °C under pressure  $3\cdot 10^8$  Pa; (d) dried silicon wafers, one of which (with thickness of silicon oxide layer of about 20 nm) were oxidized, then joined and annealed in air at 1200 °C. Note that in some cases the bonded wafers were mismatched giving twist grain boundaries either close to the  $\Sigma 3$  special orientation or with a significant misorientation angles (close to 20° or random). The 4×4 mm bicrystals were cut from central, peripheric and intermediate parts of the bonded wafers and characterized by measurements of the transversal static current-voltage (I-V), and high-frequency (0.01-1 MHz) conductance and capacitance-voltage (C-V) characteristics in the range of temperatures 77-300 K.

Our measurements have shown that the electrical properties of bicrystals studied were dependent mainly on the ambient of joining (air or deionized water) and the origin of oxide layer (native or specially grown), and to a smaller degree on the bonding ambient and misorientation angles. If wafers were joined in the air and covered with 2 nm thick native oxide, transversal I-V characteristics of bicrystals were symmetric and linear for the 77 to 300 K temperature range and practically independent on the bonding ambient (air or vacuum). This points to the absence of dangling bonds or other deep centers at such interfaces. If thick layer of silicon oxide (about 20 nm) was grown on one of the bonded wafers, transversal I-V characteristics became asymmetrical and highly nonlinear at the temperatures 77-300 K. This testifies the difference in the state of silicon-silicon oxide interfaces by both sides of the oxide layer. Provided the wafers before bonding were in contact in the deionized water, electrical properties of bicrystals studied were dependent on the part which bicrystals were cut from. The presence of silicon oxide  $\text{SiO}_x$  in the form of precipitates (islands) at the interface of such bicrystals resulted in a long-time relaxation of the charge trapped by deep interfacial states offering a hysteresis behavior of I-V and C-V characteristics, although both characteristics were symmetric.



## POSITRON AS A MICROPROBE OF OXYGEN-RELATED “AS-GROWN” DEFECTS IN Si AND 1D-ACAR SPECTROSCOPY

**N. Yu. Arutyunov and V.Yu. Trashchakov**

**Institute of Electronics of Uzbek Academy of Sciences**

**Tashkent 700143, Uzbekistan**

e-mail: [tassphy@sita.gsmmail.com](mailto:tassphy@sita.gsmmail.com)

[n\\_arutyunov@yahoo.com](mailto:n_arutyunov@yahoo.com)

Tel: (99871)-133-5330, (99871)-162-4260

Fax: (99871)-133-5330

The attraction of slow thermalized positron to the region of the negative effective charge related to the oxygen/carbon impurity centers in single crystal silicon makes it possible to apply the annihilation radiation of the electron-positron pairs for the characterization of material. In this work the one-dimensional angular correlation of the annihilation radiation (1D-ACAR) has been measured for Fz-Si and Cz-Si having different oxygen/carbon content. These data have been compared with the results obtained for SiC, C(diamond), and SiO<sub>2</sub> (quartz) where the electron structure of bonds might serve as the references to Si-C, C-O, and Si-O bonding associated with the oxygen/carbon-related point defects in silicon.

Highly-anisotropic electron momentum distribution connected with the oxygen/carbon “as-grown” impurity centers results in rather complicated picture of changes of the 1D-ACAR anisotropy. The wave functions of Si<sup>4+</sup>, C<sup>4+</sup> core electrons in both the silicon and samples of references retain mostly their atomic character and high-momentum components (HMC) of 1D-ACAR attributed to them reflect chemical nature of atoms belonging to the positron-sensitive oxygen-related centers. Our analysis has shown that relatively high partial positron annihilation rate corresponding to the HMC of the 1D-ACAR is intimately related to the average positron lifetime.

Possible impurity composition of the positron-sensitive centers in silicon is considered in the light of rather high sensitivity of the HMC of 1D-ACAR to chemical nature of the impurity atoms. In this connection the role of the effective charge of atoms of Si-O, Si-C and C-O orbitals in the process of the positron localization on the oxygen/carbon-related centers in silicon is discussed on the basis of experimental findings obtained by 1D-ACAR measurements for SiC, C (diamond), and SiO<sub>2</sub> (single crystal quartz).

There are some reasons to believe that the microstructure of electrically inactive oxygen-related impurity complexes undetectable by classical methods of defects studying (such as IR-, and EPR-spectroscopy) has become apparent in the data of 1D-ACAR measurements.





**Further development of electrical characterization method for unipolar semiconductor/semiconductor junctions and its application to studying the effect of gamma-irradiation on directly bonded p-Si/p-Si structures**

**V.A. Stuchinsky, G.N. Kamaev, K.Yu. Khoroshilov, V.V. Bolotov\*,  
and Yu.A. Sten'kin\***

Institute of Semiconductor Physics, 13 Lavrent'ev Ave., 633090 Novosibirsk, Russia

e-mail: [stuchin@isp.nsc.ru](mailto:stuchin@isp.nsc.ru), phone 7-(383-2)-332470, fax 7-(383-2)-332771

\*Institute of Sensor Microelectronics, 55a Prosp. Mira, 644077 Omsk, Russia

The paper describes further development of the characterization method for unipolar directly bonded junctions (DBJ's) previously proposed by two of the present authors [1]. In its previous version, the method enabled simultaneous determination of the energy density of interface states at the bonded interface and doping-concentration profile in its vicinity. However, it was soon recognized that real DBJ's usually contain "punctures" in their interfacial barrier, which largely distort characterization results [1]. Here, we propose a regular procedure that allows one to separate the electric current through "punctures" out of the total electric current across the whole structure. With this procedure, it becomes possible to independently determine the spreading resistance of the system of interfacial "punctures" and improve the estimate of parameters for the part of the structure with the potential barrier. As a result, we have a method that allows one to represent a real DBJ with a barrier height continuously fluctuating over the junction area with an equivalent structure that contains just two parts: quasi-ohmic "punctures" and a main bonded area with laterally uniform barrier. The latter makes it possible to trace effects of various technological and external factors on the two parts individually. Thus, amazingly rich data can be gained just from integral measurements of DBJ's, i. e., without performing any local measurements.

As an example of application of the method, electrical properties of unipolar directly bonded p-Si/p-Si junctions irradiated with  $\text{Co}^{60}$  gamma-quanta were studied. In the present paper, possible reasons for the observed increase in the d. c. conductivity of DBJ's with irradiation dose  $F$  are discussed in terms of evolution with  $F$  of the energy distribution of electronic states at the bonded interface, doping concentration in its vicinity, generation/recombination properties of the semiconductor, and density of interfacial "punctures". The current through "punctures" is shown to contribute predominantly to the total current across the structure, and this contribution increases with the total flux of gamma-quanta given to the sample. On the other hand, as  $F$  increases, the energy distribution of interface states on the area with barrier changes only insignificantly. These results strongly suggest that additional interfacial "punctures" appear during irradiation or already existing ones widen, presumably due to formation of negatively charged defects at or near the bonded interface.

[1] V.A. Stuchinsky and G.N. Kamaev, *Semiconductors*, **34** (10), 1214 (2000).



### **Study of grain boundary effect on photovoltaic parameters in polycrystalline silicon homojunction pin solar cells**

**B. Zebentout<sup>1</sup>, Z. Benamara<sup>1</sup>, H. Sehil<sup>1</sup>, H. Dib<sup>1</sup>, T. Mohammed-Brahim<sup>2</sup>**

<sup>1)</sup> Laboratoire de MicroElectronique appliquée, université Djillali Liabès,  
Sidi Bel Abbès (22000), Algérie.

<sup>2)</sup> Groupe de Microélectronique et Visualisation, université de Rennes 1,  
35042 Rennes cedex France

Recently, a particular interest is given to polysilicon material in terrestrial photovoltaic conversion devices as solar cells with weak cost and Several structures have been studied to improve the out put parameters. The aim of this work is to study the sensitivity of the light J(V) characteristics to various device and material parameters in PIN homojunction solar cells like thickness, doping profile, grain size and the high density of trap states localized at the grain boundaries and at the two interfaces. For that, we used a one dimension numerical resolution of transport equations in semiconductors (Poisson's equation and the two equations of continuity of electrons and holes) under AM1.5 solar lighting. In this simulation, we take account the intrinsic properties of polysilicon material as a density of trapping states distributed in the forbidden band according to a distribution in shape of « U » formed by two exponential band tails near the conduction and the valence band edges and gaussian state distribution for the dangling bonds characterizing the deep defects. However, the results showed that the evolution of fundamental photovoltaics parameters (fill factor, short circuit current, conversion efficiency and open circuit voltage) is strongly linked to polysilicon parameters. In the last, our simulation results have been compared with experimental I(V) obtained on PIN junction, the polysilicon has been deposited by LPCVD technique and eventually added with phosphine or diborane for doped layers. It is noted that the time of deposition depend of thickness of intrinsic layer ( $\geq 3\mu\text{m}$ ). The highly doped layers (n+ or p+) have a thin thickness in order of 1000 Å.

Finally, these cells presents a weak efficiency in order of 2%, it is owed to the presence of an important trapped density found in intrinsic polysilicon layer and at interfaces.



## ON THE PROPERTIES OF THE Be-DOPED LOW TEMPERATURE MBE GaAs LAYERS

G. Kowalski, I. Frymark, A. Krotkus\*, M. Kaminska

*Institute of Experimental Physics, University of Warsaw, Hoza 69, 00-681 Warsaw,  
Poland (E-mail [ifrymark@fuw.edu.pl](mailto:ifrymark@fuw.edu.pl), fax : +48-22-6226154)*

*\*Semiconductors Physics Institute, 2600 Vilnius, Lithuania*

Low temperature (LT) GaAs layers grown by molecular beam epitaxy (MBE) have been already applied in electronic devices making use of their high resistivity and short carrier trapping times. To improve device performance (lower trapping time) and achieve control on acceptor concentration gallium arsenide crystals are doped with beryllium (Be) atoms. Furthermore Be was found to increase thermal stability of the material [1–5]. In the present work, samples of Czochralski-grown substrate GaAs crystals with LT MBE-grown GaAs:Be layers of thickness in the range 1–5  $\mu\text{m}$  are studied. The concentration of Be atoms in the LT layer ranged from  $10^{17}$ – $10^{20} \text{ cm}^{-3}$ . The samples under investigations were annealed at temperatures ranging from 500 °C to 800°C. X-ray diffraction rocking curves and plane-wave topography were taken in order to evaluate the overall quality of the samples and their defect content. The dependencies of the FWHM's (full width at half maximum) of the layer peaks on Be concentration and the annealing temperature were measured. Information about the strain in the layers and lattice parameters is deduced from these measurements. The topography shows no misfit dislocations.

### References

- [1] Luysberg M, Specht P, Thul K, Liliental-Weber Z, Weber ER, Proc. of the 10th Conference on Semiconducting and Insulating Materials (SIMC-X), Piscataway, NJ, USA 1998, 87–92.
- [2] Haiml M, Prasad A, Morier-Genoud F, Siegner U, Keller U, Weber ER, Proc. of the 10th Conference on Semiconducting and Insulating Materials (SIMC-X), Piscataway, NJ, USA 1998, 101–104.
- [3] Lutz RC, Specht P, Zhao R, Weber ER, Proc. of the 10th Conference on Semiconducting and Insulating Materials (SIMC-X), Piscataway, NJ, USA 1998, 113–117.
- [4] Lutz RC, Specht P, Zhao R, Jeong S, Bokor J, Weber ER, Defect and Impurity Engineered Semiconductors, II. Symposium. Mater. Res. Soc. Warrendale, PA, USA 1998, 55–59.
- [5] Zhao R, Specht P, Lutz RC, Pu NW, Jeong S, Bokor J, Weber ER. Proc. of the 10th Conference on Semiconducting and Insulating Materials (SIMC-X), Piscataway, NJ, USA 1998, 130–133.



## Modelling of Be diffusion in GaAs layers grown by MBE

**R. Mosca, P. Bussei, S. Franchi, P. Frigeri and E. Gombia**

CNR -MASPEC Institute, Parco Area delle Scienze 37/A, 43010 Fontanini-Parma (Italy)  
E-mail: [mosca@maspec.bo.cnr.it](mailto:mosca@maspec.bo.cnr.it)

**A. Carnera**

Department of Physics, INFN-University of Padova, via Marzolo 8, 3513 Padova (Italy)

**M. Peroni**

Alenia Marconi Systems S.p.A., Via Tiburtina Km 12.400, 00131 Roma (Italy)

Beryllium is commonly used as a p-type dopant in GaAs grown by molecular beam epitaxy (MBE) since it allows to achieve very high hole concentrations without degradation of the surface morphology. This feature is very important in the fabrication of GaAs-based n/p/n heterojunction bipolar transistors (HBT) where highly doped p-type base layers are required to fully exploit the device capabilities. Unfortunately the high Be diffusivity is a strong disadvantage in these devices since Be-dopant outdiffusion from the base to the emitter layer during either growth or high-temperature device fabrication results in a dramatic degradation of the device performances. However it has been shown that the combined use of reduced substrate temperatures and high As/Ga flux ratios during base layer deposition is effective in reducing Be diffusion during MBE growth<sup>1</sup> as well as during post-growth annealings performed at 800 °C for 7 s.<sup>2</sup>

The Authors have recently reported the results of an investigation performed by Secondary Ion Mass Spectrometry (SIMS) on p/p<sup>+</sup> and p/p<sup>+</sup>/p GaAs structures which underwent rapid thermal annealing (RTA) experiments.<sup>3</sup> In particular it has been shown that As<sub>4</sub>/Ga flux ratio affects Be diffusion only in p/p<sup>+</sup> structures and that Be redistribution is almost independent on whether the annealing is performed at 770 °C or at 850 °C for 30s. These results have been qualitatively discussed in the frame of the Substitutional-Interstitial Diffusion (SID) model.

In order to give a more accurate description of these results, the diffusion of Be in GaAs has been modeled by following an approach that has been first proposed for Zn and Be diffusion in GaAs<sup>4</sup> and has then been applied by other authors to Be diffusion in InGaAs/InP<sup>5</sup> and InGaAs/InGaAsP heterostructures.<sup>6</sup> Following this method, the simulated Be profiles must be fitted to the experimental ones essentially by adjusting the diffusivities and concentrations of Be and Ga interstitial atoms, which are considered as fitting parameters, even if further parameters are sometimes introduced.<sup>6</sup>

In this communication the modeling procedure is critically discussed and it is shown that, in the case we are considering, unacceptable errors are introduced in the quantitative evaluation of the fitting parameters by some of the assumptions which are usually done. It is shown how the method can be refined in order to achieve a more accurate evaluation of the fitting parameters, and that it must be properly modified in order to account for the dependence of Be diffusion on the As/Ga flux ratio observed in p/p<sup>+</sup> GaAs structures.<sup>3</sup> Following this modified approach, the diffusion mechanisms originating the previously reported SIMS results in p/p<sup>+</sup> and p/p<sup>+</sup>/p GaAs structures are discussed.

---

<sup>1</sup> D.C. Streit et al., J. Vac. Sci. Technol. B 10 853 (1992)

<sup>2</sup> N. Jourdan et al., IEEE Trans. Electron Devices ED-39, 767 (1992)

<sup>3</sup> R. Mosca et al., Mater. Sci. Eng. B 80, 32 (2001)

<sup>4</sup> S. Yu et al., J. Appl. Phys. 69, 3547 (1991)

<sup>5</sup> M. Ihaddadene et al., Mater. Sci. Eng. B 80, 73 (2001)

<sup>6</sup> K. Ketata et al., Physica B 273-274, 823 (1999)

## Characterization of deep levels in rapid thermal annealing treated AlGaInP

A. Tukiainen<sup>(a)</sup>, J. Dekker<sup>(b)</sup>, T. Leinonen<sup>(a)</sup>, and M. Pessa<sup>(a)</sup>

<sup>(a)</sup>Optoelectronics Research Centre, Tampere University of Technology,  
P.O.Box 692, 33101 Tampere, Finland

<sup>(b)</sup>Laboratory of Physics, Helsinki University of Technology, 02150 Espoo, Finland

E-mail: antti.tukiainen@orc.tut.fi

Fax: +358 3 365 3400

Phone: +358 3 365 2914

AlGaInP is widely used as a cladding and a waveguide material in red LEDs and LDs. In this work we have studied the effect of rapid thermal annealing (RTA) on deep levels in AlGaInP. 2  $\mu\text{m}$  thick, lightly Si- and Be-doped, solid-source molecular beam epitaxy (SSMBE) grown  $(\text{Al}_{0.25}\text{Ga}_{0.75})_{0.51}\text{In}_{0.49}\text{P}$  layers were annealed for 1 s at temperatures between 600 °C and 925 °C. The samples were characterized by capacitance-voltage measurements (*C-V*), deep level transient spectroscopy (DLTS) and photoluminescence (PL).

Room temperature photoluminescence studies showed that the PL peak intensity of *n*-AlGaInP decreased to half of its initial value as the highest annealing temperature was used. In addition, from the *C-V* measurements it was found that the net donor concentration was inversely proportional to the annealing temperature as the annealing temperature was higher than 600 °C. Several deep levels were observed in *n*-AlGaInP samples. Two deep levels at  $0.66\pm0.02$  and  $0.96\pm0.10$  eV were attributed to originate from oxygen related defects commonly observed in AlGaInP. A deep level at  $0.42\pm0.04$  eV was identified as a Si-related DX-center. The activation energy and the capture cross section of the DX-center were found to be RTA temperature dependent. The activation energy of the defect increased from 0.38 eV to 0.46 eV as the annealing temperature was increased from room temperature to 925 °C. Higher RTA temperatures also resulted larger apparent capture cross sections of the DX-center. We assign this behaviour to be related to changes in defect configuration or defect clustering during the RTA. RTA induced an extra deep level at about 0.50 eV. In *p*-AlGaInP, the DLTS revealed four deep levels. The concentration of the  $1.30\pm0.10$  eV midgap level decreased notably at higher annealing temperatures. This defect is thought to be responsible for the observed increase in the net acceptor concentration. An additional deep level, related possibly to a native defect, was introduced during the annealing. The activation energy of this deep level was  $0.75\pm0.04$  eV.

## Electrical characterization of self-assembled InAs/GaAs Quantum Dots by capacitance techniques

E. Gombia, R. Mosca, S. Amighetti\*, C. Ghezzi\*, P. Frigeri, S. Franchi

MASPEC Institute-C.N.R., Parco Area delle Scienze 37a, 43010 Fontanini-Parma, Italy

\*Istituto Nazionale per la Fisica della Materia (INFM), Dipartimento di Fisica Università di Parma, Parco Area delle Scienze 7a, 43100, Parma, Italy

Over the past few years Quantum Dots (QDs) have attracted a growing attention both from the viewpoint of fundamental physics and for technological applications in novel optoelectronic devices such as laser and optical memory structures. For these applications the knowledge of electronic levels induced by QDs is of great relevance. Many groups have investigated, using photoluminescence techniques, the optical properties of systems containing QDs that provide information on the transition energies between electron and hole levels in QDs. However, the position of quantum levels relative to the band structure of the host matrix and the electrical characteristics of deep levels associated with growth defects induced in the dots and around them, can only be determined by electrical methods such as capacitance spectroscopy.

The aim of this work is to investigate of electronic levels induced by InAs QDs in GaAs/InAs/GaAs structures using capacitance-voltage(C-V), Admittance Spectroscopy (AS) and Deep Level Transient Spectroscopy (DLTS) techniques. The structures consist of: (i) a  $n^+$  GaAs substrate, (ii) a 1  $\mu\text{m}$  thick n-GaAs buffer layer grown by Molecular Beam Epitaxy (MBE) with electron concentration  $N = 2 \times 10^{16} \text{ cm}^{-3}$ , (iii) an InAs deposit that has coverages of 1.0 ML or 3.0 ML; in the first case it gives rise to an InAs in GaAs Quantum Well (QW), while in the second it self-assembles in a 1.6 ML Wetting Layer (WL) and in QDs (iv) a 1  $\mu\text{m}$  thick n-GaAs upper confining layer, with  $N = 2 \times 10^{16} \text{ cm}^{-3}$ . After the growth of the buffer layer at 580 °C, the substrate temperature was reduced to 460 °C for the deposition of the InAs QDs or QWs by Atomic Layer MBE (ALMBE). The upper confining layer was grown by ALMBE at 400 °C for 0.4  $\mu\text{m}$  and by MBE at 580 °C for the subsequent 0.6  $\mu\text{m}$ . The above growth procedure was adopted since it optimized the photoluminescence properties of the InAs/GaAs QDs. After the formation of the AuGe ohmic contacts on the back of the GaAs substrate, circular Au Schottky contacts, 0.4  $\mu\text{m}$  in diameter, were prepared by photolithography on the surface of the upper GaAs layer.

The apparent free carrier concentration profiles obtained by C-V measurements at 300 K show a significant carrier depletion centered around the depth of the InAs layer in both QD and QW samples. Such a depletion is attributed to a high density of deep acceptor levels associated to the InAs layer but not to the QDs. At lower temperatures (145 K) and only in QD samples an accumulation peak, whose position depends on both the temperature and the capacitance signal frequency, is clearly detected in the C-V profile. This effect is explained by accounting for the temperature dependence of the emission rate from levels induced by QDs. AS measurements carried out on samples with QDs show a low temperature conductance peak which changes the amplitude and shifts towards higher temperature with increasing the reverse bias; this peak may be associated to a distribution of levels, induced by the QDs and centered around an activation energy of 60 meV from the bottom of the GaAs conduction band.

Finally, from the analysis of the shape of the DLTS peak and from the temperature dependence of the capacitance transients following the application of positive voltage pulses, it is suggested that, for temperatures  $T < 40\text{-}50 \text{ K}$ , the emission of carriers from the QD states into the GaAs barrier is controlled by direct tunneling while, for higher temperatures, thermal emission dominates with an activation energy which is consistent with that obtained by us.

## Peculiarities of defect and impurity behavior in gallium arsenide after surface gettering

**A.T.Gorelenok<sup>\*#</sup>, V.F.Andrievskii<sup>\*\*</sup>, A.V.Kamanin<sup>\*</sup>, S.I.Kohanovskii<sup>\*</sup>,  
M.M.Mezdrogina<sup>\*</sup>, and N.M.Shmidt<sup>\*</sup>**

<sup>\*</sup> Ioffe Physico-Technical Institute, St.Petersburg 194021, Russia

<sup>\*\*</sup> Institute for Electronics, Minsk 220090, Belarus

<sup>#</sup> E-mail: kamanin@ffm.ioffe.rssi.ru, Fax: +7 (812) 247 1017, Phone: +7 (812) 247 9193

Surface gettering results of impurities and defects in 1.6 mm thick (111) GaAs plates are presented. The initial samples had the concentration of  $n = (1-3) \times 10^{15} \text{ cm}^{-3}$  and the mobility of  $1500-2000 \text{ cm}^2 \text{ V}^{-1} \text{ s}^{-1}$  at room temperature. Thin (a thickness of about 1000 Å) yttrium films vacuum or plasma deposited on either one or both sides of the GaAs samples were used for the surface gettering. Then the wafers were heat treated in ambient of hydrogen purified at temperatures of 700-800 °C during from 5 minutes till 28 hours.

It was shown, that at temperature above 700 °C, the heat treatment allowed the carrier concentration to be controlled in the range  $10^8-10^{14} \text{ cm}^{-3}$  and the mobility up to  $7000 \text{ cm}^2 \text{ V}^{-1} \text{ s}^{-1}$  in accordance with the time-temperature regime.

The C-V characteristic technique for the determination of the carrier concentration and the minor lifetime in depth was modified with a use of both photoelectrochemical and electrochemical etching of the samples for their whole thickness in one operation. The distribution profile of these parameters were given for different time-temperature regimes.

A thin (no more than 0.5 μm) near-surface layer with a p-type conductivity was found to be formed, while a uniform electron distribution was observed in the rest of the sample (about 1.5 mm thick). The investigations suggested the effect was associated with generation of anti-site defects  $\text{As}_{\text{Ga}}$  and  $\text{Ga}_{\text{As}}$  during the surface gettering. However, the significant role was played by their spatial separation rather than their annihilation.

The surface gettering opens new possibilities to create a simple and inexpensive technology for power devices and detectors of nuclear particles and irradiations. Moreover, the technology of very large and ultra speed optoelectronic circuits based on GaAs is also possible.

Low-temperature (2 K) photoluminescence has been investigated. The first Schottky barriers and X-ray detectors have been created on a basis of the material obtained.

## Electrical studies in the micro-environment of dislocations inundoped high-resistivity GaAs

W. Siegel, A. Sidelnicov, and G. Kühnel

Institut für Experimentelle Physik, TU Bergakademie Freiberg, D-09596 Freiberg,  
Germany

[winfried.siegel@physik.tu-freiberg.de](mailto:winfried.siegel@physik.tu-freiberg.de), fax: 39 4314, phone: 39 2541

Structural defects in GaAs can be connected with a change of the electrical and optical properties in their vicinity. Non-uniformities related to the cellular structure of dislocations in undoped high-resistivity LEC GaAs were intensively studied in the past<sup>1-3</sup>. In as-grown semi-insulating wafers strong differences of the electrical and optical properties have been observed between dislocation-rich cell walls and nearly dislocation-free cell interiors, e.g. by resistivity measurements, photoluminescence (PL) and IR absorption. Annealing of such wafers yielded a considerable improvement of the homogeneity.

However, the micro-environment of single dislocations was investigated up to now relatively seldom. Preferentially, optical methods were used because of their high local resolution. By micro-Raman measurements on low resistivity n-type GaAs doped by Si or Te clear changes of the carrier concentration have been detected in the vicinity of single grown-in dislocations<sup>4</sup>. Photoluminescence spectra of these zones (diameter  $\approx 20 \mu\text{m}$ ) around the dislocations were considerably different from those of the matrix and yielded information about different dopant incorporation. Much stronger changes of electrical and optical properties were observed around single dislocations in undoped p-type GaAs by spreading resistance measurements using a two-probe technique<sup>5</sup> as well as by PL intensity profiles. Zones of changed properties with a diameter of about  $100 \mu\text{m}$  were observed.

The aim of the presented paper is the investigation of electrical properties around single dislocations or other structural defects both in semi-insulating ( $\rho \geq 10^7 \Omega\text{cm}$ ) and in high-resistivity bulk GaAs ( $10^5 \leq \rho \leq 10^7 \Omega\text{cm}$ ). The local resolution of electrical methods was up to now not high enough for such investigations. PL has the necessary resolution. However, maps of the band-band PL intensity reflecting cellular structure-related non-uniformities agree mostly but not always with conductivity maps. Therefore, to detect non-uniformities of the conductivity (carrier concentration) around single dislocations in high-resistivity GaAs an *electrical* method with high local resolution is required. By improvement of a point contact current technique (PCT) using a special tip a local resolution of about  $5 \mu\text{m}$  could be achieved. In the paper is reported about the choose of optimal measuring conditions (bias voltage, force of the tip) as well as about the calibration of the point contact current to the resistivity. First results of the investigation of individual structural defects are presented. An excellent agreement was observed between the photoetching patterns and PCT maps.

<sup>1</sup> M. Müllenborn, H. Ch. Alt, and A. Heberle, J. Appl. Phys. 69 (1991), 4310

<sup>2</sup> C. Reichel, W. Siegel, G. Reichel, Inst. Phys. Conf. Ser. No. 160 (1997), 213

<sup>3</sup> W. Wickert, Dissertation, University Freiburg, 1999

<sup>4</sup> O. Pactzold, K. Sonnenberg, and G. Irmer, Inst. Phys. Conf. Ser. No. 160 (1997), 119

<sup>5</sup> K. Watanabe, H. Nakanishi, K. Yamada, and K. Hoshikawa, Appl. Phys. Lett. 45 (1984), 643





## Photoluminescence Topography, PICTS and Microwave Conductivity Investigation of EL6 in GaAs

Th. Steinegger <sup>(1)</sup>, B. Gründig <sup>(4)</sup>, M. Baeumler <sup>(2)</sup>, M. Jurisch <sup>(3)</sup>, W. Jantz <sup>(2)</sup>,  
and J.R. Niklas <sup>(4)</sup>

<sup>(1)</sup> Infineon Technologies AG, München, Germany,

<sup>(2)</sup> IAF Freiburg, Germany,

<sup>(3)</sup> Freiburger Compound Materials GmbH, Freiberg, Germany,

<sup>(4)</sup> Technical University Bergakademie Freiberg, Germany,

email: niklas@physik.tu-freiberg.de, fax: (+49)-(0)3731-39 -- 4314, phone: -- 2860

For a systematic optimization of defect-related material properties analytic results are needed that are univocally related to the defects under investigation. For GaAs a further important aspect is the spatial distribution of defect concentrations. Topographic, preferentially non-destructive measurement techniques to map the distribution patterns are required. Most suitable and predicative for this purpose is optical topography with defect-specific absorption or emission bands, provided that the recorded optical band can definitely be assigned to a specific defect.

The EL6 center is known to play a significant role in the electrical compensation process. Recent progress in material preparation techniques allowed to adjust the EL6 concentration in GaAs and to study its correlation to the EL2 defect. It has been suggested that the 0.8 eV emission band originates from EL6, but further support of this tentative assignment is desirable.

Photo-induced current transient spectroscopy (PICTS) allows a direct evaluation of the EL6 concentration. Samples have been prepared with a wide range of EL6 concentrations. We find that the 0.8 eV emission band intensity, as measured by photoluminescence spectroscopy, and the EL6 concentration, as measured by PICTS, exhibit a clear linear dependence. This correlation corroborates the quoted assignment and suggests that 0.8 eV emission topography may indeed be used to monitor EL6 defect engineering experiments.

It has been suggested that the EL6 related transition determines the carrier lifetime. However we find that the intensity of the near-bandedge photoemission decreases with increasing EL6 concentration, hence increasing 0.8 eV emission. This anticorrelation is apparent in photoluminescence topograms exhibiting the cellular structure commonly observed for LEC GaAs. It implies that EL6 does *not* determine the carrier lifetime predominantly, suggesting that other, probably nonradiative, recombination centers (NRRCs) are responsible. Indeed topograms generated with the recently developed microwave photoconductivity technique provide respective evidence, which shall be discussed.

## High-resolution photoinduced transient spectroscopy as a new tool for quality assessment of semi-insulating GaAs

**P. Kaminski and R. Kozłowski**

Institute of Electronic Materials Technology  
ul. Wolczynska 133, 01-919 Warszawa, Poland

e-mail: [Pawel.Kaminski@waw.tvp.pl](mailto:Pawel.Kaminski@waw.tvp.pl), fax: (48 22) 834 90 03, tel.: (48 22) 547 66 23

A new measuring technique called High-Resolution Photoinduced Transient Spectroscopy (HRPITS) is presented as a powerful tool for studying electronic properties of grown-in point defects in semi-insulating (SI) GaAs bulk crystals and epitaxial layers grown by molecular beam epitaxy at low temperatures (LT-GaAs). The novel method, which represents significant improvement of the earlier PITS technique, relies on the computer analysis of the photocurrent transients digitally recorded with a 12-bit resolution and sampling frequency of 1 MHz. The measurements are performed at temperatures between 20 and 320 K in 1-K steps and the HRPITS spectra are calculated using the correlation procedure with implementation of two-point weight function  $w(t, t_1, t_2) = \delta(t - t_1) - \delta(t - t_2)$ . The activation energies and apparent capture cross-sections for defect centres are obtained from Arrhenius plots determined for emission rate windows ranging from 0.5 to 100 000 s<sup>-1</sup>. The concentrations of detected defect centres are also calculated, so the energetic distributions of the defects' concentration are obtained.

Owing to the high resolution, around 20 traps are detected in a standard SI GaAs grown by the Liquid Encapsulated Czochralski (LEC) method. It is found that the concentrations of traps S1 (0.09 eV), P11 (0.12 eV), EL14 (0.22 eV), EL5 (0.42 eV), P18 (0.43 eV), EL3 (0.58 eV) and HL3 (0.60 eV), tentatively identified as: B<sub>As</sub><sup>0/-</sup>, Si<sub>Ga</sub>-Si<sub>As</sub>, V<sub>Ga</sub>-V<sub>As</sub>, As<sub>Ga</sub>-V<sub>Ga</sub>, Cu<sup>-/-</sup>, O<sub>i</sub>-V<sub>As</sub> and Fe, respectively, strongly depend on the growth conditions. Moreover, it is shown that the Hall mobility is mainly affected by the concentration of defects P23 (Fe), P18 (Cu), EL3 (O<sub>i</sub>-V<sub>As</sub>) and EL14 (V<sub>Ga</sub>-V<sub>As</sub>). For example in the SI GaAs LEC crystals with resistivity of (2.0-2.6)×10<sup>7</sup> Ωcm the increase in concentrations of these defects from 1.0×10<sup>14</sup> to 1.2×10<sup>15</sup> cm<sup>-3</sup> involves the decrease of the Hall mobility from 6900 to 5500 cm<sup>2</sup>/Vs. It should be added that the multi-step annealing of LEC GaAs crystals (1140 °C/16.5 h+555 °C/1.5 h+900 °C/4 h) results in diminishing of the concentrations of the following defects: EL3 (O<sub>i</sub>-V<sub>As</sub>), P22 (As<sub>Ga</sub><sup>+/+</sup>), P21 (V<sub>Ga</sub><sup>2-/3-</sup>), EL6 (As<sub>Ga</sub>-V<sub>As</sub>), EL5 (As<sub>Ga</sub>-V<sub>Ga</sub>), HB6 (0.29 eV), EL11 (0.17 eV), EL14 (V<sub>Ga</sub>-V<sub>As</sub>), EL17 (0.21 eV) and P12 (B<sub>As</sub><sup>-/-</sup>). For LT-GaAs the increase in the growth temperature from 300 to 400 °C manifests itself by threefold decrease in the concentrations of defects such as T5 (V<sub>Ga</sub><sup>0/+</sup>), EL9 (0.21 eV), EL10 (0.17 eV), T8 (V<sub>Ga</sub>-V<sub>As</sub>), T9 (As<sub>Ga</sub>-V<sub>As</sub>), T10 (0.36 eV) and EL8 (0.26 eV).

## Precipitation in Low Temperature Grown GaAs

**M. Herms<sup>1)</sup>, G. Goerigk<sup>2)</sup>, G. Irmer<sup>3)</sup>, E. Bedel<sup>4)</sup>, and A. Claverie<sup>5)</sup>**

<sup>1)</sup>Fraunhofer Institute of Non-destructive Testing, EADQ, Krügerstraße 22, 01326 Dresden, Germany, phone/fax: +49.351.26482.0/18, herms@eadq.izfp.fhg.de

<sup>2)</sup>Institut für Festkörperforschung, Forschungszentrum Jülich, Postfach 1913, Germany

<sup>3)</sup>Technical University Bergakademie Freiberg, 09596 Freiberg, Germany

<sup>4)</sup>LAAS/CNRS, 7 Av. du Colonel Roche 31077 Toulouse Cedex 4, France

<sup>5)</sup>CEMES/CNRS, 29 Rue Jeanne Marvig 31055 Toulouse Cedex 4, France

The electrical properties of compound semiconductors have their roots mainly in the tendency to be nonstoichiometric but the knowledge about the exact phase diagram has been still unsatisfactory. In GaAs crystals, the arsenic excess is present either as native precipitates or as point defects. In contrast to melt-grown GaAs single crystals, the arsenic excess in layers epitaxially grown at low temperatures (LT-GaAs) has been determined to  $10^{20} \text{ cm}^{-3}$  or more. These layers produced mainly by Molecular Beam Epitaxy are under discussion for optoelectronic applications. But the excess initially solved as point defects in the matrix is changing into precipitates by subsequent annealing or other thermal procedures above about 600 °C. Shape, size distribution and number density of the native precipitates are determined by time and temperature of thermal treatments and by the excess concentration being available for precipitation. Non-destructive testing tools are necessary for a better understanding of the phase diagram, the precipitation process and the optimization of device fabrication.

In this paper we present a comparative study of precipitation in LT-GaAs annealed at different temperatures by means of Transmission Electron Microscopy (TEM), Raman Scattering (RS) and Anomalous Small Angle X-ray Scattering (ASAXS). The results of TEM, RS and ASAXS experiments confirm that the average size of arsenic precipitate increases with increasing annealing temperature ( $T_{\text{ann}} = 600 - 750 \text{ °C}$ ). The formation of precipitate larger than 5 nm has a maximum between 650 and 700 °C. The ASAXS curves (see the figure below) could be fitted by use of two independent Gaussian size distribution functions. That means the arsenic precipitates in LT-GaAs has to be divided into two parts (called type 1 and 2). That reminds of the distinction between decoration and matrix precipitates in melt-grown GaAs crystals but on another scale of size. The number density of the precipitates in LT-GaAs smaller than 5 nm (type 2) has been evaluated to be at least two order of magnitudes larger than that of type 1.

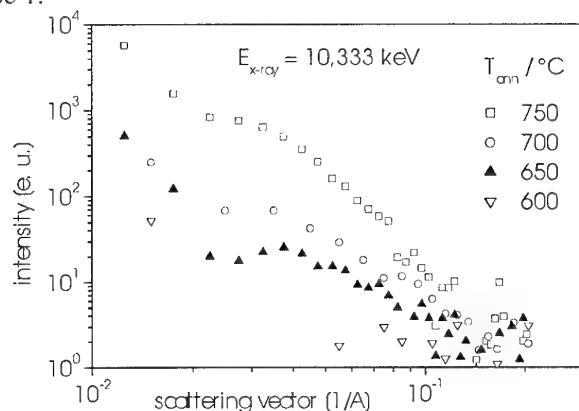


Figure 1: Small angle scattering of MBE grown GaAs-on-GaAs epilayers annealed at different temperatures  $T_{\text{ann}}$

## 2D-ACAR STUDIES ON HIGH ENERGY SWIFT HEAVY ION IMPLANTED GaAs

**K. Sivaji<sup>1</sup>, C. S. Sundar<sup>2</sup>, G. Amarendra<sup>2</sup>, S. Sankar<sup>3</sup>, P. Jayavel<sup>4</sup>  
and V. Ravichandran<sup>1</sup>**

<sup>1</sup>Materials Science Centre, Department of Nuclear Physics, University of Madras,  
Guindy Campus, Chennai – 600 025, INDIA. e- mail : k\_sivaji@yahoo.com

<sup>2</sup>Materials Science Division, IGCAR, Kalpakkam – 603 102, INDIA.

<sup>3</sup>Department of Physics, MIT Campus, Anna University, Chennai - 600 044, INDIA.

<sup>4</sup>Crystal Growth Centre, Anna University, Chennai - 600 044, INDIA.

Electron momentum distribution (EMD) imaging by positron annihilation is an investigative non-destructive technique to obtain finer details of the electronic structure as well as defects in solids. In this paper the EMD in GaAs is studied by an indigenously developed two-dimensional angular correlation of annihilation radiation (2D-ACAR) system by measuring the two dimensional EMD for selective crystallographic directions. The influence of high-energy (120 MeV) Si-implantation in GaAs (n-type) has also been studied by comparing the distributions of as-grown (semi-insulating) GaAs and Si-doped (n-type) GaAs samples.

The EMDs of as grown and Si-doped GaAs samples exhibited (i) a bone-like distribution in the low momentum region (LMR) and (ii) a hexagonal symmetry in the high momentum region (HMR). These features are characteristic of crystalline bulk semiconductors. The distributions follow the Jones zone symmetry where the momentum is finite within the zone and zero outside the zone. The dips and valleys in the projection are clearly seen in the undoped and Si-doped samples. Apart from the change of bone-like and hexagonal characteristics, a small narrow distribution in the Si- doped sample and a well-pronounced narrow distribution in the Si- implanted sample in the LMR, are observed. TRIM calculation shows the projected range of Si- ions to be 27  $\mu\text{m}$  and a large number of vacancies is created during high energy Si- implantation. The SEM studies show the end of range (EOR) of defects created and also a few clusters of Si- ions beyond the EOR. The EMDs of the Si- implanted sample show an increased distribution in the LMR compared to virgin and doped sample with a shape change in the shoulder region. The increased distribution is due to positron trapping in open volume defects, such as vacancy clusters, created by Si- ion implantation. The change of shape in the shoulder (i.e. valley) region indicates the lattice relaxation and lattice distortion around the defects. Comparing the amplitude and width of the narrow momentum component of Si- doped and Si- implanted samples, we conclude that the size of the positron trapping defect has grown; an increase in the concentration of defects in the Si- implanted sample has lead to a well-pronounced isotropic distribution.

This paper presents the details of the above studies and the results obtained.

## Application of High-Resolution X-ray Diffraction techniques to study strain status in $\text{Si}_{1-x}\text{Ge}_x/\text{Si}_{1-y}\text{Ge}_y/\text{Si}$ (001) heterostructures

**K.D. Chtcherbatchev<sup>1</sup>, A.D. Sequeira<sup>2</sup>, N. Franco<sup>2</sup>, N. Barradas<sup>2</sup>,**

**M. Myronov<sup>3</sup>, O.A. Mironov<sup>3</sup>, E.H.C. Parker<sup>3</sup>**

<sup>1</sup> Moscow State Institute of Steel and Alloys, Russian Federation, [chtrb@girnet.ru](mailto:chtrb@girnet.ru),  
fax: 07-(095)-2361205, phone: 07-(095)-9550151

<sup>2</sup> Instituto Tecnológico e Nuclear, Estrada Nacional 10, 2686-953 Sacavém, Portugal

<sup>3</sup> Department of Physics, University of Warwick, Coventry CV4 7AL, UK

The introduction of SiGe to standard Si-MOSFET technology allows bandgap engineering with enhanced performance [1,2]. High hole mobility can be realized in p-type modulation doped (MOD)  $\text{Si}_{1-x}\text{Ge}_x/\text{Si}_{1-y}\text{Ge}_y/\text{Si}$ (001) heterostructures, in which a strain-relaxed  $\text{Si}_{1-y}\text{Ge}_y/\text{Si}$ (001) buffer with low threading dislocation density has been used as a virtual substrate (VS) for the growth of  $\text{Si}_{1-x}\text{Ge}_x$  channel. To optimize the buffer design and the growth conditions, it is important to know the strain status of the VS and the channel. Apart from the traditionally used transmission electron microscopy (TEM), high-resolution X-ray reciprocal-space mapping (X-RSM) is applied for the characterization of the strain status of heterostructures. It has the advantage of being non-destructive, probing large areas and having a high sensitivity to strain variations. Samples used in this study were grown by a combination of LP-CVD and SS-MBE. Virtual substrate with a graded Ge concentration up to 35% and thickness of 1200nm was first grown on Si(001) substrate by LP-CVD. The uniform 300nm  $\text{Si}_{0.65}\text{Ge}_{0.35}$  buffer and active layers of MOD heterostructure with 4nm  $\text{Si}_{0.2}\text{Ge}_{0.8}$  channel were grown by SS-MBE.

To study the thermal stability and strain relaxation mechanisms the samples were thermally annealed after growth at 600, 700 and 750°C. The double-crystal diffractometer, *Hotbird*, equipped with 18kW Rigaku rotating anode X-ray source, Ge(444) monochromator and PSD detector was used for XRD measurements. Reciprocal space maps of both symmetrical (004) and asymmetrical (224) reflections were used in order to measure the in-plane strain. The analysis of RSM of the as-grown sample showed that the Ge concentration gradient in the VS was not linear. The behaviour of intrinsic in-plane strain along VS depth was found to be non-monotonous. The thickness of the channel was found to be non-uniform in the plane for as-grown sample because of rather wide spreading of intensity in reciprocal space. The 600°C annealing led to change of the in-plane strain depth profile, and the channel thickness becomes more uniform. The annealing at higher temperatures lead to diffusive smearing of Ge content profile. The obtained results were compared with the TEM, SIMS and RBS data.

1. U. Konig, H. Dambkes, *Solid-State Electronics* **38**(9), 1595-1602 (1995).

2. E. H. C. Parker and T. E. Whall, *Solid-State Electronics* **43**(8), 1497-1506 (1999).

## **Reconstruction of depth strain profile in ion-doped structures from High-Resolution X-ray Diffraction data using fitting procedure based on genetic algorithm**

**K.D. Chtcherbatchev**

Moscow State Institute of Steel and Alloys, Russian Federation, [chterb@girnet.ru](mailto:chterb@girnet.ru),  
fax: 07-(095)-2361205, phone: 07-(095)-9550151

The radiation point defects (RPD) depth profile can be obtained from strain depth profile that, in turn, can be reconstructed from the shape of the rocking curve in the HRXRD spectra. For the ion implantation doping processes the main contribution into strain is determined by Frenkel defects instead of impurities. Thus the profile of Frenkel defects can be calculated from the strain profile once the specific change of the matrix volume after the defect is introduced is known. However, the balance between interstitial and vacancy components of the Frenkel pairs is lost near the surface due to the different mobility of the pair components. In this case the value of Frenkel defect concentration will be underrated. Usually the problem of strain profile reconstruction from the XRD rocking curves is solved by using a trial and error method: a comparison of experimental and simulated rocking curves. The parameters of the model are changing till a good agreement according to a certain criterion (for instance,  $\chi^2$ ). The minimization of difference between experimental and simulated data is a non-linear problem. The parameter space is too complex and can contain a lot of local minima.

The autofitting procedure, which is based on genetic algorithm (GA) to reconstruct strain depth profile in ion-doped layers is developed. GA is good in finding the neighbourhood of the global minimum, however, the exact location is rarely obtained. For this reason, genetic search is followed by a local optimization step (Levenberg-Marquardt method). The structural parameters (value of strain, Debay-Waller factor (DW)) are optimization parameters. To improve a convergence of the procedure, contribution of X-ray diffuse scattering (incoherent scattering) is taken into account. The simulation block of the fitting software is based on lamellar approach to solve Takagi-Taupin equations. The procedure allows one to reconstruct the strain depth profile in ion-doped layers using a spline approximation. This approach will reduce the number of optimization parameters because 5-7 base points can describe strain and DW depth profile. In this case one does not have to change value of strain in each lamella independently.

The action of the auto-fitting procedure is demonstrated on an example of GaAs and Si substrates doped by various ions. It is shown that a significance of  $\chi^2$  criterion depends on accuracy of measurements especially for small intensities. To get the detailed information about strain profile the measurements must be done using a triple crystal arrangement that allows one to separate smooth incoherent component of X-ray scattering.



## Effect of 200 MeV $^{107}\text{Ag}^{14+}$ ion irradiation on the electrical characteristics of Ni/n-GaAs epitaxial Schottky diode

R. Singh<sup>1\*</sup>, S. K. Arora<sup>1</sup>, J. P. Singh<sup>1</sup>, Renu Tyagi<sup>2</sup>, S. K. Agarwal<sup>2</sup> and D. Kanjilal<sup>1</sup>

<sup>1</sup>Nuclear Science Centre, Aruna Asaf Ali Marg, New Delhi 110 067, India

<sup>2</sup>Solid State Physics Laboratory, Lucknow Road, Timarpur, Delhi 110 054, India

Ni/n-GaAs/Si-GaAs epitaxial Schottky diode was irradiated with 200 MeV  $^{107}\text{Ag}^{14+}$  ions. The Si dopant concentration in the 2.5  $\mu\text{m}$  thick n-GaAs epitaxial layer was  $1.5 \times 10^{17} \text{ cm}^{-3}$ . Systematic investigation of the effect of irradiation on the current-voltage (I-V) and capacitance-voltage (C-V) characteristics of the Schottky diode was performed in the fluence range of  $1 \times 10^9$  to  $5 \times 10^{11} \text{ ions cm}^{-2}$ . The I-V and C-V measurements were performed *in situ* during irradiation. From I-V characteristics various parameters of the diode like ideality factor  $n$ , reverse saturation current  $I_s$ , reverse leakage current  $I_R$ , and apparent Schottky barrier height  $\Phi_b$  were determined. The variation in these parameters with increase in irradiation fluence was studied. For pristine sample the ideality factor was 1.5. As fluence increased, it remained constant up to a fluence of  $1 \times 10^{11} \text{ ions cm}^{-2}$ , and after that it started increasing. At a fluence of  $5 \times 10^{11} \text{ ions cm}^{-2}$ , it reached a value of 1.9. The reverse leakage current (at reverse bias of 1 V) showed a peculiar behavior. Its value for unirradiated sample was  $8.7 \times 10^{-6} \text{ A}$  and as the fluence increased, it started decreasing. At a fluence of  $5 \times 10^{11} \text{ ions cm}^{-2}$ , it attained a value of  $1.7 \times 10^{-6} \text{ A}$ . The C-V measurements were performed at different frequencies of 1 MHz, 100 kHz, 10 kHz and 1 kHz, in both the reverse as well as forward bias mode. From *in situ* forward bias C-V measurements, the variation in carrier concentration as a function of fluence was studied. The variation of interface state density distribution inside the band-gap of n-GaAs with respect to fluence was calculated using the forward bias capacitance at low (1 kHz) and high (1 MHz) frequencies. The observed variations in electrical transport properties of the Ni/n-GaAs epitaxial Schottky diode have been explained considering the energy loss process of 200 MeV  $^{107}\text{Ag}^{14+}$  ions passing through the metal-semiconductor interface. The implications of elastic collisions and intense electronic excitation by swift heavy ion in affecting the electrical transport properties of n-GaAs have been discussed.

\*E-mail: [rajendra@nsc.ernet.in](mailto:rajendra@nsc.ernet.in);

Fax: +91-11-6893666

Tel.: +91-11-6893955

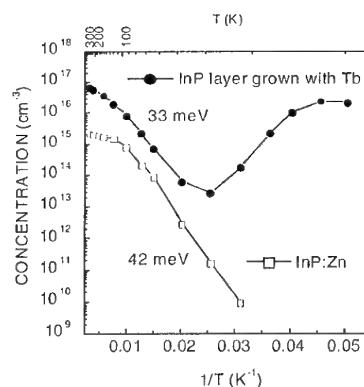
## P-type InP grown by LPE from melts with rare earth admixtures

**K. Zdansky and O. Prochazkova**

Institute of Radio Engineering and Electronics, ASCR, Chaberska 57, 18251 Prague 8, Czech Republic, email: kzdansky@ure.cas.cz, phone: 42026881804, fax: 4202688 0222

InP single crystal layers were grown by LPE on semi-insulating InP:Fe substrates with various rare earth (RE) elements added to the melt. The purpose of the RE addition was to grow InP of higher purity. Purifying effect of various RE was studied, in particular that of Er, Ho, Nd, Yb, Tb, and Pr. The concentration of the RE addition was systematically varied from zero to 0.3 wt.%. With greater RE admixtures morphologically ill layers were obtained. For characterization of the grown layers the carrier concentration and mobility were measured as a function of temperature. The InP layers grown without any RE admixture were of n-type conductivity with concentration of electrons  $4 \times 10^{17} \text{ cm}^{-3}$ . N-type InP layers with a reduced concentration of electrons were grown when a small admixture of RE, below 0.1 wt.% was used. This was true for all kinds of the RE named above. However, various RE gave various results when higher admixtures were applied. Some of them gave always n-type InP, in particular Er, Ho and Nd, and some of them gave p-type InP, in particular Yb, Tb and Pr. This result showed on different purification of the grown InP from donors and acceptors caused by different RE. Thus Er, Ho and Nd purified InP from both, donors and acceptors in the same extent. On the other hand, Yb, Tb and Pr purified InP more significantly from donors than from acceptors. This work is focused on studying p-type InP grown with RE purification by using Yb, Tb and Pr. The binding energy of the dominant acceptor in p-type InP was determined and thus the nature of the acceptor was identified. Surprisingly, dominant acceptors differ in p-InP layers purified by different RE. When Pr was used, the dominant acceptor was identified as Ge in the P lattice site of InP [1]. In the case of Tb purification, the dominant acceptor in the p-InP has been identified as Zn in the In site. The curve of the hole concentration in the Tb purified p-InP as a function of the inversion temperature  $1/T$  is shown in the figure. The binding energy of the dominant acceptor, 31 meV was determined from the linear part of the curve with a correction on the pre-exponential term  $T^{-3/2}$ . The hole concentration seemingly increases with decreasing temperature for temperatures below 40 K. This is caused by additional conductance in the acceptor impurity band. Likewise, the measured binding energy, 33 meV is smaller than the binding energy, 42 meV of a localized Zn acceptor, due to the Zn impurity band. For comparison, the curve of the hole concentration in p-InP doped with a smaller concentration of Zn is shown in the figure.

[1] K. Zdansky, J. Zavadil, O. Prochazkova and P. Gladkov, Materials Sci. Engineer. B 80, 10 (2001).







## Preparation of InP-based semiconductor materials with low density of defects: Effect of Nd, Tb and Yb addition

O. Procházková, K. Zdansky, J. Zavadil

Institute of Radio Engineering and Electronics, ASCR, Chaberská 57, 18251 Prague 8, Czech Republic, e-mail: olgap@ure.cas.cz, phone: 42026881804, fax: 4202688 0222

InP-based semiconductor materials belong to very promising candidates for wider use in ionizing radiation detectors. Parameters of the devices are determined to a large degree by properties of component materials and by technology employed in the fabrication process. Contemporary science offers a vast array of procedures designed to achieve excellent quality of bulk and layer materials. The main idea of this contribution is to exploit the specific properties of some rare earth elements (REE = Nd, Tb or Yb) to improve physical properties of InP-based layer compounds for applications. The extraordinarily high chemical reactivity of REE can be used for removal of unwanted impurities from the compounds. Combined with suitable technology, additions of REE have been shown to lead to perfect materials [1], obviating the need for prolonged (up to several days) purifying process. In the course of our study we pursued the effect of individual REE addition during the liquid phase epitaxy (LPE) on the resulting growth process and characteristics of InP-based epitaxial layers.

InP and GaInAsP single crystal layers were grown by LPE on (100) oriented InP:Sn and InP:Fe substrates with individual REE addition to the melt. The growth process was commenced under flowing high-purity hydrogen at temperature 645 °C and 660 °C with a cooling rate of 0.7-0.8 °Cmin<sup>-1</sup>. To reduce the great affinity of REE especially with respect to oxygen and hydrogen, it was necessary to prevent this metallic RE from surrounding ambient at the stage before the growth process by mechanical embedding in the melt [2]. The dependence of the layer thickness, overall morphology and defect density on the growth conditions was monitored employing scanning electron microscopy. The rough estimate of the electrical properties was gained from C-V measurements performed with the mercury probe. More substantial were results of the temperature-dependent Hall effect measurements on contacted samples in the van der Pauw configuration. The low-temperature photoluminescence (PL) spectroscopy was used to study the gettering properties of REE introduced into the growth process. We have analyzed and distinguished native and impurity-related defects from those introduced by REE admixture.

We conclude that the impact of REE admixture on structural, electrical and optical properties was quite dramatic. The density of defects was reduced by a half order of magnitude, shallow donors were reduced effectively by up to three orders of magnitude, PL spectra have been markedly narrowed and fine spectral features were resolved.

[1] Gwo-Cherng Jiang: Crystal Research and Technology 31 (1996) 365.

[2] O. Procházková and J. Zavadil: Science Foundation in China 2 (1999) 44.



## Study of high resistivity CdTe based material by PL and IR absorption

V. Corregidor<sup>a</sup>, V. Babentsov<sup>b,c</sup>, E. Dieguez<sup>a</sup>, T. Feltgen<sup>c</sup>, M. Fiederle<sup>c</sup>, K. Benz<sup>c</sup>

<sup>a</sup> Departamento Física de Materiales. Universidad Autónoma de Madrid, 28049 Madrid, Spain.

Presenting author: [ernesto.dieguez@uam.es](mailto:ernesto.dieguez@uam.es). Phone: +34 91 397 4977

Fax: +34 91 397 8579

<sup>b</sup> Institute of Semiconductor Physics, NAN of Ukraine

<sup>c</sup> Kristallographisches Institut. Universität Freiburg. Hebelstrasse 25, D-79104. Germany.

High resistivity and its origin as well as the position of deep levels in CdTe, CdZnTe is a open question discussed by several authors in the last years. High resistivity CdTe:Cl, CdTe:Zn:Cl and CdZnTe:In samples have been grown from the melt by Bridgman Method and from the vapour by Modified Markov technique.

The samples were characterized by low temperature photoluminescence and by Infrared (IR) absorption. From IR measurements an estimation of the micro-precipitates present in the samples was made.

The precipitates were detected by SEM image in CdTe:Cl sample. There is a correlation between these micro-precipitates and the shallow donor/acceptor bound exciton (BE) line's intensity and their sharpness.

Self-cleaning of the volume from the residual impurities and native defects seems to be necessary condition for the semi-insulation properties of the material. The most narrow BE lines are seen in the samples with Te rich inclusions which are getters for the residual impurities of the I group (Cu, Ag, Li, Na, etc.). After short annealing in Cd vapour these impurities can be out diffused from the inclusions decreasing resistivity and increasing the FWHM of the BE lines and a decreasing its intensity. Low concentration of micro-precipitates is also an important condition of high resistivity, probably due to deep levels, which they introduce in the band-gap.

## **Study of the defect structure, compositional and electrical properties of Er<sub>2</sub>O<sub>3</sub>-doped n-type GaSb:Te crystals grown by the vertical Bridgman technique**

**J. L. Plaza<sup>(1)</sup>, P. Hidalgo<sup>(2)</sup>, B. Méndez<sup>(2)</sup>, J. Piqueras<sup>(2)</sup> and E. Diéguez<sup>(1)</sup>**

<sup>(1)</sup>Departamento de Física de Materiales, Facultad de Ciencias, Universidad Autónoma de Madrid, Cantoblanco, 28049, Madrid, Spain.

Presenting author: Tlf: 34 91 3974977, Fax: 34 91 3978579, e-mail: ernesto.dieguez@uam.es

<sup>(2)</sup>Departamento de Física de Materiales, Facultad de Físicas, Universidad Complutense de Madrid, 28040, Madrid, Spain.

The defect structure of Te-doped GaSb samples co-doped with Er<sub>2</sub>O<sub>3</sub> and grown by the vertical Bridgman technique has been analysed in this work. This study was carried out for different Er and Te concentrations. The defect structure of the samples has been analysed by means of cathodoluminescence (CL), scanning electron microscopy (SEM) and energy dispersive X-ray microanalysis (EDAX).

The effect of the defect structure and the sample composition on the electrical properties of the material has been established taking into account the results obtained by means of the van der Pauw technique. The influence of the compensation mechanisms of the Er regarding to the n-type Te-doped GaSb matrix for the different dopant concentrations on the electrical behaviour has been studied by this technique. The type, density and mobility of the carriers and the resistivity of the samples were also measured. All these analysis were carried out for samples obtained from different regions of the ingots, providing information about the defect structure and the electrical and compositional properties for different stages of the growth.



## **Spectral characteristics of InP/InGaAsP Infrared Emitting Diodes grown by LPE**

**V. Rakovics, S. Püspöki, J. Balázs, I. Réti, and \*C. Frigeri**

Hungarian Academy of Sciences  
Research Institute for Technical Physics and Materials Science,  
1121 Budapest, Konkoly-Thege út, Hungary  
phone: (361)-3922222/3532, fax: (361)-3922237  
E-mail: rakovics@mfa.kfki.hu

\*CNR-MASPEC Institute, Parco Area delle Scienze 37/A, 43010 Parma, Italy

InP/InGaAsP double heterostructure LEDs were grown by liquid phase epitaxy using  $\langle 100 \rangle$  oriented InP substrate. Small area surface emitting LED chips were prepared to cover completely the 1000-1700 nm wavelength range. Eleven different diodes were fabricated with optimal spacing of their peak emission wavelengths in order to have sufficient overlapping of their spectra. Spectral characteristics of the different wavelength InP/InGaAsP infrared emitting diodes was studied systematically. The spectral bandwidth of the LED's were usually broader<sup>1</sup> than theoretically predicted. The broadening of the emission spectra of the LED's on the long wavelength side can be associated with non uniform active layer composition. Investigation of the cross-section of the LED structures showed, that their active layer had a thin shifted composition layer at the InP interface. The band gap difference between the bulk and the transition layer<sup>2</sup> change parallel with the long wavelength side broadening of the emission spectra of the corresponding LED's. Some diode showed spectral broadening on the opposite side, if the band gap difference of the active and the neighbouring layers was small, because low barrier height allows carrier overflow to the confining layers. Recombination in higher band gap confining layer results higher energy photon emission, broadening the spectrum on the short wavelength side. 1250-1500 nm LEDs had narrowest spectrum. High barrier at the interfaces and uniform composition inside the active layer are the most important requirements for obtaining narrow spectra.

### References

1. V. Rakovics, C. Frigeri, J. Balázs, S. Püspöki: Material Science & Engineering B 80/1-3, (2001) 18-22
2. P. E. Brunemeier, T. J. Roth, Jr. N. Holonyak, G. E. Stillman: J. Appl. Phys. 56, (1984) 1707-1716

### Acknowledgement

This work was supported by the Hungarian Research Fund (OTKA, Project numbers: T 030395 and T 035272) and by MTA and CNR (CNR-MTA Agreement).

**LPE growth and characterization of  $\text{In}_x\text{Ga}_{1-x}\text{As}_y\text{Sb}_{1-y}$  quaternary alloys****V. Rakovics, A. L. Tóth, B. Pödör, \*C. Frigeri, J. Balázs, and Z. E. Horváth**

Hungarian Academy of Sciences  
Research Institute for Technical Physics and Materials Science  
1121 Budapest, Konkoly-Thege út, Hungary,  
phone: (361)-3922222/3532, fax: (361)-3922237  
E-mail: rakovics@mfa.kfki.hu

\*CNR-MASPEC Institute, Parco Area delle Scienze, 37/A 43010 Parma, Italy

Band gap, solid phase composition and lattice mismatch data are presented characterizing  $\text{In}_x\text{Ga}_{1-x}\text{As}_y\text{Sb}_{1-y}$  layers grown by liquid phase epitaxy (LPE) on 100 oriented GaSb substrate. LPE growth was carried out in a quartz reactor tube heated by a single-zone semi-transparent furnace. The layers were grown from single-phase solutions prepared from pure In, Ga, Sb and GaAs. The melts were homogenised and purified 2 hours at 670 °C. The supersaturation of the melts was about 3 degree when the growth of quaternary layers was started at 527 °C. The cooling rate was kept constant (0.6 °C /min) until the growth was finished. 3-6 µm thick quaternary layers were deposited during 2-3 minutes. Nearly lattice-matched ( $\Delta a/a < 0.12\%$ )  $\text{In}_x\text{Ga}_{1-x}\text{As}_y\text{Sb}_{1-y}$  layers were grown over the range  $0 < x < 0.20$ . The lattice-mismatch was estimated from X-ray diffraction measurements. The composition of the grown epitaxial layers was determined by XMA analysis using In-L $\alpha$ , Ga-L $\alpha$ , As-L $\alpha$  and Sb-L $\alpha$  lines. GaAs, InSb and GaSb crystals were used as standards. The excitation electron energy was 15 keV. The measured intensities were converted to concentrations by performing atomic number, absorption and fluorescence corrections. Band gap energies from 0.726 eV to 0.55 eV were determined on different composition samples. The band gap data were obtained from infrared transmission measurements. The measured compositional dependence of the band gap shows smaller bowing than calculated using the correlated function expansion (CFE) technique<sup>1</sup>. Our experimental data are in good agreement with earlier data of two other laboratories<sup>2-3</sup>. X-ray diffraction pattern of the lowest band gap (0.55 eV)  $\text{In}_{0.2}\text{Ga}_{0.8}\text{As}_{0.17}\text{Sb}_{0.83}$  layer showed strong compositional grading, indicating the presence of miscibility gap in this material system.

**References**

- 1 - K. Shirm, H. Rabitz and P. Dutta, J. Appl. Phys., 88, 7157 (2000)
- 2 - M. Astles, H. Hill, A. J. Williams, P. J. Wrigth, and M. L. Joung, J. Electron. Mater., 24, 41 (1986)
- 3 - J. C. DeWinter, M. A. Pollack, A. K. Srivastava, and J. L. Zyskind, J. Electron. Mater., 14, 729 (1985)

**Acknowledgement**

This work was supported by the Hungarian Research Fund (OTKA, Project numbers: T 030395, and T 035272) and MTA and CNR through the CNR-MTA Agreement.

## Electric and magnetic characterization of impurity-induced states in diluted magnetic semiconductor $\text{Pb}_{1-y}\text{Yb}_y\text{Te}$

**E.P. Skipetrov<sup>1</sup>, N.A. Chernova<sup>1</sup>, L.A. Skipetrova<sup>1</sup> and E.I. Slyn'ko<sup>2</sup>**

<sup>1</sup>Physics Department, Moscow State University, 119899 Moscow, Russia

e-mail: skip@mig.phys.msu.su, fax: +7(095)932 88 76, phone: +7(095)939 44 93

<sup>2</sup>Institute of Material Science Problems, 274001 Chernivtsi, Ukraine

Temperature dependences of the resistivity  $\rho$ , Hall constant  $R_H$  and magnetic susceptibility  $\chi$  of  $\text{Pb}_{1-y}\text{Yb}_y\text{Te}$  ( $0 \leq y \leq 0.065$ ) single crystals have been investigated over the temperature range  $4.2 \leq T \leq 300$  K in magnetic field up to 0.5 T.

Temperature dependences of  $\rho$  and  $R_H$  for  $\text{Pb}_{1-y}\text{Yb}_y\text{Te}$  ( $y \leq 0.03$ ) reveal metal-like behavior, the values of  $\rho$  and  $R_H$  at 4.2 K monotonously increase with growth of Yb content. On the  $\rho(1/T)$  and  $R_H(1/T)$  curves for  $\text{Pb}_{1-y}\text{Yb}_y\text{Te}$  ( $y \approx 0.065$ ) the distinctive low-temperature activation region is observed, indicating appearance of localized states in the energy gap. From the values of free hole concentration, obtained from  $R_H$  at 4.2 K, we have determined the Fermi energy in metal-like alloys. Position of the localized states in the energy gap have been found from slope of the activation region on  $\rho(1/T)$  curve. In undoped PbTe the Fermi level appears 40 meV below the valence band edge. As Yb content grows, the Fermi level gradually approaches the valence band edge and appears above it in alloy of the highest Yb content.

In order to explain the results obtained we suppose that in PbTe ytterbium forms impurity level, which is resonant with the valence band states in alloys of low impurity content. With increase of Yb concentration, energy gap of  $\text{Pb}_{1-y}\text{Yb}_y\text{Te}$  grows, impurity level shifts to the valence band edge and finally enters the forbidden gap. The experimental results obtained allow us to determine energy position of the impurity states in alloys of various ytterbium content and propose a model of charge carriers energy spectrum in  $\text{Pb}_{1-y}\text{Yb}_y\text{Te}$ .

Investigations of magnetic properties of  $\text{Pb}_{1-y}\text{Yb}_y\text{Te}$  have revealed the Curie-Weiss impurity paramagnetic contribution to the magnetic susceptibility of alloys. From values of the Curie constant we have estimated concentration of magnetic  $\text{Yb}^{3+}(4f^{13})$  ions  $N_{\text{Yb}^{3+}}$ . It has been found that  $N_{\text{Yb}^{3+}}$  increases with Yb content, nevertheless magnetic ions make only 10-15 % of total ytterbium concentration, while the rest ions remain in non-magnetic  $\text{Yb}^{2+}(4f^{14})$  state in all the investigated alloys.

Taking into account that magnetic  $\text{Yb}^{3+}$  ions in the alloys are formed due to self-ionization of non-magnetic ytterbium ions ( $\text{Yb}^{2+} \rightarrow \text{Yb}^{3+} + e_{\text{band}}$ ) we consider that released electrons transfer to the empty states, arising due to native acceptor defects, in the valence band. On the other hand, in terms of charge carriers energy spectrum, these magnetically and electrically active ions correspond to empty states in the ytterbium impurity level. In frame of this model, we have analyzed kinetics of magnetic ions formation with doping and determined dependence of magnetic ions concentration and electron population of the impurity band on the ytterbium content in the alloys.

## On Fermi level pinning in lead telluride based alloys doped with mixed valence impurities

**E.P. Skipetrov<sup>1</sup>, E.A. Zvereva<sup>1</sup>, O.S. Volkova<sup>1</sup>, E.I. Slyn'ko<sup>2</sup>, A.M. Mousalitin<sup>3</sup>**

<sup>1</sup>Physics Department, Moscow State University, 119899 Moscow, Russia,  
tel: +7(095)9394493, fax: +7(095)9328876, email: skip@mig.phys.msu.su

<sup>2</sup>Institute of Material Science Problems, 274001 Chernovtsy, Ukraine

<sup>3</sup>Moscow State Institute of Steel and Alloys, 117936 Moscow, Russia

We report the results of our study of electron irradiation effect ( $E=6$  MeV,  $\Phi \leq 1.85 \cdot 10^{17} \text{ cm}^{-2}$ ) on the galvanomagnetic ( $4.2 \leq T \leq 300$  K,  $B \leq 0.1$  T) properties of  $n\text{-Pb}_{1-x}\text{Mn}_x\text{Te}$  ( $0.07 \leq x \leq 0.11$ ) and  $n\text{-Pb}_{1-x}\text{Ge}_x\text{Te}$  ( $0.04 \leq x \leq 0.08$ ) doped with mixed valence impurities In and Ga ( $C_{\text{In}} \approx 0.7$  mol.%,  $C_{\text{Ga}} \approx 1.5\text{-}2$  mol.%). The main objective is to clear up a mechanism of Fermi level pinning in the doped lead telluride based alloys. Changing irradiation dose was expected to alter a defect structure of the crystals, hence change a charge carrier concentration and help to elucidate a nature of impurity-induced defects in these materials.

It was established from the temperature dependencies of the resistivity and Hall constant that for both systems before irradiation the electrical properties are thermally activated that indicates existing impurity-induced defect states  $E_{\text{In}}$  and  $E_{\text{Ga}}$  within the gap. Energy positions of these states were determined and the diagrams were built for the reconstruction of the energy spectrum under the variation of the alloy composition.

Electron irradiation of doped crystals leads to a drastically different character of changing the electrical parameters of the systems with various impurities. Irradiation of the  $\text{Pb}_{1-x}\text{Mn}_x\text{Te}$  alloys doped with indium has practically no effect on their properties up to the highest irradiation fluxes. On the contrary the character of the dependencies  $\rho(1/T)$  and  $R_{\text{H}}(1/T)$  measured for the alloys  $\text{Pb}_{1-x}\text{Ge}_x\text{Te} < \text{Ga} >$  gradually changes for metallic one and activation range vanishes under irradiation. Estimations show that the rate of defect generation under irradiation is about  $dn/d\Phi = 5\text{-}6 \text{ cm}^{-1}$  that is significantly higher than typical values observed for undoped  $A^4B^6$  semiconductors [1].

An analysis of the data obtained let us make a conclusion that the level  $E_{\text{Ga}}$  does not stabilise the Fermi level in the alloys based on the lead telluride. It was shown that electron irradiation leads to the same changes in character of the  $\rho(1/T)$  and  $R_{\text{H}}(1/T)$  dependencies as ones that may be caused by increasing the gallium content. Experimental results are discussed in the frame of the model assuming that doping with gallium leads to the formation of two different defect levels in the energy spectrum of the alloys [2], generation of donor-type defects mainly and changing an electrical activity of impurity atoms under irradiation.

[1] N.B. Brandt and E.P. Skipetrov, J. Low Temp. Phys. **22**, 665 (1996).

[2] E.P. Skipetrov, E.A. Zvereva, L.A. Skipetrova, V.V. Belousov, A.M. Mousalitin, J. Cryst. Growth, **210**, 292 (2000).

## Evolution of metastable centers on the CdS surface stimulated by temperature decrease.

**B. Pavlyk, B. Tsybulyak**

Ivan Franko Lviv National University, Physics Dept., 50 Dragomanov str., 79005 Lviv, Ukraine, e-mail [pavlyk@wups.lviv.ua](mailto:pavlyk@wups.lviv.ua), tel (380) 322 794730, fax (380) 322 729467

The effect of electron emission from the basal face (0001)Cd induced by the decrease of temperature from 300° K to 80° K was observed in CdS crystals [1]. These results correlate with the data obtained by authors of [2], who investigated the anomalous temperature dependencies of surface conductivity in CdS crystals.

The experiments showed that defect structure of the undersurface layer of high-ohmic CdS crystals stimulates the electron emission (electron stream intensity 300 – 400 imp/s) and the anomalous temperature dependence of conductivity (increase of conductivity by 3 – 4 orders) on cadmium basal face (0001) as a temperature decreases. The hexagonal semiconductor CdS has a pyroelectric property. As a temperature is decreasing the basal face (0001) is charging positively. It promotes the electron accumulation on the basal face (0001). Due to this effect the compensation of the pyroelectric field is occurred. Taking into account the pyroelectric constant, the value of accumulated charge was expected to be equal to  $4 \cdot 10^{-8} \text{ C} \cdot \text{cm}^{-2}$  while the temperature decreases from 300° K to 80° K. Our calculation are showed that the required value of charge is  $2.5 \cdot 10^{-11} \text{ C} \cdot \text{cm}^{-2}$ . As long as the crystals investigated are high-ohmic and the electron concentration is rather low ( $n < 10^8 \text{ cm}^{-3}$ ) at room temperature then an additional source of electrons is required for screening the pyroelectric field and for formation of low-ohmic undersurface layer.

Investigation of the annealing effect showed the isothermal decrease of electron stream intensity with time.  $I(t)$  curve is an exponent with the activation energy  $E_a = 0.04 \text{ eV}$  and the characteristic time ( $\tau_p$ ), that depends on the temperature of previous annealing. The rate of the metastable relaxation is very low ( $\approx 3 \cdot 10^{-3} \text{ s}^{-1}$ ) at 80° K in comparison with the same rate at 200° K ( $\approx 5 \cdot 10^{-2} \text{ s}^{-1}$ )

Analysis of the data obtained allow us to assert that on the basal face (0001) of CdS crystals the metastable defects are in equilibrium and electrically neutral at room temperature. At low temperature these defects transform into electrically active, what corresponds to the low-ohmic layer formation and electron emission. The rebuilding of metastable defects is caused by interaction of interstitial cadmium and regular lattice ions. This process is accelerated by the pyrofield.

### References

1. Pavlyk B., Tsybulyak B., Horyn' Ya., Kozak I. // Functional Materials.- 1999.- V.6, \_1.- P. 83-86.
2. Korsunskaya N.E., Markevich I.V., Shulda E.V., Sheinkman M.K. // Semicond. Sci. Technol.- 1992.- V.7, \_1.- P.92-96.



## Detection of Hidden Electronic States in Semiconductors by Multi-band Cathodoluminescence Electron Microscopy

**Hiroshi Saijo, Toshiyuki Isshiki, Giuseppe Pezzotti\*, Shigehiro Nishino and Makoto Shiojiri\*\***

*Dept. Electronics and Information Science, Kyoto Institute of Technology,*

*\*Dept. Chemistry and Materials Technology, Kyoto Institute of Technology,  
Matsugasaki, Sakyo-ku, Kyoto, 606-8585, Japan*

*\*\* Prof. Emeritus, KIT, and Dept. Anatomy, Kanazawa Medical University,  
e-mail: hsaijo@dj.kit.ac.jp Fax and Phone: +81-(0)75-724-7446*

Various local structures found in solid materials have their own unique electronic structures. Local structure means different atomic arrangements from the surroundings or so-called bulk; defects, lattice distortion, adsorption, electronic excitation, etc are the local structures that create new electronic states. Steps, kinks and facets on the surface may have different electronic states. Polymorph, a new crystal structure growth, is another source of new electronic structure.

In the semiconductor technology, the specimen crystals are expected to have highly homogeneous structure except the intentionally introduced structures in the fabrication process, and the evaluation of density and distribution of foreign structures grown inside are highly required for the qualified manufacturing process.

The local foreign structures grown hidden inside are, however, hardly detectable by ordinary microscopic methods. Light emission from solids is a popular phenomenon in the study of electronic structures of solids, and the cathodoluminescence (CL), photon release by electron beam excitation, is a promised technique to detect local structures if employed in the electron microscope; *i.e.* use a scanning electron microscope with simultaneous photon detection. The wavelength and intensity in CL micrographs corresponds to the electronic structures of the specimen, and the variation of the wavelength means local electronic states created by some change of atomic arrangements. The CL micrograph is thus a map of distribution of electronic structure or states of the specimen. We took CL micrographs with three-band CL microscope\* that provides full color image of CL emitting sources in the specimen with some spectrometric accuracy.

This paper will describe various typical local structures found inside ceramic semiconductors and III-V and II-VI semiconductors. Defects, impurity distributions and lattice distortion, display color variations in CL micrographs to disclose their position, distribution and population. SiC co-grown in SiN<sub>3</sub> by HIP method proved the growth of polymorphism of SiC as identified by the difference in CL color.

\* H. Koike, T. Nakano, T. Fujimoto and K. Ogawa, "Proc. EUREM88", **3** 591 (1988). T. Nakano, T. Fujimoto, H. Koike and K. Ogawa, *Acta Histochem. Cytochem.* **23**, 753-767 (1990).



## CATHODOLUMINESCENCE DEFECTOSCOPY OF II-VI COMPOUNDS.

**M. NAZAROV**

Technical University of Moldova, MD-2012, Kishinev, Moldova.

e-mail: [nazarov@userline.ru](mailto:nazarov@userline.ru)

The quality and reliability of microelectronics materials can be dramatically changed by point and linear defects, which occur in specimens naturally, or which can be deliberately introduced. Control of defect distribution requires a measurement method capable of investigating the defects on a micrometer scale. The proposed method surveys some of the opportunities for the control of the defects in solids by using a combination of different cathodoluminescence (CL) modes including colour cathodoluminescence (CCL) in the scanning electron microscopy (SEM) with computer graphics. Several design improvements including a composite CCL+BSE-contrast in the SEM should help researchers and users better understand how annealing at different thermal environments affects the optical characteristics of materials.

The method of cathodoluminescence defectoscopy was applied to micro-characterization of commercial wide-band-gap  $A^2B^6$  semiconductors (ZnS, ZnSe) as well to the thin diffusion layers formed in these materials in processes of annealing. The host crystals were annealed in different melts: Al, Sb, Bi and Bi+BiCl<sub>3</sub> at 1200 K for 100 h with a subsequent tempering in air. In result, a complex characterization of subsurface diffusion layers formed in the annealed crystals has been achieved. It has been established that the process of annealing in the above-mentioned melts leads to a spatial redistribution of the impurity-defects by an extremely irregular way. The CCL image reveals also a good correlation with the CL and PL spectra recorded in different points of sample.

After annealing the host crystals in Bi + 10<sup>-4</sup> at % Al melt the intensity of 380 nm band increases by 63 times but the maximum at 440 nm disappears. This changing of PL spectrum of the crystals with low Al concentration can be explained by the fact, that at the concentrations of 10<sup>-4</sup>...10<sup>-3</sup> at. % of Al, the Bi melt is not Al saturated, and instead of doping, the Al extraction from the crystal occurs. So the luminescence maximum at 380 nm can be related to low Al concentration in ZnS crystals. This assumption has found its confirmation in CL investigations of ZnS:Al crystals annealed in Bi, when in a subsurface region a very bright radiation band with the luminescence maximum at 435 nm was observed [1]. The applied method of CL defectoscopy visualises dramatic roles of dislocations, temperatures and annealing atmospheres in changes of spectral luminescence composition. This method is expected to be used both for checking of the substance state and studying the characteristics of dislocations and point defects in optoelectronic and microelectronic materials.

### References

1. M.Nazarov, R.Sobolevskay, K.Sushkevich et al. /Proc of the Int. Semicond. Conf."CAS-98" - Sinaia, Romania, p.543, 1998.



## INVESTIGATION OF ELECTRICALLY ACTIVE DEFECTS IN Si-BASED SEMICONDUCTOR STRUCTURES

VLADIMIR M. POPOV, ANATOLIY S. KLIMENKO, ALEKSEY P. POKANEVICH

RES. INSTITUTE FOR MICRODEVICES, PHYS. & TECHNOL. RES.  
CERTIF. CENTER, 3, SEVERO-SYRETSKAYA, 04136, KIEV, UKRAINE  
POPOVMC@I.KIEV.UA, TEL/FAX: (044) 449-94-58

A system of methods for detailed investigation of electrically active defects (EAD) and their properties in semiconductor structures has been developed. It consists of different ways of analysis including precision measurements of local electrophysical properties of insulator – semiconductor (IS) structures, application of homeotropically oriented nematic liquid crystals (NLC), scanning electron microscopy (SEM) in electron beam induced current (EBIC) mode, x – ray microanalysis, SIMS and others. In the field of electrophysical measurements novel method of pulse modulated dynamic unsteady – state current – voltage characteristics (DUCVC) has been developed for accurate determination of metal – insulator – semiconductor (MIS) structures parameters. The main advantages of DUCVC method over traditional capacitance–voltage characteristics depend on much higher sensitivity to registration of charge generation processes in MIS structures. Depth distributions of bulk generation life – time of minority carriers in semiconductor including non – uniformly doped structures are obtained. Corresponding normalized EAD profiles in near surface region of semiconductor are calculated. NLC method gives possibility to analyse lateral distributions of defects with high local conductivity in dielectric films on semiconductor substrates. We have shown that in definite conditions EAD at silicon surface also can be distinctly revealed in IS structures. As a result non-destructive mapping of EAD distribution on semiconductor surface by means of NLC method gives opportunity for further detailed investigation of local electrophysical and chemical properties of separate defects. Combination of SEM in EBIC mode with local x – ray microanalysis is used for evaluation of chemical composition of different types of EAD responsible for recombination life – time degradation in semiconductor. For this purpose special test structures have been designed. The effectiveness of combined application of all these methods for EAD analysis in semiconductor devices manufacturing was proved by numerous investigations of Si-SiO<sub>2</sub> structures. Local characteristics of Si-SiO<sub>2</sub> structures in site of EAD in Si and thermally grown SiO<sub>2</sub> films have been determined. Local degradation processes in the region of separate EAD with high generation-recombination rates of minority carriers and micropores in SiO<sub>2</sub> have been studied. The influence of different gettering processes on EAD behaviour in active layer of Si wafers was investigated

## Effect of Light Induced Change in Built-in Potential on Carrier Lifetime in Epitaxial Wafers

**H. Väinölä, J. Storgårds, M. Yli-Koski and J. Sinkkonen**

Electron Physics Laboratory, Helsinki University of Technology, P.O.Box 3000,  
FIN-02015 HUT-Finland

E-mail: hele.vainola@hut.fi, Fax: +358 9 4515008, Tel: +358 9 4512327

The microwave photoconductive decay ( $\mu$ -PCD) measurement technique is a powerful method for characterizing semiconductor materials. To interpret the measured results of epitaxial wafers, a few models have been reported previously in the literature [1,2]. In these papers, however, the built-in potential between the epitaxial layer and the substrate has been ignored. The built-in voltage is a function of the generated excess-carrier concentration and thus it affects the measured effective lifetime. This effect should be taken into account when interpreting the measurement results.

In this paper we derive an analytical expression for the built-in potential as a function of the light generated carrier concentration. The derivation is based on the use of the injection relation whose validity is critically discussed. Then we calculate the effective lifetime from the current continuity equation. The expression for built-in potential is taken into account in boundary conditions, which allows us to study the influence of the built-in potential on the effective lifetime. Analytical solutions are verified with numerical simulations.

Results show that when the concentration of excess carriers is less than the doping density in the lightly doped side of the junction, the magnitude of the potential barrier remains constant and is the same as in thermal equilibrium. However, the potential barrier decreases as the intensity of the generation laser is increased. With typical light intensities used in  $\mu$ -PCD measurement the concentration of generated carriers exceeds the doping density in the lightly doped region. In this case the potential barrier lowering causes excess carriers to diffuse more easily across the junction, which affects considerably the measured lifetime. For example, let us consider a typical  $p/p^+$  epitaxial wafer where the bulk lifetime is much higher in the epitaxial layer than in the substrate, where Auger-recombination dominates. At low-injection conditions the potential barrier at the interface prevents the diffusion of minority carriers from the epitaxial layer into the substrate and therefore the measured lifetime is close to the lifetime in the epitaxial layer. However, when the generated carrier concentration exceeds the doping level of the epitaxial layer, the measured effective lifetime decreases even two orders of magnitude.

- [1] H. Takahashi and T. Maekawa, Jpn. J. Appl. Phys. **39**, 3854 (2000).
- [2] T. Hara, F. Tamura and T. Kitamura, J. Electrochem. Soc. **44**, L54 (1997).



## Computer Simulation of Excess Carrier Distribution for the Phase Shift Microwave Detected Photoconductivity Technique

V.V. Sirotkin, E. B. Yakimov

Institute of Microelectronics Technology RAS, Chernogolovka, 142432 Russia  
e-mail: yakimov@ipmt-hpm.ac.ru; fax: 7-095-9628047; phone: 7-09652-44161

Carrier lifetime is one of a very few parameters giving information about the defect density as low as  $10^{10}$ - $10^{11}\text{cm}^{-3}$  that is very important for the routine control of heavy metal contamination in Si wafers. Sometimes lifetime measurements allow to identify the impurity as in a case of Fe. But the reconstruction of Fe distribution is limited by the strong dependence of lifetime in Si contaminated with Fe on excitation level. Therefore for the correct reconstruction of Fe distribution from lifetime maps it is necessary to know this dependence and additionally to estimate the excitation level that for local excitation could also be a rather difficult task. A few methods are used nowadays for lifetime mapping and one of widely used techniques is based on the microwave detection of photoconductivity in the phase shift (PS) mode. In this method the laser diode intensity was modulated and the phase shift between a sinusoidal modulation of excitation and the variation of microwave reflection power is detected. As the excitation is modulated by a small amplitude sine wave, the technique is a quasi steady state one, and its main advantage is a practically constant excitation level. In the present work a computer simulation was carried out to estimate this excitation level. Under simulations the excess carrier concentration is normalized by the total generation intensity, which could be estimated experimentally for any setup used for the lifetime PS mapping. For the solution of three-dimensional diffusion equation with corresponding boundary conditions, a numerical method combining adaptive composite grids and an iterative domain decomposition algorithm is applied. Then the volume occupied by carriers presenting in equal concentration is calculated as a function of this concentration and an average phase shift is assumed to be associated with the carriers, concentration of which corresponds to a maximum in this dependence. The dependences calculated for different lifetime values are presented. It is shown that the carrier concentration determining the average phase shift has rather small dependence on lifetime that allows the correct reconstruction of Fe distribution. Besides, it is obtained that for such method the signal is mainly determined by carriers located at distances comparable with the diffusion length thus the spatial resolution is determined not by the excitation beam diameter but mainly by the diffusion length.



## **Correlation between BSE energy and X-ray spectra of multilayered microelectronics structures**

**E. I. Rau<sup>1</sup> and J. Wernisch<sup>2</sup>**

<sup>1</sup> Moscow State University, Dept. Physics, 119899 Moscow, Russia  
e-mail: [rau@pel157a.phys.msu.su](mailto:rau@pel157a.phys.msu.su) fax: 7-095-9391787; phone: 7-095-939-3895

<sup>2</sup> Technische Universität Wien, Austria

One of the problem in SEM BSE microscopy and EPMA in semiconductor microelectronics diagnostic was that of knowing the surface and subsurface structures, the quantification of the BSE tomography, i.e. the accurate measurements of the depth and thickness of separate films of multilayered structures. In this reports it is discussed the possibility of film thickness measurements by means of experimental determined mean BSE energy. Comparison of experimental BSE spectras and X-ray intensity distribution of multilayered microelectronics structures was made. It is shown that simultaneously recording of BSE and X-ray signals is very suitable for quantitative BSE microtomography of complex multilayered and other 3-D structures. The estimation of mean and most probably BSE energy and X-ray spectras was made on different samples configurations. It is shown that complete multilayered sandwich structures (including semiconductor films) characterization can be performed by use of an comparison procedure of BSE and EPMA simultaneous analysis of the thickness and the composition of all consisting films.

The authors acknowledge the support given by INTAS (project No 97-31864)

## Investigation of indium solder interfaces for high-power diode lasers

**C. Scholz, K. Boucke, R. Poprawe**

Fraunhofer Institute for Laser Technology

Steinbachstr. 15

52074 Aachen

Germany

phone: +49(0)241/8906-423

fax: +49(0)241/8906-121

email: [scholz@ilt.fhg.de](mailto:scholz@ilt.fhg.de)

During the last years high-power diode lasers became increasingly established for direct materials processing. Examples are the welding of plastics or the hardening of metal surfaces. In order to become more established and to open new fields of applications, the efficiency and the life time have to be increased.

Nowadays not only the semiconductor structure of the diode lasers has to be improved, but also the solder bond and the cooling technique. The effects of the solder layer and the structure of the heat sinks are taking a major influence on the efficiency and the life time of the diode lasers.

The solder pad has an area of approximately 1x10mm and the thickness of the solder is about 5µm. The requirements for the solder interface of high-power diode lasers in terms of thermal and electrical conductivity are considerable.

The solder layer has to be a good electrical conductor. The voltage drop has to be minimized at the solder layer. At a typical maximum current of 100A a high voltage drop creates a new heat source in the solder layer, which results in a rise of temperature in the semiconductor. To reduce the temperature in the semiconductor, the solder layer should have a good thermal conductivity. To avoid hot spots, the contact surface has to be maximized. Therefore an optimized flux resulting in almost no deposits should be chosen. To reduce the mechanical stress through thermal expansion a ductile soft solder is chosen. For all following examinations indium solder on a copper heat sink is used.

The copper heat sink is metallized with a thin gold layer. Then through vaporization the gold layer is coated with an indium layer of only a few micrometers. The contact surface of the semiconductor is gold as well.

To characterize the mechanical behavior a depth profile is prepared in order to determine the diffusion process between the indium solder and the gold contact surface. With this data a fitted simulation has been produced, in order to examine the influence of solder layers with varied thickness.

To determine the ratio of the moistened surface area, the samples are examined with an acoustic wave microscope. Therefore the thickness of the oxide film on the Indium is determined with XPS, in order to choose a good-working flux for this application. The deposits of the flux are considered with SEM.

The thermal coefficient of the solder interface is examined with a scanning near-field thermal microscope. With this data the different diffusion layers can be characterized and optimized.

These examinations are used to optimize the solder layer.

## Computer Image HRTEM Simulation of Catalytic Nanoclusters on Semiconductor Gas Sensor Materials Supports

**J. Arbiol<sup>1</sup>, F. Peiró<sup>1</sup>, A. Cornet<sup>1</sup>, J. R. Morante<sup>1</sup>, J. A. Pérez-Omil<sup>2</sup> and J. J. Calvino<sup>2</sup>**

<sup>1</sup> Departament d'Electrònica, Universitat de Barcelona, Martí i Franquès, 1, 08028 Barcelona (Spain). E-mail: [arbiol@el.ub.es](mailto:arbiol@el.ub.es) Telf.: ++34 93 402 1141

<sup>2</sup> Departamento de Ciencia de los Materiales e Ingeniería Metalúrgica y Química Inorgánica, Universidad de Cádiz, Cádiz (Spain).

In the last few years, there has been an increasing interest in the electronics world for those aspects related to semiconducting gas sensor (SGS) materials. In view of the increasingly strict legal limits for pollutant gas emissions, there is a great interest in developing high performance gas sensors for applications such as controlling air pollution and exhaust gases. In this way, semiconductor gas sensors offer advantages due to their simple implementation, low cost and good reliability for real-time control systems. The introduction of catalytic additives to the SGS materials has been reported by several authors to improve the sensitivity and selectivity of the sensor, and to reduce the response time and operating temperature of the device.

Although there exist many works in literature devoted to the electrical and general analytical characterisation as well as to the understanding of the physical mechanisms that rule the gas sensing behaviour, just few works have been dedicated to the nanostructural characterisation of semiconductor nanopowders and metal additives morphology and distribution in these SGS systems. Attending to these considerations, we have applied those nanoscopical techniques that allow the further studies needed in SGS materials field. The work performed in TEM and HRTEM and the complementary use of the Digital Image Processing and Computer Image Simulation, have given us a good understanding of the nanoscopic characteristics and behaviour of our materials.

The present study tries to be a complete overview of the catalytic distribution patterns on SGS materials: Metal Diffusion inside semiconductors bulk, Superficial Clustering and Metal Ultradispersion have been studied taking as an example the most common SGS materials ( $\text{SnO}_2$ ,  $\text{TiO}_2$ ) and catalytic metal species (Pt, Pd, Nb). We have analysed the growing mechanisms, the epitaxial relationships between metal clusters and SGS supports, the effects of sintering, the influence of catalytic species on semiconductor morphology and all the aspects related with the nanostructural properties of our systems. Using complex supercell models we could simulate the nanostructures studied, obtaining a good understanding of the results experimentally found.





## RADIATION-INDUCED POINT DEFECTS IN VITREOUS CHALCOGENIDE SEMICONDUCTORS STUDIED BY POSITRON ANNIHILATION METHOD

**O.I.SHPTYUK<sup>1,2</sup> and J.FILIPECKI<sup>2</sup>**

<sup>1</sup> Lviv Scientific Research Institute of Materials of SRC "Carat",  
202, Stryjska str., Lviv, UA-79031, Ukraine  
E-mail: shptyuk@novas.lviv.ua  
Fax: + 380 322 63-22-28

<sup>2</sup> Physics Institute of Pedagogical University of Czestochowa,  
13/15, Al. Armii Krajowej, Czestochowa, PL-42201, Poland

The physical nature of radiation-induced coordination defects formation processes was studied in chalcogenide vitreous semiconductors at the example of ternary Ge-As-S chemical system.

The radiation treatment of the investigated samples prepared by a standard melt-quenching method was performed in the normal conditions of the stationary radiation field, created in the closed cylindrical cavity owing to the concentrically established <sup>60</sup>Co (E=1.25 MeV) sources. The accumulated doses of 1÷5 MGy were chosen taking into account our previous results on radiation effects study in the binary As-based chalcogenides. The positron lifetime measurements were carried out with an ORTEC spectrometer (<sup>22</sup>Na isotope with 0.74 MBq activity). The additional information on the point defects origin were obtained owing to IR reflection spectra measuring before and three months after  $\gamma$ -irradiation in 400-200 cm<sup>-1</sup> region using a LAFS-1000 Fourier spectrometer.

The whole variety of the statistically possible coordination defects formation processes, associated with covalent chemical bonds switching in the investigated ternary As-Ge-S glass system, were analyzed. The pairs of diamagnetic over-coordinated positive ( $As_4^+$ ,  $S_3^+$ ) and under-coordinated negative ( $Ge_3^-$ ,  $As_2^-$ ,  $S_1^-$ ) point defects (the subscript - coordination number, the superscript - electrical charge excess) were supposed to be formed as a result of these transformations. The physically possible defects formation variants were experimentally selected using IR Fourier reflection spectra and then put in the ground of the developed topological model for the observed radiation-structural changes. This conclusion was confirmed entirely by positron lifetime measurements. It was shown that only lone average lifetime (near 0.35 ns) was proper to the non-irradiated glasses corresponded to low concentration of negative coordination defects. Two different lifetime components in  $\gamma$ -irradiated samples were observed, the long-living one at the level of 0.38 ns being attributed to positron annihilation on As- and Ge-based point defects and the short-living one (near 0.28 ns) - on S-based point defects in good agreement with well-known previous experimental data.

The compositional dependences of the investigated coordination defects formation processes in the above chalcogenide semiconductors were treated in the terms of average coordination number and "free" volume concepts.



## Investigations on $\text{Zn}_x\text{Cd}_{1-x}\text{O}$ Thin Films Obtained by Spray Pyrolysis.

H.Tabet-Derraz, N.Benramdane, D.Nacer, A.Bouzidi, M.Medles.

Materials and Components Physics Laboratory Djillali Liabès University, P.B. 89, 22000, Sidi Bel-Abbès, ALGERIA.

htabet@yahoo.fr. N.Benramdane@yahoo.fr A.Bouzidi@yahoo.fr,  
Tel/Fax: (213) 048 56 29 09 / 56 37 96

Keywords : Thin films, spray pyrolysis, zinc oxide, cadmium oxide, Structural, optical, electrical properties.

$\text{Zn}_x\text{Cd}_{1-x}\text{O}$  thin films were prepared on glass substrates by spray pyrolysis technique. The precursor solutions were obtained by varying the concentration of  $\text{Zn}(\text{NO}_3)_2 \cdot 6\text{H}_2\text{O}$  and the  $\text{Cd}(\text{NO}_3)_2 \cdot 4\text{H}_2\text{O}$  in a bi-distilled water. The structural properties have been studied analysing X-rays diffraction spectra. All the structures include the basic compounds, i.e.  $\text{ZnO}$  and  $\text{CdO}$ . The orientation and the crystalline phases of the deposited films were specified. With adding the Zn in the precursor solution, we can observe the preferential orientation of the  $\text{CdO}$  in the [200] direction. The electrical measurements were performed using method of four contacts. Thin films transmittances, in the 1.5-4.3 eV range, for different compositions have been measured and the optical gaps have been determined. The variations are explained considering the gaps of the two pure films. The influence of increased Cd concentration in the films on the structural, electrical and optical properties are investigated in this study.

**September 26, 14:00 - 15:15**

**POSTER Session 2**



## Characterization of thin films of n- and p-type GaN

A.Castaldini\*, A.Cavallini\*, L.Polenta\* and C.Diaz-Guerra\*<sup>#</sup>

\*INFM and Dipartimento di Fisica, Universita' di Bologna, Italy

<sup>#</sup>Permanent Address: Departamento de Fisica de Materiales, Universidad Complutense de Madrid, Spain.

Technological improvement of GaN-based devices for electronic and optoelectronic applications makes indispensable both monitoring and controlling point and extended defects, which can have detrimental effects in device performance.

It is assessed that the thickness of gallium nitride layers is a key parameter in determining the density and the distribution of defects, especially of the extended ones. In fact the strain related to the lattice mismatch between GaN and sapphire substrate enhances the formation of threading dislocations at the interface, consequently creating a highly defected layer. The dislocation density decreases with increasing the layer thickness, because the propagation of dislocations from the interface to the top layer becomes less probable.

Luminescence characteristic emissions in GaN are currently considered a sort of "signature" revealing the presence of defects; on the other side luminescence spectra are also strongly dependent on the conductivity type.

To evidence the characteristics due to different conductivity type in highly dislocated gallium nitride, n-type and p-type thin layers have been examined. The following samples have been investigated:

- p-type Mg-doped sample, 1.8  $\mu\text{m}$  thick,  $p = 1 \times 10^{17} \text{ cm}^{-3}$ , mobility  $\mu_p = 15 \text{ cm}^2/\text{Vs}$ ;
- n-type Si-doped sample, 2  $\mu\text{m}$  thick, MBE grown,  $n = 7 \times 10^{17} \text{ cm}^{-3}$ , mobility  $\mu_n = 177 \text{ cm}^2/\text{Vs}$ .

Photocurrent (PC) and Cathodoluminescence (CL) spectra have been collected at different temperatures in the range 1.6-3.4 eV to evidence the presence of emissions (blue, yellow, green) related to extended defects.

EBIC (Electron Beam Induced Current) scanning microscopy and CL (Cathodoluminescence) mapping have been carried out in order to investigate the recombination activity of extended defects and their spatial distribution.

These results have been interpreted according to the findings of DLTS analyses performed to determine the main parameters (energy, capture cross section and concentration) which describe the electrical activity of defects in the energy interval 0.1-1.2 eV from the conductance (n-type) and from the valence (p-type) band.

## Precipitates in AlGa<sub>N</sub> epilayers grown by metallorganic vapor phase epitaxy

**Junyong Kang<sup>1</sup>, Shin Tsunekawa<sup>2</sup>, Shun Itoh<sup>2</sup>**

<sup>1</sup> Department of Physics, Xiamen University, Xiamen 361005, P. R. China

E-mail: jykang@xmu.edu.cn, Fax: +86-592-2189426, Tel: +86-592-2186393

<sup>2</sup> Institute for Materials Research, Tohoku University, Sendai 980-8577, Japan

AlGa<sub>N</sub> alloy is an excellent candidate for applications in solar blind ultraviolet detectors, space communications, flame detection, and so on because of its advantages of wide direct band gaps, high temperature resistance, and good radiation hardness. Although a number of progresses have been made in metal organic vapor phase epitaxy, there is still a drawback to remove the influence of unintentional dopants. It has been observed in our previous work that the residuals O and C impurities are likely to form precipitates in nanopipes of AlGa<sub>N</sub> and Ga<sub>N</sub> epilayers. However, little information has been gained on precipitates in AlGa<sub>N</sub> epilayers without nanopipes.

The samples under study were AlGa<sub>N</sub> epilayers grown on (0001) Ga<sub>N</sub> by metallorganic vapor phase epitaxy at atmospheric pressure. A Ga<sub>N</sub> buffer layer was first deposited on the (0001) surface of an Al<sub>2</sub>O<sub>3</sub> substrate at 488 °C. Then, a 0.6-μm-thick Ga<sub>N</sub> layer was grown at 1070 °C. Finally, a 0.4-μm-thick Al<sub>0.22</sub>Ga<sub>0.78</sub>N layer was grown at 1080 °C. None of the epilayers were intentionally doped. As-grown epilayers were transparent with specular surfaces. The surface morphology of the epilayers was first imaged by a scanning electron microscope (SEM) and then by an atomic force microscope (AFM). The precipitate composition was analyzed by an energy dispersive X-ray spectroscopy (EDS) within the SEM. The precipitate structure was imaged by a transmission electron microscope (TEM).

The surface morphologies of AlGa<sub>N</sub> exhibit a number of contrast dark regions in the size of several ten-nanometers. EDS spectra of the dark regions exhibit stronger characteristic X-ray peak of C element and more recognizable peak of O element in comparison with the spectra of their bright surroundings. This indicates that the dark regions are precipitates and their bright surroundings are AlGa<sub>N</sub> matrix. The precipitates were confirmed to be tiny protuberances in specular surface by AFM observation. TEM images of the precipitates were characterized by irregular shapes of cores surrounded by interacted dislocation nets with regular patterns. The formation mechanism of the precipitates in AlGa<sub>N</sub> epilayers without nanopipes was discussed.



## **Removal of defects formed due to micro-masking on Ga-polar surface of GaN single crystals after reactive ion etching**

**G.Nowak, R.Czerwinski, M.Leszczynski, I.Grzegory**

High Pressure Research Center, Polish Academy of Science

Ul. Sokolowska 29, 01-141 Warsaw, Poland

e-mail: [grn@unipress.waw.pl](mailto:grn@unipress.waw.pl)

phone: (48-22) 632 16 35

fax : (48-22) 632 42 18

Surface of gallium nitride after mechanical polishing contains large amount of particulate contamination. During subsequent Reactive Ion etching these particulates act as micro-masks. Consequently the etched surface contains large number of defects, in form of narrow (20-30 nm diameter) pillars.

It is shown that etching in hot KOH solution completely removes those defects. After this treatment (0001) Ga-polar GaN surface slightly roughens and shallow, hexagonal etch pits are formed.

## A Raman study of GaAsN, GaInAsN layers on beveled samples

**R. Srnanek, A. Vincze, J. Kovac, I. Gregora\*, V. Gottschalch \*\***

Microelectronics Dept., Slovak University of Technology, Bratislava, Slovak Republic,  
Tel.: 421-7-60291653, Fax : 421-7-65423480, E-mail : srnanek@elf.stuba.sk

\* Institute of Physics, AS CR, Prague, Czech Republic

\*\* Fac.of Chemistry and Mineralogy, University Leipzig, D-04103 Leipzig, Germany

The ternary and quaternary alloys GaAsN and GaInAsN are promising materials for long wavelength fiber communication applications. Incorporation of relatively small concentrations of nitrogen produces a very large reduction of the band-gap energy. GaInAsN has already been shown successful to fabricate 1.3  $\mu\text{m}$  lasers and GaAsN resonant-cavity avalanche photodiode operating at 1.064  $\mu\text{m}$ . Both on GaAs substrates. Raman spectra provide sensitive tool for studying the local structure of impurity incorporation, deviation from long-range order induced by the incorporation of guest atoms. It is a technique of high spatial resolution, allowing the study of structural defects.

In this work a Raman spectra of GaAsN and GaInAsN with focus on their evolution with increasing nitrogen content up to 4 % are studied. The alloys were grown using metal organic vapor phase epitaxy (MO VPE) on (001) GaAs substrates. Raman spectra were recorded in the backscattering geometry, using the 514.5 nm line of an Ar<sup>+</sup> laser and 632.8 nm line of a He-Ne laser, respectively. Spectra were measured at room temperature and under unpolarised light. The content of nitrogen in the layers was determined by x-ray diffraction after the growth of the structures. The layer thickness varied from 130 to 300 nm and were mostly or partially relaxed. Finally a multiquantum well structure GaAsN/GaAs was studied. The structures were examined as grown and on the beveled structures prepared by chemical etching in  $\text{H}_3\text{PO}_4 : \text{H}_2\text{O}_2 : \text{H}_2\text{O}$  etchant. The prepared bevel angle was in the range  $10^{-4} - 10^{-5}$  rads.

In Raman spectra both GaAs-like and GaN-like optical phonons were observed. Because the GaAsN layers are under tensile strain LO peak is shifted from value  $292 \text{ cm}^{-1}$  to the low frequency values, to about  $288 \text{ cm}^{-1}$  for 4% N in alloys. On the beveled surface of relaxed layers the misfit dislocations and breaches were observed. The influence of these defects on Raman spectra have been examined. The main focus of our study was concentrated on changes of Raman spectra along the bevel. The ratio of TO and LO phonons (TO/LO) intensities were evaluated from these spectra. The different profiles of TO/LO dependencies along the bevel on relaxed and non relaxed layers were observed. This ratio increases from substrate-layer interface in dependence on bevel length until some "limit" thickness of GaAsN layer. In the case where the thickness of the layer is higher than this limit and the increasing of TO/LO ratio is stopped and high scattering of TO/LO is detected, this dependence corresponds to the relaxed layers. In the case when the ratio of TO/LO value doesn't stop, only the slope of the ratio is changed, this dependence correspond to the non relaxed layers. This phenomenon can be explained by presence of the defects after relaxation and by changes of the nitrogen incorporation in the alloys.





## Effect Of High Energy Nitrogen Irradiation in GaN

**M.Senthil Kumar, D.Kanjilal<sup>a</sup> and J.Kumar**

Crystal Growth Centre, Anna University, Chennai 600 025, INDIA

<sup>a</sup> Nuclear Science Centre, New Delhi, INDIA

e-mail : [senthilramu@hotmail.com](mailto:senthilramu@hotmail.com) Phone : +91-44-2352774 Fax : +91-44-2352870

Gallium Nitride (GaN) has received great interest since they have shown a great performance in light emission over short wavelength region of electromagnetic spectrum (1). It has been proved that the device performance could be improved by subjecting the devices to controlled dose of particle irradiation (2). Therefore, it is essential to analyse the defect nature as well as their influence on materials properties. The MOCVD grown GaN epitaxial layers were irradiated with 70 MeV nitrogen ion for various doses ranging from  $10^{11}$  to  $10^{14}$  cm<sup>-2</sup>. The irradiated samples have been subjected to various characterization techniques such as HALL, HRXRD and TRPL to analyse the effect of irradiation on the layer properties. The resistivity of GaN layers increases with ion fluence while their mobility and carrier concentration decreases. The defect production due to ion irradiation is increasing with ion fluence and hence the carrier trapping which is responsible for increase of resistivity also increases. HRXRD exhibits little improvement in FWHM of rocking curve due to low dose irradiation with decrease in peak intensity. TRPL measurements shows an increase in minority carrier life time with respect to ion fluence upto  $10^{13}$  cm<sup>-2</sup> and decreases for the dose  $10^{14}$  cm<sup>-2</sup>. DLTS experiments are planned in order to identify the deep level defects present in the band-gap. The results will be presented in more detail.

### References :

1. S. Nakamura and G.Fasol, The blue laser diode, Springer Verlag, 1997.
1. V.M. Rao, W.P. Hong, C. Caneau, G.K. Chang, N. Papanicolaou and H.B. Dietrich, J. Appl. Phys. 70 (1991) 3943.



## High resolution x-ray diffraction investigations of thin $\text{Al}_x\text{Ga}_{1-x}\text{N}$ films.

E. Zielińska-Rohozińska, M. Regulska, K. Pakuła, J. M. Baranowski, A. Kasińska

Institute of Experimental Physics, University of Warsaw  
Hoża 69, 00-681 Warsaw, PL  
Email: mreg@fuw.edu.pl, fax: (48-22)(622 61 54)

The x-ray diffraction measurements were performed with a triple-crystal x-ray diffractometer (MRD, Philips) with Bartels monochromator set for Ge 220 reflections of  $\text{CuK}_{\alpha 1}$  radiation. The AlGa<sub>N</sub> films used in this study were grown by MOCVD method on sapphire c plane under atmospheric pressure. The deposition procedure was sequential growth of: (1) First a low temperature (500° C) GaN buffer layer of thickness of 25 nm. (2) The growth temperature was raised then to 1100° C and 4 μm thick epitaxial films were grown in order to reduce structural defects. (3) The growth temperature was lowered then to 1025° C and 2 μm thick, undoped GaN overlayers were grown. (4) 25-30 nm thick ternary  $\text{Al}_x\text{Ga}_{1-x}\text{N}$  layers -intentionally  $x \approx 0.055$  were deposited. (5) Finally 100 nm thick, Si doped  $\text{Al}_x\text{Ga}_{1-x}\text{N}$  layers were grown. The differences in the interference pattern revealed in both, the diffraction profiles taken for scans along the diffraction vector and the reciprocal space maps [1] recorded at several places across the sample, are distinct. Moreover, "shoulders" appear on both sides of the measured diffraction peaks for scans performed in direction perpendicular to the diffraction vector at some places of sample where interference pattern is not detectable. They are resembling the intensity distribution calculated for small density of 60° glide correlated dislocations in heterostructure system [2].

Photoreflectivity measurements have been performed to determine the energy gap of AlGa<sub>N</sub>. Due to macroscopic size of light spot the optical measurements have been done on areas at which average Al composition corresponds to values of 0.053 and 0.059. Al composition derived from x-ray data is in the compositional range  $< 0.049; 0.069 >$ . The determined energy gap corresponds to 3.51 eV and 3.52 eV. These values indicate that dependence of AlGa<sub>N</sub> energy gap versus Al composition is not linear with bowing parameter  $b = 0.7$ .

Coming to conclusion; *i*) the high sensitivity to small nonuniformity of the strains recognized as changes in the interference pattern of the diffraction peak is shown, *ii*) these small inhomogeneities being significant for optical properties, are probably related to geometry of sample in MOCVD reactor during layer deposition process and allow to determine the bowing parameter for AlGa<sub>N</sub> films. The detailed analysis of strain relaxation based on numerical computer simulations is in progress.

### References

- [1] High Resolution X-ray Diffractometry and Topography, ed. D.K. Bowen and B. K.Tanner, Taylor & Francis Ltd, (1998).
- [2] V. M. Kaganer et al., Phys. Rev. B **55**, pp.1793-1810 (1997).



## Characterization of p-n Structures Grown By Sublimation Heteroepitaxy of 3C-SiC on 6H-SiC

**A.M.Strel'chuk, N.S.Savkina, A.N.Kuznetsov, A.A.Lebedev, A.S.Tregubova**

Ioffe Physico-Technical Institute of the Russian Academy of Sciences,  
Politechnicheskaya 26, St. Petersburg, 194021, Russia  
Phone: (812) 2479930, Fax: (812) 2476425,  
E-mail: Anatoly.Strelchuk@pop.ioffe.rssi.ru

The potentialities and advantages of silicon carbide as a material for commercial power semiconductor electronic devices are well known. Though SiC pn structures with high reverse voltages have already been fabricated on the basis of  $\alpha$ -SiC, however, in such structures, the maximum reverse voltage usually is lower than the calculated value. This voltage strongly depends on structural factors, which limit the device area. It is known that inclusions of cubic silicon carbide ( $\beta$ -SiC) are sometimes found in epitaxial films of wider bandgap polytypes of  $\alpha$ -SiC. Such inclusions of  $\beta$ -SiC undoubtedly affect the attainable parameters of devices based on  $\alpha$ -SiC. Therefore, studies and identification of the effects caused by the presence of  $\beta$ -SiC in  $\alpha$ -SiC are of unquestionable interest.

The investigations were performed on p-n structures grown by vacuum sublimation epitaxy on 6H-SiC Lely substrates. X-ray topographs showed that the n-type epilayer contains a large region of 3C-SiC, which consists of two double position (DP) twins with different orientations of an area about half the whole area. The p-n junction was formed by sublimation growth of  $p^+(Al)$ -layer. X-ray topographs confirmed that a  $p^+$ -3C region with DP twins of different sizes formed throughout the epilayer. A study of forward current-voltage (I-V) characteristics of p-n structures demonstrated that about 90% of all the diodes can be placed in two groups according to positions of the 3C and 6H regions and differing in parameters of the exponential dependence of the current on voltage. I-V characteristics of type I diodes display excess currents compared with currents in 6H-SiC pn structures and close in magnitude to currents in anisotype homo p-n structures based on bulk 3C-SiC, with some indications of tunneling currents. The I-V characteristics of type II diodes are close to those of anisotype homo p-n structures grown on 6H-SiC substrates. Besides, the measured I-V characteristics are compared with typical excess currents of different type and, apparently, of different nature (not related to inclusions of 3C-SiC) in  $\alpha$ -SiC based p-n structures. At forward current, diodes of both types emit in the entire visible spectral range. The longer-wavelength emission is, on the average, predominant in type I diodes, and shorter-wavelength emission in type II diodes. However, the main feature of the injection electroluminescence (IEL) is a similarity of the IEL spectra from diodes of both types. In particular, the IEL spectra of both types of diodes contain two bands ( $h\nu_{\max} \approx 2.3$  eV and  $h\nu_{\max} \approx 2.9$  eV), attributed to free exciton annihilation in 3C-SiC and 6H-SiC, respectively.

This work was supported by the Russian Foundation for Basic Research (grants N00-02-16688 and N01-02-17657).

### Characterization of 3C-SiC epilayers grown on 6H-SiC substrates by vacuum sublimation

N.Savkina, A.Tregubova, M.Scheglov, G.Mosina, L.Sorokin, V.Solov'ev,  
A.Volkova, A.Lebedev

IOFFE Institute, Polytekhnicheskaya 26, 194021 ST.-PETERBURG, RUSSIA.  
Fax: +7 (812) 2476425, Phone: +7 (812) 2479930, E-mail: [nata.sav@pop.ioffe.rssi.ru](mailto:nata.sav@pop.ioffe.rssi.ru).

Silicon carbide (SiC) semiconductor technology is developed rapidly. Sublimation epitaxy is an important part of this technology through having many potentialities. This method has been successfully used for growth of silicon carbide layers. It is well known that SiC exhibits numerous structural variants called polytypes. All polytypes except one occur in hexagonal (H) or rhombohedral (R) structures and are denoted as  $\alpha$ -SiC. One polytype occurs in a zinc blend structure with cubic (C) symmetry and is denoted as  $\beta$ -SiC. It must be noted,  $\beta$ -SiC (3C) is a metastable polytype and forms at lower temperature than  $\alpha$  polytypes. Growth of  $\alpha$ -SiC (6H-SiC in our case) epilayers on basal orientation substrates of 6H-SiC is accompanied by growth of inclusions of 3C-SiC or transformation all 6H-SiC epilayer into 3C-SiC epilayer.

In this paper growth of 3C-SiC was performed on Si face on-axis 6H-SiC Lely substrates by sublimation in vacuum. Deposition of 3C layer corresponds to the island growth resulting in double position boundaries (DPB's) and stacking fault (SF) formation. Modifying growth conditions in the growth zone it is possible to obtain various density of DPB's and SF.

The purpose of this work is to characterize of as-grown 3C-SiC layers with different DPB's and SF density by several methods. Such the complex method of approach to the problem allowed us to receive more information about transformation one polytype to another. First the polytype, DPB's and SF distributions of 3C layers were mapped with optical microscope after the layers were oxidized and those having various DPB's density were extracted. Then the grown films were investigated more carefully by X-ray diffraction technique (topography and diffractometry). The transmission topography, the back-reflection technique in an asymmetric geometry and double-crystal topography were used in this study. The topographs of selected structures will be presented. These pictures clearly show that 3C layers consist of twins having various sizes. In this paper 3C-SiC twin areas from  $0.1\text{mm}^2$  to  $25\text{mm}^2$  have been studied. The interface 3C-SiC layer - 6H-SiC substrate has been investigated by TEM (transmission electron microscopy), SEM (secondary electron microscopy), the electron beam-induced current (EBIC) method and the results obtained will be discussed.

This work is supported by RFBI grants # 00-02-16688, # 01-02-17657.

## Contactless Characterization of Surface and Interface Band-bending in Silicon-On-Insulator (SOI) Structures

T. Okumura, A. En, K. Eguchi and M. Suhara

Department of Electrical Engineering, Tokyo Metropolitan University

1-1 Minami-ohsawa, Hachioji, Tokyo 192-0397, Japan

Email: okumura@eei.metro-u.ac.jp, Fax: +81-426-77-2756, Phone: +81-426-77-2760

A silicon-on-insulator (SOI) material is offering several advantages over the bulk LSI technology for high speed as well as low-power applications. As the thickness of the top-Si layer in the SOI materials is reduced, electric properties of the surface as well as the buried Si/SiO<sub>2</sub> (BOX) interfaces become crucial to the device performance in addition to the quality of the top Si layer.

In this paper, we demonstrate that the Kelvin-probe method is capable of determining electrical properties of the surface as well as the near-surface region of the SOI material without any device preparation process and completely in a nondestructive manner. With the use of ultraviolet (UV) light source for the surface-photovoltage (SPV) measurement, the surface band-bending of very thin SOI layers can be characterized, because of very short penetration depth of the UV light (several 10<sup>2</sup> nm @340 nm). On the other hand, infrared (IR)-illumination (the penetration depth of several μm) is capable of searching deeper region, such as the BOX-substrate interface.

Figure 1 shows the "contactless *I-V* characteristics", i.e. the light-intensity dependence of the surface photovoltage (SPV). Two SOI materials were fabricated by completely different processes, although the thickness of the top-Si layer is in the same order of magnitude. Just prior to the measurement, both samples were precleaned by the RCA method followed by dipped into a 4.5% HF solution. The experimental results show that there is a significant band-bending both at the top surface (UV) and the BOX-substrate interface (IR) for sample #1, while negligibly small band-bending is observed at the BOX-substrate for sample #2.

The details of the experimental method and the other data will be discussed in the presentation.

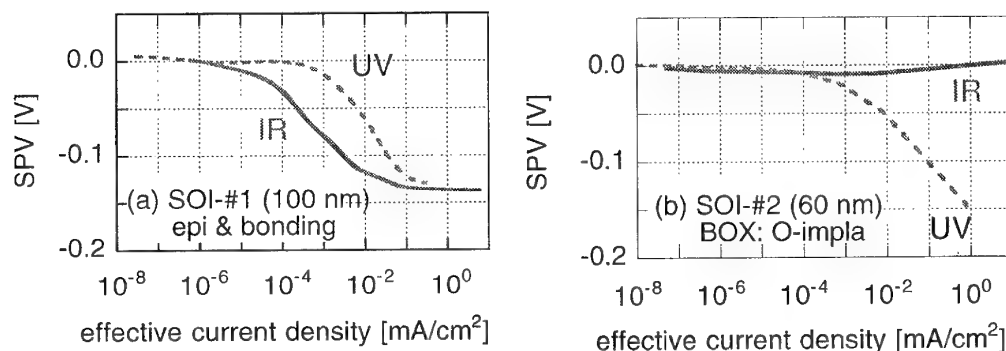


Fig. 1 Contactless *I-V* characteristics for two different kinds of SOI (p on p) materials. The negative polarity of SPV indicates downward bending of the energy band.

## Scanning Kelvin Probe and Surface Photovoltage Analyses of Polycrystalline Silicon

A.Castaldini, D.Cavalcoli, A.Cavallini, M.Rossi

INFM and Physics Department, viale Berti Pichat 6/2, I- 40127, Bologna, Italy.  
Tel: +39 051 2095806 Fax: +39 051 2095153 e-mail: mrossi@df.unibo.it.

The aim of this work is to show physical principles, technical details and capabilities of two non-contact techniques used for the characterization of polycrystalline silicon: Scanning Kelvin Probe (SKP) [1] and Surface Photovoltage (SPV) [2].

We have implemented these two techniques on the same stage to characterize polycrystalline wafers for photovoltaic application. The implementation of the two probes on the same stage is of wide interest for in-line applications in photovoltaic and microelectronics industries. SKP and SPV can measure important parameters affecting device performance, such as minority carrier diffusion length, work function, detection of organic contaminants and surface doping density.

The results concerning the application of these methods to the characterization of different polycrystalline Si wafers for photovoltaic application will be reported.

The minority carrier diffusion length is evaluated from the SPV signal obtained by the spectral response of the wafer to a low intensity photon excitation in the range (850-950nm), while the majority carrier concentration in the near-surface region (Surface Charge Profiling technique, SCP [3]) is measured from the SPV signal obtained by a low intensity blue light (wavelength equal to 450nm).

SKP has been used to measure the contact potential difference, and hence the work-function. As the work-function resulted to be correlated to the presence of organic contaminants on the Si surface, work-function maps of the whole area of the samples have been achieved to determine the distribution of the organic contamination.

All the parameters have been mapped (the wafers were 10x10cm<sup>2</sup> large) by these three methods.

All the experimental methods have been performed in non-contact mode and by means of the same experimental apparatus: in this respect the capabilities of these methods for fast and in-line characterization in the photovoltaic industry have been explored.

The research is being performed in the framework of the FAST-IQ European Project (Fast in line characterization tools and process control for crystalline silicon material for photovoltaic industry applications) financed by E.U. (Fifth Framework Program).

[1] I. D. Baikie and P. J. Estrup *Rev. Sci. Instrum.* **69**, 11 (1998).

[2] J. Lagowski, P. Edelman, M. Dexter and W. Henley *Semicond. Sci. Technol.* **7**, A185 (1992).

[3] E. Kamieniecki *J. Vac. Sci. and Techn.* **20**, 3 (1992).

## Photoacoustic (PA) evaluation of defects and thermal conductivity in the surface layer of ion implanted semiconductor

Nobuya Takabatake, Takeshi Kobayashi, Yoshiyuki Show\*, and Tomio Izumi\*

Department of Electrical and Electronic Engineering, Kanagawa Institute of Technology, 1030 Shimo-ogino, Atsugi, Kanagawa, 2430292 JAPAN

E-mail: batake@ele.kanagawa-it.ac.jp Fax: +81-46-242-6089

\* Departments of Electrics, School of Engineering, Tokai University

### 1. Introduction

In recent years, it becomes more difficult to characterizing crystalline defects in a surface of semiconductor, as LSIs become more integrated. A photoacoustic (PA) method is potentially a suitable measurement technique for local thermal conductivity in the vertical-depth direction of specimen. We measured annealing behavior of thermal conductivity in the surface of ion implanted semiconductor by using the PA method. Defects were evaluated through annealing behavior of thermal conductivity.

### 2. Experiment and results

The specimen consisted of an implanted part A and an unimplanted part B. The thermal characteristics of part B were known. The thermal conductivity was measured from the phase difference of the PA signals between part A and part B<sup>1)</sup>. Silicon substrates were implanted with Si ions at 150 keV with an implantation dose from  $1 \times 10^{12}$  to  $1 \times 10^{16}$  ion/cm<sup>2</sup>. The thickness of the implantation layer was 100 nm, which measured by TEM. Annealing behavior of the thermal conductivity for each specimen are shown in Fig. 1. The thermal conductivity values after ion implantation divided into two ranges: about 3 and 0.3 Wm<sup>-1</sup>K<sup>-1</sup>. Those respective thermal conductivity values are about 1/50 and 1/500 of the value for the unimplanted specimen.

The thermal conductivity began to increase with temperature rising from 600°C, and recovered for the value of unimplanted specimen after annealing at 750°C. The recovery of the thermal conductivity by the annealing means the removal of the defects in ion implanted layer. Therefore, the PA method is effective for the evaluation of the defects in the thin films with submicron thickness. We will report in detail the annealing behavior of the thermal conductivity at the conference.

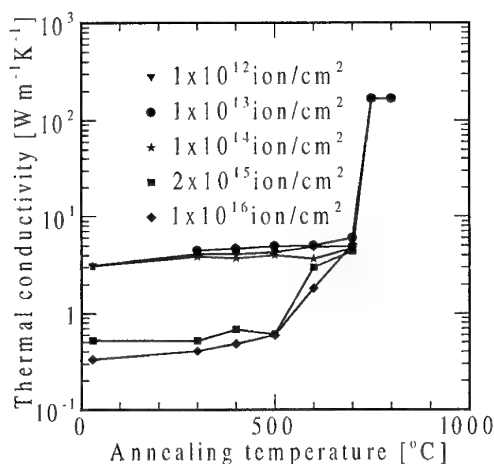


Fig.1 Annealing curve of the thermal conductivity.

1) N. Takabatake, T. Kobayashi, D. Sekine and Tomio Izumi, Appl. Surf. Sci. 159-160 pp594-598(2000)



## **The optoelectronic characterization of the silicon/silicon nitride interface**

**G. Citarella, O. Abdallah and M. Kunst**

Hahn-Meitner-Institut, Dept. Solare Energetik (SE5), Glienicker Strasse 100, 14109  
Berlin, Germany; e-mail: citarella@hmi.de, phone: 0049 (0)30 80622189,  
fax: 0049 (0)30 80622434

Plasma enhanced chemical vapour deposited (PECVD) silicon nitride (SiN) films are of growing interest in the semiconductor industry. They are extensively used as oxidation and diffusion masks, dielectrics and play also an essential role in nonvolatile memories and thin film transistors. These films are excellent anti-reflection and passivation coatings of silicon.

In this work the Si/SiN interface is studied by contactless, transient and frequency resolved photoconductivity measurements in the microwave frequency range.

Volume excitation (by 1064 nm light) and surface excitation (by 532 nm light) are used to induce the signals.

It is shown that the covering of one surface of a nSi wafer with a SiN film leads to a strong increase of the photoconductivity decay time. The decay is mainly determined by diffusion controlled surface recombination at the uncovered surface. The SiN covered surface can be considered as a reflecting wall for excess charge carriers. This passivation is due to the suppression of defects and the formation of an accumulation layer at the nSi/SiN interface. Experimental evidence suggests that the main effect is field induced passivation. In nSi wafers covered at both surfaces with SiN it is observed that the lifetime measured approaches the volume lifetime.

The behaviour is more complicated in pSi wafers coated with SiN. In these samples a depletion-inversion layer is formed at the junction leading to the separation and storage of excess charge carriers. The effective surface lifetime depends strongly on the injection level. The extraction of the interface state density from the lifetimes measured will be discussed taking into account the space charge field and the cross-sections. Exemplary scanning measurements with relatively high resolution will be presented.



## Extraction of Parameters of Deep Centers and Interface Traps in SOI Structures With Using of DLTS Measurements

I.V.Antonova

Institute of Semiconductor Physics, Novosibirsk, 630090, Lavrentieva 13, Russia

E-mail: [antonova@isp.nsc.ru](mailto:antonova@isp.nsc.ru), Tel: (7-3832)-33-24-93, Fax: (7-3832)-33-27-71

A production of the main parts of the integral circuits in modern microelectronics based on bulk silicon will be in near future screwed by silicon-on-insulator (SOI) structures. The most advantageous methods of SOI fabrication use a technology of wafer bonding and hydrogen cutting of a thin layer (Smart-Cut technology [1], Genesis Process [2], and modified Smart-Cut technology [3]). The interface states and deep levels are very important parameters of SOI material and devices. Traditional capacitance DLTS (C-DLTS) is powerful technique for identification of interface states and deep levels in semiconductor volume. Charge DLTS (Q-DLTS) extends range of method possibilities especially for the MOS-like structures. The aim of the present report is extraction of parameters of the deep centers and interface traps in the SOI structures with using of C- and Q-DLTS.

The different ways for deriving distribution of interface states in Si band gap are compared and demonstrated on the example of the SOI structure fabricated with using of wafer bonding and hydrogen slicing. The high frequency capacitance – voltage (C-V) technique, charge and capacitance DLTS (Q- and C-DLTS) were used for investigation. The operational frequencies were 1 KHz and 8 MHz for Q- and C-DLTS, respectively.

If the top Si layer and the substrate have the same type of conductivity, C-V characteristics allow one to choose the voltage intervals which correspond to the regimes where the substrate is in depletion and the top Si layer is in accumulation, or the substrate is in accumulation and the top Si layer is in depletion regime, respectively. Thus, one can investigate separately by DLTS the substrate and the buried oxide/substrate interface, or the Si film and the top Si/SiO<sub>2</sub> interface. DLTS peaks have to be divided into two groups. The first group is corresponded to interface traps, the second are connected with the “volume” deep levels. The methods of separation and analyzes of continuous distribution of traps are suggested in the report.

The Si/thermal SiO<sub>2</sub> interface in investigated SOI is obtained to characterize by continuous distribution of interface states. Whereas in the case of bonded Si/SiO<sub>2</sub> interface a blurred system of levels  $E_c - 0.22$ ,  $E_c - (0.31-0.33)$  eV in upper half of band gap was observed. Deep levels with  $E_c - 0.39$  eV and  $\sigma = 1 \times 10^{-15}$  cm<sup>2</sup>, and  $E_c - 0.58$  eV,  $\sigma = 4 \times 10^{-14}$  cm<sup>2</sup> observed in top Si layer up to the depth of 0.21  $\mu$ m from surface most likely correspond to extended radiation damages located in near surface area of the SOI.

### References

- 1- M.Bruehl, NIM, vol. B 108, pp.313-319, February 1996.
2. Y.A.Li, R.W.Bower, Jpn. J. Appl. Phys., vol.39, pp. 275-276, January 2000.
3. V.P.Popov, I.V.Antonova, V.F.Stas, L.V.Mironova, E.P.Neustroev, A.K.Gutakovskii, A.A.Franzusov, G.N.Feofanov, in Perspectives, Science and Technologies for Novel Silicon on Insulator Devices, P.L.F.Hemment et al. (eds.) pp.47-54, 2000



## Cathodoluminescence of thin films of silicon oxide on silicon

M.V.Zamoryanskaya, V.I.Sokolov, I.M.Kotina

Ioffe Physico-Technical Institute, 194021, SPetersburg, Russia, email:  
zam@pop.ioffe.rssi.ru, fax.: (812)2471017, tel.: (812)2479382

Reliability and characteristics of planar devices depend on the properties of interface  $\text{SiO}_2/\text{Si}$ . In this work we studied the properties of thin chemical silicon oxide with thickness 2-5nm and the evaluation of natural oxide on silicon.

The properties of thin silicon oxide on silicon was studied using the cathodoluminescence (CL) method. This method is very sensible to the changes of the structure, structure defects and impurities in silicon oxide. This spectrometer is connected with electron probe microanalyzer "Camebax". The high sensibility of our optical CL spectrometer gives the possibility to measure the CL of the thin layers with thickness of 1-2nm. The time resolution method ( $5\mu\text{s}$ ) permits to mark out the emission bands related with intrinsic defects of  $\text{SiO}_2$  films at 2.65eV and 1.9eV with time rise 1ms and  $14\mu\text{s}$ .

CL spectra of thin silicon oxide films don't like on the one of bulk silicon oxide or thick films with thickness more than 10nm. The band at 1.9eV (nonbridging oxygen) was not observed in CL spectra of all the thin films we studied. All the CL spectra of the thin films consist of very broad band with halfwidth 0.8-1.0eV and with maximum at 2.0-2.5eV. In same case two maximum of CL intensity were observed in spectra. The position of the maximum of CL emission depends on the method of the preparation of silicon surface, on the type of silicon and on the film growth technique. The natural and chemical films on chemical polished silicon with high conductivity ( $2\text{-}40\text{k}\Omega/\text{cm}^2$ ) had a maximum of CL emission at 2.4-2.6eV. CL spectra of the thin films on silicon with low conductivity ( $0.01\text{-}450\Omega/\text{cm}^2$ ) had two maximum at 2.0-2.1eV and 2.3-2.5eV.

We studied the evolution of natural silicon oxide on "pure" chemical polished silicon with conductivity  $40\text{ k}\Omega/\text{cm}^2$ . The surface of this sample was passivated by hydrogen. In this case one intensive band at 3.4eV is observed in CL spectrum. It may be relate with direct transition of the silicon  $\Gamma_{c25}-\Gamma_{v15}$ . After tow weeks the intensity of the band at 3.4eV decreased and in the same time the broad band with maximum at 2.4-2.5eV appears in CL spectrum.

We relate the CL bands at 2.0-2.6eV in thin  $\text{SiO}_2$  films with silicon "islands" with size 15-25Å appeared in silicon oxide during the process of oxidation

## APPLICATION OF GASKETED DIAMOND ANVIL CELL FOR OPTICAL AND SPECTROSCOPICAL STUDY OF SEMICONDUCTORS UNDER PRESSURE

<sup>1</sup>Efros B.M., <sup>2</sup>Misiuk A, <sup>1</sup>Shishkova N.V., <sup>1</sup>Prudnikov A.M.

<sup>2</sup>Institute of Electron Technology, Warszawa, Poland

<sup>1</sup>Phys.& Tech. Institute, NASc, Donetsk, Ukraine

e-mail:efros@hpress.dipt.donetsk.ua

High pressure is an immensely useful tool in the study of semiconductors. With this aim the gasketed diamond anvil cell (DAC) based device for optical and spectroscopical investigations under pressure and pressure measuring has been developed on the basis of optical microscope and different spectrometers.

The deformable gasket material was 301 stainless steel; the disk-shaped gaskets (diameter 3-4 mm, thickness 150-250  $\mu\text{m}$ ) after pre-strengthening treatment were tested in screw-lever DAC at pressures up to 70 GPa. In the gasketed DAC, a sample hole of radius  $r_g$  is formed in the centre of the gasket, filled with pressure-transmitting fluid, ideally with shear strength  $k = 0$ . While increasing pressure, the cell seals by virtue of the pressure between the gasket and anvil being greater than the hydrostatic pressure by an amount equal to the shear strength in the thick gasket, and greater still in the thin gasket.

Optical transmission measurements in the gasketed DAC are performed by introducing radiation through the lower diamond and detecting through the upper diamond. The pressure transmitting fluid was a 4:1 mixture of methanol and ethanol. High pressure was measured using the ruby fluorescence method. The latter is a purely optical method based upon the shift with pressure of the doublet fluorescence normally found at 0,6942  $\mu\text{m}$ , commonly known as the *R* line. Using of spectrometer with linear dispersion 4.5  $\text{\AA}/\text{mm}$  allows one to measure by ruby a pressure with the accuracy of 30 MPa. This device allows one to study optical absorption, reflection and luminescence of studied samples under pressure in situ with minimum area  $20 \times 20 \mu\text{m}^2$  into spectral range 0.25-1.8  $\mu\text{m}$ . There is a high sensible television camera at this device allowing one to observe sample behaviour in situ in this wavelength range.

In this work, we shall present some typical experimental data on the high pressure behaviour of different semiconductors among them Si, Si-O, Ge and so on. Discussed results include metal- semiconductor transitions, electronic transitions, phase and structure transformations. Basic effects of pressure on semiconductors are the increase of direct band gap with the density of the crystal, the consequent band crossovers, and the increase in phonon frequencies.



## DAC OPTICAL ABSORPTION STUDIES OF THE Si-O ( $\text{SiO}_{2-x}$ ) SEMICONDUCTOR SYSTEM

B.Efros<sup>1</sup>, N.Shishkova<sup>1</sup>, A.Misiuk<sup>2</sup> and A.Prudnikov<sup>1</sup>

<sup>1</sup>Donetsk Physics & Technology Institute, Ukraine Academy of Sciences,  
Donetsk, Ukraine

<sup>2</sup>Institute of Electron Technology, Warsaw, Poland  
e-mail:shishkov@kinetic.ac.donetsk.ua

Extensive experiments studies of the – IV elements have been made in recent years. Motivations have included the rich variety of phase and structural transitions.

Different  $\text{SiO}_{2-x}$  defects can be created in Czochralski grown silicon, Cz – Si, by appropriate pre-annealing at atmospheric pressure ( $10^5$  Pa). Some data concerning the effect of enhanced hydrostatic pressure on creation of defects in the Si –  $\text{SiO}_{2-x}$  system have been reported for defects – containing Cz – Si subjected to the cyclic hydrostatic pressure treatment.

An attempt to observe the mentioned hydrostatic pressure – induced effect of massive creation of “new” defects in Cz – Si with oxygen – related defects were undertaken in this work.

The increase of defect concentration in the hydrostatic pressure – treated Cz- Si samples with initially present  $\text{SiO}_{2-x}$  precipitates can be considered as a proof of hydrostatic pressure – induced massive creation of defects on before – created oxygen – related defects. However, in the case of some DAC – treated samples, a misfit dislocation network was not directly proved to be created because of too small sample dimension in comparison to the resolution of the spectroscopy and X– ray methods.

The samples of this system, having minimum (Fz-Si) and maximum (Cz-Si) oxygen contents and, consequently, different defects present at the initial state, have been studied by optical microscopy. The studied samples were placed in the DAC and subjected to quasi-hydrostatic pressure at pressure up to 20 GPa. Structural investigations of the studied samples were carried out in situ under pressure at different pressures.

The study of these samples was carried out by spectroscopical methods under pressure too. In particular, it was revealed that the sample with high defect density indicated the transparency ~ 55-70% in the wavelength range 800-1100 nm with some maximum at 930 nm at the initial state the effect possibly connected with the sample non-homogeneity. At application of the high pressure (~5GPa) the value of transparency decreases up to 10% in the wavelength range of 800-925nm and later on transparency value increases sharply up to ~100% at 1100 nm wavelength. Further pressure rise (up to ~10 GPa) resulted in an increase of the transparency value up to 20% at 800-900 nm range and later on it increases up to 55% at 1100 nm wavelength. Thus with the pressure rise, the absorption edge of forbidden zone moved to higher wavelengths.

It follows that investigation in the DAC is a useful method to study structural and phase transformation also in non-homogeneous semiconductor materials likes Si- $\text{SiO}_{2-x}$ .



## THE IMPACTS OF NITROGEN ON POWER DIODE CHARACTERISTICS

Jinggang. Lu, Deren Yang\*, Luixin Fan, Xiangyang Ma, Liben Li, Duanlin Que

State Key Laboratory of Silicon Materials, Zhejiang University,  
Hangzhou 310027, People's Republic of China

KEYWORDS: NITROGEN, DIODE, REVERSE BREAKDOWN VOLTAGE, REVERSE RECOVERY TIME

Nitrogen in Czochralski (CZ) silicon has many interesting behaviors. It is well known that nitrogen in silicon can increase mechanical strength of silicon wafers by locking dislocations. It is found that nitrogen in silicon can influence the shape of voids and enhance the formation of oxide precipitates. However, many aspects of nitrogen in CZ silicon remain still unclear. In this paper, the impacts of nitrogen on the power diode characteristics are investigated.

Nitrogen doped CZ silicon (NCZ-Si) samples grown under reduced nitrogen atmosphere were used for manufacturing diodes. After diffusion and Nickel silicidation process, the wafers were cut into 1.2mmx1.2mm square chips which were then divided into center, middle and edge groups according their position in wafers. From each group, 50 chips were randomly chosen out to manufacture diodes. The diode characteristics: reverse breakdown voltage( $V_r$ ), forward voltage drop( $V_f$ ) and reverse recovery time( $T_{rr}$ ) were then tested on routinely diode analyzer. After diode process, the preferential etched specimens were examined by an optical microscope. For comparison, the common CZ silicon (ACZ-Si) samples grown under argon ambient with almost the same oxygen concentration and the thermal history were also used in our experiments. It was found that nitrogen doping has no influence on diodes' forward voltage drop, but decrease diodes'  $T_{rr}$  and  $V_r$  slightly, particularly for high interstitial oxygen specimens. It was also found that high density dislocations were formed in edge portion of both NCZ and ACZ silicon wafers during diode process. Compared with those made from center or middle portion of the wafer, diodes made from the edge portion have relative lower  $V_r$  and  $T_{rr}$ . It can be concluded that nitrogen has no important influence on the characteristics of diodes if the initial interstitial oxygen concentration is not too high ( $>10^{18}\text{cm}^{-3}$ ) in NCZ silicon. During the heat-up and cool-down process of phosphorous and boron diffusion, large amounts of dislocations were generated at the edge portion of the wafer. Nitrogen doping has no influence on the generation of these thermal stress induced dislocations which result in lower  $T_{rr}$  and  $V_r$ .

---

\* To whom correspondence should be addressed.



# CHARACTERIZATION OF STRUCTURAL, ELECTRICAL AND OPTICAL PROPERTIES OF RARE-EARTH DOPED Si-BASED LIGHT-EMITTING DIODES

N.A.Sobolev

Ioffe Physico-Technical Institute, St.-Petersburg, Russia

E-mail: [nick@sobolev.ioffe.rssu.ru](mailto:nick@sobolev.ioffe.rssu.ru), fax: (812)2471017, phone: (812)2473885

Light-emitting diodes (LEDs) based on Er-doped monocrystalline Si have attracted considerable interest for optoelectronic applications. To produce such structures, the solid phase epitaxial (SPE) technique is usually used. Er and O ion co-implantation is conventionally carried out into (100)-oriented substrates at room temperature. SPE recrystallization of layers amorphysed by the implantation is followed by the formation of end-of-range defects and hairpin dislocations, which are responsible for a relatively low intensity of Er-related luminescence. To improve the properties of Si:(Er,O) LEDs, we have suggested to implant Er ions into (111)-oriented substrates [1]. The purpose of this paper is to overview our recent results demonstrating the possibilities of the suggested modification of the SPE technique for the engineering of structural defect and electrically and optically active center as well as for improvement of the properties of Si:(Er,O) LEDs. Structural, electrical and optical properties in Ho and O ion co-implanted Si were also studied to determine some details of defect formation and luminescence processes.

Co-implantation of Er or Ho ions at  $0.8\pm 2.0$  MeV energies and  $1\times 10^{14}\div 9\times 10^{14}$  cm<sup>-2</sup> doses and O ions at  $0.06\pm 0.25$  MeV energies and  $1\times 10^{15}\div 9\times 10^{15}$  cm<sup>-2</sup> doses in n-Cz-Si as well as annealing at  $600\div 900^\circ\text{C}$  for  $0.25\div 4$  h in various ambient surroundings were carried out to produce the electrically and optically active centers. Implantation of B and P ions, titanium and gold sputtering, photolithography as well as chemical etching were performed to prepare LEDs with a mesa-like edge contour. TEM, SIMS, RBS, X-ray diffraction, DLTS, capacitance-voltage, photo- and electroluminescence (EL) techniques were used to study the properties of Si:(Er,O) and Si:(Ho,O) structures.

The suggested SPE technique allowed us to modify the spectra of structural defects, electrically and optically active centers in the samples, observe some new effects and improve the characteristics of LEDs. The formation of microtwins and dislocations in very high densities gave a possibility to prepare avalanching and tunneling diodes characterized by uniform breakdown over the whole area of p-n junction and working at room temperature. Temperature enhancement of the rare-earth-related EL intensity in (111) LEDs is observed under avalanche and tunnel breakdown of p-n junctions. The enhancement is related to the formation of process-induced deep level centers. New centers emitting under reverse bias and characterized by the highest effective cross section for the excitation of Er<sup>3+</sup> ions were firstly observed. The LEDs with EL of Ho<sup>3+</sup> ions at room temperature have firstly been prepared.

[1]. A.M.Emel'yanov, N.A.Sobolev et al. Appl. Phys. Lett. **72**, 1223 (1998).



## X-ray diffractometry of Si epilayers grown on porous silicon

**V.Bondarenko, V.Yakovtseva, L.Dolgyi,  
M.Balucani\*, G. Lamedica\* and A.Ferrari\***

Belarussian State University of Informatics & Radioelectronics, Minsk, Belarus  
vitaly@bsuir.edu.by, tel: 375 17 2398843, fax: 375 17 2310914

\* INFN Unit 6, University of Rome "La Sapienza", Rome, Italy

Porous silicon (PS) is of great scientific and practical interest because of its structural features. PS is produced when single-crystal Si is anodized in certain electrolytes. Anodic etching results in a porous layer containing pores of a few nanometers in diameter and Si crystallites of the same scale.

Both salient features of PS – crystallinity and porosity – depend strongly on regimes of the PS formation and are useful for one or other applications. The crystal structure of PS allows epitaxial layers to be grown on its surface. These are used for SOI-structure named ELTRAN (Epitaxial Layer TRANSfer) originated in Canon Inc. [1]. The key ELTRAN processes are CVD Si epitaxial growth on PS, bonding and splitting the bonded wafers along the PS layer. It is evident that the perfect structure of the Si epitaxial layer is desirable because this is the layer that is employed for active device fabrication. So, it is of importance to correlate structural perfection and strains of the grown epitaxial layer with the properties (thickness and porosity) of the seed PS layer.

The present paper reports the double crystal x-ray diffractometry for exploring the lattice mismatch and strains of epitaxial Si layers grown on the PS layers of various thickness and porosity.

N<sup>+</sup>-type (111) Czochralski Si wafers of 0.01 Ohm·cm resistivity were anodized in HF electrolytes to form PS layers of 1-5 μm thickness and 10-65% porosity. Then CVD Si epitaxy was performed by the pyrolysis of SiH<sub>4</sub> in hydrogen to grow 2 μm Si epitaxial layer on PS. X-ray rocking curves were recorded on a double crystal diffractometer using Cu K<sub>α</sub> radiation and a Si block as reference crystal.

For all values of PS thickness and porosity, lattice parameter of the PS layer was disclosed to be greater than that of the single-crystal Si substrate. The increased thickness of the PS layer increases the amplitude of the diffraction peaks from PS. The increase in PS porosity increases significantly the PS lattice parameter. High temperature annealing changes both value and direction of PS lattice deformation. The lattice parameter of annealed PS appears to be smaller than that of the single-crystal Si substrate. The increase in PS porosity is accompanied by the fitting of the diffraction peaks of annealed PS to the substrate peak.

The initial PS thickness and porosity were shown to be responsible for the lattice mismatch, strains and defect densities of epitaxial layers. Perfect Si epitaxial layers were grown on the PS layer of optimal parameters. Correlation between the structural perfection and strains of the grown epitaxial layer with the properties of the seed PS layer is discussed.

[1] <http://www.canon.co.jp/ELTRAN>

## Damage profiles determination in ultra-shallow implantated Si by triple crystal x-ray diffraction

<sup>1</sup>C. Bocchi, <sup>1</sup>F. Germini, <sup>2</sup>E. Kh. Mukhamedzhanov, <sup>1</sup>L. Nasi, <sup>3</sup>V. Privitera  
and <sup>3</sup>C. Spinella

<sup>1</sup>CNR-MASPEC Institute, Parco Area delle Scienze 37/A, I-43010 Fontanini-Parma, Italy

<sup>2</sup>A. V. Shubnikov's Institute of Crystallography of Russian Academy of Sciences,  
Leninskiy pr. 59, 117333 Moscow, Russia

<sup>3</sup>CNR-IMETEM Institute, Str.le Primosole 50, 95121 Catania, Italy

Actual challenge for the ion implantation technology is the achievement of both ultra-shallow p<sup>+</sup> and n<sup>+</sup> source/drain structures, necessary for the Complementary Metal-Oxide-Semiconductor (CMOS) technology. A common approach is to use very low implantation energies giving rise to extremely thin doped layers. As for a p<sup>+</sup> junction realization, B ions have been implanted in Si at ultra-low energies. Lattice distortion and disorder due to the implantation process have been investigated by means of a high resolution x-ray diffraction method. Due to a very low implantation depth (tens of nm), the x-ray diffraction measurements were carried out by a triple-crystal diffractometry (TCD) with a Si double reflections monochromator for selecting the CuK $\alpha_1$  radiation as a probe and a high quality Si analyzer crystal, both [001] oriented. This TCD configuration made it possible to separate the elastic component of the measured intensity from that diffused in the same angular range by lattice defects, considerably improving the signal-to-noise ratio. A Rigaku RU-200 rotating anode generator was used as the radiation source. The 004 reflection was selected for all of the samples. The specimens investigated were implanted at different energies: 0.25, 0.5 and 1keV by an Applied Materials xR LEAP, and at different doses:  $1 \times 10^{14}$ ,  $1 \times 10^{15}$  cm<sup>-2</sup>. For the analysis of the experimental curves, the subsurface region was divided in several thin layers. The layer thickness, the static DW factor, which is related to the lattice damage, and the lattice spacing modification were the parameters of the fitting procedure. Despite of the thinness of the "subsurface-damaged area", it was possible to obtain the behaviour of the main parameters describing the depth distribution of the lattice distortions in the analyzed crystals.



# **Characterization of ultrathin wafers by X-ray topography and micrometer-resolved area diffraction**

**T. Baumbach<sup>1)</sup>, L. Helfen<sup>1)</sup>, P. Pernot<sup>1)</sup>, M. Herms<sup>1)</sup>, C. Landesberger<sup>2)</sup>, and G. Schwinn<sup>2)</sup>**

<sup>1)</sup>*Fraunhofer Institute of Non-destructive Testing, EADQ., Krügerstraße 22, 01326 Dresden, Germany, phone/fax: +49.351.26482.0 / 17, baumbach@eadq.izfp.fhg.de*

<sup>2)</sup>*Fraunhofer Institute for Reliability and Microintegration, Hansastrasse 27d, 80686 München, Germany*

The majority of micro- and opto-electronic devices is fabricated on silicon substrates. The trend to higher integration in microelectronics requires new packaging solutions. One way of achieving that is the preparation of flexible electronic devices on ultrathin wafers, for example flat flexible peripheral modules. These ultrathin wafers are cut from melt-grown single crystals and thinned down subsequently to several micrometers by specially developed steps of grinding and etching. Then, the wafers have to be glued on supporting foils or substrates for a better handling. Advanced techniques for non-destructive testing are required for the optimization of the whole procedure, that means for the minimization of several remaining damages and strain of the crystal structure and to insure the subsequent costly device fabrication.

In this paper we present X-ray topography and micrometer-resolved area diffraction studies of 20  $\mu\text{m}$  thick silicon wafers glued on 4 inch standard silicon substrates performed at the European Synchrotron Radiation Facility, Grenoble (beamline ID19). The lateral distribution of defects and strain induced by the procedure of thinning and glueing will be discussed (see for instance the figures below).

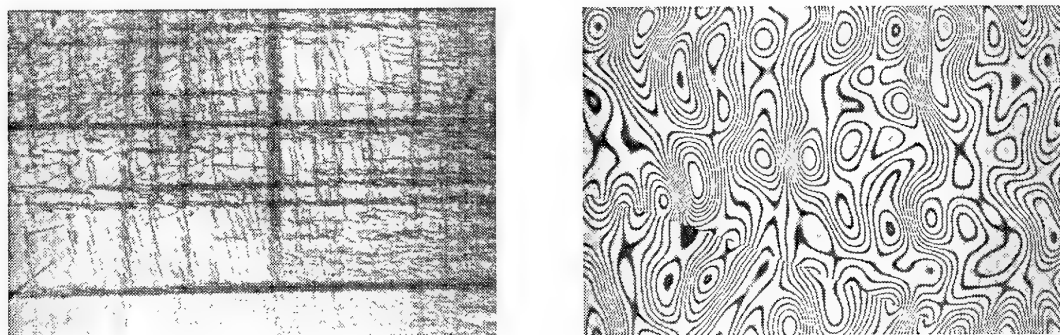


Figure 1: White beam topography (140 mm  $\times$  90 mm): Distribution of dislocation (left) and "Zebra-scan" of lattice strain (right).



## 2D-ACAR STUDIES ON MICROSTRUCTURE CHARACTERISTICS OF POROUS SILICON

**K. Sivaji<sup>1</sup>, C. S. Sundar<sup>2</sup>, R. Rajaraman<sup>2</sup>, Padma Gopalan<sup>2</sup>, S. Sankar<sup>3</sup>  
and V. Ravichandran<sup>1</sup>**

<sup>1</sup>Materials Science Centre, Department of Nuclear Physics, University of Madras,  
Guindy Campus, Chennai – 600 025, INDIA. e- mail : k\_sivaji@yahoo.com

<sup>2</sup>Materials Science Division, IGCAR, Kalpakkam – 603 102, INDIA.

<sup>3</sup>Department of Physics, MIT Campus, Anna University, Chennai - 600 044, INDIA

Mapping of the electron momentum distribution (EMD) by positron annihilation technique allows one to obtain finer details of the electronic structure and microstructure characteristics of porous silicon (PS). These characteristics studied by indigenously developed two-dimensional angular correlation of positron annihilation radiation (2D-ACAR) are reported in this paper. PS samples were prepared under different current densities (CD) to change the etching rate and hence the porosity, while keeping HF concentration and anodization time constant. The annihilation characteristics have yielded valuable information on the open volume defects associated with vacancies and their complexes present on the pore (columnar) surfaces of PS.

Photoluminescence (PL) measurements of these samples yielded the size of the nanocrystallites. In the present studies the size of the crystallites (17 Å) is found to be almost constant reaching a saturation at low CD itself. The EMD of all the samples featured a narrow component in the low momentum region. This arises due to formation of positronium by the pick-off annihilation at the surface of pores. The narrow component is superimposed over a broad distribution from the crystalline Si-substrate. The positronium formation can be attributed to the presence of a large number of Si:H complexes present at the pore surface. Apart from the substrate annihilation, positrons seem to annihilate in the open volume defects like vacancy complexes on the pore surface. Positronium component peak in the 2D-ACAR spectrum is found to be symmetric irrespective of the CD. This suggests that positronium is formed at the voids on the pore surface. The width (FWHM) and intensity of the narrow component are strongly influenced by the pore size and hence the porosity. From the width of the narrow component, the pore size is estimated as 15 – 18 Å. Increasing CD increases the concentration of nanocrystallites (from PL studies) leading to a decrease of the pore size (from 2D-ACAR studies) and hence porosity.

The paper will present the details of these studies and bring out the power of 2D-ACAR as an important technique to understand the electronic structure and defects of porous silicon.



## DLTS-analysis of kinetics of charge-carrier capture by dense planar array of deep traps

V. A. Stuchinsky

Institute of Semiconductor Physics, 13 Lavrent'ev Ave., 633090 Novosibirsk, Russia

e-mail: [stuchin@isp.nsc.ru](mailto:stuchin@isp.nsc.ru), phone 7-(383-2)-332470, fax 7-(383-2)-332771

Over many years, deep-level transient spectroscopy (DLTS) has been predominantly used to study comparatively sparse spatial distributions of deep traps in semiconductors, except for the case of defect clusters produced by heavy particles (neutrons or ions). Novel trends in semiconductor technology made other dense systems of traps (e. g., planar arrays of quantum dots in heteroepitaxial structures or planar interfaces with interfacial states in directly bonded structures), a matter of an intense scientific inquiry. In this paper, the use of DLTS for analyzing kinetics of charge-carrier capture by dense planar ensembles of deep traps is discussed. The capture of carriers by a portion of traps raises the electrical potential in neighboring local regions with still empty traps, thus decreasing there the concentration of free carriers available for further capture. As a result, the capture kinetics slows down, extending in time by several orders of magnitude. If the traps are randomly distributed in the plane, then the log-log plot of the logarithm of the ratio of the initial capture rate to the instantaneous one vs the concentration of trapped carriers  $n_t$  is expected to be a curve the slope of which changes from about 1/2 to about 2 as a continuous depletion region develops around traps (which happens at  $n_t \approx N^{2/3}$ , where  $N$  is the doping concentration); afterwards, this dependence increases abruptly as  $n_t$  approaches its steady-state value  $n_t(t \rightarrow \infty)$ . Involvement of traps into the planar array in the form of linear subarrays (dislocations, etc.) results in appearance of another part in the above curve the slope of which roughly equals to unity. The above analysis, together with examination of the temperature dependence of  $n_t(t \rightarrow \infty)$  and transient capacitance, can be used to independently estimate the quantities governing the capture kinetics (concentration of traps, "Coulomb radius" for them, etc.) and establish particular arrangement of traps in the array. It can be also helpful in analyzing other possible reasons for non-exponential capture kinetics (such as, for instance, dispersion of capture cross-sections in quantum-dot arrays, etc.).



## **Comparison of the scanning electron microscopy methods of semiconductors: SEBIV, SEAM, SCEBIC**

**E. I. Rau**

Moscow State University, Dept. of Physics. 119899 Moscow, Russia  
e-mail: [rau@pel157a.phys.msu.su](mailto:rau@pel157a.phys.msu.su) fax: 7-095-9391787; phone: 7-095-939-3895

It was discussed the physical origins of three contactless methods of scanning electron microscopy: Scanning electron beam induced voltage (SEBIV), Scanning electron acoustic microscopy (SEAM), and Single contact electron beam induced current (SCEBIC). The transient characteristics of the signals are considered. The images of semiconductor barrier structures in different scanning electron microscope (SEM) modes are compared and the disputable questions of the thermal acoustic waves microscopy of semiconductor crystals is demonstrated. The influence of capacitive coupling in all experimental circuits have been studied and taken into account by interpretation of the results.

The aim of the present paper is to provide a comparative analysis of the three above mentioned methods of semiconductor diagnostics in the SEM, to compare and correlate the image contrast mechanisms and to show the reasons for differences observed in the detected signals. The methods are considered regarding their preferable applications in testing particular objects or obtaining complementary information.



## DETERMINATION OF DIFFUSION LENGTH AND SURFACE RECOMBINATION VELOCITY BY THE SURFACE ELECTRON BEAM INDUCED VOLTAGE METHOD

E.I. Rau, E.B. Yakimov

Institute of Microelectronics Technology RAS, Chernogolovka, 142432 Russia,  
e-mail: rau@pel157a.phys.msu.su; fax: 7-095-9628047; phone: 7-095-9393895

The Surface Electron Beam Induced Voltage (SEBIV) could be considered as an electron beam based analog of well-known photovoltage technique. In this method the samples under study is excited with the focused electron beam and the induced voltage is detected by capacitively coupled electrode. The possibilities of contactless measurements of minority carrier diffusion length  $L$  and surface recombination velocity  $S$  in semiconductor crystals with and without p-n using this method are discussed. In the first case for geometry, when the p-n plane is parallel to the electron beam, the beam is scanned across the junction and the SEBIV signal is measured as a function of distance to the junction at a few different beam energies. In samples without p-n junctions or Schottky barriers  $L$  can be obtained from the dependence of the SEBIV signal on the primary electron energy. This dependence is more complex than the EBIC one because the SEBIV signal depends also on the width of generation region, which increases with an electron energy. A program for simulation of both SEBIV signals was developed. A comparison of simulated dependences with measured ones revealed a good correlation that allows to obtain nondestructively the  $L$  value from the SEBIV measurements. In the samples with barrier structures besides  $L$  the surface recombination velocity can be also obtained from fitting. The experimental and simulated dependencies demonstrating the possibility of  $L$  and  $S$  reconstruction are presented. It is shown that the reconstruction will be more reliable when the condition of constant  $I_b \cdot E_b$  is used and measurements are carried out for a few  $I_b \cdot E_b$  values.



## **Multi-electrode LBIC method for characterization of 1D “hidden” defects**

**V. Sirotkin, S. Zaitsev, E. Yakimov**

Institute of Microelectronics Technology Russian Academy of Sciences,  
142432 Chernogolovka, Moscow district, Russia  
e-mail: [yakimov@ipmt-hpm.ac.ru](mailto:yakimov@ipmt-hpm.ac.ru), fax: 7(095)9628047, phone: 7(09652)44161

The aim of the paper is to evaluate possibility of a multi-electrode LBIC (light beam induced current) method for characterization of individual 1D defects located under the surface. In the presented method, several Schottky contacts are used to obtain a collection volume of a special form. For defect region parameters reconstruction the collected current dependence on the depletion region width is used. In order to improve the sensitivity of the method, the implementation of the modulation techniques (the measurements of first derivative of collected current depending on applied bias) is proposed.

Using the computer simulation it is demonstrated that the considered method offers a significant advantage over the “standard” EBIC (electron beam induced current) as well as over the multi-electrode EBIC methods for the investigated defects.

For the computer simulation of LBIC and EBIC signals, a drift-diffusion approach is used. The mathematical model is solved by a numerical method based on a combination of adaptive composite grids and an iterative domain decomposition algorithm.



## **Optical profilometry applied to the characterization of surfaces in the microelectronic field.**

**J.Ph. Piel, A. Dubois\*, L. Vabre\*, P. Boher, L. Escadafals, R. Tirmarche,  
A.C. Boccara\*, J.L. Stehlé.**

SOPRA

26 rue P. Joigneaux, 92270 Bois-Colombes, France

Tel : 01 46 49 67 52, Fax : 01 42 42 29 34, E-mail : [dev@sopra-sa.com](mailto:dev@sopra-sa.com)

\* Laboratoire d'Optique, Ecole Supérieure de Physique et Chimie Industrielles,  
CNRS, UPR A0005

10 rue Vauquelin, 75005 Paris, France

Tel : 01 40 79 45 90, Fax : 01 40 79 46 03, E-mail : [dubois@optique.espci.fr](mailto:dubois@optique.espci.fr)

Phase-shifting interference microscopy is a technique of choice to visualize and characterize the surface state of materials used in various domains. In particular, the surface topography of microelectronic devices with patterns can be studied. Optical profilometry has the advantage to be non-destructive, non-invasive, fast, and easy-to-process. Vertical resolutions as good as 1 nm and lateral resolutions better than 1  $\mu$ m can be obtained.

We will present an interference microscope that permits to acquire topographic images at high speed. Images can be obtained within 50 ms with high signal to noise ratio. The acquisition speed allows one to work in an industrial environment where vibrations are present.

The instrument can also be used to visualize buried structures under transparent layers. It is then possible to extract the topography of the substrate surface.

The accurate determination of heights is however a difficult problem. The phase of the interference signal, proportional to the path differences of the beams reflected by the reference surface and by the studied surface is highly affected by the nature of the material of the surface itself through the refractive index and by the propagation of light through superficial layers. Multiple interferences can also occur in multi-layer samples. These phenomena must be taken into account to get accurate measurements.

To illustrate the various possibilities of our system, we will present different applications belonging to the microelectronic world.



**In-situ time-resolved reflectivity:  
a technique useful for solid-state transformations**

**F.Corni, R.Tonini**

I.N.F.M. – Dipartimento di Fisica, Università di Modena, Italy  
Email: [corni@unimo.it](mailto:corni@unimo.it), fax ++39 059 367488, tel ++39 059 2055249

**G.Pavia, G.Queirolo, R. Zonca**

STMicronics, Agrate Brianza, Italy

Information about the solid-state transformations occurring in thin films can be obtained by directing a laser beam on the sample surface and measuring the reflected intensity by means of a photodiode. The technique, called Time-Resolved Reflectivity, is an in-situ technique very fast and simple. In proper conditions, it allows the entire evolution of a transformation to be followed while it occurs during a thermal treatment, then allowing the kinetics of the process to be studied.

In this work we present some results obtained on layered samples, interesting for the microelectronic industry. The surface reflectivity, in this case, depends on the refractive indices of the materials employed and on the physical dimensions of the layers. The results, extracted from the raw reflectivity data by means of few simple assumptions, are discussed and compared to those obtained with more conventional, but in most cases, destructive and ex-situ techniques.





## Effect of minority charge carrier lifetime general form on EBIC - Case of Au-nSi Schottky diode -

Ma.Bouloudenine<sup>(1)</sup>, D.E.Mekki<sup>(1)</sup> and R.J.Tarento<sup>(2)</sup>

(1): Université de Annaba, Faculté des sciences, Département de physique -BP 12  
23000 Annaba (Algérie).

(2): Université de Paris Sud - Laboratoire de physique des solides, Bt 510, 91405  
Orsay (France).

Theoretical model, which takes into account the influence of the minority charge carrier lifetime,  $\tau_p$ , on curves representing the evolution of Electron Beam Induced Current (EBIC) efficiency as a function of Beam energy,  $E_0$ , is elaborated.

The adopted calculation procedure consists to resolve the continuity equations for both majority and minority excess carriers, via the hall Shockley Read (SRH) theory and the equality between electron and hall recombination rates and this, with conferring a  $\tau_p$  general spatially dependence form.

Such a model is then successfully applied to an Au-nSi Schottky diode leading to satisfactory agreements between theory and experiment.

The effect of the minority diffusion length,  $L_p$ , the interfacial recombination speed,  $S_p$ , and the doping concentration,  $N_d$ , is also studied.



## Studies of growth bands in Si:Ge crystals

K. Wieteska<sup>1</sup>, W. Wierzchowski<sup>2</sup>, W. Graeff<sup>3</sup>, M. Lefeld-Sosnowska<sup>4</sup>, M. Regulska<sup>4</sup>

<sup>1</sup>Institute of Atomic Energy, Otwock-Świerk, Poland

<sup>2</sup>Institute of Electronic Materials Technology, Warsaw, Poland

<sup>3</sup>HASYLAB at DESY, Hamburg, Germany

<sup>4</sup>Institute of Experimental Physics, University of Warsaw, Warsaw, Poland  
[mreg@fuw.edu.pl](mailto:mreg@fuw.edu.pl), fax: 48 22 622 61 54

Reduction of germanium segregation is the most important problem in technology of Si:Ge crystals. On this reason it is of great importance to improve methods of characterization allowing studies and evaluation of segregation effects in these crystals. In actual case Si:Ge crystals with approximately 3% of germanium were studied with various topographic methods using both conventional and synchrotron sources of X-rays. Present investigation included in particular various types of white beam synchrotron topography and conventional Lang topographic methods. The topographic investigations were completed by recording of rocking curves and lattice parameter measurements with Bond method.

The topographic results obtained with various methods were dominated by strong contrast caused by growth bands and only in some transmission topographs it was possible to reveal the dislocation lines. The particularly useful in studying of growth bands were the methods realized in back-reflection geometry using white synchrotron radiation. In this case the beam entered the crystal at a relatively low glancing angle 4 or 10° and a single exposure provided a set of different Laue spots indexed with special program. Taking projection topographs with relatively large beam size it was possible to reproduce the distribution of growth bands at the surface of the sample. Contrary to that taking the section topographs with the beam front limited to 5 µm the topographs provided the distribution of growth bands inside the crystals. Thanks to the low glancing angle the section topographs provided many information about the shape of growth surface despite small thickness of investigated wafers. By taking the topographs with very large film-to-crystal distances it was also possible to reveal the character of lattice deformation across the striations and the information about germanium distribution.

## Acoustic-wave effects on space charge defect states in SiGe heterostructures

A. A. Podolyan and O. A. Korotchenkov

Faculty of Physics, Kiev University, Kiev 03680, Ukraine  
e-mail: olegk@mail.univ.kiev.ua

A variety of acoustically driven junction space charge and photoelectric techniques are employed in order to reveal defect states in SiGe heterostructures. These include DLTS and steady-state capacitance measurements, the spectral distribution and decay properties of a photovoltage. Several defect-mediated phenomena are discussed which may particularly be important for applications utilising accumulation of charge carriers and photovoltage effects.

The structure consists of a CVD-grown  $\text{Si}_{0.83}\text{Ge}_{0.17}$  layer of thickness  $\approx 1 \mu\text{m}$  and a (100)Si substrate of thickness  $\approx 300 \mu\text{m}$ . The back electrical contact is ohmic and the front rectifying contact is formed through a thin gold layer. The junction space charge measurements are done utilizing a DLS-83D spectrometer. The light excitation beam either cw or pulse-chopped is achieved with LEDs. The plate acoustic waves are introduced by placing a piezoceramic transducer on top of the sample. A rf power supply is used to feed into the transducer allowing acoustic strain amplitudes as high as  $\sim 5 \times 10^{-6}$  at frequency of about 3 MHz. The measurements are performed in the temperature range from 77 to 300K.

The DLTS spectra of the sample consist of two peaks revealing two deep levels located at about 0.2 (peak A) and 0.4 (peak B) eV. The peak B appears to be remarkably quenched in acoustic fields whereas the peak A remains almost unaffected. It is suggested that the observed features reveal acoustically driven defect recharge which undergoes an enhancement in the junction area. The latter is likely to be due to acoustically-induced accumulation of stress and charge at the interface, and turns out to be used for recognition of defect states localized in the interface.

Further evidence of the suggested picture is discerned by analyzing the capacitance-voltage (C-V) curves as well as the photovoltage response of the structure. The plot  $1/C^2$  against reverse bias voltage  $V$  produces a nearly straight line for reverse bias from 0 to 7V. This is no longer valid when acoustic waves are applied. The capacitance exhibits a considerable decrease (up to 30%) for the bias from 0 to 2.5V which is sensitive to the strain amplitude in the wave. Moreover, the photovoltage signal is found to change its sign in the spectral range from 1 to 1.2 eV when driven by acoustic waves. Furthermore, the rapid decrease in photovoltage seen just after the light is off is followed by the signal increase with a subsequent long-time relaxation.

The model attempting to explain the observed effects by acoustically-induced recharge of defect states in the accumulation regions is outlined.

## Ultrasonic manipulation of bound exciton luminescence in GaAs quantum wells

**O. A. Korotchenkov<sup>1</sup> and D. S. Kim<sup>2</sup>**

<sup>1</sup> Faculty of Physics, Kiev University, Kiev 03680, Ukraine

e-mail: olegk@mail.univ.kiev.ua

<sup>2</sup> Department of Physics, Seoul National University, Seoul 151-742, Korea

We report a first experimental observation of a striking narrowing of the exciton emission linewidths in a quantum well structure driven by ultrasonic vibrations. We believe that the results are of fundamental interest for externally influencing the dynamics of photoexcited carriers in low-dimensional semiconductors, and they may pave new ways in realizing acoustically pumped lasing.

Measurements are performed on alternating 100 Å wide undoped GaAs quantum wells and 100 Å wide  $\text{Al}_{0.5}\text{Ga}_{0.5}\text{As}$  barriers (30 periods) grown on top of the (001)  $n^+$ -GaAs substrate. Resonant ultrasonic vibrations are achieved at about 1 MHz frequency by mounting the sample onto the  $\text{LiNbO}_3$  piezoelectric plate driven by a pulse generator. Low-temperature photoluminescence (PL) is excited by a He-Ne laser, and PL spectra are taken over the duration of ultrasonic pulses using either Model 162 Boxcar Averager or 72080 Perkin Elmer lock-in amplifier.

In the absence of ultrasonic driving, the PL spectrum is dominated by a single emission line arising from the recombination of mobile excitons confined in the quantum well. The full widths at half maximum (FWHM) of the line is 6.4 meV. Application of ultrasonic vibrations makes the PL line progressively weaker in intensity, it becomes broader (to about 8 meV), and experiences a low-energy shift. Further increasing the ultrasonic amplitude above some threshold value changes the PL spectrum quite remarkably, such that narrow emission lines which are less than 1.8 meV FWHM are resolved.

An evidence is presented that allows to treat the observed phenomenon in the framework of piezoelectric field effects on the exciton relaxation in the quantum well. The influence of the driving field is suggested to narrow and red-shift the exciton emission lines due to the exciton relocalization to lower-energy sites at interface roughness potentials. This is accomplished by field-ionizing the excitons, their drift in the driving field within the plane of the quantum well, and the subsequent triggering of the radiative recombination in the bound exciton emission band when electrons and holes are captured at the interface localization potential containing a trapping defect. An ultrasonically pumped lasing is expected to occur in the presented structure by optimizing the cavity design.



## Spontaneous Quantum Dot Formation at $\text{In}_x\text{Ga}_{1-x}\text{As}/\text{In}_y\text{Ga}_{1-y}\text{As}$ Interfaces

**M. Righini<sup>1</sup>, F. Fernández-Alonso<sup>1</sup>, A. D'Andrea<sup>3</sup>, D. Schiumarini<sup>2</sup>, S. Selci<sup>1</sup>  
and N. Tomassini<sup>3</sup>**

<sup>1</sup>Istituto di Struttura della Materia - CNR, via del Fosso del Cavaliere 100, 00133 Roma, Italy. Fax: +39 06 4993 4153; phone: +39 06 4993 4166; e-mail: righini@ism.rm.cnr.it.

<sup>2</sup>Istituto di Chimica dei Materiali - CNR, c.p.10, 00016 Monterotondo Scalo (Roma) Italy

<sup>3</sup>Istituto di Metodologie Avanzate Inorganiche - CNR, c.p.10, 00016 Monterotondo Scalo (Roma) Italy

We have performed reflectivity (R) and photoluminescence (PL) measurements on a set of  $\text{In}_x\text{Ga}_{1-x}\text{As}/\text{In}_y\text{Ga}_{1-y}\text{As}/\text{GaAs}(001)$  asymmetric quantum wells (AQW) with an intentionally abrupt change of indium composition ( $x = 0.149$ ,  $y = 0.064$ ). These measurements have been compared against extensive spectroscopic data gathered on a set of symmetric quantum wells (SQW) of similar structural parameters. All samples have also been routinely characterized by RHEED and high resolution X-ray diffraction.

The results of the structural and optical characterization (R and PL) of the SQW samples agree very well with theoretical calculations [1]. Such an agreement is a clear marker of the high quality of the SQW samples, i.e., the homogeneity of the InGaAs alloy material as well as the behavior of the GaAs/InGaAs interfaces as ideal barriers. Also, the AQW R spectra agree well with model calculations, both in terms of peak energy position and line shape [2]. The AQW PL spectra, however, display peculiar spectroscopic features. Among these we may cite: (a) a composite peak with the greatest part of the PL emission at recombination energies significantly lower than the corresponding reflectivity peak (i.e., large Stokes shift); (b) a blue-shift of the PL and an almost constant peak width with increasing temperature; (c) an incipient saturation of the PL peak as the excitation power is increased. We will discuss the consistence of these experimental findings with the hypothesis of zero-dimensional exciton confinement induced by local and random potential fluctuations at the In-alloy/In-alloy interface. A brief examination of the possible formation mechanisms leading to the formation of such "natural quantum dots" at this poorly studied interface will be presented.

### References:

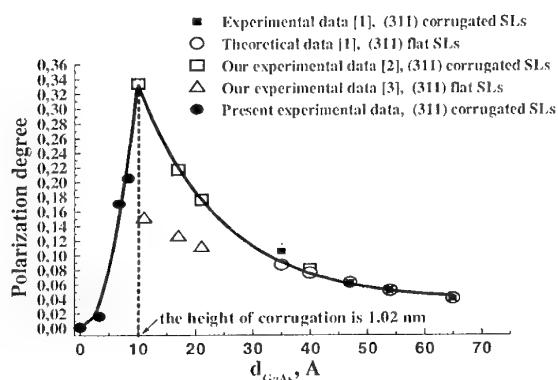
- [1] A. D'Andrea, N. Tomassini, L. Ferrari, M. Righini, S. Selci, M.R. Bruni, M.G. Simeoni and N. Gambacorti, *Phys. Rev. B* **52** (1995) 10713.
- [2] N. Tomassini, A. D'Andrea, M. Righini, S. Selci, L. Calcagnile, R. Cingolani, D. Schiumarini and M.S. Simeone, *Appl. Phys. Lett.* **73** (1998) 2245.

## Polarization resolved-photoluminescence for study of GaAs/AlAs interfaces in corrugated and flat ultra-short-period superlattices

G.A.Lyubas, V.V.Bolotov

United Institute of Semiconductor Physics, Siberian Branch, Russian Academy of Sciences, prosp. Lavrentyeva 13, Novosibirsk, 630090 Russia, Tel: +7-3832-332834, Fax: +7-3832-332771, e-mail: lubas@isp.nsc.ru

We have improved a method of polarization resolved-photoluminescence and applied this technique in order to investigate the corrugated and flat GaAs/AlAs ultra-short-period superlattices (SLs). The flat SLs (i.e. without corrugation) were grown using molecular beam epitaxy technique on (311)B and (100) surfaces. The corrugated SLs (CSLs) were grown on faceted (311)A GaAs surfaces. The thickness of GaAs layers in the SLs was varied from 3.4 to 40 Å. The phenomenon of photoluminescence polarization anisotropy was observed (see Fig.). The polarization nature of the *I<sub>ehh</sub>*



transitions is explained by valence band anisotropy in the case of a (311)A corrugated SLs with a GaAs layer thickness of more than 35 Å. For a thickness of less than 35 Å, the *I<sub>ehh</sub>* polarization anisotropy is explained by both valence band anisotropy and anisotropy associated with interface corrugation. It was determined that the SLs grown on faceted (311)A GaAs substrates contain periodic corrugated GaAs and AlAs layers (see Fig.). The

period of corrugation is 32 Å along the [01-1] direction, the height of corrugation is 10.2 Å. This correlates with the model [4] and contrasts with the model [5], where the height of corrugation is 3.4 Å. Latter the 10.2 Å interface corrugation of GaAs and AlAs layers in these (311)A SLs was directly observed by TEM. The CSLs with average GaAs layer thickness of less than 10.2 Å exhibited considerably lower polarization anisotropy (see Fig.). In this case quantum-well clusters were formed. The length of clusters is about 4-5 nm along the [01-1] direction. The formation of clusters reduce the polarization degree. These results are important for development of CSL-based devices [6]. This work was supported by the Zamaraev International Charitable Scientific Foundation.

1. M.V.Belousov, V.L.Berkovits, A. O. Gusev, *et al.*, Phys. Solid State, **36** (1994) 596.
2. G.A. Lyubas, V.V. Bolotov, JETP Lett., **72** (2000) 205.
3. G.A. Lyubas, Phys. Low-Dim. Struct., 11/12 (2000) 161.
4. R.Nötzel, N.N.Ledentsov, L.A.Daweritz, *et al.*, Phys. Rev. Lett., **67** (1991) 3812.
5. M.Wassmermeier, J.Sudijono, M.D.Johnson, *et al.*, J. Cryst. Growth, **150** (1995) 425.
6. V.V.Bolotov, G.A.Lyubas, IEEE Electron Devices and Materials 2000, No1(2000) 36.

## The investigation of quantum islands structures on (001) GaAs surface at submonolayer MBE growth from calculation of phonon spectrum

V. V. Bolotov, V. A. Sachkov

Institute of Sensor Microelectronics SB RAS, 644077 Omsk, Pr. Mira 55a, Russia  
e-mail: bolotov@phys.omsu.omskreg.ru, tel. (+7)381-2-663606, fax (+7)381-2-64-8676

The theoretical calculations of phonon spectra for the structure determination of quantum GaAs islands on (001) reconstructed (2x4) surfaces are presented. The calculations of phonon frequencies have been done for 8 neighbours at Born approximation. The Coulomb interaction influence in dipole approximation has been considered.

The best fitting of calculations and experimental results are observed for quantum GaAs islands which are quantum wires of endless length along the direction [110], containing two Ga and As atoms, divided by 4 Al and As atoms and one atom Ga, which is below on one layer (along the growing directions) and also for similar quantum GaAs wires, which lengths are limited by 6 Ga atoms and are divided by the barrier of 2 Al atoms.

On the figure the experimental Raman spectrum [1] in comparison with the calculated spectrum for the contribution of 20 different small island are shown. The picture shows the well correspondence of the theory and the experiment.

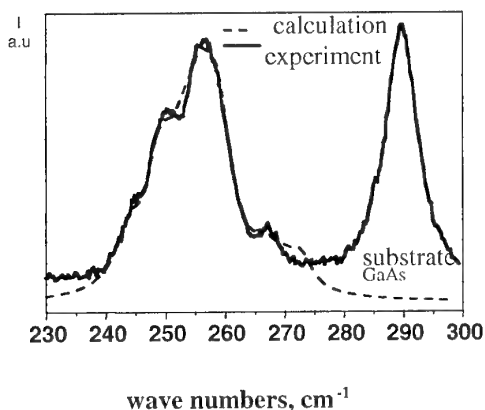


Figure. The experimental ( $\lambda_{ex} = 488$  nm) and calculated Raman spectra of the GaAs<sub>0.6</sub>/AlAs<sub>5</sub> superlattice which were grown on the reconstructed surface (001)-(2x4) and containing the GaAs quantum island.

### References

- [1]. M. D. Efremov, V. A. Volodin, V. A. Sachkov, V. V. Preobrazenskiy, B. R. Semyagin, V. V. Bolotov, E. A. Galaktionov, A. V. Kretinin. Pis'ma Zh. Eksp. Teor. Fiz., **70** (1999) 73.

## Properties of AlGaAs layers grown on Si by the Conformal method

**O. Martínez<sup>1</sup>, M. Avella<sup>1</sup>, A. M. Ardila<sup>1,2</sup>, J. Jiménez<sup>1</sup>, B. Gérard<sup>3</sup>  
and M. Philippens<sup>4</sup>**

<sup>1</sup>Dpto. Física de la Materia Condensada, E.T.S.I.I., 47011, Valladolid, Spain.

Tlf: +34 983 423572. Fax: +34 983 423192. E-mail: oscar@fmc.uva.es

<sup>2</sup>Dep. de Física, Universidad Nacional de Colombia, Ciudad Universitaria, Santa Fe de Bogotá, Colombia

<sup>3</sup>THALES ICR, Domaine de Corbeville, 91404 Orsay, France.

<sup>4</sup>RWTH Institut für Halbleitertechnik, Lehrstuhl I, Templergraben 55, DE-52056 Aachen, Germany

The growth of III-V compound layers on Si substrates presents a high interest in order to integrate the high performance of III-V devices with the mature technology of Si. However, the large lattice mismatch and the thermal strain reduces the quality of the epilayers [1]. We have demonstrated that it is possible to obtain high quality GaAs/Si by HVPE or MOVPE using the conformal growth method. This method is basically a confined lateral growth [2]. In order to realise interesting lateral devices (LED's, LD, etc.), AlGaAs has to be conformally grown by MOVPE. Here we present a study of these AlGaAs conformal layers by means of Cathodoluminescence, microRaman and PLI (PhotoLuminescence Imaging) techniques.

The main issues regarding these layers are analysed, e.g. Al distribution, presence of crystal defects, the homogeneity of the layers and the influence of the growth parameters. In particular the Al content, obtained from the Raman data, is deeply discussed. The presence of free carriers in the layers (some of them intentionally doped), which leads to the presence of LOPC (Longitudinal Optic phonon Plasmon Coupled) modes in the Raman spectra, can influence the estimated Al content. A detailed study shows a maximum Al content of about 22% in some of the conformal layers.

The results obtained show that it is possible to improve the quality of AlGaAs/Si by the conformal method, but the growth process by MOVPE presents much more difficulties than were found for conformal GaAs layers grown by HVPE.

- [1] S. F. Fang, K. Adomi, S. Iyer, H. Morkoc, H. Zabel, C. Choi, N. Otsuka, J. Appl. Phys. 68, R31 (1990)
- [2] O. Martínez, M. Avella, E. de la Puente, J. Jiménez, B. Gerard and E. Gil-Lafon, J. Cryst. Growth, 210, (2000) 198





### **Raman Investigation of Interface Atomic Reconstructions in Superlattices GaAs/AlAs grown on (100) Substrates.**

**M.D.Efremov<sup>1</sup>, V.A.Volodin<sup>1</sup>, V.A.Sachkov<sup>2</sup>, V.V.Preobrazhenski<sup>1</sup>, B.R.Semyagin<sup>1</sup>**

<sup>1</sup> Institute of Semiconductor Physics of SB RAS, pr.ak.Lavrentjeva 13, Novosibirsk 630090, Russia. , E-mail: [efremov@isp.nsc.ru](mailto:efremov@isp.nsc.ru), phone; +7(3832)332470

<sup>2</sup> Institute of Sensor microelectronics of SB RAS, pr.Mira 55A, Omsk 644077, Russia.

Surface reconstructions are intensively studied by means of scanning tunnelling microscopy, electron diffraction and other direct methods. Is atomic structure conserved during growth of heterostructures in conditions of surface reconstruction? To solve the question, Raman scattering in superlattices GaAs/AlAs grown in conditions of reconstruction (2x4) of (100) surface was investigated. To study atomic structure of interface submonolayers of GaAs were grown by means of MBE techniques on reconstructed surface of AlAs. In that case GaAs islands only partially covered the surface, so finish heterostructure represented a periodical system of GaAs islands embedded in AlAs matrix. Raman spectra of optical phonons contained triplet peak indicating periodicity of the system not only in direction of growth but in planar one. In order to connect obtained experimental data with atomic structure of interface modelling of phonon frequencies of GaAs islands were applied. Calculations were performed within "rigid ions" model, taking into account several neighbouring coordination spheres and coefficients fitted to bulk properties of GaAs. Using derived eigenvectors for phonon modes theoretical Raman spectra were calculated in Volkenstein polarizability model. Calculated Raman spectra were shown strongly depends on atomic structure of the islands, what allow to distinguish them on size and shape. Among modelled configuration several were selected, which Raman active phonons modes are bunching in triplet. Weights of Raman contributions for selected modes were fitted to experiment. Just obtained atomic structure of interface possessed staggering similarity to experimental data obtained by STM method for atomic structure of GaAs islands formed on the surface (100) in condition of reconstruction (2x4). Moreover, calculated covering of the surface coincided with experimental one and corresponded to 0.6ml. Thus, Raman spectroscopy combined with theoretical calculations gave information about atomic structure of heterojunction for SLs grown in conditions of surface reconstruction. One can examine also tunnelling properties in the case of ultra thin layers in doped SLs. In tunnelling doped SLs Raman scattering on phonon-plasmon modes was observed, but theoretical description of that process is difficult, because of lack of suitable results in literature. Within this work an attempt was made to describe dynamical screening of phonons in electron gas in the case of tunnelling SLs.

## Influence of disorder on Raman spectra of GaAs quantum wires grown with partial filling of corrugated (311)A AlAs surfaces

M.D.Efremov<sup>1</sup>, V.A.Volodin<sup>1</sup>, V.A.Sachkov<sup>1</sup>, V.V.Preobrazhenski<sup>1</sup>, B.R.Semyagin<sup>1</sup>,  
N.N.Ledentsov<sup>2</sup>, V.M.Ustinov<sup>2</sup>, I.P.Soshnikov<sup>2</sup>, D.Litvinov<sup>3</sup>, D.Gerthsen<sup>3</sup>

1- Institute of Semiconductor Physics of SB RAS, pr.ak.Lavrentjeva 13, Novosibirsk, Russia, E-mail: [efremov@isp.nsc.ru](mailto:efremov@isp.nsc.ru), fax: +7(3832)332771, phone; +7(3832)332470

2- Institute of A.F. Ioffe Institute of the RAS, S.-Peterburg, Russia

3- Laboratory of Electron Microscopy, University of Karlsruhe, Germany

Raman spectroscopy powered by theoretical modeling of vibrational modes was shown to be an effective tool to examine interface structure of superlattices. In this work we study GaAs<sub>n</sub>/AlAs<sub>m</sub> corrugated superlattices (CSLs) grown on (311)A GaAs substrates using Raman spectroscopy and HRTEM. GaAs (311)A surface may be spontaneously nanofaceted with a period of 3.2 nm in the (0-11) direction, with a height of the corrugation of 1 nm [1]. The polarization-sensitive splitting of the TO modes was observed in our (311)A SLs. Moreover, we found strong increase in the value of splitting for (311)A superlattices, with decrease in the average thickness of the GaAs layers to 1 nm or slightly less. As opposite, SLs grown side-by-side on (311)B surfaces, where no corrugation was expected, demonstrated no TO-line splitting. Thus, one can conclude, that the splitting is, indeed, caused by the interface corrugation of GaAs/AlAs (311)A SLs and the formation of dense arrays of GaAs quantum wires (QWWs) [2]. The direct HRTEM data confirmed that the CSLs have QWW-like structure the corrugation height of 1 nm. Perfect 3.2nm periodicity was revealed in Fourier-transforms of the randomly-chosen processed HRTEM images of SLs with layer thickness above 1nm [3]. A checkerboard arrangement of the spots was also found in agreement with the fact that both GaAs and AlAs layers are corrugated. SLs with GaAs layer thickness below 1nm in addition to 3.2nm periodicity demonstrated a non-perfect lateral periodicity of 1.6–2nm due to coexistence of the two similar corrugated, but phase-shifted surface domains in this case. On the basis of HRTEM we also estimated that for the length of the GaAs QWWs in the (-233) direction is only 4-5 nm in the structure with partial surface filling. The calculations of Raman spectra of GaAs QWWs of finite length along [-233] were performed according to HRTEM results. The phonon spectra were calculated in rigid ions model and the Raman spectra in different polarizations were calculated using Wolkenstain bond polarisability model. Comparison of the calculated and the experimental Raman spectra demonstrated good agreement between theory and experiment. The finite size of the QWW and the related disorder was shown to influence strongly the frequencies of the phonon modes.

[1] R.Nötzel, N.N.Ledentsov, L.Dawerits, M.Hohenstein, and K.Ploog, *Phys. Rev. Lett.*, **67**, 3812 (1991).

[2] V.A.Volodin, M.D.Efremov, V.V.Preobrazhenskii, B.R.Semyagin, V.V.Bolotov, *Superlattices and Microstructures*, **26**, 11 (1999).

[3] N.N. Ledentsov, D.Litvinov, A.Rosenauer, D.Gerthsen, I. P.Soshnikov, V.A.Shchukin, V.M.Ustinov, A.Yu.Egorov, A.E.Zukov, V.A.Volodin, M.D.Efremov, V.V.Preobrazhenskii, B.P.Semyagin, D.Bimberg and Zh.I.Alferov, *Journal of Electronic Materials* 30 (5) (2001), *in print*.



## **On the morphology and composition of InAs/GaAs quantum dots**

**Vincenzo Grillo, Laura Lazzarini, Thilo Remmele\***

Maspec-CNR, Parco Area delle Scienze 37/A, 43010 Fontanini-Parma, Italy

\*University of Erlangen, Germany

The interpretation of the TEM pictures of quantum dots either in plan or cross sectional geometry is an open problem, due to the difficulty of separating the contributions coming from the chemical and strain contrast.

As the system InAs/GaAs is concerned, the dot morphology has not been assessed and recently, indications have been found of In segregation and Ga diffusion, which lead to an inhomogeneity of the dot composition.

Plan view investigations of uncapped and embedded dots strongly suggest that the dot base is round shaped.

From the comparison between the DALI elaborations and the FE simulations of cross sectional images the following results have been obtained:

- 1 - In segregates at the top of the dots.
- 2 - Neither the lens shape nor the pyramidal shape can account for the observed strain patterns. A possible explanation of this fact can come from the In segregation itself or from the modelling of an intermediate shape of the dots (i.e. faceted dome). Continuum elasticity approximation limits should be otherwise taken into account.

Further, the induced artifacts due to the thin foil prepared for TEM observations have been studied, as they can produce totally misleading features in the images.



## **Optical and structural characterization of LP MOVPE grown lattice matched GaInP/GaAs heterostructures**

**C. Pelosi, G. Attolini, S. Scardova, F. Germini**

MASPEC-CNR Institute, Parco Area Delle Scienze, 37/A Fontanini  
43010 PARMA (Italy)

**O. Martínez, L.F. Sanz, M.A. González, J. Jiménez**

Física de la Materia Condensada, ETSII, 47011 Valladolid (Spain)

InGaP alloy is gaining an increasing interest because it can be matched to GaAs( $\text{In}_{0.51}\text{Ga}_{0.49}\text{P}$ ) and some unique characteristics of this material system ( large valence band discontinuity, stability, it can be prepared without significant donor-related deep traps). It offers good performance in light emitting devices, solar cells and heterojunction bipolar transistors. However, some disadvantages are the presence of an ordered phase and a strong dependence of the lattice parameter with composition. Lattice matched GaInP can be under an ordered phase with CuPt ordering in the cation sublattice, where In and Ga occupy alternate (-111) planes. Ordering is undesirable for device applications since it shrinks the band gap lowering the emission energy. On the other hand ordering inhomogeneities reduce the device performance.

In addition to order, similar effects can be produced by composition fluctuations. Both ordering and composition are related to the growth conditions, i.e. growth temperature, V/III ratio and the substrate properties.

We present herein a morphologic, structural and optical characterization of lattice matched GaInP/GaAs heterostructures grown by LP MOVPE on either undoped or Si-doped substrates. The characterization of the layers is carried out by AFM, X-Ray diffraction, TEM Raman spectroscopy and PL mapping. The results are discussed in terms of ordering and composition with respect to the growth conditions. Attention should be paid to the homogeneity and the discrimination between ordering and composition fluctuations.

## AFM and TEM study of the lateral composition modulation in the etched and photoetched $\text{In}_x\text{Ga}_{1-x}\text{P}$ epitaxial layers

V.Eremenko<sup>a</sup>, L.Gonzalez<sup>b</sup>, Y.Gonzalez<sup>b</sup>, V.Vdovin<sup>c</sup>,  
L.Vazquez<sup>d</sup>, G.Aragon<sup>e</sup>, M.Herrera and F.Briones<sup>b</sup>

<sup>a</sup> Institute of Microelectronics Technol.,RAS,142432 Chernogolovka,Moscow District, Russia, Fax: (095)962-8047, Ph.:(095)962-80-74, e-mail: eremenko@ipmt-hpm.ac.ru

<sup>b</sup> Inst. de Microelectronica de Madrid,CNM-CSIC,I.Newton,8-PM,28760, Madrid, Spain

<sup>c</sup> Institute for Chem.Probl. of Microelectronics,B.Tolmach.per.5,109017 Moscow, Russia

<sup>d</sup> Dept. of Surf. Physics and Eng. Instituto de Ciencia de Materiales de Madrid, CSIC, Cantoblanco, 28049 Madrid, Spain

<sup>e</sup> Dept. de Ciencia de los Materiales e Ingenieria Metalurgica y Quimica Inorganica. Universidad de Cadiz .Apdo.40, Puerto Real, 11510- Cadiz, Spain

The layers of ternary system  $\text{In}_x\text{Ga}_{1-x}\text{P}$  grown by MBE in the miscibility gap show after TEM observations specific defect as lateral composition modulation over range from few to hundreds of nanometers. Fine scale modulation is associated now with spinodal decomposition. Long wavelength quasi-periodic modulations are also supposed to be decomposition related. Nevertheless, the origin and properties as well as many peculiarities of lateral composition modulation remain unclear. An understanding of the microscopic nature of this phenomenon is very important, due to its influence on the semiconductor band structure and scattering of charge carriers as well as on the performance of optoelectronic devices. On the other hand, understanding and control of the composition modulation can provide a new approach for band structure engineering or, on the contrary, suppressing decomposition.

In this paper, an alternative way to characterize  $\text{In}_x\text{Ga}_{1-x}\text{P}$  composition modulation features by selective etching and photoetching techniques is presented for the first time. High sensitivity of selective etching and photoetching to local chemical inhomogeneities and elastic stresses, as well as to local electronic properties of the semiconductor are used.  $\text{In}_x\text{Ga}_{1-x}\text{P}$  layers studied in this work have been grown by ALMBE at substrate temperature of 420°C. AFM and TEM techniques were applied for analysis of chemically etched layers. AFM imaging of selectively etched n-type, p-type and undoped layers has revealed characteristic quasi-periodic structures consisting of ridges oriented along  $\langle 110 \rangle$  with periodicity of 300-500nm. Shape and length of the ridges are strongly dependent on doping type. In particular, topological features are quite peculiar in p-type material, which is well known to have anomalous low carrier mobility. Our TEM observations show contrast periodicity similar to that found in AFM measurements as well as additional fine features of the relief of the ridges in undoped material. We think that morphology features observed in our experiments are related to composition modulation effect. Photoetching reveals finer surface topography as hillocks with indications of self-organization. The mechanisms of defect revealing, and possibility of application of high resolution SNOM technique for analysis of the nature of composition modulation are finally discussed.

## INVESTIGATIONS ON SWIFT HEAVY ION IMPLANTATION ON SEMI-INSULATING GaAs

**P. Jayavel<sup>a</sup>, K. Santhakumar<sup>b</sup> and J.Kumar<sup>c</sup>**

<sup>a</sup>AIST Central – 2, Research Institute of Photonics, Tsukuba – 305 8568, Japan.

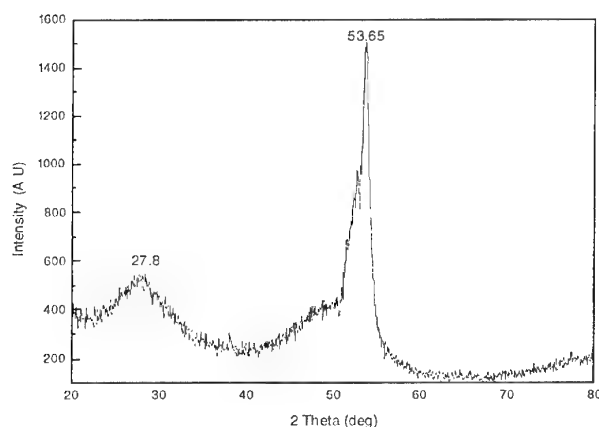
<sup>b</sup>Materials Science Division, IGCAR Kalpakkam - 603102, India

<sup>c</sup>Crystal Growth Centre, Anna University, Chennai - 600025, India

Tel.+81 298 613390; Fax:+ +81 298 613357, E-mail:jpachi@usa.com

Ion implantation in Gallium Arsenide (GaAs) has been extensively investigated for VLSI applications and for the realisation of novel electronic devices. The direct band gap and high electron mobility allows the production of discrete and integrated optoelectronic devices and to fabricate very high speed transistors, quantum well diodes, laser diodes and microwave oscillators [1]. In large scale integrated circuit fabrication using GaAs, nitrogen implantation is used to form isolated GaN buried layers. In view of the increasing application of N<sup>+</sup> implantation to device fabrication, it is of interest to investigate the damage introduced by the N<sup>+</sup> implantation and to study their effect on the annealing in GaAs.

For the present investigations, LEC grown undoped Semi-Insulating (SI) GaAs (100) single crystal substrates were used. 120 keV mass analyzed N<sup>+</sup> has been implanted on the samples to the fluences of  $1 \times 10^{15}$ ,  $1 \times 10^{16}$  and  $1 \times 10^{17}$  cm<sup>-2</sup> at room temperature under a vacuum of  $1 \times 10^{-7}$  mbar. Secondary Ion Mass Spectroscopy (SIMS) and Glancing angle XRD (GXRD) experiments have been carried out on the implanted samples. Figure shows the GXRD peak



intensity versus 2 theta of the implanted (fluence  $1 \times 10^{17}$  cm<sup>-2</sup>) sample. It is observed that a predominant peak at  $2\theta = 27.2$ , due to the formation of GaN<sub>x</sub>As<sub>1-x</sub>. Further the complex formation has been confirmed by SIMS analysis of the implanted samples. Detailed investigations on the 120 keV N<sup>+</sup> implanted with various ion fluences on GaAs substrates will be presented.

### References

1. D.S.McGregor, R.A.Rojeski, G.F.Knoll, F.L.Terry, J.J.East and Y.Eisen, Nucl. Instr. and Meth. A, 343 (1994) 527.



## Improvement of the parameters of devices on the base of GaAs epilayers by isovalence dope at liquid phase epitaxy

S.K.Guba, S.I.Krukovsky, A.B.Smirnov, A.I.Vlasenko

Institute of Semiconductor Physics NAS Ukraine, 45 pr.Nauki, Kiev, 03028, Ukraine  
E-mail:tenet@alfa.semicond.kiev.ua

At the present time the development of the III-V semiconductor devices production technology is the prevalent trend of microelectronics. Because of this, a search for ways of improving stability of III-V semiconductor-based devices such as photodetectors, Shottky barrier transistors, power GaAs bipolar transistors etc., are of considerable practical interest.

It was established that the rare-earth elements application in III-V semiconductor liquid-phase epitaxy considerably reduces concentration of accidental impurities (by 1,5-2 orders), has resulted in a increasing mobility of majority carriers and improving the stochiometry of grown epilayers. Such effect is stipulated by gettering operation of rare-earth elements. The degree of clearing depends on materials purity and features of a technical process.

We have determined the mechanism of influence of rare-earth elements on forming of the epitaxial layers properties. The doping of the melt with a low concentration of Yb and Sc resulted in gettering of residual impurities [1]. Moreover, at doping by Yb of Ga melt there is exist some range of his concentrations ( $N_{Yb} \leq 0,5 \times 10^{-4}$  at. p.), at which one begins possible to receive pure at enough acting eptaxial layers GaAs with a stoichiometric correlation of components  $A_3$  and  $B_5$  and perfect physical properties. The padding isovalence doping of a melt by bismuth reduces normal (directional normally to the surface substrates) integrate growth of epitaxial layers, that reduces probability of creation of structural defects.

Besides it is established that the simultaneous doping of Ga melt by Al and Yb in specially fitted proportions allows to receive uncompensated poor doping layers with concentration of carriers  $10^9 \text{ cm}^{-3}$  ( $\rho > 10^5 \text{ Ohm} \times \text{cm}$ ). And the effect of "cleaning" of epitaxial layers shows at minor concentrations of alloying elements (Yb, Al), reducing probability of pollution by unchecked impurity from an alloying material.

Such features of our method allow to receive epitaxial structure with low charge of states on interface, that improves noise performances of devices. Thus the high-purity and stoichiometric epilayers for device application can be obtained.

We also researched the predominant processes of a defect formation in composite specially doped iGaAs - nGaAs - n+GaAs structures with aim to produce criteria of building of the stable element base in conditions of external factors .

1. E.F. Venger, G.N. Semenova, S.I. Krukovski, T.G. Kryshab, M.O. Litvin, R. Merker Rare-earth applications in  $A_3B_5$  liquid-phase epitaxy *Opto-Electronics Review* Vol. 5, N 3 (1997).



## Investigations on Surface Defects of GaAs Grown by Molecular Beam Epitaxy

**M. Kaniewska and K. Klima**

Institute of Electron Technology, Al. Lotnikow 32/46, 02-668 Warsaw, Poland

E-mail: [kaniew@ite.waw.pl](mailto:kaniew@ite.waw.pl), fax: +48 22 847 06 31, tel: +48 22 548 77 93

The presence of surface macroscopic defects is a characteristic feature of GaAs epitaxial layers grown by molecular beam epitaxy (MBE). The surface defects, which are difficult to be avoided because of growth non-uniformity in MBE, are a trouble problem for optoelectronic and microelectronic devices. With respect to their shape and size the defects have been classified into a few groups. On the basis of this fact it has been suggested that defects have many different origins. The defects of irregular shape are attributed to macroscopic contamination, mainly caused by substrate preparation effects. The defects of oval shape are related to excess Ga atoms or to surface microscopic contamination. On the other hand it has been shown that the oval defects density is related to the Ga cell temperature and the growth time. It indicates that the substrate is not a particular source of oval defects and some of the defects are growth-induced. In this paper results of investigations of the surface macroscopic defects as a function of growth parameters are presented. We have observed that the normalized global defect density, on the As-stabilized surface of the GaAs layers, was thermally activated and varied from 40 to  $3 \times 10^3 \text{ cm}^{-2}$ , while changes in the temperature of the Ga cell covered the growth rate in the range 0.2-2.5  $\mu\text{m}$ . The defects can essentially be divided into two groups. We distinguish defects which characterize a large core region and defects which do not possess a distinct core particulate. As we observed, a mutual proportion of the oval defects without cores to the defects with cores changed with the substrate temperature as well as with the growth rate. Small oval defects without cores were the dominant defects if growth under As-rich conditions was performed at an elevated temperature and a low growth rate. The defect densities on the Ga-stabilized surfaces were in the same range of magnitude comparing to the defect densities on the As-stabilized surfaces. However large defects, with their size up to 20  $\mu\text{m}$ , with a large core in the middle, were the most dominant defects on the surface. Images of the defects with irregular shape and other results, presented in our previous paper [1], evidence that out-diffusion of atoms from Ga droplets takes place on the surface and the process shows a directional anisotropy. This can suggest that large defects at higher substrate temperature undergo evolution as well as that the effect can be a cause of the formation of elongated small defects. The results suggest that some defects differing in their size and shape can have the same origin and unbonded Ga atoms have to be taken into consideration in the process of the defect formation. In the process of evaluating the GaAs layers room-temperature photoluminescence spectroscopy was used. An interesting aspect of the study is a correspondence established between the efficiency of photoluminescence resulted from epitaxial layers and the kind of the dominant surface defects.

[1] M.Kaniewska, K.Klima, K.Reginski, Proc.SIMC-XI, Canberra, Australia, July, 2000





### Doping and impurity defect formation in epitaxial GaAs

**Bobrovnikova I.A.\***, **Lavrentieva L.G.\*\***, **Ivonin I.V.\***, **Subach S.V.\***, **Vilisova M.D.\***, **Preobragenski V.V.\*\*\***, **Putjato M.A.\*\*\***, **Semjagin B.R.\*\*\***

\*Siberian Physical Technical Institute State University, Tomsk, Russia,  
tel: (3822)556374, fax: (3822)233034, e-mail: bia@ic.tsu.ru;

\*\* , Tomsk State University, Tomsk, Russia;

\*\*\*Institute of Semiconductor Physics SB RAS, Novosibirsk, Russia.

Epitaxial growth occurs at relatively low temperatures. That is why the growth and doping of epitaxial layer are determined by surface kinetics. Surface structure and adsorption layer composition can sufficiently effect the doping and formation of defects. The components existing in vapour phase and in adsorption layer not only in atomic forms but also in a form of compound molecules can incorporate into the solid phase without their preliminary dissociation.

This paper is aimed at studying the impurity incorporation in a simple form and in a complicated one into the epitaxial grown GaAs and revealing mechanisms of formation of simple and complicated impurity defects during the vapour phase (VPE) and molecular beam (MBE) epitaxy. For this purpose the effect of growth conditions (As and impurity pressure, growth temperature, crystallographic surface orientation) on the impurity incorporation kinetics has been investigated for some impurities (S, Te, Sn, Ge) in VPE and Si – in MBE systems. Epitaxial layers have been grown on GaAs substrates of different orientations ((111)A, (100) and low angle deviations from main plains) in chlorine VPE system at 750°C and in MBE system at 480-520°C. The methods of electron microscopy, photoluminescence, and Hall-measurements have been used for investigations.

It was shown, that IV and VI groups impurities incorporate into the GaAs not only as simple donors and acceptors but also as more complicated defects: complexes, including impurity atom and a vacancy. Relative concentrations of various forms of impurity in the layers depends on the growth conditions. It was found, that the character of these dependences for simple impurity defects differs significantly from that for complicated defects.

Calculation of equilibrium adsorption layers composition on the surface of GaAs in VPE and MBE systems has been made in a wide diapason of growth conditions. It was shown that the IV and VI group impurities exist in adsorption layer not only in atomic form, but also in a form of diatomic molecules. Relative concentration of different impurity species in adsorption layer depends on the conditions of epitaxial growth.

Comparison of experimental and calculation data revealed some certain correlations between the concentration of impurity in different forms in the solid phase and in the adsorption layers. Analysis of these correlations allowed us to suggest a model of defect formation during the epitaxial growth of GaAs, according to which the formation of simple impurity defects (donors and acceptors) occurs due to the incorporation of adsorbed impurity atoms into the growing layer, and the formation of the complicated defects (impurity-vacancy complexes) occurs due to the capture of diatomic impurity molecules without their preliminary dissociation. The suggested mechanism is in a good accordance with the experimental VPE and MBE data.



## Transformation of defect structure and electrophysical properties of III-V semiconductors by pulsed laser irradiation

V.A. Gnatyuk

Institute of Semiconductor Physics of National Academy of Sciences of Ukraine  
Prospekt Nauki 45, UA-03028 Kyiv, Ukraine  
Tel.: +38 044 2645796, Fax.: +38 044 2649511, E-mail: gnatyuk@mailcity.com

Irradiation of semiconductors with nanosecond laser pulses results in creation and multiplication of the simplest defects, formation of complexes, development of dislocation structure, migration of impurities and intrinsic defects. This has opened up fresh opportunities for modifying the electrical and photoelectric parameters of III-V semiconductors. We have shown [1, 2] that irradiation of InSb and high-resistivity GaAs crystals with nanosecond ruby laser pulses resulted in modification of the photoconductivity spectra and change of the conductivity, surface recombination rate and nonequilibrium carrier lifetime. The phenomena of a giant increase in the conductivity of GaAs [2] and in the photoconductivity of InSb crystals after laser irradiation were discovered [1].

The present work is devoted to studying the reasons for the laser-stimulated phenomena in InSb and GaAs and determining the mechanism of laser radiation effect on defect structure of the semiconductors. Studies of the conductivity, photoconductivity, temperature dependence of the nonequilibrium carrier lifetime of various InSb and GaAs crystals irradiated with different numbers of laser pulses, carried out in a wide range of intensities, revealed the features associated with the highly critical dependence of the phenomena on the initial structure and state of the crystal surface as well as on a radiation intensity. The semi-insulator properties of original GaAs crystals have been attributed to the deep donor centers EL2 (probably based on antisites  $As_{Ga}$ ) counter-balanced by shallow-level accidental acceptors. A considerable rise (by a factor of  $10^2$ - $10^3$ ) of the conductivity of irradiated GaAs was due to the modification of a system of both intrinsic and impurity point defects. Irradiation of GaAs crystals caused a depletion of As atoms from the surface layer as a result of laser desorption. This layer became enriched with Ga and consequently the probability of the formation of point defects  $Ga_{As}$  (acting as acceptors) increased. Laser-stimulated diffusion of accidental impurities (Cu, C, Ca, Zn, Si atoms) from surface into the interior of crystals also formed shallow acceptor levels in a bandgap of GaAs causing the disruption in the donor-acceptor counter-balanced conditions. The laser-stimulated photosensitization of InSb crystals (integral photoconductivity increased by a factor of  $10^1$ - $10^2$ ) was attributed to gettering of electrically active point defects (acting as recombination centers) by extended defects (acting as sinks) as a result of action of laser-induced stress and shock waves.

1 - V.A.Gnatyuk, *Journal of Physics D: Applied Physics* **32**, No 20 (1999) 2687-2691.

2 - V.A.Gnatyuk, O.S.Gorodnychenko, P.O.Mozol', O.I.Vlasenko, *Quantum Electronics and Optoelectronics* **3**, No 1 (2000) 26-30.



## Correlation of crystal defects and galvanomagnetic parameters of semi-insulating InP with performance of radiation detectors fabricated from characterized materials

D. Korytar<sup>1</sup>, P. Bohacek<sup>1</sup>, C. Ferrari<sup>2</sup>, B. Surma<sup>3</sup>, F. Dubecky<sup>1</sup>, J. Huran<sup>1</sup>, B. Zatko<sup>1</sup>,  
V. Smatko<sup>1</sup>, R. Fornari<sup>2</sup>, and S. Strzelecka<sup>3</sup>

<sup>1</sup>Institute of Electrical Engineering, Slovak Academy of Sciences  
Dubravska cesta 9, Bratislava, SK-842 39 Slovakia, (korytar@svspn.sk,  
bohacek@svspn.sk)

<sup>2</sup>MASPEC CNR Institute, Parco Area delle Scienze 37/A, I-43100 Parma, Italy

<sup>3</sup>Institute of Electronic Materials Technology, Wolczynska 133, Warsaw, PL-01-919  
Poland

Crystal defects in semiconducting materials play a crucial role in determining the electrical properties and performance of electronic devices. This is especially important in the case of radiation detectors since their active region is given by the bulk of semiconductor substrate itself. Recently, bulk semi-insulating GaAs has found application as a promising basic material for detectors of ionising radiation (mainly X- and  $\gamma$ -rays), operated at room temperature (see e. g. [1] and references therein). However, SI InP offers better perspectives owing to the higher atomic number of In, which results in a 2-3x higher stopping efficiency with respect to GaAs, and to higher maximum electron drift velocity which allows 2-3x faster counting rate. Moreover, InP radiation detector is a potential candidate for detection of solar neutrino [2]. It should be noted that so far InP was only marginally considered for applications in the field of radiation detectors. The first paper in this area appeared till in 1998 [3].

In this work, bulk SI InP wafers of various producers have been examined by several characterization techniques with the aim to correlate the observed results with the detection performance of detectors. Conductivity and Hall parameters of the crystals have been measured using van der Pauw techniques. Crystal imperfections were assessed by high resolution double crystal X-ray topography and chemical etching to find density and distribution of dislocations. (004) rocking curves half-width have been taken as a parameter to classify the overall crystal perfection of wafers. The microprecipitates were studied by infrared light scattering tomography. The homogeneity of detector charge collection was investigated by scanning EBIC. The tested detectors were fabricated from the different materials in just one run in order to be sure that their performances were not influenced by technological process steps carried out in a different way.

For conclusion, the observed structural and physical characteristics of bulk SI InP crystals are correlated with the performance of radiation detectors based on tested materials. In general, the charge collection efficiency and energy resolution of radiation detectors fabricated from the bulk SI InP materials showed strong dependence on substrate quality.

- [1] T. E. Schlesinger, R. B. James, (vol. eds.): Semiconductors for Room Temperature Nuclear Detector Applications, Semiconductors and Semimetals, vol. 43, eds. R. K. Willardson, A. C. Beer, E. R. Weber, Academic Press, San Diego 1995.
- [2] P.G. Pelfer, F. Dubecky, R. Fornari, M. Pikna, E. Gombia, J. Darmo, M. Krempasky, and M. Sekacova, Nucl. Instr. Meth. **A 458** (2001) 400.
- [3] J. C. Lund, F. Olschner, F. Sinclair, M. R. Squillante: Nucl. Instr. Meth. **A 272** (1998) 885.



## Characterization of Defects and Whole Wafer Uniformity of Annealed Undoped Semi-insulating InP Wafers

Youwen Zhao<sup>1</sup>, Niefeng Sun<sup>2</sup>, Hongwei Dong<sup>1</sup>, Jinghua Jiao<sup>1</sup>, Jianqun Zhao<sup>1</sup>,  
Zhengping Zhao<sup>2</sup>, Tongnian Sun<sup>2</sup> and Lanying Lin<sup>1</sup>

<sup>1</sup>P.O.Box 912, Material Science Laboratory, Institute of Semiconductors, Chinese Academy of Sciences, Beijing 100083, P.R. China

Email: [zhaoyw@red.semi.ac.cn](mailto:zhaoyw@red.semi.ac.cn) phone number: 86-10-82304513

<sup>2</sup> P.O.Box 179-40, Hebei Semiconductor Research Institute, Shijiazhuang, Hebei, P. R. China

Email: [tnsun@public.sj.he.cn](mailto:tnsun@public.sj.he.cn) phone number:86-0311-7814737

Semi-insulating (SI) InP wafers of 2 inch and 3 inch diameters have been prepared by annealing undoped LEC InP at 900°C for 80h under pure phosphorus ambient (wafer A) and iron phosphide ambient (wafer B). The electrical uniformity of the two wafers, along with a Fe-doped as-grown SI LEC InP wafer, has been characterized by whole wafer PL mapping and radial Hall measurements. Defects in these wafers have been detected by photo-induced current transient spectroscopy (PICTS). The results indicated that uniformity of wafer B is much better than those of wafer A and as-grown Fe-doped SI InP wafers. Compared with wafer A and Fe-doped SI InP, there are less and low concentration of defects in wafer B, as evidenced by PICTS. Either the concentrations of defects are high or the defects are numerous in Fe-doped SI InP and wafer A. The good uniformity of wafer B is related with the nonexistence of high concentration of thermally induced defects. The mechanism for this phenomenon has been discussed based on the results.



## CHARACTERISATION OF BULK CRYSTALS AND STRUCTURES BY LIGHT-INDUCED TRANSIENT GRATING TECHNIQUE

**K. Jarasiunas<sup>1</sup> and N. Lovergine<sup>2</sup>**

<sup>1</sup>Institute of Materials Science, Vilnius University, Lithuania.

e-mail: [kestutis.jarasiunas@ff.vu.lt](mailto:kestutis.jarasiunas@ff.vu.lt), fax (3702) 366003, tel.(3702) 366036

<sup>2</sup>INFM, and Dipartimento di Ingegneria dell'Innovazione, Università di Lecce, Italy.

Light induced transient grating technique (TGT) is an implementation of the time-resolved four-wave mixing (FWM) spectroscopy in the pico- and nano-second time domain. Particular strength of this technique is its capability to monitor deep-impurity governed carrier generation, their transport and recombination in a nondestructive all-optical way. Additional advantage is its sensitivity to surface recombination velocity, as well as to the quality of heterostructure interfaces, if two different wavelengths are used to excite a carrier packet at the surface region and to monitor its in-depth propagation. We review applications of TGT in its various configurations (light self-diffraction and degenerate/nondegenerate FWM) using picosecond and nanosecond laser pulses.

We investigate by TGT at 1.06  $\mu\text{m}$  laser wavelength the role of charge state of deep vanadium impurity in bulk semi-insulating CdTe crystals, co-doped with shallow donors (Cl) or acceptors (As). Sub-nanosecond free-carrier grating decay in CdTe:V,Cl allow to reveal the role of residual Cd divacancies, estimate their density and recombination activity. A three-fold enhancement of electron generation rate in CdTe:V,Cl is attributed to the photo-excitation of associations of defects, presumably vacancy-donor complexes.

In GaAs crystals, a temporary transfer of EL2 levels to metastable state appears at RT by nanosecond laser excitation and we apply this feature to determine the deep donor compensation ratio in LEC- and Bridgman-grown wafers. By monitoring the light diffraction efficiency across the wafer area a W-shaped spatial distribution of EL2 states and its correlation with dislocation density is also revealed. Picosecond dynamics of free carrier grating reveals the charge state of EL2 levels, carrier generation rate, electron-to-hole density ratios and the feedback of light-induced space-charge field to carrier transport.

Two-colour TGT investigations were carried out on MOVPE-grown ZnTe/GaAs and CdTe/ZnTe/GaAs heterostructures. We compare the carrier dynamics in a thin CdTe layer (thickness  $d_1=770$  nm) and a thick one ( $d_2=1600$  nm) and determine similar carrier diffusion coefficients ( $D \approx 29$  cm<sup>2</sup>/s), but different lifetimes ( $\tau_1=1.1$  ns and  $\tau_2=0.3$  ns for the thickness above, respectively). Similarly,  $D$  and  $\tau$  close to 32 cm<sup>2</sup>/s and 1.7 ns are found for carriers in ZnTe/GaAs. Whilst these lifetimes are typical of excited II-VI semiconductors, values of diffusion coefficients above indicate a transfer from light-induced bipolar plasma to quasi-monopolar transport of carriers due to fast and effective electron trapping.

The use of a tuneable source picosecond parametric laser for TGT spectroscopy is shown as an essential innovation to study carrier dynamics in compensated bulk crystals, as well as a way to get deeper insight into role of interfaces in epitaxial heterostructures.

## Crystal defects and optical transitions in high purity, high resistivity CdTe for device applications

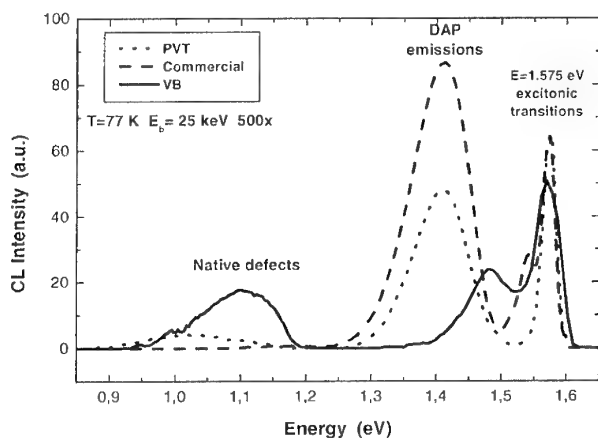
N. Armani, C. Ferrari, G. Salvati, F. Bissoli, M. Zha, L. Zanotti

CNR – MASPEC Institute, Parco Area delle Scienze, 37/A 43010 Fontanini, PARMA, Italy  
Tel. +39 0521 269250 - Fax +39 0521 269206, e-mail [narmani@maspec.bo.cnr.it](mailto:narmani@maspec.bo.cnr.it)

Cadmium Telluride (CdTe) is a very attractive semiconductor material for a large number of applications in the X- and  $\gamma$ -ray detectors and electro-optical devices. However, all the above mentioned applications require a reproducible electrical resistivity larger than  $10^7 \Omega \text{ cm}$  which, till now, has been obtained by selecting suitable doping elements even if the intentional doping of the crystals may lead to a very poor crystalline quality due to the constitutional supercooling effect.

In this work, high purity undoped semi-insulating CdTe crystals have been grown by Physical Vapour Transport (PVT) and by modified Vertical Bridgman (VB) from 7N source elements by direct synthesis [A. Zappettini et al. *J. Cryst. Growth* **214-215**, 14 (2000)] and by the heat treatment to adjust the stoichiometry [M. Zha et al. to be presented at ICCG-13 Kyoto, Japan, July 30 – August 04, 2001].

The structural and optical studies have been systematically performed by high resolution X-ray diffraction and cathodoluminescence (CL) techniques respectively before and after thermal annealing procedures. The density and distribution of native dislocations and precipitates have been determined by comparing chemical etching, X-ray topography and panchromatic CL maps imaging. Dislocations were found to arrange in cellular structures of 2-300  $\mu\text{m}$  in diameter while precipitates were homogeneously distributed on the growth plane.



The CL emissions from low and high resistivity samples have been studied by spectrally resolved CL at  $77 < T < 300 \text{ K}$ . An example of CL spectra from high resistivity specimens is shown in the figure. In addition to the usual optical transitions [see for instance A. Castaldini et al. *J. Appl. Phys.* **83**, 2121 (1998)], a new interesting result comes up by comparing the integrated intensities of the deep level-related band at 1.1 eV from the VB and PVT specimens. This

difference is discussed in terms of the different growth conditions, electrical properties and annealing procedures. Finally, cross section CL maps and spectral analyses have also been carried out in order to assess the in depth defect distribution and optical properties homogeneity along the growth axis.

**DEFECTS IN CdTe FILMS DOPED WITH Zn and Ge****V. Corregidor<sup>a</sup>, E. Saucedo<sup>b</sup>, L. Fornaro<sup>b</sup>, E. Diéguez<sup>a</sup>**<sup>a</sup> Dept. Física de Materiales. Universidad Autónoma de Madrid, 28049 Madrid. Spain.Presenting author: [ernesto.dieguez@uam.es](mailto:ernesto.dieguez@uam.es) Phone: +34913974977; Fax: +34913978579<sup>b</sup> Radiochemistry Department, Universidad de la República, 11800, Uruguay

CdTe films are been widely studied in recent years due to their different applications, such as solar cells (CdS/CdTe heterojunction), optoelectronic and detectors devices. The cristallinity needed for such applications is variable, for solar cells the polycrystalline state is the appropriate while for optoelectronic high cristallinity is required.

In this work CdTe films are grown by physical vapour transport onto different substrates. Synthesized CdTe was charged in an evacuated ampoule and sealed, then it was put in a two independent zones controlled furnace, using both, horizontal and vertical arrangement. According to the furnace set-up different the source and the substrates temperatures can be achieved. Several substrates are used like n-Si, p-Si and alumina, in this way different quality of the film growth can be obtained as a function of the mismatch substrate-film. Experiments are carried out at a source temperature in the range 500-850°C and at substrates temperatures 250-800°C. Growth duration is variable between 24 and 96 hours. After films growth, atoms like Ge and Zn, are evaporated and diffused into the film by heating the substrate.

The layers are characterized by HRXRD and low angle diffraction to study the cristallinity grade and for determination of growth direction, mostly (111). Photoluminescence at 4K and other temperatures was used for determination of the luminescence behaviour. A wide band in the region of 1,4 eV is present, as well as the excitonic lines due to the recombination of the acceptors/donors impurities presents in the film, although in some cases these lines are not clearly observed. Depending of the material cristallinity, the diffused atoms can be accumulated in the boundary grain and in dislocations, which increases the amount of inclusions, observed by EDAX and SEM. Distribution of these atoms are studied along the film thickness. Electrical and detection properties of the films are studied by assembling detectors. For this purpose, Au was deposited by thermal evaporation as a real contact onto the substrate and as a front contact onto the film substrate, Au wires 0.001 inches in diameter were attached using graphite suspension in water and finally the detector is encapsulated with an acrylic coating. Room temperature I-V curves were performed for determining dark current and apparent resistivity and X-Ray response was carried out irradiating with a collimated <sup>241</sup>Am source. Correlation between growth parameters, dopants, physical, electrical and detection capabilities are included. Finally, the results obtained for the different substrates and dopant atoms are compared with previous reported data.

## BEHAVIOUR OF DEFECTS IN ZnSe CRYSTALS AT LASER SHOCK WAVE PASSAGE

A. Baidullaeva, O.I.Vlasenko, P.O.Mozol'

Institute of Semiconductor Physics  
National Academy of Sciences of Ukraine,  
45, Prospekt Nauki, 03028, Kiev-28, Ukraine  
E-mail: baidulla@class.semicond.kiev.ua  
Tel.: (+38) 044-265-18-75, fax: (+38) 044 265-83-42

Irradiation of II-VI crystals with nanosecond laser pulses of subthreshold power alters considerably of their physical properties. These changes are due to laser induced defect formation. Among the factors being to able to cause the laser defect formation one can be named heating, acoustic wave and shock wave (SW).

In this paper SW influence on defect structure modification of ZnSe crystals was investigated. The investigated high-resistivity ZnSe crystals were distinguished in accordance with the concentration of accidental impurities into three types with concentrations  $n \sim 10^{15}$ ,  $10^{16}$ ,  $10^{17} \text{ cm}^{-3}$  respectively. The Q-switched ruby laser pulses of power density  $10^7$ - $10^8 \text{ W/cm}^2$  was used to generate the SW. The depths of SW formation were 110 and 77  $\mu\text{m}$  when power density of laser pulses was equal 40 and 80  $\text{MW/cm}^2$  accordingly. In these cases corresponding pressures of the SW were 3.64 and 5.14 kbar.

The spectra of photoconductivity (PC) thermally stimulated conductivity and temperature dependences of dark and photocurrents of ZnSe crystals before and after SW passage were investigated. It was established that changes of the properties depend on accidental impurity concentration at SW passage through samples. The decrease in the PC value also PC spectra shape in ZnSe-2 crystals ( $n \sim 10^{15} \text{ cm}^{-3}$ ) was observed after SW passage. In ZnSe-3 ( $n \sim 10^{14} \text{ cm}^{-3}$ ) magnitude of PC rises before and reduces after SW pressure increase. Here the spectrum shape is remained. The range of activation in dark current temperature dependence of ZnSe-2 emerges at lower SW pressures in comparison with ZnSe-3. Photo current extinguish temperature location alters in ZnSe-2 after SW passage with  $P=3.64 \text{ kbar}$ .

Experimental data analysis shows that above mentioned changes of studied crystals' properties at SW passage could be explained by new defects formation with energetic positions  $E_1 = 0.03 \text{ eV}$ ,  $E_2 = 0.11 \text{ eV}$  and  $E_3 = 0.68 \text{ eV}$  in ZnSe-2 and ZnSe-3 respectively. Mechanisms of these defects formation are discussed. It is assumed that increase of defect concentration may be caused by liberation of residual impurities from impurity accumulation (clusters) when a SW passes through the crystal.



## Transient and stable absorption of radiation induced defects in oxide crystals

D.Sugak<sup>1,2</sup>, A.Matkovskii<sup>1,3</sup>, A. Durygin<sup>4</sup>, A. Suchocki<sup>4</sup>, P.Potera<sup>3</sup>

<sup>1</sup> State University Lviv Polytechnic, 12 Bandera St., 79646 Lviv, Ukraine,  
tel/fax: 0380322742164, e-mail: crystal@polynet.lviv.ua

<sup>2</sup> Institute of Materials, SRC «Carat», 202 Stryjska St., 79031 Lviv, Ukraine

<sup>3</sup> Institute of Physics, HPS, Rejtana 16 A str, 35-310 Rzeszow, Poland,  
e-mail: matk@atena.univ.rzeszow.pl

<sup>4</sup> Institute of Physics, PAS, 32/46 A I. Lotnikow, 02668 Warsaw, Poland

The results of investigation of the UV, gamma, electron and neutron irradiation influence on optical properties of rare-earth doped  $\text{YAlO}_3$  (YAP),  $\text{Gd}_3\text{Ga}_5\text{O}_{12}$  (GGG) and  $\text{LiNbO}_3$  (LN) crystals are presented. YAP, GGG and LN crystals doped with rare-earth ions ( $\text{Nd}^{3+}$ ,  $\text{Ho}^{3+}$ ,  $\text{Tm}^{3+}$ ,  $\text{Er}^{3+}$ ,  $\text{Yb}^{3+}$ ) are most prospective materials for laser engineering. The presence of defects (color centers) in laser crystals is one of major factors determining their quality and efficiency.

Growth defects recharging mechanism forms the main contribution in changes of optical properties of UV and gamma-irradiate crystals. The generated color centers (CC) are both stable (SCC) and transient (TCC) at room temperature. Transient CC are stable at temperatures  $T < 100$  K and have life time of few ms at room temperature. The models of color centers and the role of rare-earth impurities in radiation induced transformations of crystals are discussed. The TCC are a source of energy losses in laser rods due to a re-absorption of laser radiation. The SCC also contribute to losses mainly via unproductive absorption of pumping light.

In irradiated GGG-Nd crystals the additional absorption (AA) spectrum consists at least of two bands with peaks  $30000$  and  $23000 \text{ cm}^{-1}$  and the clearing near the absorption edge occur. The value of AA increases with the irradiation dose and at  $D > 10^4$  Gy its saturation takes place. In Er-doped crystals, generating in  $3 \mu\text{m}$  range, CC may fulfill a function of sensibilizers providing an increasing of the laser output energy.

In YAP crystals irradiation leads to appearance of AA in the range of  $48000$ - $10000 \text{ cm}^{-1}$  with maxima at  $45000$ ,  $40000$ ,  $32000$ ,  $23000$ ,  $20000 \text{ cm}^{-1}$  and  $16000 \text{ cm}^{-1}$ . The AA bands are connected with the hole centers  $\text{O}^\cdot$  which can be stabilized by  $\text{Fe}^{2+}$  ions, F-centers. Transient AA in range of  $\nu < 18000 \text{ cm}^{-1}$  is connected with centers of  $\text{F}^+$  type. In all doped and undoped  $\text{LiNbO}_3$  crystals irradiation results in a complex AA band in the  $29000$ - $13000 \text{ cm}^{-1}$  region. Introducing trivalent dopands alone causes an increase in AA in comparison with pure crystals. At the same time the AA intensity decreases for all samples co-doped with  $\text{Mg}^{2+}$ .

Irradiation of crystals with high energy electrons and neutrons results in formation of displacement defects at high levels of particle fluence (more then  $10^{17} \text{ cm}^{-2}$ ) due to the relative high values of threshold energy (more then  $40 \text{ eV}$ ).



## Surface states of $\text{Cd}_{1-x}\text{Zn}_x\text{Te}$ crystals

Belyaev S.V., Zhovnir G.I., Sypko S.A.

Institute of Semiconductor Physics NAS Ukraine  
Kiev-28, pr. Nauki (ç, Kiev 03028, Ukraine  
tel.: 380 (44) 265-96-51, 555-08-75; fax: 380 (44) 265-41-10  
e-mail: AVL@mizar.semicond.kiev.ua

High specific resistance is one of the main conditions for the use  $\text{Cd}_{1-x}\text{Zn}_x\text{Te}$  single crystals as substrate material for epitaxy. High values of the Debye screening length can sufficiently change surface conductivity, which leads to the lowering of the physical parameters of the matrix photoreceivers.

This report is concerned with the investigations of the influence of oxygen adsorption on the physical properties of the (111) surface in the commercially produced  $\text{Cd}_{1-x}\text{Zn}_x\text{Te}$  single crystals. In order to prevent the formation of the oxides on the freshly etched surface of the film the 5% bromine solution the non-aqueous organic solvent was used as polishing etching solution. Thoroughful rinsing of the surface was carried out in several stages with the use of the high purity organic solvents. On the prepared freshly etched surface the contacts immediately were deposited, accompanied by investigations of the photoconductivity spectra (FC) and electrical resistance. In the following the surface was stabilized in the air atmosphere during time ranging from 1 up to 100 hours. Then mentioned above investigations were again carried out. At a result of the series of carried out investigations the monotonic decrease of the surface resistance, increase of the intrinsic maximum in the FC spectra and increase of the inclination angle of its short wavelength wing was established. The latter is characteristic for the increased concentration of the point defects in the subsurface layer of the crystal. Taking into account the maximal reticular density of (111) face it is possible to consider that the adsorption is small and inversion layer with the different sign of majority carriers is absent.

The established regularities are determined by the change of the surface charge and by the decrease of the concentration of the minority carries in the surface layer of the Debye screening length.

## Heterojunction and periodical structures in MCT solid solution : the results of laser annealing

M.M. Pociask and E.M. Sheregii

Institute of Physics, Pedagogical University in Rzeszów,  
Rejtana 16a Str., 35-310 Rzeszów, Poland  
e-mail: pociask@atena.univ.rzeszow.pl  
Fax: +48 17 8526792, Phone: +48 17 8625628

Mercury cadmium telluride (MCT) solid solution, still one of the most important material for infrared devices has a serious fault: the weak mercury bond in crystal net. This peculiarity - the weak HgTe bond - has another aspect: the possibility to modify the properties of that material by an external influences, for example, by laser irradiation.

In semiconductors of MCT a prominent role is played by intrinsic defects such as vacancies of mercury atoms, which are acceptors, and interstitial mercury atoms (IMA), which are donors. At high temperature the main model of diffusion of IMA in HgCdTe is a vacancy mechanism, which allows the chemical diffusion of mercury. This diffusion process of IMA determines the concentration of both donors and acceptors and brings about a change in chemical composition of the material [1].

In this paper it is shown that the diffusion processes of atoms at laser annealing of  $\text{Hg}_{0.8}\text{Cd}_{0.2}\text{Te}$  can cause the specific conditions of decomposition of solid solution, which determine its inner periodic structure.

The idea of the possible formation of *p-n* heterojunction as a result of defects migration, which was shown by computer modelling of mass transportation processes under laser treatment of the MCT was experimentally realized. MCT samples were irradiated without melting with neodymium laser. The presence of a heterojunction on a surface not far below the upper, annealed surface has been verified by photovoltaic measurements and X-ray microanalysis as well as by current-voltage characteristics. That heterojunction is photosensitive in the range 9-11  $\mu\text{m}$  [2-3].

1. R.Ciach, M.Faryna, M.Ku\_ma, M.Pociask, E.Shererii, "Segregation of impurities and defects in  $\text{Hg}_{0.8}\text{Cd}_{0.2}\text{Te}$  by laser annealing", *Thin Solid Films* **241**, pp. 151-154, 1994.
2. E.Shererii, M.Ku\_ma, C.Abeynayake, M.Pociask, "Creation of a *p-n* heterojunction in  $\text{Cd}_x\text{Hg}_{1-x}\text{Te}$  ( $x=0.2$ ) by laser annealing", *Can. J. Phys.* **73**, pp. 174-176, 1995.
3. R. Ciach, M. Faryna, C. Abeynayake, M. Pociask, E. Sheregii, "Oscillations of the composition of HgCdTe solid solution after laser annealing", *Journal of Crystal Growth* **161**, pp. 234-238, 1996.



## Using spatially resolved techniques for investigating defects through HgCdTe IR FPA technological process

**Pavel Y. Pak, Valeriy V. Shashkin**

Institute of Semiconductor Physics, 630090, Novosibirsk 90, Russia

E-mail: pak@thermo.isp.nsc.ru; tel.: +7-3832-331954

Performance of IR FPA photodetectors strongly suffers from spatial nonuniformity of base material. Therefore, spatially resolved investigating material parameters is very important for developing high-performance FPAs.

We applied both destructive and nondestructive techniques to  $\text{Hg}_{1-x}\text{Cd}_x\text{Te}$  (MCT) epilayers ( $x=0.2-0.3$ ) grown by MBE on GaAs substrates as well as to MCT photodiode array structures for long-wavelength infrared (LWIR) and midwavelength infrared (MWIR) spectral region. Nondestructive Scanning Laser Microscopy (SLM) technique based on Laser Beam Induced Current (LBIC)<sup>1</sup> effect was used for spatial mapping electrically active regions in MCT. Temperature conditions of experiments were different depending on type of material: 78K for MCT with  $x=0.2-0.24$  and 300K for  $x>0.28$ . Destructive technique of Secondary Ion Mass Spectroscopy (SIMS) was used for imaging background impurity distribution in MCT epilayers.

We compared results of SLM imaging of a fragment of a LWIR photodiode array structure with current-voltage dependencies of diodes measured after forming contacts. Strong correlation between qualitative estimation by SLM and quantitative measurements of diode current-voltage dependencies has been found.

In order to find out distribution of electrically active nonuniformities in the volume of the MCT film, MBE grown  $\text{Hg}_{0.78}\text{Cd}_{0.22}\text{Te}/\text{GaAs}$  epilayers were measured by SLM through step-by-step etching. Obtained images show similar plane distribution of electrically active nonuniformities from etching to etching down to substrate. Since that we concluded about intergrowing in vertical plane character of defects.

It is known that background impurities in semiconductor crystals may be concentrated on crystal structure defects. We obtained SIMS images with a 5- $\mu\text{m}$  resolution reproducing a background impurity distribution in a fragment of MCT epilayer ( $x=0.3$ ). Distributions of carbon, arsenic, lithium and copper concentration are similar. Comparing these results with SLM images shows existence of electrically active nonuniformities in the regions where background impurities have concentration peaks. We assume that crystal structure nonuniformities concentrate background impurities during film growth process. The same crystal structure defects cause appearing electrical nonuniformities, registered by SLM.

1. J. Bajaj, W. E. Tennant, R. Zucca and S. J. C. Irvine, *Semicond. Sci. Technol.*, vol.8 (1993), p.872

# Author Index

Abdallah O.	P2-12	Bonafos C.	P1-09
Agarwal S. K.	P1-35	Bondarenko V.	P2-19
Ahoujja M.	S10-3	Borionetti G.	S5-1
Alex V.	S7-2	Börner F.	S5-4
Aleynikov A.	S6-2	Boscherini F.	S13-5
Amarendra G.	P1-32	Bosi M.	P1-01
Amighetti S.	P1-26	Boucke K.	P1-51
Andrievskii V. F.	P1-27	Bouloudenine Ma.	P2-29
Angelis C. T.	S13-3	Bouzidi A.	P1-54
Antonova I. V.	P2-13	Braun W.	S12-2
Aragon G.	P2-41	Breitenstein O.	S14-4
Arakawa Y.	S10-4	Briggs G. A. D.	S4-3
Arbiol J.	P1-52	Briones F.	P2-41
Ardila A. M.	P2-36, S3-4	Broqua N.	S14-5
Armani N.	P1-01, P2-50, S10-5	Brunner K.	S2-3
Arora S. K.	P1-35	Bünger Th.	S1-2
Arutyunov N. Yu.	P1-20	Bussei P.	P1-24
Asaad I.	S14-5	Calvino J. J.	P1-52
Attolini G.	P2-40	Cantelli R.	S13-4
Avella M.	P2-36, S3-4, S14-5	Carnera A.	P1-24
		Carrada M.	P1-09
Babentsov V.	P1-38	Cassidy T. D.	S1-1
Baeumler M.	P1-29, S1-2	Castaldini A.	P2-01, P2-10, S10-5
Baidullaeva A.	P2-52	Cavalcoti D.	P2-10
Balázs J.	P1-40, P1-41	Cavallini A.	P2-01, P2-10, S10-5
Balucani M.	P2-19	Cesca T.	S13-5
Baranowski J. M.	P2-06	Chante J. P.	P1-08
Barradas N.	P1-33	Chen Y. H.	S3-2
Bärwolff A.	S2-3, S14-2	Chernova N. A.	P1-42
Batson P. E.	S8-1	Cherns D.	S10-1
Baumbach T.	P2-21	Chtcherbatchev K. D.	P1-33, P1-34
Bedel E.	P1-31	Chu T.	S7-2
Belyaev S. V.	P2-54	Ciatto G.	S13-5
Benamara Z.	P1-22	Cirlin G.	S2-5
Benatmane A.	S3-6	Citarella G.	P2-12, S6-5
Benelová M.	S4-2	Claeys C.	S7-1
Benramdane N.	P1-54	Claverie A.	P1-31
Benz K.	P1-38	Cordero F.	S13-4
Berenguer M.	S1-4	Cornet A.	P1-52
Bergman J. P.	S14-3	Corni F.	P2-28
Bertulis K.	P1-23	Corregidor V.	P1-38, P2-51
Bettiati M.	S14-5	Cremades A.	P1-05
Bickermann M.	S3-5	Czerwinski R.	P2-03
Bissoli F.	P2-50		
Bluet J. M.	S1-4	D'Andrea A.	P2-33
Bobrovnikova I. A.	P2-45	Daub E.	S2-4
Boccaro A. C.	P2-27	Däweritz L.	S12-2
Bocchi C.	P2-20	Dekker J.	P1-25
Bochem H. P.	P1-06	Diaz-Guerra C.	P2-01
Bohacek P.	P2-47	Dib H.	P1-22
Boher P.	P2-27	Dieguez E.	P1-38, P1-39, P2-51
Bolotov V. V.	P1-21, P2-34, P2-35		

Dimitriadis C. A.	S13-3	Germini F.	P2-20, P2-40
Dobis P.	S4-2	Gerth G.	S2-5
Dobrowolski W.	S9-2	Gerthsen D.	P2-38
Dolgyi L.	P2-19	Ghezzi C.	P1-26
Donecker J.	S7-2, S14-2	Giannazzo F.	S6-4
Dong Hongwei	P2-48	Gil-Lafon E.	S3-4
Donoval D.	S8-3	Girard P.	S1-4
Dubecky F.	P2-47	Gnatyuk V. A.	P2-46
Dubois A.	P2-27	Goerigk G.	P1-31
Durygin A.	P2-53	Goldfarb I.	S4-3
Ebling D. G.	S12-1	Gombia E.	P1-24, P1-26
Edelman P.	S6-2	Gonzalez L.	P2-41
Efremov M. D.	P2-37, P2-38	González M. A.	P1-09, P2-40
Efros B.	P2-15, P2-16	Gonzalez Y.	P2-41
Egorov V. A.	S2-5	González-Varona O.	P1-09
Eguchi K.	P2-09	Gopalan P.	P2-22
Ehlert A.	S2-4	Gorelenok A. T.	P1-27
El Habra N.	S13-5	Gosele U.	S2-5
Elsaesser T.	S2-3, S4-1	Gottschalch V.	P2-04
Emel'yanov E. M.	P1-17	Graeff W.	P2-30
Emiliani V.	S4-1	Gramlich S.	S2-3
En A.	P2-09	Grazzi C.	P1-02
Engler N.	S8-2	Gregora I.	P2-04
Enisherlova K.	P1-19	Grillo V.	P2-39
Eremenko V.	P2-41	Grmela L.	S4-2
Escadafals L.	P2-27	Gründig B.	P1-29, S9-3
Evangelou E. K.	S13-3	Grzegory I.	P2-03
Fan Luixin	P2-17	Guadalupi G. M.	S13-4
Fedotov A.	P1-19	Guba S. K.	P2-43
Feltgen T.	P1-38	Guillot G.	S1-4
Fernández P.	S11-5	Günther T.	S2-3, S4-1
Fernández-Alonso F.	P2-33	Hageman P.	S10-2
Ferrari A.	P2-19	Hanaue Y.	S3-3
Ferrari C.	P2-47, P2-50,	Hanaue Y.	S9-4
	S12-4	Hara T.	P1-12
Fiederle M.	P1-38	Harada H.	P1-15
Figielski T.	S9-2	Hardalov Ch.	S11-5
Filipecki J.	P1-53	Haroutyunian V. S.	P1-03
Fitzgerald E. A.	S12-4	Hasegawa T.	P1-10
Fogarassy E.	S3-6	Hastas N. A.	S13-3
Fornari R.	P1-01, P2-47	Heera V.	P1-08
Fornaro L.	P2-51	Helfen L.	P2-21
Fraboni B.	S13-5	Hengehold R. L.	S10-3
Franchi S.	P1-24, P1-26	Herms M.	P1-31, P2-21
Franco N.	P1-33	Herrera M.	P2-41
Frigeri C.	P1-13, P1-40,	Herres N.	S12-1
	P1-41	Hidalgo P.	P1-39
Frigeri P.	P1-24, P1-26	Hilpert U.	S11-4
Frymark I.	P1-23	Hirano Y.	S5-3
Fujimori H.	S5-3	Hirose T.	S2-2, S5-5
Fukuda K.	P1-16	Höring L.	S11-4
Fukuzawa M.	S9-4	Horváth Z. E.	P1-41
Garrido B.	P1-09	Hoshikawa K.	S12-3
Gasparotto A.	S13-5	Hoshino K.	S10-4
Gebauer J.	S5-4	Huang X.	S12-3
Geiler H. D.	S2-4	Hubbard S. M.	S11-2
Gelly G.	S14-5	Huran J.	P2-47
Gérard B.	P2-36, S3-4	Ibuka S.	S2-1
Gerhardt A.	S14-2	Imscher K	S9-1
		Inoue N.	P1-15, S5-2

Intonti F.	S4-1	Kovac J.	P2-04
Irisawa T.	P1-13	Kovacsics Csaba	P1-14
Irmer G.	P1-31	Kowalski G.	P1-23
Ishiyama T.	P1-16	Kozlowski J.	P1-04
Ishizuka Yoshimori	P1-11	Kozlowski R.	P1-30
Islam M. R.	S3-3	Krause-Rehberg R.	S5-4
Isshiki T.	P1-45, S11-3	Krotkus A.	P1-23
Ito S.	S8-4	Krukovsky S. I.	P2-43
Itoh Shun	P2-02	Kühnel G.	P1-28
Ivonin I.V.	P2-45	Kumar J.	P2-05, P2-42
Iwagami Y.	P1-16	Kunst M.	P2-12, S6-5
Izumi T.	P1-12, P2-11	Kuznetsov A. N.	P2-07
Jahn U.	S11-1	Lagowski J.	S6-2
Jantz W.	P1-29, S1-2	Lamedica G.	P2-19
Janzén E.	S14-3	Landesberger C.	P2-21
Jarasiunas K.	P2-49	Landesman J. P.	S3-1
Jayavel P.	P1-32, P2-42	Langenkamp M.	S14-4
Jenichen B.	S12-2	Latini G.	S4-5
Jiao Jinghua	P2-48	Lavrentieva L. G.	P2-45
Jiménez J.	P1-09, P2-36, P2-40, S3-4, S14-5	Lazar M.	P1-08
Jurisch M.	P1-29, S9-3	Lazzarini L.	P2-39
Kaganer V. M.	S12-2	Lebedev A.	P2-07, P2-08
Kamaev G. N.	P1-21	Ledentsov N. N.	P2-38, S2-5
Kamakura Y.	S2-2, S5-5	Lefeld-Sosnowska M.	P2-30
Kamanin A. V.	P1-27	Lei H.	S8-2
Kamata N.	S10-4	Leinonen T.	P1-25
Kaminska M.	P1-23	Leipner H. S.	S8-2
Kaminski P.	P1-30	Leszczynski M.	P2-03
Kamiura Y.	P1-16	Li Liben	P2-17
Kanai A.	S8-4	Lienau Ch.	S2-3, S4-1
Kang Junyong	P1-07, P2-02	Lin Lanying	P2-48
Kaniewska M.	P2-44	Litvinov D.	P2-38
Kanjilal D.	P1-35, P2-05	Locatelli M. L.	P1-08
Karge H.	S2-4	Logothetidis S.	S13-3
Kashima K.	S5-3, S7-3	Lovergine N.	P2-49
Kasinska A.	P2-06	Lu Jinggang	P2-17
Khoroshilov K. Yu.	P1-21	Lyubas G. A.	P2-34
Kim D. S.	P2-32	Ma M.	P1-13
Kim R.	S2-2, S5-5	Ma Xiangyang	P2-17
Kinoshita K.	S3-3	Maaßdorf A.	S2-3
Kinoshita K.	S9-4	Macht L.	S10-2
Kirste L.	S12-1	Maier M.	S1-2
Kishino S.	P1-11	Makosa A.	S9-2
Kiskinova M.	S13-1	Malyarchuk V.	S2-3
Kitaia A. H.	S13-2	Martínez O.	P2-36, P2-40, S3-4
Klima K.	P2-44	Martinuzzi S.	S6-3
Klimenko A. S.	P1-47	Masarotto L.	S1-4
Kobayashi T.	P2-11	Mascher P.	S13-2
Kodama S.	S3-3	Matkovskii A.	P2-53
Kögler R.	S5-4	Matsumoto T.	S5-2
Kohanovskii S. I.	P1-27	Mazanik A.	P1-19
Köhler K.	S12-1	Mazur Y. I.	S2-3
Koidl P.	S12-1	McFall J. L.	S10-3
Konofaos N.	S13-3	Medles M.	P1-54
Kordos P.	P1-06	Mekki D. E.	P2-29
Korotchenkov O. A.	P2-31, P2-32	Méndez B.	P1-39
Korytar D.	P2-47	Mezdrogina M. M.	P1-27
Kotina I. M.	P2-14	Mikayama T.	P1-15
		Mironov O. A.	P1-33

Misiuk A.	P2-15, P2-16		S11-5
Mohammed-Brahim T.	P1-22	Pizzini S.	P1-17
Molinas B.	S13-4	Plaza J. L.	P1-39
Montgomery P. C.	S3-6	Ploog K. H.	S12-2
Morante J. R.	P1-09, P1-52	Pociask M. M.	P2-55
Moreira E. C.	S13-5	Podolyan A. A.	P2-31
Moriya K.	S3-7	Pödör B.	P1-41
Mosca R.	P1-24, P1-26	Pokanevich A. P.	P1-47
Mosina G.	P2-08	Polenta L.	P2-01, S10-5
Mousalitin A. M.	P1-43	Pommies M.	S14-5
Moussavi-Zarandi A.	P1-18	Ponpon J. P.	S3-6
Mozol' P. O.	P2-52	Popov V. W.	P1-47
Mukhamedzhanov E.	P2-20	Poprawe R.	P1-51
Murase T.	P1-10	Potera P.	P2-53
Myronov M.	P1-33	Preobrazhenski V. V.	P2-37, P2-38, P2-45
Nacer D.	P1-54	Priolo F.	S13-5
Namizaki T.	P1-10	Privitera V.	P2-20
Nasi L.	P2-20	Prochazkova O.	P1-36, P1-37
Navarro J.	S6-2	Prudnikov A.	P2-15, P2-16
Nazarov M.	P1-46	Püspöki S.	P1-40
Nickel D.	S2-3	Putjato M. A.	P2-45
Niklas J. R.	P1-29, S9-3	Que Duanlin	P2-17
Nishihori F.	S7-3	Queirolo G.	P2-28
Nishimura S.	S7-4		
Nishino S.	P1-45, S11-3	Raineri V.	S6-4
Nowak G.	P2-03	Rajaraman R.	P2-22
Obloh H.	S12-1	Rakotoniaina J. P.	S14-4
Odawara M.	S4-4	Rakovics V.	P1-40, P1-41
Ogawa T.	P1-13	Rau E. I.	P1-50, P2-24, P2-25
Ohkubo I.	P1-15	Ravichandran V.	P1-32, P2-22
Okamoto W.	S10-4	Redmann F.	S5-4
Okumura T.	P2-09	Regulska M.	P1-03, P2-06, P2-30
Orsal B.	S14-5	Remmele T.	P2-39
Ottaviani L.	P1-08	Réti I.	P1-40
Pak Pavel Y.	P2-56	Richter E.	S2-3
Pakula K.	P1-03, P2-06	Riemann H.	S7-2
Palais O.	S6-3	Righini M.	P2-33, S4-5
Palumbo O.	S13-4	Rossetto G.	S12-4
Panayiotatos Y.	S13-3	Rossi M.	P2-10
Parker E. H. C.	P1-33		
Paszkiewicz B.	P1-04	Sachkov V. A.	P2-35, P2-37, P2-38
Paszkiewicz R.	P1-04	Saijo H.	P1-45, S11-3
Pavia G.	P2-28	Salviati G.	P2-50, S10-5
Pavlidis D.	S11-2	Sankar S.	P1-32, P2-22
Pavlyk B.	P1-44	Santhakumar K.	P2-42
Pécz B.	S9-2	Sanz L. F.	P1-09, P2-40
Peiró F.	P1-52	Saramad S.	P1-18
Pelosi C.	P2-40	Sasaki S.	P1-12
Pelya O.	S9-2	Satka A.	S8-3
Peransin J. M.	S14-5	Saucedo E.	P2-51
Pérez-Omil J. A.	P1-52	Savkina N.	P2-08
Pérez-Rodríguez A.	P1-09	Savkina N. S.	P2-07
Pernot P.	P2-21	Savtchouk A.	S6-2
Peroni M.	P1-24	Scamarcio G.	S13-5
Pessa M.	P1-25	Scardova S.	P2-40
Pezzotti G.	P1-45	Scheglov M.	P2-08
Philippens M.	P2-36	Schippan F.	S12-2
Philippens M.	P2-27		
Piel J. Ph.	P2-27		
Piqueras J.	P1-05, P1-39,		



Schiumarini D.	P2-33	Subach S.V.	P2-45
Scholz C.	P1-51	Suchocki A.	P2-53
Schreiber J.	S11-4	Sugak D.	P2-53
Schroder D. K.	S6-1	Suhara M.	P2-09
Schwinn G.	P2-21	Sun Niefeng	P2-48
Sehil H.	P1-22	Sun Tongnian	P2-48
Sekiguchi T.	S8-4, S11-5	Sundar C. S.	P1-32, P2-22
Selci S.	P2-33, S4-5	Surma B.	P2-47
Semyagin B. R.	P2-37, P2-38, P2-45	Sypko S. A.	P2-54
Senthil Kumar M.	P2-05	Tabet-Derraz H.	P1-54
Sequeira A. D.	P1-33	Taishi T.	S12-3
Shano T.	S5-5	Tajima M.	S2-1
Shashkin Valeriy V.	P2-56	Takabatake N.	P2-11
Shek E. I.	P1-17	Taniguchi K.	S2-2, S5-5
Shen Yaowen	P1-07	Tarento R. J.	P2-29
Sheregii E. M.	P2-55	Terashima K.	S7-4
Shiojiri M.	P1-45, S11-3	Tichelaar F. D.	S10-2
Shirai H.	S5-3	Tiginyanu I. M.	S11-2
Shirakawa T.	S14-1	Ting Wei-Yuan	S13-2
Shiraki H.	P1-10	Tirmarche R.	P2-27
Shishkova N.	P2-15, P2-16	Tlaczala M.	P1-04
Shmidt N. M.	P1-27	Tokuda Y.	P1-10
Show Y.	P2-11	Tománek P.	S4-2
Shpotyuk O. I.	P1-53	Tomassini N.	P2-33
Shyano T.	S2-2	Tomm J. W.	S2-3, S14-2
Sidelnicov A.	P1-28	Tonini R.	P2-28
Siegel W.	P1-28	Tóth A. L.	P1-41
Simoen E.	S7-1	Tränkle G.	S2-3
Singh J. P.	P1-35	Trashchakov V. Yu.	P1-20
Singh R.	P1-35	Tregubov A.	P2-08
Sinkkonen J.	P1-48	Tregubova A. S.	P2-07
Sirotkin V.	P1-49, P2-26	Trequattrini F.	S13-4
Sivaji K.	P1-32, P2-22	Triftshäuser W.	S5-4
Skipetrov E. P.	P1-42, P1-43	Tsuji H.	S2-2, S5-5
Skipetrova L. A.	P1-42	Tsunekawa Shin	P2-02
Skorupa W.	P1-08, S5-4	Tsybulyak B.	P1-44
Skriniarová J.	P1-06	Tukiainen A.	P1-25
Slyn'ko E. I.	P1-42, P1-43	Tyagi R.	P1-35
Smatko V.	P2-47		
Smirnov A. B.	P2-43	Uchihashi T.	P1-11
Sobolev N. A.	P1-17, P2-18	Ueda K.	S4-4
Sokolov V. I.	P2-14	Urbietta A.	S11-5
Solov'ev V.	P2-08	Ustinov V. M.	P2-38, S2-5
Someya T.	S10-4		
Sorokin L.	P2-08	Vabre L.	P2-27
Soshnikov I. P.	P2-38	Väinölä H.	P1-48
Sperr P.	S5-4	Valiaev V.	S11-2
Spinella C.	P2-20	van der Hart A.	P1-06
Srnanek R.	P2-04	Van Nostrand J. E.	S10-3
Starck C.	S14-5	Vazquez L.	P2-41
Stehlé J. L.	P2-27	Vdovin V.	P2-41
Steinegger Th.	P1-29	Vdovin V. I.	P1-17
Sten'kin Yu. A.	P1-21	Verma P.	S3-3
Stenzenberger J.	S1-2	Vilisova M. D.	P2-45
Stevens-Kalceff M. A.	S11-2	Vincze A.	P2-04
Storgårds J.	P1-48	Vlasenko A. I.	P2-43
Straubinger T. L.	S3-5	Vlasenko O. I.	P2-52
Strel'chuk A. M.	P2-07	Voelskow M.	P1-08
Strunk H. P.	P1-02	Volkova A.	P2-08
Strzelecka S.	P2-47	Volkova O. S.	P1-43
Stuchinsky V. A.	P1-21, P2-23	Volodin V. A.	P2-37, P2-38

Volovik B. V.	S2-5
von Aichberger S.	S6-5
Wagner J.	S12-1
Wagner M.	S2-4
Wang Z. G.	P1-07, S3-2
Watanabe M.	S7-3
Weingärtner R.	S3-5
Wellmann P. J.	S3-5
Werner P.	S2-5
Wernisch J.	P1-50
Weyers M.	S2-3
Weyher J. L.	S10-2
Wierzchowski W.	P2-30
Wieteska K.	P2-30
Wilson M.	S6-2
Winnacker A.	S3-5
Wosinski T.	S9-2
Xu Bo	S3-2
Yakimov E. B.	P1-49, P2-25, P2-26, S6-3
Yakovtseva V.	P2-19
Yamada K.	S10-4
Yamada M.	S3-3, S7-2, S9-4
Yamanaka Y.	S5-2
Yamashita Y.	P1-16
Yang Deren	P2-17
Ye Xiaoling	S3-2
Yeo Y. K.	S10-3
Yli-Koski M.	P1-48
Yonenaga I.	S12-3
Yoshida H.	P1-11
Yoshida M.	S9-4
Yoshimoto M.	S1-3
Yoshimura M.	S4-4
Yugova T. G.	P1-17
Zaitsev S.	P2-26
Zalharov N. D.	S2-5
Zamoryanskaya M. V.	P2-14
Zanardi Ocampo J. M.	S10-4
Zandbergen H. W.	S10-2
Zanotti L.	P2-50
Zatko B.	P2-47
Zavadil J.	P1-37
Zdansky K.	P1-36, P1-37
Zebentout B.	P1-22
Zha M.	P2-50
Zhao Jianqun	P2-48
Zhao Youwen	P2-48
Zhao Zhengping	P2-48
Zhovnir G. I.	P2-54
Zielinska-Rohozinska E.	P1-03, P2-06
Zonca R.	P2-28
Zvereva E. A.	P1-43

## DRIP IX PROGRAM

<b>MONDAY 24 September</b>	
	16:00 – 20:00 Registration & Reception 20:00 – 21:30 Welcome Dinner
<b>TUESDAY 25 September</b>	
08:45 – 09:00 Opening Address 09:00 – 10:25 <b>SESSION 1</b> 10:25 – 10:55 Coffee Break 10:55 – 12:35 <b>SESSION 2</b> 12:35 – 14:10 Lunch	14:10 – 15:50 <b>SESSION 3</b> 15:50 – 16:20 Coffee Break 16:20 – 16:50 <b>SESSION 3</b> 16:50 – 18:30 <b>SESSION 4</b> 18:45 – 20:00 <b>POSTER SESSION 1</b> 20:00 – 21:30 Dinner
<b>WEDNESDAY 26 September</b>	
08:30 – 10:10 <b>SESSION 5</b> 10:10 – 10:40 Coffee Break 10:40 – 12:20 <b>SESSION 6</b> 12:20 – 14:00 Lunch	14:00 – 15:15 <b>POSTER SESSION 2</b> 15:15 – 16:40 <b>SESSION 7</b> 16:40 – 17:10 Coffee Break 17:10 – 18:35 <b>SESSION 8</b> 18:35 – 20:00 <b>SESSION 9</b> 20:00 – 21:30 Dinner
<b>THURSDAY 27 September</b>	
08:30 – 10:10 <b>SESSION 10</b> 10:10 – 10:40 Coffee Break 10:40 – 12:20 <b>SESSION 11</b> 12:20 – 13:40 Lunch	13:40 – 19:30 <b>EXCURSION to URBINO</b> 20:00 – 23:00 <b>GALA DINNER</b>
<b>FRIDAY 28 September</b>	
09:00 – 10:25 <b>SESSION 12</b> 10:25 – 10:50 Coffee Break 10:50 – 12:30 <b>SESSION 13</b> 12:30 – 13:50 Lunch	13:50 – 15:30 <b>SESSION 14</b> 15:30 – 15:45 Closing ceremony